

University of Alberta

**AMPAKINE AND OPIOID MODULATION
OF RESPIRATORY NEURAL CONTROL**

by

Floriane Lenal

A thesis submitted to the Faculty of Graduate Studies and Research
in partial fulfillment of the requirements for the degree of

Doctor of Philosophy

Centre for Neuroscience

©Floriane Corinne Lenal

Spring 2013

Edmonton, Alberta

Permission is hereby granted to the University of Alberta Libraries to reproduce single copies of this thesis and to lend or sell such copies for private, scholarly or scientific research purposes only. Where the thesis is converted to, or otherwise made available in digital form, the University of Alberta will advise potential users of the thesis of these terms.

The author reserves all other publication and other rights in association with the copyright in the thesis and, except as herein before provided, neither the thesis nor any substantial portion thereof may be printed or otherwise reproduced in any material form whatsoever without the author's prior written permission.



Library and Archives
Canada

Published Heritage
Branch

395 Wellington Street
Ottawa ON K1A 0N4
Canada

Bibliothèque et
Archives Canada

Direction du
Patrimoine de l'édition

395, rue Wellington
Ottawa ON K1A 0N4
Canada

Your file Votre référence

ISBN: 978-0-494-96408-8

Our file Notre référence

ISBN: 978-0-494-96408-8

NOTICE:

The author has granted a non-exclusive license allowing Library and Archives Canada to reproduce, publish, archive, preserve, conserve, communicate to the public by telecommunication or on the Internet, loan, distribute and sell theses worldwide, for commercial or non-commercial purposes, in microform, paper, electronic and/or any other formats.

The author retains copyright ownership and moral rights in this thesis. Neither the thesis nor substantial extracts from it may be printed or otherwise reproduced without the author's permission.

AVIS:

L'auteur a accordé une licence non exclusive permettant à la Bibliothèque et Archives Canada de reproduire, publier, archiver, sauvegarder, conserver, transmettre au public par télécommunication ou par l'Internet, prêter, distribuer et vendre des thèses partout dans le monde, à des fins commerciales ou autres, sur support microforme, papier, électronique et/ou autres formats.

L'auteur conserve la propriété du droit d'auteur et des droits moraux qui protègent cette thèse. Ni la thèse ni des extraits substantiels de celle-ci ne doivent être imprimés ou autrement reproduits sans son autorisation.

In compliance with the Canadian Privacy Act some supporting forms may have been removed from this thesis.

While these forms may be included in the document page count, their removal does not represent any loss of content from the thesis.

Conformément à la loi canadienne sur la protection de la vie privée, quelques formulaires secondaires ont été enlevés de cette thèse.

Bien que ces formulaires aient inclus dans la pagination, il n'y aura aucun contenu manquant.

Canada

“Only those who attempt the absurd can achieve the impossible”

- Albert Einstein -

*A la mémoire de
Wilson, Tertulie
Et Marie-Madeleine*

Je dédie cette thèse à Henri Lenal

Abstract

The inspiratory phase of the breathing cycle is thought to be generated by a network of neurons within a region of the ventrolateral medulla called the preBötzinger complex (preBötC). Synaptic transmission mediated by the neurotransmitter glutamate acting via α -amino-3-hydroxy-5-methyl-4-isoxazolepropionate (AMPA) receptors is critical for the normal functioning of the preBötC network and its rhythmogenic activity. Ampakines are synthetic molecules designed to readily cross the blood-brain barrier and allosterically bind to AMPA receptors (AMPA receptors) to modulate certain kinetics of their channel such as slowing channel closing or decreasing desensitization and/or deactivation rates. This may prolong current flow through AMPARs and enhance endogenous glutamatergic synaptic transmission. Previous studies have demonstrated that the two broad classes of ampakines (high- and low-impact) alleviate opioid-induced respiratory depression in rodents *in vivo* and *in vitro*. This thesis aimed to investigate the cellular mechanisms underlying these actions.

I determined that the mu-opioid receptor agonist [D-Ala², N-MePhe⁴, Gly⁵]-enkephalin (DAMGO) differentially affected synaptic inputs within the preBötC. AMPA-mediated ionic currents in single preBötC neurons were potently enhanced by the high-impact ampakines CX614 and CX546 and this clearly amplified the recruitment of endogenous inspiratory-drive conductances to promote respiratory rhythmogenesis. In addition to the preBötC effects, it was determined that DAMGO may significantly suppress

respiratory frequency by acting through raphé nucleus obscurus (RNO) neurons. Electrophysiological data showed that DAMGO decreased the excitability of RNO neurons. Immunohistochemical data demonstrated that mu-opioid receptors are uniquely expressed among excitatory RNO neurons. Finally, the mode of action of the low-impact ampakine CX717 (which alleviates severe opioid-induced respiratory depression) was examined. Surprisingly, CX717 showed little to no augmenting action of AMPA mediated conductances on preBötC neurons. However, it markedly increased N-methyl-D-aspartic acid (NMDA)-mediated responses that were decreased by glycine, and a high expression of the subunit NR3A was found within the preBötC. This led to my hypothesis that CX717 is acting as an allosteric modulator on the glycine binding NMDA receptor subtype NR3, known to negatively influence conventional NMDA receptor conductance. These data provide a foundation for further exploring a completely novel model of CX717 action and the previously unexplored role of NR3 function in central respiratory control.

Table of Contents

CHAPTER 1 INTRODUCTION.....	1
1.1 OVERVIEW.....	2
1.2 OBJECTIVES.....	3
1.3 ANATOMY OF NEURAL CONTROL OF BREATHING: RESPIRATORY RHYTHM GENERATORS AND IMPORTANT NUCLEI.....	4
1.3.1 A brief historical perspective.....	4
1.3.2 The preBötzinger complex: a inspiratory rhythm generator located in the ventral respiratory column of the medulla.....	6
1.3.3 Additional important nuclei of the rostral VRC.....	15
1.4 PHARMACOLOGY OF NEURAL CONTROL OF BREATHING: KEY NEUROMODULATORS OF CENTRAL RESPIRATORY DRIVE.....	20
1.4.1 Peptides.....	20
1.4.2 Glutamatergic ionotropic receptors.....	25
1.4.3 Serotonin modulation of respiratory drive.....	31
1.5 REFERENCES.....	44
CHAPTER 2. MATERIAL AND METHODS	73
2.1 MATERIAL AND METHODS FOR ELECTROPHYSIOLOGICAL RECORDINGS...	74
2.1.1 Brainstem spinal cord preparation.....	74
2.1.2 Medullary slice preparation.....	74
2.1.3 Whole-cell patch-clamp recording technique.....	75
2.1.4 Drug application.....	77
2.1.5 Data acquisition, protocols and statistical analysis.....	78

2.2 METHODOLOGY FOR IMMUNOHISTOCHEMISTRY AND	
IMMUNOCYTOCHEMISTRY.....	83
2.2.1 Immunohistochemistry of transverse medullary slices.....	83
2.2.2 Immunocytochemistry of HEK293 cells.....	85
2.3 MATERIAL AND METHODS FOR PROTEIN EXPRESSION IN HEK293 CELLS.	86
2.3.1 HEK293 cell culture.....	86
2.3.2 HEK293 cell transfection with recombinant receptors.....	87
2.3.3 Electrophysiology of transfected HEK293 cells.....	88
2.4 REFERENCES.....	93
CHAPTER 3. MODULATION OF RESPIRATORY NEURAL ACTIVITY	
BYOPIOIDS AND HIGH-IMPACT AMPAKINES.....	94
3.1 ABSTRACT.....	95
3.2 INTRODUCTION.....	96
3.3 RESULTS.....	98
3.3.1 DAMGO modulates inspiratory motor output <i>in vitro</i>	98
3.3.2 Mu-opioid receptor expression in the ventrolateral medulla.....	99
3.3.3 Whole-cell patch-clamp analysis of damgo-mediated modulation of respiratory neurons and synaptic drive.....	101
3.3.4 CX614 modulates inspiratory motor output.....	106
3.3.5 CX614 potentiates AMPA receptor conductance on respiratory preBötC neurons.....	107
3.3.6 Synaptic analysis of CX614 effect on preBötC neurons.....	110
3.3.7 Other allosteric modulators of AMPA receptors.....	114
3.4 DISCUSSION.....	116
3.4.1 Differential disruption of synaptic transmission among respiratory preBötC neurons by opioids.....	116
3.4.2 Cellular mechanisms underlying the increase of inspiratory rhythm by ampakines.....	120
3.4.3 AMPA receptor conductance and inspiratory rhythm.....	121

3.5 REFERENCES.....	145
CHAPTER 4. OPIOID-MEDIATED RESPIRATORY DEPRESSION VIA ACTIONS IN THE RAPHE NUCLEUS.....	153
4.1 ABSTRACT.....	154
4.2 INTRODUCTION.....	155
4.3 RESULTS.....	157
4.3.1 Mu-opioid receptor activation in the raphe nucleus obscurus can depress inspiratory drive <i>in vitro</i>	157
4.3.2 Distribution of mu-opioid receptors among excitatory and inhibitory RNO neurons.....	159
4.3.3 DAMGO modulates respiratory RNO neurons.....	161
4.3.4 Ampakine modulation of RNO respiratory neurons and network.....	164
4.4 DISCUSSION.....	167
4.4.1 Modulation of the RNO-preBötC loop by mu-opioid receptors....	167
4.4.2 Potential postsynaptic effects of damgo on respiratory raphe neurons underlying respiratory depression.....	169
4.4.3 Summary.....	171
4.5 REFERENCES.....	186
CHAPTER 5. CELLULAR MECHANISMS UNDERLYING THE ALLEVIATION OF RESPIRATORY DEPRESSION BY LOW-IMPACT AMPAKINES.....	192
5.1 ABSTRACT.....	193
5.2 INTRODUCTION.....	194
5.3 RESULTS.....	196
5.3.1 Low-impact ampakines alleviate damgo-induced respiratory depression <i>in vitro</i>	196

5.3.2 Modulation of respiratory neural circuitry by CX717 in baseline conditions.....	197
5.3.3 Single-cell analyses of CX717 modulation of preBötC neuron activity following damgo-induced respiratory depression.....	200
5.3.4 Modulation of NMDA receptor conductance by CX717.....	203
5.4 DISCUSSION.....	210
5.4.1 Low-impact ampakines and AMPA receptors.....	210
5.4.2 CX717 and NMDA receptor conductance.....	211
5.4.3 A state-dependent potentiation of inspiratory rhythm generation by CX717.....	214
5.4.4 Behind the scenes: the presence or the induction of a glycinergic signal ?.....	214
5.5 REFERENCES.....	239
 CHAPTER 6. REVIEW AND DISCUSSION.....	243
6.1 MU-OPIOID RECEPTORS OF THE RAT PREBÖTC.....	244
6.2 RAPHE OBSCURUS INFLUENCE ON RESPIRATORY NETWORK ACTIVITY.....	247
6.3 ALLOSTERIC MODULATORS OF AMPA RECEPTORS MODIFY RESPIRATORY NEURON FUNCTION.....	250
6.4 THE PARTICULAR CASE OF CX717, A WINDOW TO A NMDA RECEPTOR- DRIVEN RESPIRATORY RHYTHM GENERATION HYPOTHESIS.....	252
6.5 FUTURE DIRECTIONS.....	256
6.6 CONCLUDING REMARKS.....	259
6.7 REFERENCES.....	262

List of Figures

Figure 1.1 Schematic representations of respiratory related regions in the rodent brainstem.	33
Figure 1.2 NK1 receptors in the rostral VRC of the mouse.....	35
Figure 1.3 Schema of the rat brainstem spinal cord and medullary slice.....	36
Figure 1.4 Caudal medullary raphé nuclei and their 5HT neuronal cell bodies.	37
Figure 1.5 Overall view of the μ -opioid receptor structure.....	39
Figure 1.6 Overall structure and classical function of the glutamate ionotropic AMPA and NMDA receptors.	40
Figure 1.7 Ampakine actions on excised patches and hippocampal slices.	42
Figure 2.1 Photograph of the electrophysiological chamber used for recording inspiratory activity from a medullary slice preparation.	89
Figure 2.2 Schematic diagram of a rhythmically-active medullary slice preparation used for recordings of preBötC neurons and hypoglossal nerve activity.	90
Figure 2.3 Schematic diagram of the medullary slice preparation and the recording of a respiratory neuron of the RNO.	91
Figure 3.1 Local activation of μ -opioid receptors within the preBötzinger complex (preBötC) in <i>in vitro</i> medullary slice preparation of neonatal rat depresses inspiratory rhythm.	124
Figure 3.2 μ -opioid receptor 1a is expressed in the preBötC of new born rat.....	125
Figure 3.3 Expression of MOR1a, NK1R, and ChAT in a transverse section of the medulla in neonatal rat.....	127

Figure 3.4 DAMGO differentially affects respiratory neurons of preBötC in <i>in vitro</i> medullary slice preparation of neonatal rats.....	128
Figure 3.5 Differential effects of DAMGO on inspiratory currents of preBötC neurons.....	130
Figure 3.6 Differential effect of DAMGO on interburst synaptic events in inspiratory neurons of the preBötC.	132
Figure 3.7 Bath application of CX614 alleviates DAMGO-induced inspiratory drive frequency depression in <i>in vitro</i> rat medullary slice preparation.	133
Figure 3.8 Local application of CX614 into the preBötC alleviates opioid-induced inspiratory rhythm depression.....	134
Figure 3.9 AMPA-mediated current load is increased by CX614 in respiratory preBötC neurons.....	135
Figure 3.10 CX614 increases the AMPA component of preBötC inspiratory drive potentials independently of external calcium.....	136
Figure 3.11 CX614 alone augments excitatory currents on respiratory preBötC neurons and increasing inspiratory frequency.....	138
Figure 3.12 CX614 effect on preBötC neuronal postsynaptic activity subsequent to DAMGO-induced suppression of inspiratory drive.	140
Figure 3.13 Allosteric modulation of AMPA receptors by the high impact ampakine CX546 increases inspiratory envelope of preBötC neurons in basic physiological conditions.	141
Figure 3.14 Ampakine CX546 increases inspiratory currents in weak endogenous inspiratory drive.....	143
Figure 3.15 Cyclothiazide reverses DAMGO-induced inspiratory drive depression in <i>in vitro</i> medullary slice of neonatal rat.	144
Figure 4.1 Local injection of the mu-opioid agonist DAMGO in the most ventral part of the RNO decreases inspiratory motor output rhythm in <i>in vitro</i> neonatal rat medullary slice.	173
Figure 4.2 Mu-opioid receptors (MOR)-expressing neurons of the RNO highly co-localize with serotonin (5HT)-expressing neurons in the RNO of P2 rat transverse medullary slice.....	174

Figure 4.3 Transverse sections of the medulla of P2 rat immunostained for 5HT, substance P (SP) and NK1R at different rostral (upper end) to caudal (lower end) levels.	176
Figure 4.4 A subpopulation of serotonergic neurons in the ventral RNO expresses both SP and MOR.	177
Figure 4.5 Characteristics of respiratory neurons of the RNO in medullary slice preparation.	179
Figure 4.6 DAMGO decreases excitability of respiratory-related RNO neurons.	181
Figure 4.7 Postsynaptic effect of DAMGO on RNO neurons.	182
Figure 4.8 Respiratory raphé neurons contain functional AMPA receptors which conductance can be modulated by the high-impact ampakine CX614.	183
Figure 4.9 Independent action of the ampakine CX614 within the RNO sensitive area can increase inspiratory drive frequency in presence of DAMGO.	185
Figure 5.1 Bath application of CX717 alleviates DAMGO-induced depression of inspiratory frequency in <i>in vitro</i> medullary slice preparation.	217
Figure 5.2 Local application of CX717 into preBötC counters respiratory drive inhibition induced by DAMGO.....	218
Figure 5.3 Bath application of CX717 does not change baseline inspiratory activity in <i>in vitro</i> neonatal rat models.....	220
Figure 5.4 CX717 alone does not change synaptic input current size nor decay kinetics on inspiratory preBötC neurons.....	222
Figure 5.5 CX717 alone can change excitatory synaptic input currents on expiratory preBötC neurons.....	224
Figure 5.6 Ampakine CX717 augments inspiratory currents suppressed by DAMGO on preBötC neurons.....	226
Figure 5.7 CX717 action on AMPA-mediated currents on respiratory preBötC neurons.....	227
Figure 5.8 Effect of CX717 on inspiratory activity after DAMGO-induced respiratory depression and in presence of the NMDA receptor blocker MK801.....	228

Figure 5.9 NMDA-mediated depolarizing responses are increased by CX717 following glycine exposure in some preBötC neurons.....	229
Figure 5.10 NR3A receptor is expressed in the ventrolateral medulla of newborn rats.....	230
Figure 5.11 Colocalization of NR3A and NK1R is prominent in the preBötC of perinatal rat.....	232
Figure 5.12 HEK293T cells transfected with NR1/NR3A display excitatory inward currents in response to glycine puff.....	233
Figure 5.13 CX1763 can alleviate DAMGO-induced suppression of inspiratory frequency.	234
Figure 5.14 CX1942 can alleviate DAMGO-induced suppression of inspiratory frequency.	235
Figure 5.15 Comparison between CX1942 and CX1763 counteractions of DAMGO-induced inhibition of respiratory rate <i>in vitro</i>	236
Figure 5.16 CX1739 can alleviate DAMGO-induced suppression of inspiratory frequency.	238
Figure 6.1 Putative “two arms” system of neuromodulation of the inspiratory drive by opioids and ampakines.....	260
Figure 6.2 A candidate binding site for a low-impact ampakine.....	261

Table and Annexes

Table 2.1 List of primary antibodies used in immunohistochemistry studies.....	92
Annex 1. Schematic representation of the NR3A/pcDNA3.1 plasmid map.	270
Annex 2. Schematic representation of the NR3B/pcDNA3.1 plasmid map.	271

CHAPTER 1

INTRODUCTION

1.1 OVERVIEW

The complex and highly organized respiratory system has evolved remarkably since the first living organisms where oxygenation was largely fulfilled via passive diffusion. In mammals, it has developed into a respiratory system composed of interconnected peripheral components ensuring coordinated breathing movements controlled by central respiratory networks that sense and generate breathing signals. Breathing is a vital biological function that commences *in utero* and persists until death, thus any significant disturbance in respiratory drive or function can become life-threatening. Loss or impairment of respiratory functions can be caused by a variety of conditions. These include stroke; lung diseases such as pulmonary fibrosis, chronic obstructive pulmonary disease, asthma, or cystic fibrosis; diaphragm abnormalities such as congenital diaphragm hernia; genetic diseases such as Prader-Willi and Rett Syndromes; sleep-related respiratory diseases such as central and obstructive sleep apnea. Respiratory dysfunctions that result from failure of appropriate central respiratory drive are relevant to this thesis work.

Reduced central drive, referred to as respiratory depression, can result from both disease and administration of drugs that include anaesthetic and analgesic agents. For example, commonly used opioid analgesics such as morphine and fentanyl can have dramatic depressing effects on central respiratory drive that is a major undesirable side effect. In recent years, efforts have been made to develop agents that are either capable of more specifically targeting pain pathways or that are capable of counteracting the depression of the central respiratory drive induced by analgesics without affecting their pain reducing properties. This dissertation pertains to the latter, with a systematic study of ampakines, which are positive allosteric modulators of amino-3-hydroxy-5-methyl-4-isoxazolepropionate (AMPA) receptors and have shown promise as emerging therapeutics to counter central respiratory depression without removal of opioid analgesics effects.

1.2 OBJECTIVES

In this dissertation, opioid-induced central respiratory depression and integrative physiological properties of ampakines were investigated using *in vitro* newborn rodent models, with the objective of understanding the cellular mechanisms underlying the modulation of breathing by opioids and ampakines. Experimental approaches used include motor output recordings in acute rhythmic medullary slice preparations combined with immunohistochemistry and whole-cell patch-clamp electrophysiological analysis of respiratory related neurons of the preBötC and the raphé nucleus obscurus. Three main questions were addressed:

1. What are the cellular mechanisms underlying μ -opioid agonist-induced respiratory depression, and where are μ -opioid receptors expressed in the inspiratory network?

2. How do ampakines and opioids modulate synaptic transmission within the preBötC?

3. Which receptor proteins are targeted by the different types of ampakines in preBötC neurons, how do ampakines modulate those receptors, and to what extent can each unique modulation result in an increase of inspiratory rhythmogenesis?

The results of this study should increase our current knowledge on the underlying neurotransmitters and synaptic mechanisms implicated in the regulation of preBötzinger complex (preBötC) rhythmogenesis and the neural control of breathing, as well as providing at least a partial mechanistic understanding of ampakine function. Ultimately, the exploration of ampakine function on preBötC neurons and their effects on specific conductances could provide the basis for synthesizing clinically relevant compounds capable of specifically counteract respiratory depression. This first chapter introduces the field of central respiratory control by providing an overview of the literature pertaining to the physiology, anatomy and pharmacology of breathing rhythmogenesis. The techniques used for the experimental research are described

in the second chapter, followed by chapters 3, 4 and 5 that describe the main body of data. The last chapter is dedicated to a general discussion of the results and delineates future directions.

1.3 ANATOMY OF NEURAL CONTROL OF BREATHING: RESPIRATORY RHYTHM GENERATORS AND IMPORTANT NUCLEI

1.3.1 A BRIEF HISTORICAL PERSPECTIVE

The mammalian brainstem contains multiple nuclei of neuronal assemblies dedicated to lower and basic functions of life, and it conveys neuronal activity necessary for maintaining what has been referred to as ‘a vegetative state of life’. One of the earliest reports suggesting that respiratory activity was generated in the brainstem dates back to 1812, when Le Gallois described the “medulla spinalis” as being important for respiratory and cardiac activities (Le Gallois, 1812). The French physiologist Pierre Flourens described a “nœud vital” in the brainstem as being the source of respiratory rhythmogenesis (Flourens, 1842; Flourens, 1851). From 1876, when the Cruelty to Animals Act legalized animal experimentation in the United Kingdom, animal research was permitted and this gave rise to a new era of scientific research. Different types of models and techniques (*in vivo*, *in vitro*) emerged and helped researchers understand the anatomical and physiological basis of central respiratory control. In the 1880’s, pioneering work by Sydney Ringer demonstrated the importance of potassium, calcium and sodium ions in the solution perfusing a frog heart in order to produce long-lasting heart beating (Ringer, 1883; reviewed in Miller, 2004) and defined the physiological basis of saline solution used to study normal cell function *in vitro*. Electrophysiological work by Lumsden (1923a, b, c) and Stella (1938) involving brain transections and lesioning techniques in vagotomized animals laid out the fundamental organization of the central respiratory network. Two parts of the

brainstem were found to be important for central control of breathing: the pons and the medulla oblongata (Lumsden 1923 a, b, c; Stella, 1938).

Extracellular and intracellular single-cell recording techniques combined with histological approaches helped identify and characterize a multitude of respiratory-related neurons within the brainstem (Merrill, 1970; Richter and Heyde, 1974; Lipski and Merrill, 1980; Lipski, 1981; reviewed in Kalia, 1981; Onimaru and Homma, 1987). Respiratory-related neurons are typically classified according to their firing pattern, the timing of their discharge and changes of their membrane potential in respect to the respiratory cycle. Respiratory-related neurons fall into two basic classes: inspiratory and expiratory neurons, although each class can be divided into several subtypes (Ezure et al., 1988; Ezure, 1990; Smith et al., 1990; Schwarzacher et al., 1995). These neurons project to cranial and spinal respiratory motoneurons responsible for controlling the contraction of respiratory muscles located in the upper airways, ribcage, diaphragm and abdomen.

Several studies demonstrated that respiratory neurons located close to the ventral surface of the medulla are organized in a columnar fashion (ventral respiratory column, VRC; Merrill, 1970; Bianchi et al., 1973; Bianchi, 1974; reviewed in Mitchell and Berger, 1977). It was later found that the VRC comprises a subcomponent that constitutes an essential network for respiratory rhythmogenesis (Smith et al., 1989; Smith et al., 1991; Onimaru and Homma, 2003). In addition, the VRC has the ability to integrate a variety of afferent inputs originating from different brain regions (including the brainstem itself) to produce a breathing pattern that must be sustainable throughout life and capable of adapting to various challenges (e.g. exercise activity) (reviewed in Feldman et al., 2003). Specifically, central chemoreceptors [e.g. retrotrapezoid neurons (Mulkey et al., 2004); raphé nuclei neurons (reviewed in Richerson, 2004)] and peripheral chemoreceptors [aortic and carotid bodies via the nucleus tractus solitarius (Nattie and Li, 2002)] project to VRC respiratory neurons providing sensory feedback in order to adjust respiration to meet changes in pH, carbon dioxide and oxygen blood concentrations (reviewed in Feldman et al., 2003). The VRC includes, in a

rostral-caudal order, the retrotrapezoid nucleus/parafacial respiratory group (RTN/pFRG), the Böttinger complex (BötC) and the preBöttinger complex (preBötC), which all contain many respiratory propriobulbar neurons (Ellenberger and Feldman, 1990; Schreihofer et al., 1999; Guyenet et al., 2002; Tan et al., 2010; reviewed in Wong-Riley and Liu, 2005 and in Alheid and McCrimmon, 2008). The location of these nuclei within the mammalian brainstem is shown in Figure 1.1 which displays their distribution in parasagittal and longitudinal perspectives within the rat brainstem.

1.3.2 THE PREBÖTZINGER COMPLEX: A INSPIRATORY RHYTHM GENERATOR LOCATED IN THE VENTRAL RESPIRATORY COLUMN OF THE MEDULLA

1.3.2.1 Identification of the preBöttinger complex locus and function

The preBötC is located ventral to the semi-compact division of the nucleus ambiguus (NA_{sc}) and rostral to the anterior tip of the lateral reticular formation (Smith et al., 1991; Gray et al., 1999; Wong-Riley and Liu, 2005). It was initially described in a seminal study published in *Science* (Smith et al., 1991). That particular study involved serial transections of the brainstem in order to isolate a restricted area of the medulla, necessary and sufficient to generate inspiratory rhythm *in vitro*. Within that area, a kernel of voltage-dependent rhythmogenic inspiratory neurons was identified as being functionally essential for generating inspiratory activity. The “nœud vital” of Flourens was found: the preBötC was defined as a respiratory control generator and was named after its location within the medulla, which is in close vicinity to the previously characterized Böttinger complex (note that it should have been termed the post-Böttinger complex based on correct anatomical terminology). The study triggered a surge of interest and progress towards understanding central respiratory control.

Subsequent studies explored potential molecular markers capable of distinguishing the preBötC within the VRC. The preBötC is highly immunoreactive for the neurokinin-1 receptor (NK1R) that binds substance P

(Gray et al., 1999) (see Fig. 1.2). NK1R expressing preBötC neurons are excitatory glutamatergic cells (Wang et al., 2001; Guyenet et al., 2002) that include predominantly small propriomedullary cells and, in the caudal region of the preBötC, larger cells with spinal projections (Guyenet et al., 2002; Stornetta et al., 2003). In addition, studies demonstrated that the inception of respiratory activity measured by either *in vivo* fetal breathing movements (Kobayashi et al., 2001), or *in vitro* respiratory-related motor activity (Greer et al., 1992; Di Pasquale et al., 1996; Pagliardini et al., 2003) coincided with the inception of NK1R expression in the rat preBötC (Pagliardini et al., 2003) at embryonic age (E) 17, approximately 5 days before birth.

Fluorescent tagging of substance P (Pagliardini et al., 2005), combined with epifluorescence imaging and electrophysiological techniques was used to visualize *in vitro* neurons that have internalized their substance P receptors for examination of their morphological and electrophysiological characteristics (Pagliardini et al., 2005; Hayes et al., 2007; Montandon et al., 2011). NK1R positive (NK1R⁺) neurons include neurons with and without respiratory-related activity. NK1R⁺ inspiratory neurons vary in size as indicated by capacitance measurements [range of ~45pF to ~85pF; Hayes and Del Negro, 2007]. Importantly, some NK1R⁺ preBötC neurons have the electrophysiological characteristics of early-inspiratory cells (Guyenet and Wang, 2001; Pagliardini et al., 2005; Hayes and Del Negro, 2007). Analysis of whole-cell recordings of preBötC neurons led to a classification of inspiratory preBötC neurons (Rekling et al., 1996a). Some inspiratory neurons (type I or early-inspiratory cells) display depolarizing ramps with onsets before the hypoglossal nerves discharge, have rhythmogenic bursting-like behaviour and can be depolarized by thyrotropin-releasing hormone (TRH) (Rekling et al., 1996b). Other inspiratory neurons (type II) are insensitive to TRH and do not display any rhythmogenic property (Rekling et al., 1996a, 1996b). Both types I and II preBötC neurons are sensitive to substance P (Gray et al., 1999). A subset of small fusiform NK1R⁺ preBötC neurons contains μ -opioid receptors and whole-cell recordings in presence of tetrodotoxin (TTX) demonstrated the presence of functional μ -opioid receptors

only on type I neurons (Gray et al., 1999). In a subsequent study, substance P tagged inspiratory preBötC neurons were shown to be sensitive to μ -opioid agonist (Montandon et al., 2011).

In vivo studies in adult rats have shown that killing a subset of NK1R positive neurons within the preBötC using substance P conjugated to the toxin saporin (SP-SAP) led to marked disturbances of breathing (Gray et al., 2001). As the preBötC dysfunction progresses after bilateral injection of SP-SAP, breathing pattern is initially disrupted during rapid eye movement (REM) sleep, then also during non-REM sleep and eventually during wakefulness (McKay et al., 2005). On the other hand, genetic deletion of NK1R does not alter spontaneous respiratory activity *in vitro* nor breathing *in vivo* (De Felipe et al; 1998; Ptak et al., 2000b). Collectively these data indicated that the activation of NK1R itself is not necessary for respiration, but NK1R⁺ preBötC neurons are critical to maintain a stable rhythmogenic drive.

In the adult rat, a subpopulation of NK1R⁺ preBötC neurons also expresses the neuropeptide somatostatin (STT) (Stornetta et al., 2003). Retrograde labeling and tracing studies showed that STT-positive preBötC neurons are propriobulbar neurons (Stornetta et al., 2003, Tan et al., 2010), and *in situ* hybridization studies showed that most of them contain vesicular glutamate transporter 2 mRNA while only few contain glutamic acid decarboxylase (GAD-67) mRNA or the opioid precursor preproenkephalin mRNA (Stornetta et al., 2003), suggesting that most STT-positive neurons are excitatory. Development of allatostatin-coupled adeno-associated viruses driven by the somatostatin promoter enabled acute silencing of STT-expressing preBötC neurons, which led to severe suppression of respiratory activity and lack of respiratory movements (Tan et al., 2008).

Overall these results demonstrated that NK1R (see Fig. 1.2) and somatostatin expression are valuable markers to identify critical preBötC neurons. More recently, those markers were also used to provide the first anatomical identification of the preBötC in humans (Lavezzi and Maturri, 2008; Schwarzacher et al., 2011).

1.3.2.2 Theories and concepts on respiratory rhythmogenesis

The dynamic neuronal organization of the preBötC and the underlying mechanisms necessary to generate spontaneous respiratory rhythmicity within the preBötC are still not fully understood. One of the first approaches used toward understanding preBötC rhythmogenesis was to identify intrinsic physiological properties in respiratory preBötC neurons. Electrophysiological whole-cell patch-clamp techniques permitted the identification of several pacemaker-type currents and synaptic neurotransmitter conductances. Initially, two models were proposed: the “synaptic network model” proposed that recurrent inhibitory synaptic transmission is essential for respiratory rhythmogenesis (Bradley et al., 1975; Feldman and Cowan, 1975; Richter, 1982), while the “pacemaker model” proposed that neurons with pacemaker properties generate rhythmicity (Smith et al., 1991; Johnson et al., 1994; Koshiya and Smith, 1999).

In the first model, synaptic inhibitory interactions were believed to account for the mutually exclusive respiratory patterns of inspiratory and expiratory cells, as well as for the generation of the ramp-like inspiratory phase observed *in vivo* (reviewed in Richter, 1982). Classical glycine and γ -aminobutyric acid type A (GABA_A) receptor agonists modulate respiratory rhythm (Brockhaus and Ballanyi, 1998; Ren and Greer, 2006), depending on chloride (Cl⁻) co-transporter expression (Ren and Greer, 2006). However, *in vitro* studies demonstrating that block of GABAergic and glycinergic Cl⁻-mediated inhibition does not abolish respiratory rhythm (Feldman and Smith., 1989; Onimaru et al., 1990) favoured the pacemaker hypothesis. Several pacemaker-type currents were then proposed as being critical for rhythmogenesis.

In the mouse model, a subpopulation of preBötC respiratory neurons have a cationic conductance activated by hyperpolarization which produces a depolarizing inward current known as the hyperpolarized-activated current (I_h; Thoby-Brisson et al., 2000). I_h is known to participate in automaticity properties of cardiac pacemaker cells (DiFrancesco, 1993; reviewed in Pape, 1996). However, although pharmacological blockers of I_h can modulate respiratory rhythm *in vitro*, none of the I_h blockers affect respiratory neuron membrane

potential (Thoby-Brisson et al., 2000), which suggests that the contribution of I_h is not necessary to produce persistent bursting behaviour in these neurons.

Computational simulation studies (Butera et al., 1999) have proposed that fast activation of the persistent sodium current (I_{NaP}) could contribute to burst-generating pacemaker properties in preBötC neurons. The I_{NaP} is a voltage-dependent inward sodium (Na^+) current that is activated approximately 10 mV negative to the classic transient Na^+ current and was first described in cerebellar Purkinje cells as being capable of evoking prolonged plateau potentials (Llinas and Sugimori, 1980). I_{NaP} displays a characteristic voltage slope inward rectification that is blocked by tetrodotoxin (TTX) and may be carried by a subset of non-inactivating Na^+ channels (reviewed in Crill, 1996). Another current that contributes to plateau potentials, a common feature shared with the I_{NaP} in the ability to generate bursts, is the calcium-induced non-specific cationic current (I_{CAN}) (Rekling and Feldman, 1997a). I_{CAN} is an inward current that has poor selectivity for specific cations but excludes anions and is triggered by cytoplasmic calcium (Ca^{2+}) (reviewed in Partridge and Swandulla, 1988). Calcium-activated non-specific (CAN) channels are non-inactivating channels that can be further activated by either their own Ca^{2+} influx or Ca^{2+} influx derived from I_{CAN} -dependent and independent depolarizations (Tatsumi and Katayama, 1994; Partridge and Valenzuela, 1999). In rat and mouse models, whole-cell recording studies have demonstrated the presence of both the I_{NaP} (Thoby-Brisson and Ramirez, 2001; Del Negro et al., 2002; Del Negro et al., 2005) and the I_{CAN} (Del Negro et al., 2005) in preBötC respiratory neurons. Importantly, I_{NaP} and I_{CAN} blockade leads to silencing of the respiratory network (Peña et al., 2004; Del Negro et al., 2002; Del Negro et al., 2005). However, some of the pharmacological blockers used in those experiments, namely riluzole (RIL) and flufenamic acid (FFA), lack specificity. RIL and FFA have been found to lower neuronal excitability via inhibitory effects on voltage-gated sodium channels (Yau et al., 2010) and glutamatergic receptors (Doble, 1996; Wang et al., 2004; Lamanauskas and Nistri, 2008). Therefore, the loss of respiratory rhythmicity induced by RIL and FFA might have been due to an overall decrease of neuronal

excitability in the network. Moreover, specific injection of RIL in presence of FFA into the midline raphé obscurus nucleus can completely block respiratory drive activity *in vitro* (Pace et al., 2007a), indicating that those drugs can suppress respiratory rhythm via an indirect action outside the preBötC.

Finally, the NACLN protein that conducts a TTX and cesium (Cs^+) - resistant voltage-independent leak sodium current that contributes to the classical background Na^+ conductance (Hodgkin and Katz, 1949) has been recently identified by Lu and colleagues (Lu et al., 2007). Because genetic deletion of NACLN is fatal in the neonatal period due to abnormal breathing, it was proposed to be essential for respiratory rhythmogenesis (Lu et al., 2007). The NALCN channel is described as a four domain non-selective channel, constitutively active, expressed in mammalian neurons and responsible for setting resting membrane potential. Interestingly, the expression of NALCN with the conserved cytosolic UNC79 and UNC80 proteins (types of *unc* (uncoordinated) proteins, components of the synaptic active zone) enables the cell to sense changes in extracellular calcium ($[\text{Ca}^{2+}]_e$), where an increase in $[\text{Ca}^{2+}]_e$ inhibits I_{NALCN} but a reduction in $[\text{Ca}^{2+}]_e$ increases I_{NALCN} (Lu et al., 2010). This effect may play a role in determining the sensitivity of $[\text{Ca}^{2+}]_e$ on neuronal excitability and may explain, at least in part, why a small raise in $[\text{Ca}^{2+}]_e$ can inhibit spontaneous respiratory activity and *vice versa* (Ruangkittisakul et al., 2007; Panateiscu et al., 2009; reviewed in Ruangkittisakul et al, 2011).

Excitatory synaptic modulation through glutamatergic AMPA receptors has been shown to play a very important role in respiratory rhythmogenesis since pharmacological blockade of those receptors slows and eventually eliminates respiratory rhythm (Greer et al., 1991; Smith et al., 1991; Funk et al., 1993; Thoby-Brisson et al., 2000; Pace et al., 2008). Further, mutant mice lacking the vesicular glutamate transporter 2 gene die of respiratory failure (Wallen-Mackenzie et al., 2006). Subsequently, the idea that neurons with intrinsic pacemaker properties could be synchronized by excitatory AMPA receptor-mediated interactions emerged. Using the competitive blocker of AMPA receptors 6-cyano-7-nitroquinoxaline-2, 3-dione (CNQX), Koshiya and Smith tested this

pacemaker-network hypothesis in rat medullary slice by demonstrating that, in some inspiratory preBötC neurons, rhythmic calcium transients and voltage-dependent oscillatory bursts persist and are desynchronized in the absence of inspiratory network motor output (Koshiya and Smith, 1999). In the same study, the authors showed that the frequency of isolated pacemaker intrinsic inspiratory bursts depends on the level of excitation and can be regulated by extracellular potassium concentration (Koshiya and Smith, 1999). In the mouse model, two types of CNQX-resistant pacemaker neurons have been described: one being cadmium (Cd^{2+}) and FFA-sensitive, the other being Cd^{2+} -insensitive with Na^+ -dependent bursting properties (Thoby-Brisson and Ramirez, 2001; Peña et al., 2004), respectively similar to I_{CAN} and I_{NaP} of preBötC neurons characterized in the rat model (Del Negro et al., 2005).

Although several studies had identified and confirmed the importance of AMPA receptors for preBötC inspiratory rhythmogenesis, the signal transduction pathways involved had not been fully described. Two-photon imaging experiments and patch-clamp studies of inspiratory drive potentials on inspiratory preBötC neurons showed that conductances mediated by AMPA and glutamate metabotropic receptors activation can cooperatively trigger the release of intracellular calcium ($[\text{Ca}^{2+}]_i$) via inositol 1,4,5-trisphosphate (IP_3) signalling pathway, which in turn evokes somatic transient receptor potential (TRP) channels and I_{CAN} conductance (Pace et al., 2007; Mironov, 2008; Pace and Del Negro., 2008). Those experiments suggested an “emergent network properties model” for respiratory rhythmogenesis, where a synaptically-activated network (gated by glutamatergic receptors) can increase bursting conductance (such as I_{CAN}) by inducing an increase in $[\text{Ca}^{2+}]_i$. Subsequent to those studies, mathematical modelling studies underlined the possibility for the burst-generating I_{CAN} conductance and Na^+ accumulation to evoke different outward currents which can cause burst termination (Rubin et al., 2009). This series of experiments fed the more recent theory of the “group-pacemaker model” which is a hybrid of the pacemaker model and the synaptic network model (Del Negro et al., 2010).

In summary, whether the preBötC circuitry function arises from intrinsic properties of individual neurons or from their synaptic connections remains an unresolved question, although the latest theory postulates that both are important (reviewed in Feldman and Del Negro., 2006 and Del Negro and Hayes, 2008).

1.3.2.3 The Dbx1 mouse model

In an attempt to characterize preBötC respiratory neurons, a developmental approach has been adopted towards understanding what controls the acquisition of the cellular identity of respiratory preBötC neurons and how they develop into a dynamic, complex and highly organized network that produces inspiratory rhythmic drive. Genetic techniques in mouse models not only allow the tracing of neural progenitors (present at very early embryonic stages and crucial for the proper development of the CNS) to study their origin and migration to their final location, but also allow for the deletion of progenitors in order to determine their functional role. Progenitors expressing the homeodomain transcription factor Dbx1 have been characterized as determinant for spinal commissural interneurons that coordinate locomotion (Pierani et al., 2001; Lanuza et al., 2004). Recently, a subset of Dbx1-expressing progenitors in the hindbrain was found to migrate to the preBötC. Importantly, perinatal Dbx1 mutant mice do not generate rhythmic breathing movements, and preBötC Dbx1-expressing neurons have the electrophysiological characteristics of inspiratory neurons (Bouvier et al., 2010; Gray et al., 2010). Although several models with respiratory phenotypes (Phox2b mutants, Math1 mutation, Egr2 mutation) have been developed for studying the origin of brainstem respiratory neurons (Dubreuil et al., 2008, Onimaru et al., 2008; Rose et al., 2009; Thoby-Brisson et al., 2009), the Dbx1 model is so far the only model related directly to the origin of preBötC neurons in rodents (Bouvier et al., 2010; Gray et al., 2010).

1.3.2.4 *In vitro* rodent models

An important advancement in the field of respiratory control was the development of two *in vitro* experimental models: the medullary slice and the brainstem-spinal cord preparation. In 1984, Suzue developed an elegant *in vitro* experimental approach to study the neural control of breathing (Suzue, 1984). By isolating the brainstem and spinal cord of newborn rodents *in vitro*, and artificially perfusing this preparation with a modified Ringer's solution, it was possible to record spontaneously generated neural rhythmic activity that correlated with respiratory movements of the attached diaphragm and ribcage. Suzue demonstrated that it was also possible to modulate this respiratory rhythmic activity by including pharmacological agents to the perfusate (Suzue, 1984). The brainstem-spinal cord preparation (Fig. 1.3A), which is commonly used for studying respiratory neurobiology studies, provided the experimental grounds for subsequent studies by multiple laboratories leading to fundamental advances in our understanding of respiratory control. Since then respiratory neurobiology has been studied in a range of vertebrates including cats, goats, turtles, frogs and monkeys, but the rodent models remain the most used models for studying basic mechanisms of breathing.

In vitro isolation of the inspiratory generator (preBötC) led to the development of the rhythmic medullary slice preparation (Fig.1.3B). The advantage of this preparation is that it allows for experimental manipulations to study the role of pharmacological agents or external factors on inspiratory drive in conjunction with direct access to visualizing single-cells (interneurons, motoneurons or glial cells) for targeted whole-cell patch recordings. Although the slice preparation presents the advantage of recording cells embedded in their natural milieu, it should be noted that neurons located on the surface of the preparation (those most typically recorded) will have lost portions of their dendritic projections. This *in vitro* model, typically bathed in an artificial cerebrospinal fluid with an elevated potassium concentration, produces a very robust and long lasting endogenous fictive inspiratory rhythmic activity that can be recorded directly from the preBötC area or through its motor output at the level

of the hypoglossal nerves (Fig 1.3B). Structure-function studies of the preBötC included systematic studies of “calibrated” newborn rodent medullary slices (Ruangkittisakul et al., 2006; Ruangkittisakul et al., 2008). The latter study involved a serial restriction of excitatory inputs to further refine the functional boundaries necessary for obtaining a viable inspiratory rhythmic activity. The authors concluded that a transverse medullary slice as thin as 175µm was sufficient to generate inspiratory rhythmic activity.

Both *in vitro* models have additional caveats to consider. They are only viable in fetal and early postnatal periods (up to postnatal day P22 for mouse models slices (Ramirez et al., 1997; 1998), and P5 for rat models). This is due in part to the fact that diffusion of glucose and oxygen to the interstitial space between cells becomes more difficult as neuronal density augments with age. Another caveat is that the inspiratory bursts pattern generated in both *in vitro* models (rapid inspiratory onset, and rapid post-inspiratory decline) is clearly different from the one observed *in vivo* (augmenting inspiratory bursts followed by a slow post-inspiratory decline) (Bianchi et al., 1995). This difference is mainly attributed to the reduction of excitatory afferent inputs and the cooler ambient temperature used in *in vitro* preparations. Plus, differences in PO₂ and pH between *in vivo* and *in vitro* models have been reported (Okada et al., 1993; Mulkey et al., 2001; Dean et al., 2004). This can have implications on neuronal firing properties and synaptic activity (Brockhaus et al., 1993; Garcia et al., 2010; Hill et al., 2011). Despite those limitations, *in vitro* models remain a mainstay to address and manipulate central respiratory circuitry.

1.3.3 ADDITIONAL IMPORTANT NUCLEI OF THE ROSTRAL VRC

1.3.3.1 Expiratory related nuclei

The Bötzing Complex (BötC, Fig.1.2A) is located rostral to the preBötC and ventral to the compact division of the NA and contains glycinergic expiratory neurons (Tian et al., 1998; Tian et al., 1999; Schreihofer et al., 1999). Expiratory BötC neurons have been identified in both juvenile and adult animals, where some

behave as pre-inspiratory cells in extremely hypoxic conditions (Fortuna et al., 2008). Bötc also contains some cranial motoneurons and is believed to be an important source of synaptic inhibition for the nucleus of the tractus solitarius (Merrill et al., 1983; Fedorko and Merrill, 1984), other VRC inspiratory neurons (Fedorko and Merrill, 1984) and spinal cord phrenic motoneurons (Merrill and Fedorko, 1984).

The Retrotrapezoid Nucleus (RTN) is an assembly of neurons located ventral to the VII_n and appears to be a major site for central chemoreception (Mulkey et al., 2004). The RTN contains glutamatergic neurons that specifically express the transcription factor Phox2b. Although not indispensable for maintaining breathing and blood CO₂ homeostasis (Rammanantsoa et al., 2011), Phox2B expressing neurons in the RTN have an important role in regulation of breathing (Abbott et al., 2011), central chemosensory control (Marina et al., 2010), and have excitatory glutamatergic projections to the preBötC (Weston et al., 2004; Bochorishvili et al., 2012). Beside Phox2b-expressing neurons, glial cells in the RTN were also found to contribute to chemoreception in this region (Gourine et al., 2010).

The parafacial respiratory group (pFRG; Figs. 1.1 and 1.2A) is also located ventral to the VII_n and was functionally characterized as an area containing many neurons with rhythmogenic properties that spontaneously depolarize prior to the onset of inspiratory activity (referred to as pre-inspiratory cells by Onimaru and Homma, 1987). Initially hypothesized as an alternative site for respiratory rhythmogenesis (Onimaru et al., 1995; Onimaru and Homma, 2003), this view has been challenged by the findings that pFRG activity correlates with expiratory related motoneurons and muscle activity (Janczewski et al., 2002; Mellen et al., 2003). Thus, the pFRG may function as a generator of expiratory rhythmic activity and be coupled with preBötC inspiratory rhythm generator in order to regulate respiration in both juvenile and adult rats (Janczewski and Feldman, 2006). However, although RTN/pFRG expiratory neurons may be active in some conditions (Pagliardini et al., 2011), spontaneously active pre-inspiratory neurons remain to be identified in adult rats (Fortuna et al., 2008).

Although questions regarding how the pFRG and the preBötC interact and synchronize in the whole animal requires further investigation (Thoby-Brisson et al., 2012), *in vitro* transections of the *en bloc* preparation between the two nuclei have demonstrated that the two respiratory generators can oscillate independently (Janczewski et al., 2006; Onimaru et al., 2006; Thoby-Brisson., 2009). In addition, their respective developmental onsets do not coincide with each other (Pagliardini et al., 2003; Onimaru and Homma, 2005; Thoby-Brisson et al., 2009), and the development of one does not seem to be essential for the development of the other (Thoby-Brisson et al., 2009; reviewed in Fortin and Thoby-Brisson, 2009 and Champagnat et al., 2011). Thus, there is a general consensus for considering the pFRG and the preBötC as two distinct central respiratory rhythmogenic entities.

1.3.3.2 Modulatory and putative chemosensitive sites

The dorsolateral side of the medullary slice contains the rostral part of the nucleus tractus solitarius (NTS). The NTS is part of the dorsal respiratory group (DRG) of neurons that are not essential for respiratory rhythmogenesis but capable of modulating respiratory rhythm (reviewed in Alheid and McCrimmon, 2008). The NTS is a relay for many primary afferents with cardiorespiratory function (Lopes and Palmer, 1976) and other visceral sensory receptors such as pulmonary stretch receptors (Berger and Dick, 1987; Bonham et al., 1993; reviewed in Kubin et al., 2006). Some NTS neurons fire action potentials in phase with inspiratory related motor output (Champagnat et al., 1983) and their activity has been associated with feedback information processing (reviewed in Bianchi et al., 1995, Feldman et al., 2003 and Kubin et al., 2006) along with relaying information arising from the carotid bodies involved in peripheral chemoreception (reviewed in Nattie, 1999).

Raphé nuclei are the main source of endogenous serotonin (5-hydroxytryptamine, 5HT) in the brain. Raphé nuclei are typically divided into: rostral (or superior) and caudal (or inferior) raphé nuclei groups. The rostral group of raphé nuclei is located in the mesencephalon and rostral pons, which is outside

the scope of the thesis work and thus will not be reviewed here. The caudal group of raphé nuclei (MR; Fig. 1.1 and 1.4) is an assembly of neurons clustered around the midline and extend from the caudal pons to the caudal portion of the medulla oblongata. The MR includes the raphé magnus nucleus, raphé obscurus nucleus and the raphé pallidus nucleus.

MR nuclei are part of the pain descending pathway (involved in opioid induced analgesia) via their spinal projections to pain sensing regions (Mayer and Price, 1976; reviewed in Basbaum and Fields, 1984). Although MR neurons have been shown to express abundant μ -opioid receptors (Ding et al., 1996), raphé nuclei physiology appears to be very complex because they contain cells that can be inhibited (Deakin et al., 1977; Fields and Anderson, 1978; Duggan and North, 1983; Chiang and Pan, 1985) and/or excited (Basbaum et al., 1976; Anderson, Basbaum and Fields, 1977) by opioids. These neurons are classified as ON and OFF cells of the raphé (reviewed in Mason, 2001). MR nuclei are thought to influence respiratory activity because they project extensively to respiratory-related nuclei, including the NTS (reviewed in Thor and Helke, 1987), phrenic and hypoglossal motoneurons (Holtman et al, 1984; Henry and Manaker, 1998) and the preBötC (Ptak et al., 2009). Hypoplasia and under development of MR have been associated with sudden unexplained death syndrome (SIDS) and sudden intrauterine death (SIUD) in humans (Lavezzi et al., 2009).

MR 5HT neurons are postulated to be intrinsically chemosensitive *in vitro* (reviewed in Corcoran et al., 2009) based on the fact that they increase their firing rate in response to increasing CO₂ (Richerson, 1995) even after synaptic isolation in rat and mouse brains slices (Bradley et al., 2002), and they can respond to pH changes in culture (Wang et al., 1998). The “state-dependent central chemoreception” hypothesis postulates that, while RTN chemoreceptors would be relatively important during wakefulness, the implication of chemosensitive raphé neurons would be more prominent in sleep state (Nattie and Li, 2001; Nattie 2001; Buchanan and Richerson, 2010).

1.3.3.3 Pattern forming respiratory motoneurons pools

Neurons in the nucleus ambiguus (NA) contribute to glossopharyngeal, vagal and accessory innervation (Bieger and Hopkins, 1987) and have direct projections to hypoglossal inspiratory motor nucleus (Rekling and Feldman, 1997b). The NA is also a critical site for cardiorespiratory efferents due to its large number of preganglionic cardiac vagal neurons (Gunn et al., 1968; Stuesse, 1982; reviewed in Salo et al., 2006).

Rostral hypoglossal nerves are used to record inspiratory related activity in the medullary slice preparation. Hypoglossal motoneurons (XII MNs) are located on either side of the midline, ventral to the fourth ventricle, and represent a heterogeneous population of motoneurons comprised of non-respiratory and respiratory-related cells. In rats, respiratory XII MNs of the dorsal subdivision of the XII nucleus innervate styloglossus and hyoglossus retrusor tongue muscles, important for upper airways patency and coordination of upper airway muscles with respiratory movements. XII MNs located in the ventral division of the hypoglossal nucleus innervate the genioglossus muscles, major tongue protruders and upper airways dilators (McClung and Goldberg, 1999; McClung and Goldberg, 2000). Synaptic tracing experiments helped to locate XII inputs. XII MNs receive inputs from preMNs localized dorsal to the NA (Peever et al., 2002; Dobbins and Feldman., 1995) and also from dorsolateral respiratory group preMNs (Ezure and Tanaka, 2006). More recently, calcium imaging experiments in medullary slice preparations confirmed that inspiratory XII MNs received inputs from a cluster of ipsilateral inspiratory preMNs that have their soma located just dorsal to the NAsc and the lateral paragigantocellular reticular nucleus (Koizumi et al., 2008).

1.4 PHARMACOLOGY OF NEURAL CONTROL OF BREATHING: KEY NEUROMODULATORS OF CENTRAL RESPIRATORY DRIVE

1.4.1 PEPTIDES

1.4.1.1 Opioids and respiratory depression

Opioid receptors and function

Opioids have been used for centuries to treat pain and remain the principal pharmacological agents used for acute and chronic pain management today. Opioids exert their analgesic effect by targeting membrane receptors located on neurons that are sensitive to noxious stimuli and lowering their excitation threshold and/or inhibiting their neurotransmission (reviewed in Hill, 1994; Yaksh, 1997). The receptors for opioids have been classified into three subtypes: mu (μ), kappa (κ) and delta (δ) opioid receptors (reviewed in Knapp et al., 1995). This nomenclature is based on pharmacological studies that demonstrated the selective binding of *morphine* to μ -opioid receptors (MOR) and *ketocyclazocine* to κ -opioid receptors (KOR) (Lord et al., 1977), while δ -opioid receptors (DOR) were first characterized in *vas deferens* mouse tissue (Lord et al., 1977; reviewed in Pasternak, 1993). Opioid receptors can also bind endogenous ligands that include endorphins (Waterfield et al., 1977), enkephalins (Hughes et al., 1975) and dynorphins (Chavkin et al., 1982), which preferentially bind MOR, DOR/MOR and KOR respectively and have all been reported to participate in endogenous pain relief mechanisms (reviewed in Jacob and Ramabadran, 1981; Yatsh, 1997). However the ubiquitous distribution of opioid receptors in and outside the central nervous system (Atweh and Kuhar, 1977; Tempel and Zukin, 1987; Giolli et al., 1990; Mansour et al., 1994; Arvidsson et al., 1995; Ding et al., 1996; Bagnol et al., 1997; Stein and Lang, 2009) also suggested a broader action for opioids and helped clarify the basis for the side effects associated with the

administration of opioid drugs, including respiratory depression (Duthie and Nimmo, 1987; De Schepper et al., 2004; reviewed in Benyamin et al., 2008).

Opioid receptors are part of the large family of G-protein-coupled receptors, characterized by a seven trans-membrane domain structure, an extracellular N-terminal region, and an intracellular C-terminal region (reviewed in Knapp et al., 1995; Fig. 1.5). Their exact atomic structure is only starting to be determined (Manglik et al., 2012; Wu et al., 2012) and has revealed the association of μ -opioid receptors in linked pairs (as seen in Fig. 1.5; Manglik et al., 2012). Opioid receptor activation produces predominantly inhibitory responses mediated by an increase in postsynaptic K^+ channel conductances and/or a decrease in presynaptic voltage-gated Ca^{2+} channels via the activation of G proteins (reviewed in Grudt and Williams, 1995). After its activation, the opioid receptor phosphorylates and couples with arrestins to be internalized (reviewed in Ferguson, 2001).

Genetic manipulations including MOR knockout mouse models and G_i -proteins antisense oligonucleotides have suggested that opioids exert their analgesic effects primarily through the MOR/ $G_{i\alpha}$ -protein signalling (Raffa et al., 1994; Matthes et al., 1997). Cloning analysis of the MOR gene have led to the identification of an increasing number of mRNA splice variants, promoters and RNA transcripts in the human, rat and mouse species (Thompson et al., 1993; Wang et al., 1993; Pan et al., 1999; Pan et al., 2000; Pan et al., 2001; Pasternak, 2004; Pan et al., 2005; Xu et al., 2011). This indicates that MOR can be expressed in many different forms that may be coupled to distinct G-proteins and therefore act distinctively on their host cells. Thus, binding of any opioid ligand onto its receptor can induce diverse intracellular cascades and physiological responses (Ling et al., 1985; Zhang and Pasternak, 1981; Borgland et al., 2003).

Opioids and neural control of breathing

Opioid receptor expression has been reported in the medulla (Atweh and Kuhar, 1977), in structures associated with cardiorespiratory function such as the nucleus ambiguus (Irnaten et al., 2003), the NTS (Aicher et al., 2000), and the preBötC (Gray et al., 1999). Some neurons located in the brainstem produce and

secrete endogenous enkephalins (Elde et al., 1976; Simantov et al., 1977; Stornetta et al., 2001; Guyenet et al., 2002), including bulbospinal cells of the ventrolateral medulla (Guyenet et al., 2002; Stornetta et al., 2003) that can be strongly barosensitive (Stornetta et al., 2001). Enkephalins can inhibit pontine and medullary respiratory neurons activity *in vivo* by decreasing the efficacy of glutamate synaptic neurotransmission (Denavit-Saubie et al., 1978; Morin-Surun et al., 1984a).

Respiratory activity in neonatal and adult animals *in vivo* is markedly perturbed by opioids, specifically by δ - and μ -opioid receptor agonists (Ward and Holaday, 1983; Morin-Surun et al., 1984b; Lalley, 2003; reviewed in Pattinson, 2008). Systemic delivery of opioids depresses respiratory frequency and tidal volume in *in vivo* adult rats (Morin-Surun et al., 1984b; Pazos and Florez, 1984; Manzke et al., 2003) and those effects are thought to be mediated by functional DOR and MOR found on respiratory neurons (Morin-Surun et al., 1984a). Bilateral microinjections of a MOR agonist into the adult rat preBötC induces severe respiratory depression in freely moving rats, and can cause apnea in anaesthetized rats (Montandon et al., 2011).

Experiments in *in vitro* preparations of neonatal rodents determined that the decrease of respiratory rhythm was caused by MOR activation (Greer et al., 1995; Ballanyi et al., 1997; Takita et al., 1997; Ballanyi et al., 2009). Whole-cell recordings of respiratory neurons in medullary slice and *en bloc* preparation have shown that the membrane potential of some inspiratory neurons are hyperpolarized by the MOR agonist D-Ala², NMe-Phe⁴, Gly-ol⁵-enkephalin (DAMGO), with a decreased input resistance and a reversal potential between -85 and -70 mV [close to the equilibrium potential of potassium (Nernst $E_K \sim -90$ mV)], consistent with a direct postsynaptic increase in K^+ conductance (Gray et al., 1999; Takeda et al., 2003). Specifically NK1R-expressing inspiratory preBötC neurons are particularly sensitive to MOR agonists (Gray et al., 1999; Montandon et al., 2011). Interestingly, not all respiratory neurons respond to opioids. Indeed, pre-inspiratory pFRG neurons and expiratory neurons appear to be resistant to μ -opioid receptors agonists (Takeda et al., 2001; Janczewski et al., 2002; Mellen et

al., 2003; Onimaru et al., 2006), even at embryonic stages (Fortin and Thoby-Brisson, 2009). The selective inhibition of preBötC neurons by DAMGO was shown to produce a “quantal slowing” of inspiratory burst frequency (in reference to missing inspiratory bursts rather than mere decrease in frequency; Mellen et al., 2003), suggesting that DAMGO could uncouple the two respiratory oscillators (pFRG and preBötC). Quantal slowing has also been reproduced *in vivo* by the μ -opioid agonist fentanyl, in juvenile vagotomized and anesthetized rats (Janczewski and Feldman, 2006). Other investigators propose that preBötC neurons do not express μ -opioid receptors postsynaptically and that the respiratory depression is due solely to presynaptic effects of MOR activation (Krause et al., 2009; Ballanyi et al., 2010). One goal of the present thesis research is to determine whether MOR agonists have a pre- or post-synaptic effect on preBötC respiratory neuron and to confirm MOR expression in the preBötC.

The widely used μ -opioid receptor antagonist naloxone can antagonize the inhibition of respiratory rhythm induced by opioids both *in vivo* and *in vitro*. But it has limitations to its therapeutic use since it antagonizes both respiratory depression and analgesic effect and its duration of action is relatively short (McGillard and Takemori, 1978).

1.4.1.2 Substance P and somatostatin role in respiratory control

Substance P (SP) has a very potent excitatory effect on the respiratory network (Suzue, 1984), including the preBötC and inspiratory-related motoneurons such as phrenic motoneurons (Gray et al., 1999; Ptak et al., 2000a; Pagliardini et al., 2005). Endogenous SP is believed to be released by raphé nuclei, the NTS and the parapyramidal region (Holtman and Speck., 1994; Ptak et al., 2009). When SP is perfused with the bathing medium in *in vitro* preparations, it induces a large increase in inspiratory burst frequency, a slow depolarization of membrane potential in preBötC respiratory neurons (Pagliardini et al., 2005) and a voltage-insensitive inward current with increase in input resistance (Hayes and Del Negro, 2007). SP binds to three types of G-protein coupled receptors namely neurokinin (NK) 1, NK2 and NK3 receptors. Although NK1 receptors (NK1R)

are known to be essential for SP effect on respiratory network (Monteau et al., 1996; Ptak et al., 2000b), recent work has shown that NK1R non-expressing neurons could also undergo large membrane depolarization upon SP bath application (Hayes and Del Negro, 2007). As discussed in that study, this suggests that SP-evoked electrical and neuronal changes in NK1R expressing neurons can diffuse to surrounding NK1R non-expressing cells, probably via gap junctions.

The mechanisms underlying SP potent excitatory effects on respiratory rhythm have also been investigated in medullary slice preparations. In XII MNs, SP was found to inhibit the two-pore domain TWIK-related acid sensitive potassium channel (TASK) (Talley et al., 2000; Adachi et al., 2010). Two-pore domain channels conduct background K^+ currents that help maintain the membrane potential to negative resting values and counterbalance depolarization (Duprat et al., 1997; reviewed in Enyedi and Czirjak., 2010). By inhibiting TASK channels and therefore regulating the cellular excitability, SP can promote depolarization of XII MNs. In addition to the suppression of K^+ leak current, SP can modulate the Na^+ leak current I_{NALCN} (Lu et al., 2009), discussed earlier on this Chapter. SP modulates I_{NALCN} via a G-protein-independent mechanism and requires the expression of UNC79 and UNC80 proteins to exert this effect (Lu et al., 2009). Interestingly, SP has been reported to increase Na^+ leak conductance in preBötC neurons (Peña and Ramirez, 2004; Ptak et al., 2009). Finally, a study on the excitatory effect of SP on preBötC neurons demonstrated that SP can activate transient receptor protein canonical (TRPC) channels, leading to enhanced I_{CAN} conductance (Ben-Mabrouk and Tryba, 2010). The effect is likely mediated by TRPC3 and TRPC7 channels expressed in the VRC (Ben-Mabrouk and Tryba, 2010).

In contrast to SP, somatostatin (STT) has an inhibitory effect on respiratory rhythm (Suzue et al., 1984; Chen et al., 1990; Chen et al., 1991). Although exogenous bath application of STT has been shown to induce '*quantal slowing*' of respiratory drive frequency in rodent brainstem-spinal cord preparation at extremely low concentrations ($1 \cdot 10^{-13}$ to $1 \cdot 10^{-12}$ mol.L⁻¹) (Gray et al., 2010), endogenous release of STT in the preBötC has only been reported in

rabbit (Pantaleo et al., 2011). Endogenous STT has been suggested in the rat NTS (Kalia et al., 1984), where STT was shown to decrease neuronal excitability and increase the muscarinic non-inactivating potassium current (I_M) (Jacquin et al., 1988). Specific silencing of STT-producing cells in the preBötC can induce persistent apnea in adult awake rats (Tan et al., 2008) and STT/NK1R/STR2a expressing preBötC neurons are derived from Dbx1 expressing neurons (Gray et al., 2010). Somatostatin receptors are G-protein-coupled receptors of which five types have been cloned (SSTR1-5) (reviewed in Patel, 1999). Despite the common belief that STT receptors desensitize quickly (due to their very high sensitivity to agonists) their exact mechanism of action upon STT binding is still unclear. The mechanism that transduces the inhibition of preBötC neurons by STT remains to be established.

1.4.2 GLUTAMATERGIC IONOTROPIC RECEPTORS

1.4.2.1 AMPA receptors

AMPA receptors structure and gating properties

AMPA receptors mediate fast excitatory synaptic transmission in the central nervous system. Native AMPA receptors are tetrameric membrane proteins composed of two dimers (reviewed in Gouaux, 2004). Each dimer can have a homomeric (same subunits) or heteromeric (two distinct subunits) structure, and is capable of binding one agonist molecule. So far, four different subunits have been cloned, commonly named GluR1, GluR2, GluR3 and GluR4 (Hollman and Heineman, 1994; Sobolevsky et al., 2009), also known as GluA1-4 under the latest nomenclature revised by the International Union of Basic and Clinical Pharmacology committee (IUPHAR; Collingridge et al., 2009). Each subunit can have their mRNA alternatively spliced to give either a “flip” or “flop” isoform (Sommer et al., 1990). Under physiological conditions AMPA receptors are ion channels that are permeable to sodium, calcium and potassium ions. More specifically, AMPA receptors containing GluR2 subunits display linear current-

voltage (I/V) plot and low calcium permeability. AMPA receptors lacking the GluR2 subunit are however highly permeable to calcium and display an inwardly rectifying I/V plot (Keller et al., 1993; Wollmuth and Sakmann 1998; Figs.1.6A and B).

One important characteristic of the AMPA receptors is their high affinity for the neurotransmitter glutamate and their capacity to display a very fast deactivation (channel closure upon removal of agonist molecule) and desensitization (channel closure upon continuous exposure to the agonist) (Jonas and Spruston., 1994; Raman and Trussell, 1995). Structure-function studies have demonstrated that desensitization is mediated by movements between the receptor dimers (Du et al., 2005; Sun et al., 2002; Gonzalez et al., 2010).

Positive allosteric modulators of AMPA receptors are molecules that bind to specific sites of AMPA receptors (distinct from the agonist binding site) and, upon binding of the agonist, modulate desensitization and/or deactivation rate of the receptor with differential subunit affinity. Because AMPA receptor subunits are differently distributed throughout the brain, allosteric modulators of AMPA receptors have distinct regional effects. Aniracetam was one of the first allosteric modulators characterized (Ito et al., 1990). Ampakines family of compounds is derivative of aniracetam and is classified in two main groups: high-impact and low-impact ampakines (reviewed in Lynch and Gall, 2006).

“High-impact” ampakines (e.g. CX546, CX614) were the first group developed by Cortex Pharmaceuticals (Irvine, CA) and have common binding site with the benzothiadiazide cyclothiazide (Arai et al., 2000; reviewed in Traynelis et al., 2010; see Fig. 6A), which is a very well characterized AMPA receptor modulator that slows the desensitization of AMPA receptors (Arai et al., 2000). Some high-impact ampakines also have the interesting property of activating the expression of additional genes, such as brain neurotrophic factor gene (BDNF; Lauterborn et al., 2000; Ogier et al., 2007; Simmons et al., 2009; Lauterborn et al., 2009). Electrophysiological studies have shown that the high-impact ampakine CX546 binds to non-desensitized AMPA receptors and decreases their desensitization rate by increasing the agonist affinity (Nagarajan et al., 2001).

Aniracetam and CX614 however slow the receptor deactivation rate by stabilizing the receptor dimer in its closed conformation (Jin et al., 2005; see Fig. 1.7 for mechanism details).

“Low-impact” ampakines have been developed more recently and have distinct binding sites, different from one another (CX717, CX1763, CX1739 and others). Although their exact chemical structures have not yet been released by Cortex Pharmaceuticals Inc., it is known that low-impact ampakines do not share common binding sites with cyclothiazide, and that they were designed to be less potent and thus safer than their counterparts. The exact mechanism of action of those newer compounds remains to be determined through molecular and pharmacological analysis.

Pharmacology of AMPA receptors and application in respiratory control

AMPA synaptic transmission is a key component in respiratory control (Greer et al., 1991; Funk et al., 1993). Bath and local applications of the AMPA receptor antagonist 6-Cyano-7-nitroquinoxaline-2, 3-dione (CNQX) in the preBötC region of *in vitro* rat preparations reversibly abolish respiratory rhythm (Greer et al., 1991; Funk et al., 1993), suggesting the presence of endogenous release of glutamate in this region of the VRC and the importance of AMPA receptors activation for respiratory rhythm generation. RT-PCR analysis of preBötC neurons has shown that GluR2 subunits are present in preBötC neurons (Paarman et al., 2000) and whole-cell recordings of inspiratory preBötC neurons confirmed that functional AMPA receptors were mainly Ca²⁺ impermeable (Pace et al., 2007b; Pace and Del Negro, 2008).

Deactivation and desensitization of AMPA receptors (see Fig. 1.7) are two characteristics that allow for a very precise, quick and efficient glutamatergic synaptic transmission which can readily tune synaptic plasticity within a neuronal network. Because allosteric modulators of AMPA receptors have the ability to modulate those very same characteristics (deactivation and/or desensitization), they have been considered as potential therapeutic drugs to increase excitatory efficacy within the respiratory neuronal network. Cyclothiazide was shown to increase inspiratory network motor output and inspiratory-related currents on XII

MNs (Funk et al., 1995). Unlike cyclothiazide, ampakines readily cross the blood brain barrier, which gives them their potential therapeutic significance. The high-impact ampakine CX546 is able to counteract respiratory depression induced by opioids *in vitro*, and was also shown to reverse respiratory depression in *in vivo* (Ren et al., 2007). A study on Rett-syndrome model showed that CX546 could significantly improve respiratory function by inducing expression of endogenous BDNF levels (Ogier et al., 2007). Also, the low-impact ampakine CX717 was shown to protect against breathing depression induced by opioids in rodents (Ren et al., 2009) and humans (Oertel et al., 2010).

1.4.2.2 NMDA receptors

NMDA receptors structure and gating properties

N-Methyl-D-aspartic acid (NMDA) receptors are hetero-tetrameric membrane proteins that mediate synaptic plasticity in the central nervous system (reviewed in Collingridge and Singer, 1990; Malenka and Nicoll, 1993). Unlike AMPA receptors, NMDA receptors are activated by both glycine and glutamate which implies 2 different agonist recognition sites on the same receptor (Johnson and Ascher, 1987; Benveniste and Mayer, 1991). To date, three subunits have been cloned: the glycine-binding NR1 subunit, the glutamate binding NR2 subunit and the glycine-binding NR3 subunit (also known as GluN1-3, under IUPHAR nomenclature; Collindridge et al., 2009). Each subunit has the same structure: an amino terminus composed of a large extracellular amino-terminal domain and a ligand-binding domain (S1-S2), a transmembrane region (M1, M3 and M4) with a re-entrant membrane loop (M2), and a cytoplasmic carboxyl terminus. The transmembrane region is considered as the functional hallmark of the receptor as it determines the ion channel formation as well as the receptor subunit assembly (crucial for protein expression at the membrane) (Furukawa et al., 2005). NMDA receptors are commonly known as hetero-tetramers composed of the assembly of two dimers; each dimer containing one NR1 subunit together with NR1, NR2 or NR3 subunit. The NR1 subunit must be present in one dimer before assembly

with another dimer can occur; its presence is therefore a prerequisite for the receptor to be translated into a functional protein (Moriyoshi et al., 1991; Meguro et al., 1992; Ishii et al., 1993; Perez-Otaño et al., 2001; Schuler et al., 2008). NMDA receptors may also be expressed as triheterodimers (Chazot et al., 1994; Hatton and Paoletti, 2005), and although there has been much emphasis on NR2 subunits-containing triheterodimers (Chazot and Stephenson, 1997; Brickley et al., 2003) NR3-containing triheterodimers have recently been reported in native neurons (Pilli and Kumar, 2012).

Because conventional NMDA receptors require the release of Mg^{2+} block via depolarization or clearance of extracellular Mg^{2+} and bind both glycine and glutamate neurotransmitter (Verdoorn et al., 1987; Kleckner and Dingledine, 1988), NMDA receptors are considered as activity-dependent molecular “coincidence detectors” (Edwards et al., 1998; see Fig. 1.6C). They transduce environmental chemical signals (glutamate, glycine and $[Mg^{2+}]_e$) into an ionic current highly permeable for calcium that is triggered by the activation of the ionic channel (reviewed in MacDonald and Nowak, 1990; Sakurada et al., 1993; Edwards et al., 1998). The NR1 and NR3 subunits may also form a functional excitatory receptor that binds glycine but is not sensitive to NMDA or glutamate (Ciabarra et al., 1995; Das et al., 1998; Chatterton et al., 2002; Matsuda et al., 2002; Piña-Crespo et al., 2010), and whose function do not depend on $[Mg^{2+}]_e$ and membrane potential (Chatterton et al., 2002; Sasaki et al., 2002). Functional NR1/NR3 receptors have been found in primary mammalian cultured cells but questions remain as to how are they expressed in native cells. Interestingly the co-expression of a NR2 subunit with NR1 and NR3 not only obliterate any sensitivity to glycine alone, but the presence of NR3 negatively influences the conventional NR1/NR2 receptor response to NMDA or glutamate (Das et al., 1998; Chatterton et al., 2002).

Pharmacology of NMDA receptors and its application in respiratory control

Single-cell RT-PCR analysis of newborn rat respiratory preBötC neurons revealed a very heterogenous distribution of NMDA receptor subunits: NMDA

receptors of preBötC neurons are composed of all three NMDA subunits: NR1, NR2 and NR3 (Paarman et al., 2005). That particular study, despite the lack of physiological analysis, indicated a heterogeneous expression of NMDA receptors composition in respiratory preBötC neurons, with the particularity that all preBötC respiratory neurons tested contained the NR3A subunit subtype (Paarman et al., 2005). Furthermore, immunohistochemical studies of respiratory nuclei in the VRC in postnatal rats demonstrated dynamic changes in NMDA receptor subunit expression level throughout the development, (Liu and Wong-Riley, 2010b). In particular, the subunit NR2D expression level dramatically declines with age, as opposed to the subunit NR3B expression level which increases during postnatal development (Liu and Wong-Riley, 2010b). NMDA receptors were found to be capable of mediating respiratory drive in the preBötC even in the absence of AMPA receptors function (Morgado-Valle and Feldman, 2010). However, unlike the AMPA receptor antagonist CNQX, *in vitro* bath application of the NMDA receptor blocker APV only attenuates inspiratory drive potentials of preBötC neurons, without affecting XII burst frequency (Pace et al., 2007b). NMDAR1 mutant mice were used to evaluate the contribution of NMDA receptors functions into central inspiratory drive using *in vitro* neonatal preparations (Funk et al., 1997). It was suggested that NMDA receptors were dispensable for the development of spontaneous inspiratory drive generation even if exogenous NMDA could strongly increase respiratory rhythm (Greer et al., 1991; Funk et al., 1993).

1.4.2.3 Kainate receptors

Kainate receptors represent the third class of glutamatergic ionotropic receptors. GluR5-GluR7 and KA1-2 subunits have been cloned (also known as GluK1-5, under IUPHAR nomenclature; Collindridge et al., 2009). While AMPA and NMDA receptors have been extensively characterized, much less is known about kainate receptors despite their evident role in modulating synaptic transmission and plasticity in the brain (Wisden and Seeburg, 1993; Cossart et al.,

1998; Bortolotto et al., 1999; Sallert et al., 2007). Also, we know that kainate receptors are expressed in respiratory nuclei of the ventrolateral medulla (Robinson and Ellenberger, 1997; Garcia Del Cano et al., 1999; Paarman et al., 2000) but the involvement of kainate receptors in respiratory control has been poorly investigated (Ireland et al., 2008).

1.4.3 SEROTONIN MODULATION OF RESPIRATORY DRIVE

Endogenous release of serotonin (5HT) was originally described as a blood-borne “serum” factor that affected blood vessel “tonus” (reviewed in Jacobs and Azmitia, 1992). 5HT neurons of the brainstem project to several nuclei of the VRC (Al-Zubaidy et al., 1996; Onimaru et al., 1998; Peña and Ramirez, 2002; Manzke et al., 2003; Ptak et al., 2009). However, depending on the receptor subtype on which it binds to, 5HT can have inhibitory or excitatory effects on its target. In fact, while 5HT_{1a} agonists can cause respiratory depression (via the decrease of cyclic AMP), 5HT_{4a} and 5HT₂ a, b and c receptor agonists increase respiratory rhythm (via an increase of cAMP or phospholipase C signalling, respectively) (Manzke et al, 2003; reviewed in Richter et al., 2003).

In addition to a modulatory effect of 5HT on respiratory neurons, several studies suggest that 5HT may also be important for the proper development of respiratory control centers (Hodges et al., 2009) and central chemoreflexes (Ray et al., 2011). Some mouse pups lacking 5HT neurons have severe apnea (Hodges et al., 2009), and specific silencing of 5HT neurons in the brainstem of mice severely disrupts chemosensitive and thermoregulatory reflexes (Ray et al., 2011). Also, endogenous release of 5HT by raphe neurons terminals onto preBötC neurons was proposed to be part of a feedback excitatory loop between the raphe and the preBötC in rat medullary slice preparation (Ptak et al., 2009). 5HT has been shown to increase pacemaker related conductances such as NALCN-like current (Ptak et al., 2009) or persistent and transient Na⁺ currents (Peña and Ramirez, 2002) in respiratory preBötC neurons. It was proposed from *in vitro* experiments that 5HT acting through 5HT₂ receptors is critical for the generation of fictive

eupnea (Peña and Ramirez, 2002) and gasping (Tryba et al., 2006). However, experiments using an *in situ* preparation and the application of specific pharmacological serotonin receptor antagonists demonstrated that 5HT₁ and 5HT₂ receptors are not essential for eupnea or gasping (Toppin et al., 2007). In addition, experiments using genetically engineered mice that lack the majority of 5-HT producing neurons generated eupneic breathing and gasping (Hodges et al., 2008; St-John et al., 2009).

Recently, developmental studies in rat demonstrated that 5HT receptors subunits 5HT₁ and 5HT₂ undergo a significant and abrupt decrease in expression level in all major respiratory nuclei of the VRC with postnatal development (Liu and Wong-Riley, 2010a), suggesting that the influence of serotonergic transmission has on respiratory control is developmentally regulated. That study emphasized the important modulatory and trophic role of serotonin during development, which has been reported in other parts of the brain (reviewed in Lauder, 1990; Jacobs and Azmitia, 1992; Whitaker-Azmitia et al., 1996; Hodges and Richerson, 2008).

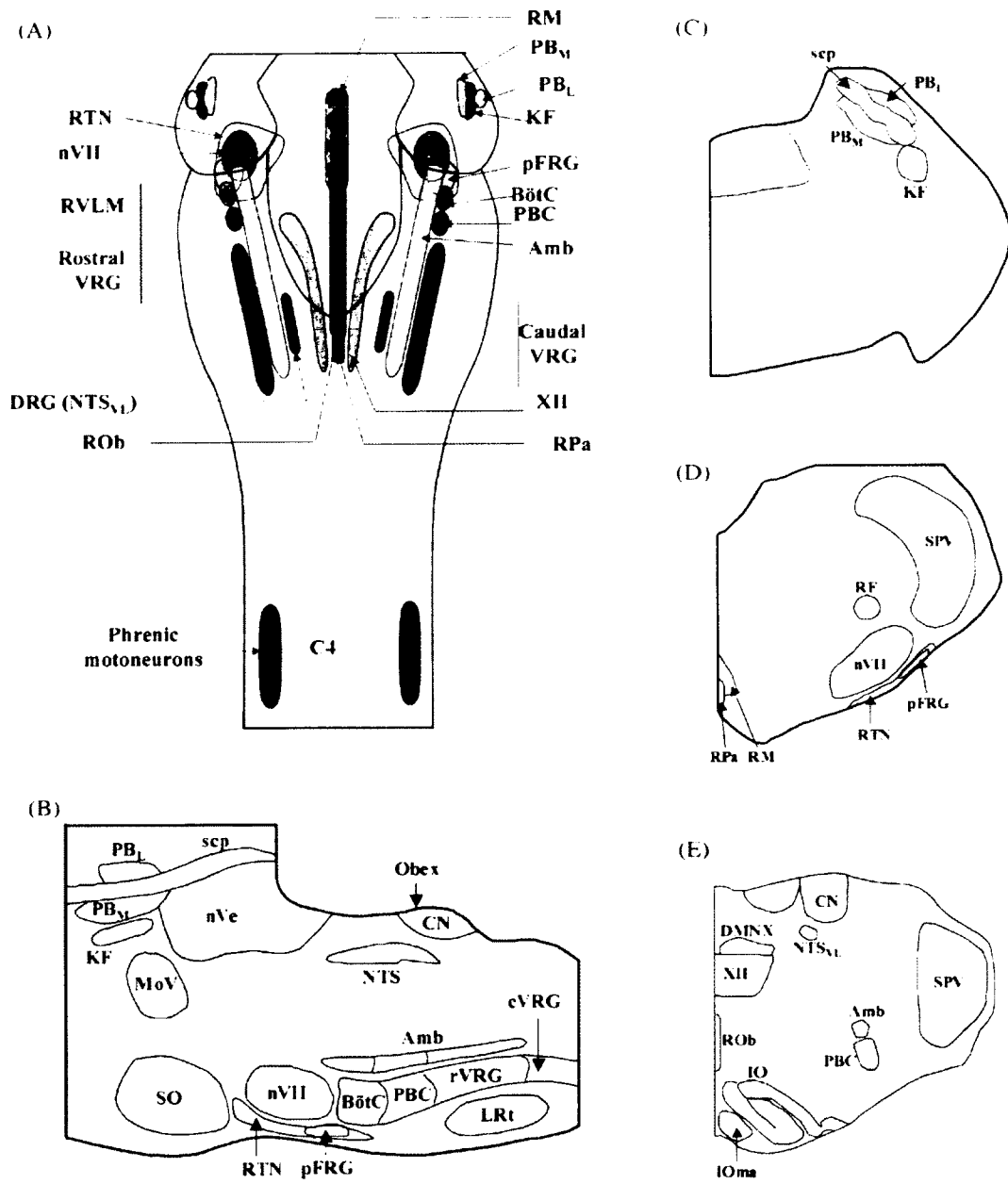


Figure 1.1 Schematic representations of respiratory related regions in the rodent brainstem.

Previous Page

Figure 1.1 Schematic representations of respiratory related regions in the rodent brainstem.

The boundaries delineating the different compartments reflect functional nuclei or areas defined to date. (A) Schematic longitudinal representation of brain stem nuclei that are associated with respiratory control. Amb, nucleus ambiguus; BötC, Bötzinger complex; DRG, dorsal respiratory group; KF, Kölliker-Fuse nucleus; NTS, nucleus tractus solitarius; RM, raphé magnus; PBC, preBötzinger complex; PBL, lateral parabrachial nucleus; PBM, medial parabrachial nucleus; pFRG, parafacial respiratory group; RM, raphé magnus; ROb, raphé obscurus; RPa, raphé pallidus; RVLM, rostroventrolateral medulla; VRG, ventral respiratory group; XII, hypoglossal nucleus. For landmark reference: C4, cervical 4 level; nVII, facial nucleus. (B) Schematic parasagittal representation of brain stem respiratory nuclei. LRt, lateral reticular nucleus; RTN, retrotrapezoid nucleus. For landmark reference: CN, cuneate nucleus; MoV, motor nucleus of trigeminal nerve; nVe, vestibular nuclei; SO, superior olivary nucleus. (C)-(E) Schematic representation of coronal sections of the rat brain stem at pontine (C), rostral medullary (D), and caudal medullary (E) levels. DMNX, dorsal motor nucleus of the vagus nerve; IO, inferior olivary nucleus; IOma, medial accessory olivary nucleus. For landmark reference: RF, retrofacial nucleus; scp, superior cerebellar peduncle; SPV, spinal nucleus of trigeminal nerve.

Figure 1 from Wong-Riley and Liu (2005) *Resp. Physiol. Neurobiol.* 149(1-3): 83-98.

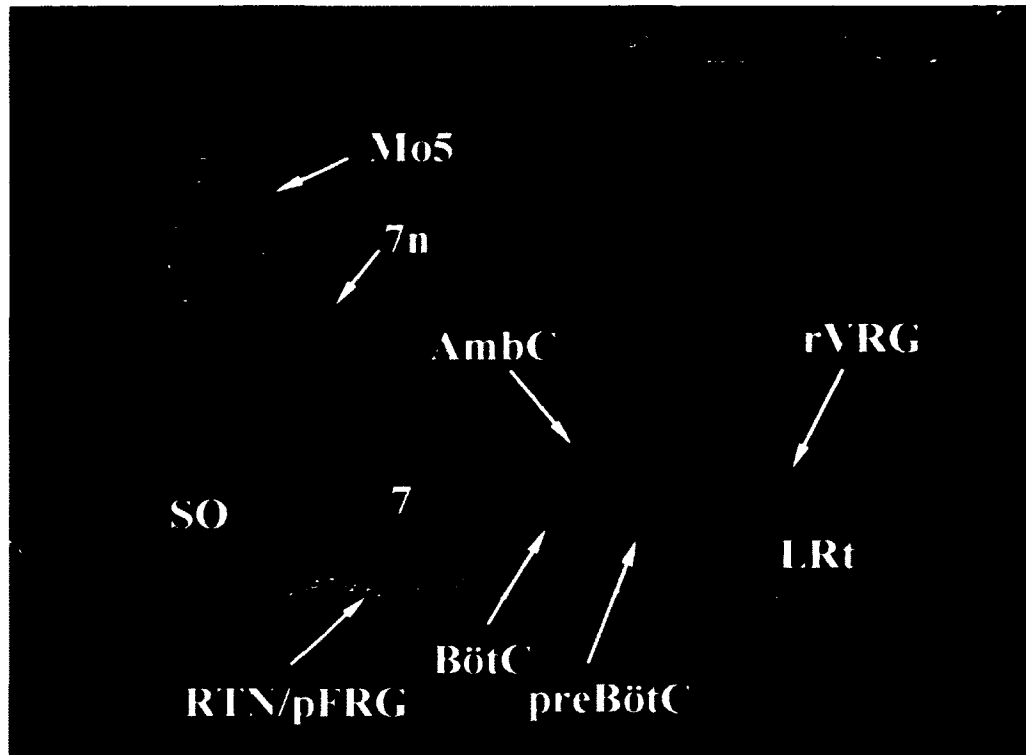


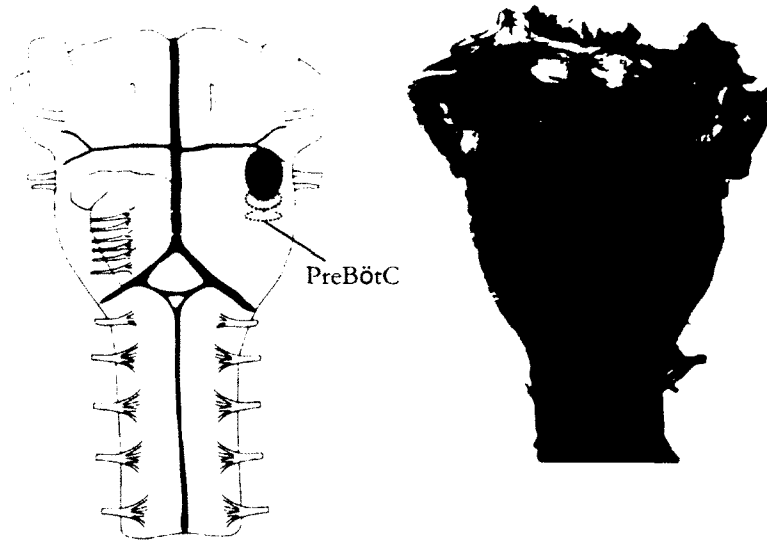
Figure 1.2 NK1 receptors in the rostral VRC of the mouse.

Pseudocolored sagittal section through the rhombencephalon of the adult mouse with immunolabeled NK1 receptors (cyan). Note the dense labeling at the level of the preBötC and also at the ventral and caudal portions of the facial nucleus. Areas such as the superior olive (SO) and lateral reticular nucleus (LRt) are essentially unstained for NK1 receptors. Few areas of the VRC (i.e. BötC or rVRG) can be considered devoid of NK1 receptors. Following immunolabeling with diaminobenzidine as the chromogen, the section was subsequently counterstained with ethidium bromide (red) as a fluorescent Nissl stain. Grayscale images of the NK1 receptors were inverted with respect to black and white and copied to the green and blue channels of an RGB image. A grayscale image of the Nissl staining was copied to the red channel of the same image to produce the final composite image.

Adapted from Figure 4 of Alheid and McCrimmon (2009) *Respir. Physiol. Neurobiol.* 164(1-2):3–

11.

A



B

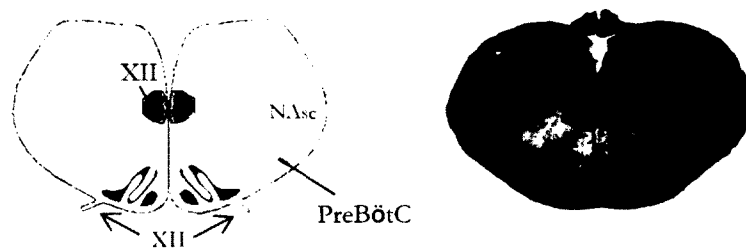


Figure 1.3 Schema of the rat brainstem spinal cord and medullary slice.

A. Picture of a brainstem spinal cord preparation on its ventral side on the right, and its corresponding schema (on the left) which highlights important respiratory nuclei present in its preparation: the pFRG (blue), the BötC (Grey) and the preBötC (pink). The dashed line indicates the rostral and caudal edges of the medullary slice **B.** Picture of a transverse medullary slice preparation is shown on the right. The schema on the left highlights the preBötC (pink), the semi-compact division of the nucleus ambiguus (NAsc) the XII nuclei and rostral XII nerves (arrows) present in this preparation.

Reproduced and adapted from Ruangkittisakul et al. (2007) *Journal of Physiology* 584 (Pt 2):489-508.

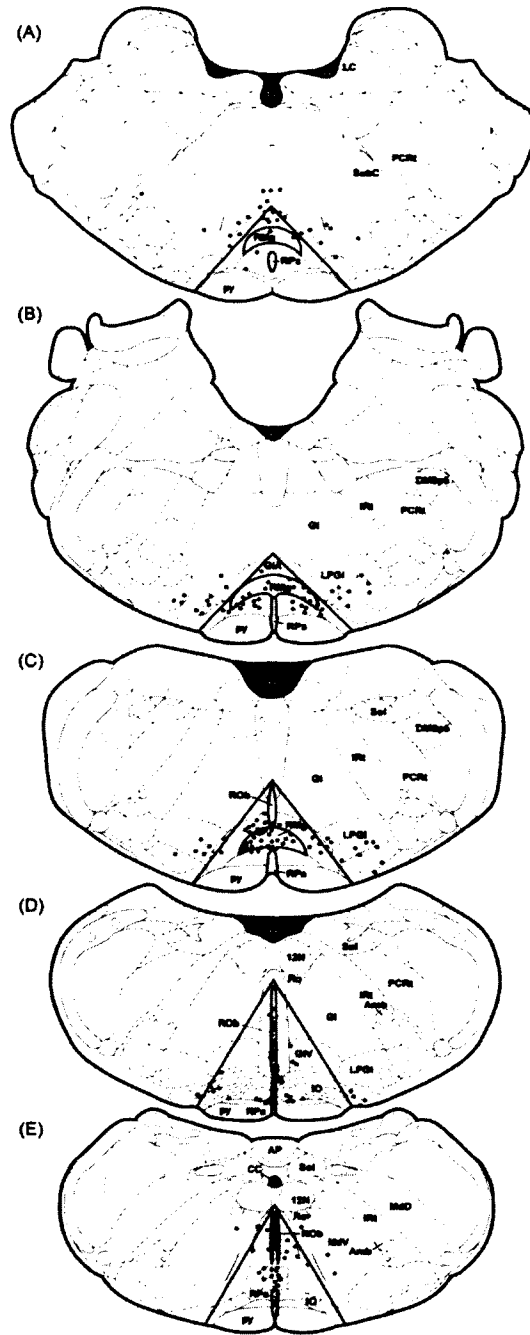


Figure 1.4 Caudal medullary raphé nuclei and their 5HT neuronal cell bodies.

Figure 3 from Baker et al. (2009) *Respir Physiol Neurobiol.* 165(2-3):175-84.

Previous Page

Figure 1.4 Caudal medullary raphé nuclei and their 5HT neuronal cell bodies.

Diagram of representative coronal sections through the caudal raphé nuclear region showing the distribution of neurons stained for tryptophanhydroxylase (TPH) immunoreactivity in a male rat. Each dot represents one TPH immunoreactive neuron. Borders of the caudal raphé nuclei were defined according to the Rat Brain Atlas, 5th Edition (Paxinos and Watson, 2005). (A) Bregma -10 mm; (B) Bregma -11 mm; (C) Bregma -12 mm; (D) Bregma -13 mm; (E) Bregma -14 mm. The triangular area indicates the boundaries of the parapyramidal region as used in the present study. Amb, nucleus ambiguus; AP, area postrema; CC, central canal; DMSp5, dorsomedial spinal trigeminal nucleus; GiA, gigantocellular reticular nucleus pars alpha; GiV, gigantocellular reticular nucleus pars ventralis; IO, inferior olivary nuclei; IRt, intermediate reticular nucleus; LC, locus coeruleus, MdD, medullary reticular nucleus dorsal division; MdV, medullary reticular nucleus ventral division; Ro, nucleus of Rölller; Sol, nucleus of the solitary tract; SubC, subcoeruleus nucleus; LPGi, paragigantocellular reticular nucleus; PCRt, parvicellular reticular nucleus; 12N, hypoglossal nucleus; py, pyramidal tract; 4V, fourth ventricle; RMg, nucleus raphé magnus; RPa, nucleus raphé pallidus; Rob, nucleus raphé obscurus; ppa, parapyramidal region.

Figure 3 from Baker et al. (2009) *Respir Physiol Neurobiol.* 165(2-3):175-84.

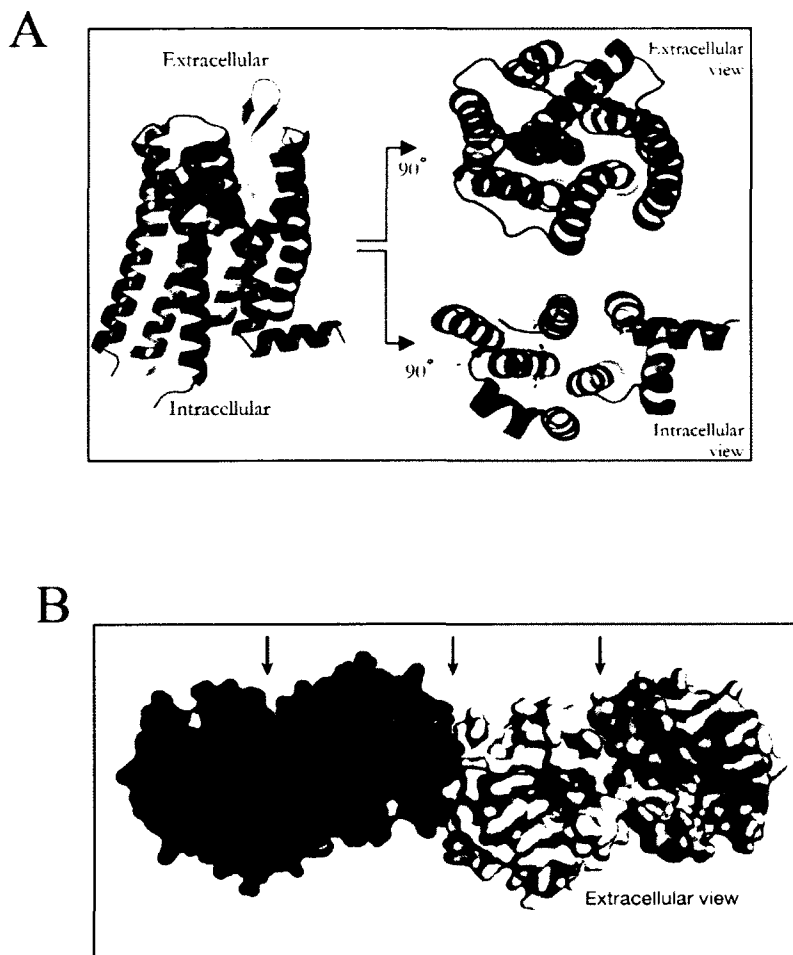
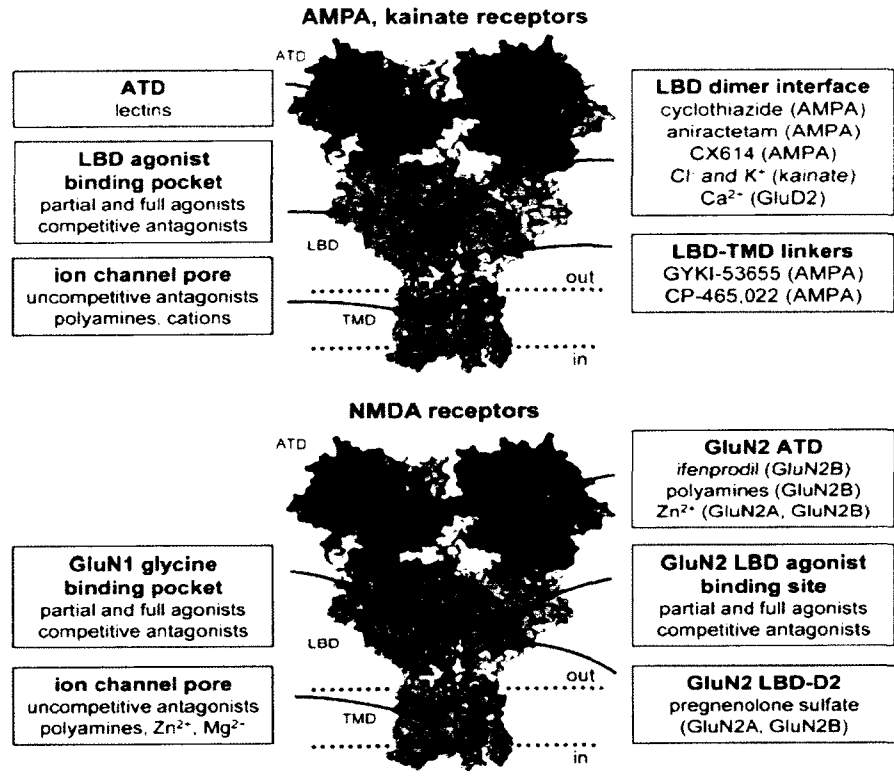


Figure 1.5 Overall view of the μ -opioid receptor structure.

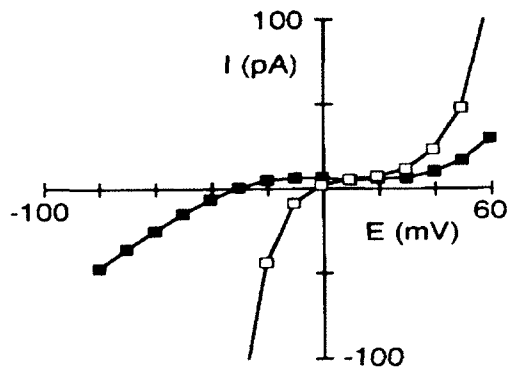
A. Views from within the membrane plane (left), extracellular side (right top) and intracellular side (right bottom) show the typical seven-pass transmembrane GPCR architecture of the μ -opioid receptor. The ligand, b-FNA, a semisynthetic opioid antagonist derived from morphine, shown in shown in green spheres. **B.** The μ -opioid receptor crystallized as intimately associated pairs, with two different interfaces. Black arrows show the transmembrane (TM) domains (TM5-TM6; TM1-TM2-H8 and TM-TM6 respectively, from left to right). The interface defined by TM5-TM6 is more extensive than the one defined by TM1-TM2-H8.

Figure 1 and 4 adapted from Manglik et al (2012) *Nature* Mar 21; 485(7398):321-6.

A



B



C

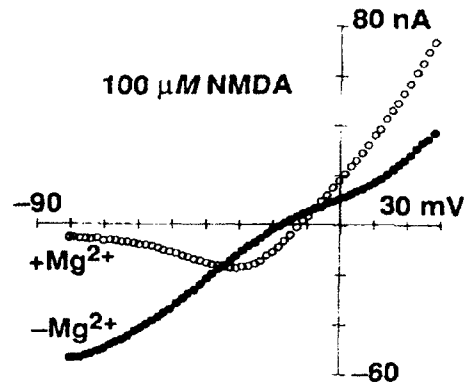


Figure 1.6 Overall structure and classical function of the glutamate ionotropic AMPA and NMDA receptors.

Previous Page

Figure 1.6 Overall structure and function of the glutamate ionotropic AMPA and NMDA receptors.

A. Schematic structure of a glutamate receptors and binding sites for various agonists, antagonists and modulators. ATD: amino terminal domain; LBD: ligand binding domain; TMD: trans-membrane domain. [Figure 9 from Traynelis et al. *Pharmacol.Rev.* 62(3):405-96]. B. Peak IV relation for whole-cell glutamate-activated currents recorded in a HEK293 cell expressing GluR1 (Q) bathed either in CsCl or CaCl₂. The IV shows a strong double rectification due to a voltage-dependent block of Ca²⁺ permeable AMPAR channels by intracellular polyamines. The glutamate-mediate currents in CsCl solution (empty squares) cross the voltage axis near -4 mV. When Ca²⁺ replaces Cs⁺ (black squares) the IV relation remains strongly doubly rectifying with the reversal potential shifted leftward, consistent with Ca²⁺ being more permeant than monovalent alkali cations [Figure 6 from Wollmuth and Sakmann (1998) *J.Gen.Physiol.* 112(5):623-36]. C. The ionic current produced by 100 μM NMDA in an oocyte injected with NMDAR mRNA was plotted as a function of voltage in the absence (black circles) and presence (empty circles) of 1mM Mg²⁺. The perfusion solution also contained 3μM glycine. [Figure 1B from Verdoorn et al. (1987) *Science* 238(4830):1114-6].

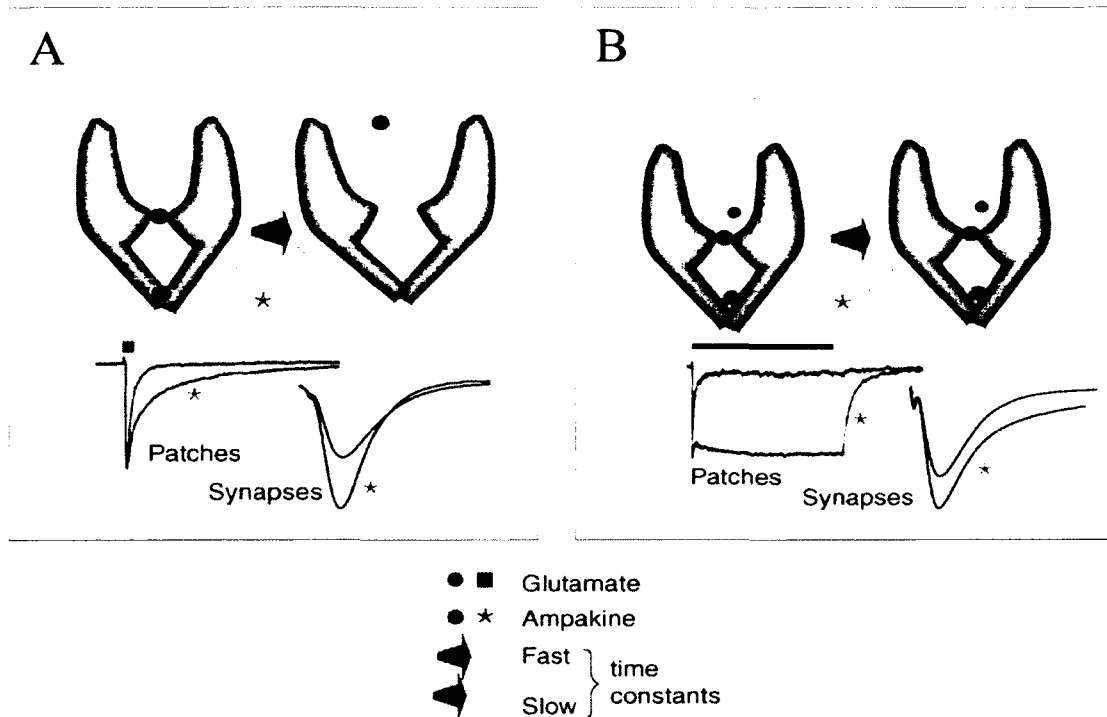


Figure 1.7 Ampakine actions on excised patches and hippocampal slices.

A. The probabilistic movement of a receptor subunit from its transmitter-bound, channel open state to the unbound, channel-closed state occurs with a mean time constant (blue arrow). Binding of an ampakine to a strategic site at the hinge of the extracellular domains increases the time constant (orange arrow), and thereby delays the closing of the channel. The traces below the schematic are from experiments using excised patches or hippocampal slices. In the patches, a one-millisecond pulse of glutamate (short red bar) caused a sharp inward flux of current that decayed back to baseline following washout; the rate of decay is a measure of receptor deactivation. Addition of an ampakine (orange asterisk) prolonged the duration of the current (i.e. increased the time constant of deactivation). An ampakine that acts predominately on deactivation increased the amplitude of synaptic responses in the hippocampus (right-hand traces) but had little effect on their duration. **B.** Binding of the transmitter can also disturb the dimerization of AMPA receptor subunits. Most ampakines, by binding within the dimer interface, increase the time constant for this effect (orange arrow), as can be seen in the traces from an excised patch experiment. In this study, a 500 ms pulse of glutamate (long red bar) produced an inward current that returned to a near baseline level despite the continued presence of the transmitter; this is desensitization. Addition of the ampakine caused the

receptors to continue passing current throughout the duration of the glutamate pulse. The synaptic effects of an ampakine that slows both deactivation and desensitization are illustrated in the right-hand traces, from an experiment using hippocampal slices. Note that the drug increases both the amplitude and duration of the postsynaptic response.

Figure 1 from Lynch and Gall (2006) *Trends in Neurosciences* 29(10):554-62

1.5 REFERENCES

- ABBOTT SB, STORNETTA RL, COATES MB, GUYENET PG (2011) Phox2b-expressing neurons of the parafacial region regulate breathing rate, inspiration, and expiration in conscious rats. *J. Neurosci.* 31(45):16410-22.
- ADACHI T, HUXTABLE AG, FANG X, FUNK GD (2010) Substance P modulation of hypoglossal motoneuron excitability during development: changing balance between conductances. *J. Neurophysiol.* 104(2):854-72.
- AICHER SA, GOLDBERG A, SHARMA S, PICKEL VM (2000) Mu-opioid receptors are present in vagal afferents and their dendritic targets in the medial nucleus tractus solitarius. *J. Comp. Neurol.* 422(2):181-90.
- ALHEID GF, MCCRIMMON DR (2008) The chemical neuroanatomy of breathing. *Respir. Physiol. Neurobiol.* 164(1-2):3-11.
- AL-ZUBAIDY ZA, ERICKSON RL, GREER JJ (1996) Serotonergic and noradrenergic effects on respiratory neural discharge in the medullary slice preparation of neonatal rats. *Pflugers Arch.* 431(6):942-9.
- ANDERSON SD, BASBAUM AI, FIELDS HL (1977) Response of medullary raphe neurons to peripheral stimulation and to systemic opiates. *Brain Res.* 123(2):363-8.
- ARAI AC, KESSLER M, ROGERS G, LYNCH G (2000) Effects of the potent ampakine CX614 on hippocampal and recombinant AMPA receptors: interactions with cyclothiazide and GYKI 52466. *Mol. Pharmacol.* 58(4):802-13.
- ARVIDSSON U, RIEDL M, CHAKRABARTI S, LEE JH, NAKANO AH, DADO RJ, LOH HH, LAW PY, WESSENDORF MW, ELDE R (1995) Distribution and targeting of a mu-opioid receptor (MOR1) in brain and spinal cord. *J. Neurosci.* 15(5 Pt 1):3328-41.
- ATWEH SF, KUCHAR MJ (1977) Autoradiographic localization of opiate receptors in rat brain. I. Spinal cord and lower medulla. *Brain Res.* 124, 53.
- BAGNOL D, MANSOUR A, AKIL H, WATSON SJ (1997) Cellular localization and distribution of the cloned mu and kappa opioid receptors in rat gastrointestinal tract. *Neuroscience* 81(2):579-91.
- BARKER JR, THOMAS CF, BEHAN M (2009) Serotonergic projections from the caudal raphe nuclei to the hypoglossal nucleus in male and female rats. *Respir. Physiol. Neurobiol.* 165(2-3):175-84.

- BALLANYI K, LALLEY PM, HOCH B, RICHTER DW (1997) cAMP-dependent reversal of opioid- and prostaglandin-mediated depression of the isolated respiratory network in newborn rats. *J. Physiol.* 504 (Pt 1):127-34.
- BALLANYI K, PANAITESCU B, RUANGKITTISAKUL A (2010) Indirect opioid actions on inspiratory pre-Bötzinger complex neurons in newborn rat brainstem slices. *Adv. Exp. Med. Biol.* 669:75-9.
- BALLANYI K, RUANGKITTISAKUL A, ONIMARU H (2009) Opioids prolong and anoxia shortens delay between onset of preinspiratory (pFRG) and inspiratory (preBötC) network bursting in newborn rat brainstems *Pflugers Arch.* 458(3):571-87.
- BASBAUM AI, CLANTON CH, FIELDS HL (1976) Opiate and stimulus-produced analgesia: functional anatomy of a medullospinal pathway. *Proc Natl Acad Sci U S A.* 73(12):4685.
- BASBAUM AI, FIELDS HL (1984) Endogenous pain control systems: brainstem spinal pathways and endorphin circuitry. *Annu. Rev. Neurosci.* 7:309-38.
- BEN-MABROUK F, TRYBA AK (2010) Substance P modulation of TRPC3/7 channels improves respiratory rhythm regularity and ICAN-dependent pacemaker activity. *Eur. J. Neurosci.* 31(7):1219-32.
- BENVENISTE M, CLEMENTS J, VYKLYCKY LJ, MAYER ML (1990) A kinetic analysis of the modulation of N-methyl-D-aspartic acid receptors by glycine in mouse cultured hippocampal neurones. *Journal of Physiology (Lond.)* 428, 333-357.
- BENVENISTE M, MAYER ML (1991) Kinetic analysis of antagonist action at N-methyl-D-aspartic acid receptors. Two binding sites each for glutamate and glycine. *Biophys. Journal* 59: 560-573.
- BENYAMIN R, TRESHOT AM, DATTA S, BUENAVENTURA R, ADLAKA R, SEHGAL N, GLASER SE, VALLEJO R (2008) Opioid complications and side effects. *Pain Physician.* 11(2 Suppl):S105-20.
- BERGER AJ, DICK TE (1987) Connectivity of slowly adapting pulmonary stretch receptors with dorsal medullary respiratory neurons. *J. Neurophysiol.* 58(6):1259-1274.
- BIANCHI AL (1974) Modalities of discharge and anatomo-functional properties of medullary respiratory neurons]. [Article in French] *J. Physiol. (Paris)*.68(5):555-87.

BIANCHI AL, DENAVIT-SAUBIE M, CHAMPAGNAT J (1995) Central control of breathing in mammals: neuronal circuitry, membrane properties and neurotransmitters. *J. Physiol. Rev.* 75:1-45.

BIANCHI AL, DUSSARDIER M, BARILLOT JC, PLANCHE D (1973) Anatomical and functional heterogeneity of the medullary respiratory neurons. *Acta Neurobiol. Exp. (Wars)*. 33(1):319-28.

BIEGER D, HOPKINS DA (1987) Viscerotopic representation of the upper alimentary tract in the medulla oblongata in the rat: the nucleus ambiguus. *J. Comp. Neurol.* 262(4):546-62.

BOCHORISHVILI G, STORNETTA RL, COATES MB, GUYENET PG (2012) Pre-Bötzinger complex receives glutamatergic innervation from galaninergic and other retrotrapezoid nucleus neurons. *J. Comp. Neurol.* 520(5):1047-61.

BONHAM AC, COLES SK, MCCRIMMON DR (1993) Pulmonary stretch receptor afferents activate excitatory amino acid receptors in the nucleus tractus solitarius in rats. *J. Physiol.* 464:725-45.

BORGLAND SL, CONNOR M, OSBORNE PB, FURNESS JB, CHRISTIE MJ. (2003) Opioid agonists have different efficacy profiles for G protein activation, rapid desensitization, and endocytosis of mu-opioid receptors. *J. Biol. Chem.* 278(21):18776-84.

BORTOLOTTO ZA, CLARKE VR, DELANY CM, PARRY MC, SMOLDERS I, VIGNES M, HO KH, MIU P, BRINTON BT, FANTASKE R, OGDEN A, GATES M, ORNSTEIN PL, LODGE D, BLEAKMAN D, COLLINGRIDGE GL (1999) Kainate receptors are involved in synaptic plasticity. *Nature*. 402(6759):297-301.

BOUVIER J, THOBY-BRISSON M, RENIER N, DUBREUIL V, ERICSON J, CHAMPAGNAT J, PIERANI A, CHÉDOTAL A, FORTIN G (2010) Hindbrain interneurons and axon guidance signaling critical for breathing. *Nat. Neurosci.* 13(9):1066-74.

BOYDEN ES, ZHANG F, BAMBERG E, NAGEL G, DEISSEROTH K (2005). Millisecond-timescale, genetically targeted optical control of neural activity. *Nat. Neurosci.* 8(9):1263-8.

BRADLEY GW, VON EULER C, MARTTILA I, ROOS B (1975) A model of the central and reflex inhibition of inspiration in the cat. *Biol. Cybern.* 19(2):105-16.

BRADLEY SR, PIERIBONE VA, WANG W, SEVERSON CA, JACOBS RA, RICHERSON GB (2002) Chemosensitive serotonergic neurons are closely associated with large medullary arteries. *Nat. Neurosci.* 5(5):401-2.

BRICKLEY SG, MISRA C, MOK MH, MISHINA M, CULL-CANDY SG (2003) NR2B and NR2D subunits coassemble in cerebellar Golgi cells to form a distinct NMDA receptor subtype restricted to extrasynaptic sites. *J. Neurosci.* 23(12):4958-66.

BROCKHAUS J, BALLANYI K (1998) Synaptic inhibition in the isolated respiratory network of neonatal rats. *Eur J Neurosci.* 10(12):3823-39.

BROCKHAUS J, BALLANYI K, SMITH JC, RICHTER DW (1993) Microenvironment of respiratory neurons in the *in vitro* brainstem-spinal cord of neonatal rats. *J Physiol.* 462:421-45.

BUCHANAN GF, RICHERSON GB (2010) Central serotonin neurons are required for arousal to CO₂. *Proc Natl Acad Sci U S A.* 107(37):16354-9.

BUTERA RJ JR, RINZEL J, SMITH JC (1999) Models of respiratory rhythm generation in the pre-Bötzinger complex. I. Bursting pacemaker neurons. *J. Neurophysiol.* 82(1):382-97.

CAO JY, QIU S, ZHANG J, WANG JJ, ZHANG XM, LUO JH (2011) Transmembrane region of N-methyl-D-aspartate receptor (NMDAR) subunit is required for receptor subunit assembly. *J. Biol. Chem.* 286(31):27698-705.

CHAMPAGNAT J, DENAVIT-SAUBIE M, SIGGINS GR (1983) Rhythmic neuronal activities in the nucleus of the tractus solitarius isolated *in vitro*. *Brain Res.* 280(1):155-9.

CHAMPAGNAT J, MORIN-SURUN MP, BOUVIER J, THOBY-BRISSEON M, FORTIN G (2011) Prenatal development of central rhythm generation. *Respir Physiol Neurobiol.* 178(1):146-55.

CHATTERTON JE, AWOBULUYI M, PREMKUMAR LS, TAKAHASHI H, TALANTOVA M, SHIN Y, CUI J, TU S, SEVARINO KA, NAKANISHI N, TONG G, LIPTON SA, ZHANG D (2002) Excitatory glycine receptors containing the NR3 family of NMDA receptor subunits. *Nature* 415(6873):793-8.

CHAVKIN C, JAMES IF, GOLDSTEIN A (1982) Dynorphin is a specific endogenous ligand of the kappa opioid receptor. *Science* 215(4531):413-5.

CHAZOT PL, COLEMAN S, CIK M, STEPHENSON FA (1994) Molecular characterization of N-methyl-D-aspartate receptors expressed in mammalian cells yields evidence for the coexistence of three subunit types within a discrete receptor molecule. *J Biol Chem.* 269(39):24403-9.

CHAZOT PL, STEPHENSON FA (1997) Molecular dissection of native mammalian forebrain NMDA receptors containing the NR1 C2 exon: direct demonstration of

NMDA receptors comprising NR1, NR2A, and NR2B subunits within the same complex. *J. Neurochem.* 69(5):2138-44.

CHEN ZB, HEDNER T, HEDNER J (1990) Local application of somatostatin in the rat ventrolateral brain medulla induces apnea. *J. Appl. Physiol.* 69(6):2233-8.

CHEN ZB, ENGBERG G, HEDNER T, HEDNER J (1991) Antagonistic effects of somatostatin and substance P on respiratory regulation in the rat ventrolateral medulla oblongata. *Brain Res.* 556(1):13-21.

CHIANG CY, PAN ZZ (1985) Differential responses of serotonergic and non-serotonergic neurons in nucleus raphé magnus to systemic morphine in rats. *Brain Res.* 337(1):146-50.

CIABARRA AM, SULLIVAN JM, GAHN LG, PECHT G, HEINEMANN S, SEVARINO KA (1995) Cloning and characterization of chi-1: a developmentally regulated member of a novel class of the ionotropic glutamate receptor family. *J. Neurosci.* 15(10):6498-508.

CLEMENTS JD, WESTBROOK GL (1991) Activation kinetics reveal the number of glutamate and glycine binding sites on the N-methyl-D-aspartate receptor. *Neuron* 7:605-613.

COLLINGRIDGE GL, OLSEN RW, PETERS J, SPEDDING M (2009) A nomenclature for ligand-gated ion channels. *Neuropharmacology* 56(1):2-5.

COLLINGRIDGE GL, SINGER W (1990) Excitatory amino acid receptors and synaptic plasticity. *Trends Pharmacol. Sci.* 11(7):290-6.

CORCORAN AE, HODGES MR, WU Y, WANG W, WYLIE CJ, DENNERIS ES, RICHERSON GB (2009) Medullary serotonin neurons and central CO₂ chemoreception. *Respir. Physiol. Neurobiol.* 168(1-2):49-58.

COSSART R, ESCLAPEZ M, HIRSCH JC, BERNARD C, BEN-ARI Y (1998) GLUR5 kainate receptor activation in interneurons increases tonic inhibition of pyramidal cells. *Nat Neurosci.* 1(6):470-8.

CRILL WE (1996) Persistent sodium current in mammalian central neurons. *Annu Rev Physiol.* 58:349-62.

DAS S, SASAKI YF, ROTHE T, PREMKUMAR LS, TAKASU M, CRANDALL JE, DIKES P, CONNER DA, RAYUDU PV, CHEUNG W, CHEN HS, LIPTON SA, NAKANISHI N (1998) Increased NMDA current and spine density in mice lacking the NMDA receptor subunit NR3A. *Nature* 393(6683):377-81.

- DEAKIN JF, DICKENSON AH, DOSTROVSKY JO (1977) Morphine effects on rat raphé magnus neurones [proceedings]. *J. Physiol.* 267(1):43P-45P.
- DEAN JB, MULKEY DK, HENDERSON RA 3RD, POTTER SJ, PUTNAM RW (2004) Hyperoxia, reactive oxygen species, and hyperventilation: oxygen sensitivity of brain stem neurons. *J Appl Physiol.* 96(2):784-91.
- DE FELIPE C, HERRERO JF, O'BRIEN JA, PALMER JA, DOYLE CA, SMITH AJ, LAIRD JM, BELMONTE C, CERVERO F, HUNT SP (1998) Altered nociception, analgesia and aggression in mice lacking the receptor for substance P. *Nature* 392(6674):394-7.
- DEL NEGRO CA, HAYES JA (2008) A 'group pacemaker' mechanism for respiratory rhythm generation. *J. Physiol.* 586(9):2245-6.
- DEL NEGRO CA, HAYES JA, PACE RW, BRUSH BR, TERUYAMA R, FELDMAN JL (2010) Synaptically activated burst-generating conductances may underlie a group-pacemaker mechanism for respiratory rhythm generation in mammals. *Prog. Brain Res.* 187:111-36.
- DEL NEGRO CA, KOSHIYA N, BUTERA RJ JR, SMITH JC (2002) Persistent sodium current, membrane properties and bursting behavior of pre-Bötzinger complex inspiratory neurons *in vitro*. *J. Neurophysiol.* 88(5):2242-50.
- DEL NEGRO CA, MORGADO-VALLE C, HAYES JA, MACKAY DD, PACE RW, CROWDER EA, FELDMAN JL (2005) Sodium and calcium current-mediated pacemaker neurons and respiratory rhythm generation. *J. Neurosci.* 25(2):446-53.
- DENAVIT-SAUBIÉ M, CHAMPAGNAT J, ZIEGLGÄNSBERGER W (1978) Effects of opiates and methionine-enkephalin on pontine and bulbar respiratory neurones of the cat. *Brain Res.* 155(1):55-67.
- DE SCHEPPER HU, CREMONINI F, PARK MI, CAMILLERI M (2004) Opioids and the gut: pharmacology and current clinical experience. *Neurogastroenterol Motil* 16:383-394
- DING YQ, KANEKO T, NOMURA S, MIZUNO N (1996) Immunohistochemical localization of mu-opioid receptors in the central nervous system of the rat. *J. Comp. Neurol.* 367(3):375-402.
- DI FRANCESCO D (1993) Pacemaker mechanisms in cardiac tissue. *Annual Rev. Physiol.* 55:455-72.
- DI PASQUALE E, TELL F, MONTEAU R, HILAIRE G (1996) Perinatal developmental changes in respiratory activity of medullary and spinal neurons: an *in vitro* study on fetal and newborn rats. *Brain Res Dev Brain Res.* 91(1):121-30.

- DOBBINS EG, FELDMAN JL (1995) Differential innervation of protruder and retractor tongue muscles of rat. *J. Comp. Neurol.* 357:376–394.
- DOBLE A (1996) The pharmacology and mechanism of action of riluzole. *Neurology.* 47(6 Suppl 4):S233-41.
- DU M, REIDS SA, JAYARAMAN V (2005) Conformational changes in the ligand-binding domain of a functional ionotropic glutamate receptor. *The journal of Biological Chemistry* 280(10): 8633-8636.
- DUBREUIL V, RAMANANTSOA N, TROCHET D, VAUBOURG V, AMIEL J, GALLEGO J, BRUNET JF, GORIDIS C (2008) A human mutation in Phox2b causes lack of CO2 chemosensitivity, fatal central apnea, and specific loss of parafacial neurons. *Proc. Natl. Acad. Sci. U S A* 105:1067-1072.
- DUGGAN AW, NORTH RA Electrophysiology of opioids (1983) *Pharmacol Rev.* 35(4):219-81.
- DUPRAT F, LESAGE F, FINK M, REYES R, HEURTEAUX C, LAZDUNSKI M (1997) TASK, a human background K⁺ channel to sense external pH variations near physiological pH. *EMBO J.* 16(17):5464-71.
- DUTHIE DJ, NIMMO WS (1987) Adverse effects of opioid analgesic drugs. *Br J Anaesth.* 59(1):61-77.
- EDWARD SD, YEH SR, KRASNE FB (1998) Neuronal coincidence detection by voltage-sensitive electrical synapses. *Proc. Natl. Acad. Sci. USA* 95:7145–7150.
- ELDE R, HÖKFELT T, JOHANSSON O, TERENIUS L (1976) Immunohistochemical studies using antibodies to leucine-enkephalin: initial observations on the nervous system of the rat. *Neuroscience* 1(4):349-51
- ELLENBERGER HH, FELDMAN JL (1990) Brainstem connections of the rostral ventral respiratory group of the rat. *Brain Res.* 513(1):35-42.
- ENYEDI P, CZIRJÁK G (2010) Molecular background of leak K⁺ currents: two-pore domain potassium channels. *Physiol. Rev.* 90(2):559-605.
- EZURE K (1990) Synaptic connections between medullary respiratory neurons and considerations on the genesis of respiratory rhythm. *Prog. Neurobiol.* 35:429- 450.
- EZURE K, TANAKA I (2006) Distribution and medullary projection of respiratory neurons in the dorsolateral pons of the rat. *Neuroscience* 141(2):1011-23.
- EZURE K, MANABE M, YAMADA H (1988) Distribution of medullary respiratory neurons in the rat. *Brain Res.* 455:262-270.

- FELDMAN JL, COWAN JD (1975) Large-scale activity in neural nets II: A model for the brainstem respiratory oscillator. *Biol. Cybern.* 17(1):39-51.
- FELDMAN JL, MITCHELL GS, NATTIE EE (2003) Breathing: rhythmicity, plasticity, chemosensitivity. *Annu. Rev. Neuroscience* 26:239-66.
- FELDMAN JL, DEL NEGRO CA (2006) Looking for inspiration: new perspectives on respiratory rhythm. *Nat. Rev. Neuroscience* 7: 232-242.
- FEDORKO L, MERRILL EG (1984) Axonal projections from the rostral expiratory neurones of the Bötzing complex to medulla and spinal cord in the cat. *J. Physiol.* 350: 487-496.
- FERGUSON SS (2001) Evolving concepts in G protein-coupled receptor endocytosis: the role in receptor desensitization and signaling. *Pharmacol Rev.* 53(1):1-24.
- FIELDS HL, ANDERSON SD (1978) Evidence that raphé-spinal neurons mediate opiate and midbrain stimulation-produced analgesias. *Pain* 5(4):333-49.
- FLOURENS MJP (1842) Recherches expérimentales sur les propriétés et les fonctions du system nerveux dans les animaux vertèbres (2d ed.). Paris: Baillière.
- FLOURENS MJP (1851) Comptes Rendus de l'Académie des Sciences (Paris) 33:437.
- FONG TM, YU H, STRADER CD (1992) The extracellular domain of substance P (NK1) receptor comprises part of the ligand binding site. *Biophys. J.* 62(1): 59-60.
- FORTIN G, THOBY-BRISSEON M (2009) Embryonic emergence of the respiratory rhythm generator. *Respir. Physiol. Neurobiol.* 168(1-2):86-91.
- FORTUNA MG, WEST GH, STORNETTA RL, GUYENET PG (2008) Botzinger expiratory augmenting neurons and the parafacial respiratory group. *J. Neurosci.* 28(10):2506-15.
- FUNK GD, SMITH JC, FELDMAN JL (1993) Generation and transmission of respiratory oscillations in medullary slices: role of excitatory amino acids. *J. Neurophysiol.* 70(4):1497-515.
- FUNK GD, SMITH JC, FELDMAN JL (1995) Modulation of neural network activity *in vitro* by cyclothiazide, a drug that blocks desensitization of AMPA receptors. *J. Neurosci.* 15(5 Pt 2):4046-56.

FUNK GD, JOHNSON SM, SMITH JC, DONG XW, LAI J, FELDMAN JL (1997) Functional respiratory rhythm generating networks in neonatal mice lacking NMDAR1 gene. *J. Neurophysiol.* 78(3):1414-20.

FURUKAWA H, SINGH SK, MANCUSO R, GOUAUX E (2005) Subunit arrangement and function in NMDA receptors. *Nature.* 438(7065):185-92.

GARCIA AJ 3RD, PUTNAM RW, DEAN JB (2010) Hyperbaric hyperoxia and normobaric reoxygenation increase excitability and activate oxygen-induced potentiation in CA1 hippocampal neurons. *J Appl Physiol.* 109(3):804-19.

GARCÍA DEL CAÑO G, MILLÁN LM, GERRIKAGOITIA I, SARASA M, MATUTE C (1999) Ionotropic glutamate receptor subunit distribution on hypoglossal motoneuronal pools in the rat. *J Neurocytol.* 28(6):455-68.

GIOLLI RA, BLANKS RH, TORIGOE Y, CLARKE RJ, FALLON JH, LESLIE FM (1990) Opioid receptors in the accessory optic system of the rat: effects of monocular enucleation. *Vis Neurosci.* 5(5):497-506.

GONZALEZ J, DU M, PARAMESHWARAN K, SUPPIRAMANIAM V, JAYARAMAN V (2010) Role of dimer interface in activation and desensitization in AMPA receptors. *Proc Natl Acad Sci U S A.* 107(21):9891-6.

GOUAUX E (2004) Structure and function of AMPA receptors. *J. Physiol.* 554 (Pt 2):249-53.

GOURINE AV, KASYMOV V, MARINA N, TANG F, FIGUEIREDO MF, LANE S, TESCHEMACHER AG, SPYER KM, DEISSEROTH K, KASPAROV S (2010) Astrocytes Control Breathing Through pH-Dependent Release of ATP. *Science* 329 (5991): 571-575.

GRAY PA, REKLING JC, BOCCHIARO CM, FELDMAN JL (1999) Modulation of respiratory frequency by peptidergic input to rhythmogenic neurons in the preBötzinger complex. *Science* 286(5444):1566-8.

GRAY PA, JANCZEWSKI WA, MELLEN N, MCCRIMMON DR, FELDMAN JL (2001) Normal breathing requires preBötzinger complex neurokinin-1 receptor-expressing neurons. *Nat. Neurosci.* 4(9):927-30.

GRAY PA, HAYES JA, LING GY, LLONA I, TUPAL S, PICARDO MC, ROSS SE, HIRATA T, CORBIN JG, EUGENÍN J, DEL NEGRO CA (2010) Developmental origin of preBötzinger complex respiratory neurons. *J. Neurosci.* 30(44):14883-95.

- GREER JJ, SMITH JC, FELDMAN JL (1991) Role of excitatory amino acids in the generation and transmission of respiratory drive in neonatal rat. *J. Physiol.* 437:727-49.
- GREER JJ, SMITH JC, FELDMAN JL (1992) Respiratory and locomotor patterns generated in the fetal rat brain stem-spinal cord *in vitro*. *J. Neurophysiol.* 67(4):996-9.
- GREER JJ, CARTER JE, AL-ZUBAIDY Z (1995) Opioid depression of respiration in neonatal rats. *J. Physiol.* 485 (Pt 3):845-55.
- GUNN CG, SEVELIUS G, PUIGGARI J, MYERS FK (1968) Vagal cardiomotor mechanisms in the hindbrain of the dog and cat. *Am. J. Physiol.* 214(2):258-62.
- GUO-FENG T, PEEVER JH, DUFFIN J (1998) Bötzinger-complex expiratory neurons monosynaptically inhibit phrenic motoneurons in the decerebrate rat. *Experimental Brain Research* 122(2): 149-156.
- GUYENET PG, WANG H (2001) Pre-Bötzinger neurons with preinspiratory discharges 'in vivo' express NK1 receptors in the rat. *J. Neurophysiol.* 86, 438-446.
- GUYENET PG, SEVIGNY CP, WESTON MC, STORNETTA RL (2002) Neurokinin-1 receptor-expressing cells of the ventral respiratory group are functionally heterogeneous and predominantly glutamatergic. *J. Neurosci.* 22(9):3806-16.
- HATTON CJ, PAOLETTI P (2005) Modulation of triheteromeric NMDA receptors by N-terminal domain ligands. *Neuron* 46(2):261-74.
- HAYES JA, DEL NEGRO CA (2007) Neurokinin receptor-expressing pre-botzinger complex neurons in neonatal mice studied *in vitro*. *J. Neurophysiol.* 97(6):4215-24.
- HENRY JN, MANAKER S (1998) Colocalization of substance P or enkephalin in serotonergic neuronal afferents to the hypoglossal nucleus in the rat. *J. Comp. Neurol.* 391(4):491-505.
- HILL AA, GARCIA AJ 3RD, ZANELLA S, UPADHYAYA R, RAMIREZ JM (2011) Graded reductions in oxygenation evoke graded reconfiguration of the isolated respiratory network. *J Neurophysiol.* 105(2):625-39.
- HILLE B (1994) Modulation of ion-channel function by G-protein-coupled receptors. *Trends Neurosci.* 17(12):531-6.
- HILLE B (2001) *Ion Channels of Excitable Membranes*, 3rd Edition (Sunderland MA: Sinauer Associates).

- HODGES MR, RICHERSON GB (2008) Contributions of 5-HT neurons to respiratory control: neuromodulatory and trophic effects. *Respir Physiol Neurobiol.* 164(1-2):222-32.
- HODGES MR, TATTERSALL GJ, HARRIS MB, MCEVOY SD, RICHERSON DN, DENERIS ES, JOHNSON RL, CHEN ZF, RICHERSON GB (2008) Defects in breathing and thermoregulation in mice with near-complete absence of central serotonin neurons. *J Neurosci.* 28(10):2495-505
- HODGES MR, WEHNER M, AUNGST J, SMITH JC, RICHERSON GB (2009) Transgenic mice lacking serotonin neurons have severe apnea and high mortality during development. *J. Neurosci.* 29(33):10341-9.
- HODGKIN AL, KATZ B (1949) The effect of sodium ions on the electrical activity of giant axon of the squid. *J. Physiol.* 108(1):37-77.
- HOLTMAN JR, NORMAN WP, GILLIS RA (1984) Projections from the raphé nuclei to the phrenic motor nucleus in the cat. *Neurosci Lett.* 44(1):105-11.
- HOLTMAN JR, SPECK DF (1994) Substance P immunoreactive projections to the ventral respiratory group in the rat. *Peptides* 15(5):803-8.
- HOLLMANN M, HEINEMANN S (1994) Cloned glutamate receptors. *Annu.Rev. Neurosci.* 17, 31–108.
- HUGHES J, SMITH TW, KOSTERLITZ HW, FOTHERGILL LA, MORGAN BA, MORRIS HR (1975) Identification of two related pentapeptides from the brain with potent opiate agonist activity. *Nature* 258(5536):577-80.
- IRELAND MF, LENAL FC, LORIER AR, LOOMES DE, ADACHI T, ALVARES TS, GREER JJ, FUNK GD (2008) Distinct receptors underlie glutamatergic signalling in inspiratory rhythm-generating networks and motor output pathways in neonatal rat. *J Physiol.*586(9):2357-70.
- IRNATEN M, AICHER SA, WANG J, VENKATESAN P, EVANS C, BAXI S, MENDELOWITZ D (2003) Mu-opioid receptors are located postsynaptically and endomorphin-1 inhibits voltage-gated calcium currents in premotor cardiac parasympathetic neurons in the rat nucleus ambiguus. *Neuroscience* 116(2):573-82.
- ISHII T, MORIYOSHI K, SUGIHARA H, SAKURADA K, KADOTANI H, YOKOI M, AKAZAWA C, SHIGEMOTO R, MIZUNO N, MASU M, (1993) Molecular characterization of the family of the N-methyl-D-aspartate receptor subunits. *J. Biol. Chem.* 268(4):2836-43.

ITO I, TANABE S, KOHDA A, SUGIYAMA H (1990) Allosteric potentiation of quisqualate receptors by a nootropic drug aniracetam. *J. Physiol.* 424:533-43.

JACOBS BL, AZMITIA EC (1992) Structure and function of the brain serotonin system. *Physiol Rev.* 72(1):165-229.

JACOB JJ, RAMABADRAN K (1981) Role of opiate receptors and endogenous ligands in nociception. *Pharmacol Ther.* 14(2):177-96.

JACQUIN T, CHAMPAGNAT J, MADAMBA S, DENAVIT-SAUBIÉ M, SIGGINS GR (1988) Somatostatin depresses excitability in neurons of the solitary tract complex through hyperpolarization and augmentation of IM, a non-inactivating voltage-dependent outward current blocked by muscarinic agonists. *Proc Natl Acad Sci U S A.* 85(3):948-52.

JANCZEWSKI WA, ONIMARU H, HOMMA I, FELDMAN JL (2002) Opioid-resistant respiratory pathway from the preinspiratory neurones to abdominal muscles: *in vivo* and *in vitro* study in the newborn rat. *J. Physiol.* 545(Pt 3):1017-26.

JANCZEWSKI WA, FELDMAN JL (2006) Distinct rhythm generators for inspiration and expiration in the juvenile rat. *J. Physiol.* 570(Pt 2):407-20.

JIN R, CLARK S, WEEKS AM, DUDMAN JT, GOUAUX E, PARTIN KM (2005) Mechanism of positive allosteric modulators acting on AMPA receptors. *J. Neurosci.* 25(39):9027-36.

JOHNSON JW, ASCHER P (1987) Glycine potentiates the NMDA response in cultured mouse brain neurons. *Nature* 325, 529-531.

JOHNSON SM, SMITH JC, FUNK GD, FELDMAN JL (1994) Pacemaker behavior of respiratory neurons in medullary slices from neonatal rat. *J. Neurophysiol.* 72(6):2598-608.

JONAS P, SPRUSTON N (1994) Mechanisms shaping glutamate-mediated excitatory postsynaptic currents in the CNS. *Curr. Opin. Neurobiol.* 4(3):366-372.

KALIA MP (1981) Anatomical organization of central respiratory neurons. *Annu Rev Physiol.* 43:105-20.

KALIA M, FUXE K, HÖKFELT T, JOHANSSON O, LANG R, GANTEN D, CUELLO C, TERENIUS L (1984) Distribution of neuropeptide immunoreactive nerve terminals within the subnuclei of the nucleus of the tractus solitarius of the rat. *J. Comp. Neurol.* 222(3):409-44.

KELLER BU, BLASCHKE M, RIVOSECCHI R, HOLLMANN M, HEINEMAN SF, KONNERTH A (1993) Identification of a subunit-specific antagonist

AMPA/Kainate receptor channels. *Proceeding of the National Academy of Sciences* 90(2):605-609.

KNAPP RJ, MALATYNSKA E, COLLINS N, FANG L, WANG JY, HRUBY VJ, ROESKE WR, YAMAMURA HI (1995) Molecular biology and pharmacology of cloned opioid receptors. *FASEB J.* 9(7):516-25.

KOBAYASHI K, LEMKE RP, GREER JJ (2001) Ultrasound measurements of fetal breathing movements in the rat. *Journal of Applied Physiology* 91(1) 316-320.

KOIZUMI H, WILSON CG, WONG S, YAMANISHI T, KOSHIYA N, SMITH JC (2008) Functional imaging, spatial reconstruction, and biophysical analysis of a respiratory motor circuit isolated *in vitro*. *J. Neurosci.* 28(10):2353-65.

KOSHIYA N, SMITH JC (1999) Neuronal pacemaker for breathing visualized *in vitro*. *Nature.* 400(6742):360-3.

KRAUSE KL, NEUMUELLER SE, MARSHALL BD, KINER T, BONIS JM, PAN LG, QIAN B, FORSTER HV (2009) Micro-opioid receptor agonist injections into the presumed pre-Bötzinger complex and the surrounding region of awake goats do not alter eupneic breathing. *J. Appl. Physiol.* 107(5):1591-9.

KUBIN L, ALHEID GF, ZUPERKU EJ, MCCRIMMON DR (2006) central pathways of pulmonary and lower airway vagal afferents. *J. Appl. Physiol.* 101:618-27.

LALLEY PM (2003) Mu-opioid receptor agonist effects on medullary respiratory neurons in the cat: evidence for involvement in certain types of ventilatory disturbances *Am J. Physiol. Regul. Integr. Comp. Physiol.* 285(6):R1287-304.

LAMANAUSKAS N, NISTRI A (2008) Riluzole blocks persistent Na⁺ and Ca²⁺ currents and modulates release of glutamate via presynaptic NMDA receptors on neonatal rat hypoglossal motoneurons *in vitro*. *Eur. J. Neurosci.* 27(10):2501-14.

LANUZA GM, GOSGNACH S, PIERANI A, JESSELL TM, GOULDING M (2004) Genetic identification of spinal interneurons that coordinate left-right locomotor activity necessary for walking movements. *Neuron* 42(3):375-86.

LAUDER JM (1990) Ontogeny of the serotonergic system in the rat: serotonin as a developmental signal. *Ann N Y Acad Sci.* 600:297-313; discussion 314.

LAUTERBORN JC, LYNCH G, VANDERKLISH P, ARAI A, GALL CM (2000) Positive modulation of AMPA receptors increases neurotrophin expression by hippocampal and cortical neurons. *J Neurosci.* 20(1):8-21.

LAUTERBORN JC, PINEDA E, CHEN LY, RAMIREZ EA, LYNCH G, GALL CM (2009) Ampakines cause sustained increases in brain-derived neurotrophic factor

signaling at excitatory synapses without changes in AMPA receptor subunit expression. *Neuroscience* 159(1):283-95.

LAVEZZI AM, CASALE V, ONEDA R, WEESE-MAYER DE, MATTURRI L (2009) Sudden infant death syndrome and sudden intrauterine unexplained death: correlation between hypoplasia of raphé nuclei and serotonin transporter gene promoter polymorphism. *Pediatr. Res.* 66(1):22-7.

LAVEZZI AM, MATTURRI L (2008) Functional neuroanatomy of the human pre-Bötzinger complex with particular reference to sudden unexplained perinatal and infant death. *Neuropathology* 28(1):10-6.

LE GALLOIS JJC (1812) Expériences sur le principe de la vie, notamment sur celui des mouvements du cœur, et sur le siège de ce principe. *D'Hautel, Paris.*

LING GS, SPIEGEL K, LOCKHART SH, PASTERNAK GW (1985) Separation of opioid analgesia from respiratory depression: evidence for different receptor mechanisms. *J. Pharmacol. Exp. Ther.* 232(1):149-55.

LIPSKI J (1981) Antidromic activation of neurones as an analytic tool in the study of the central nervous system. *J. Neurosci. Methods* 4(1):1-32.

LIPSKI J, MERRILL EG (1980) Electrophysiological demonstration of the projection from expiratory neurones in rostral medulla to contralateral dorsal respiratory group. *Brain Res.* 197(2):521-4.

LIU Q, WONG-RILEY MT (2010a) Postnatal changes in the expressions of serotonin 1A, 1B, and 2A receptors in ten brain stem nuclei of the rat: implication for a sensitive period. *Neuroscience.* 165(1):61-78.

LIU Q, WONG-RILEY MT (2010b) Postnatal development of N-methyl-D-aspartate receptor subunits 2A, 2B, 2C, 2D, and 3B immunoreactivity in brain stem respiratory nuclei of the rat. *Neuroscience* 171(3):637-54.

LLINÁS R, SUGIMORI M (1980) Electrophysiological properties of *in vitro* Purkinje cell somata in mammalian cerebellar slices. *J. Physiol.* 305:171-95.

LOPES OU, PALMER JF (1976) Proposed respiratory 'gating' mechanism for cardiac slowing. *Nature* 264: 454-456.

LORD JA, WATERFIELD AA, HUGHES J, KOSTERLITZ HW (1977) Endogenous opioid peptides: multiple agonists and receptors. *Nature* 267:495-499.

LU B, SU Y, DAS S, LIU J, XIA J, REN D (2007) The neuronal channel NALCN contributes resting sodium permeability and is required for normal respiratory rhythm. *Cell* 129(2):371-83.

- LU B, SU Y, DAS S, WANG H, WANG Y, LIU J, REN D (2009) Peptide neurotransmitters activate a cation channel complex of NALCN and UNC-80. *Nature* 457(7230):741-4.
- LU B, ZHANG Q, WANG H, WANG Y, NAKAYAMA M, REN D (2010) Extracellular calcium controls background current and neuronal excitability via an UNC79-UNC80-NALCN cation channel complex. *Neuron* 68(3):488-99.
- LUMSDEN T (1922-1923A) Observations on the respiratory centres in the cat. *J. Physiology* 57:153-160.
- LUMSDEN T (1922-1923B) Observations on the respiratory centres. *J. Physiology* 57:354-367.
- LUMSDEN T (1922-1923C) The regulation of respiration: part I. *J. Physiology* 58:81-91.
- LYNCH G, GALL CM (2006) Ampakines and the threefold path to cognitive enhancement. *Trends Neurosci.* 29(10):554-62.
- MACDONALD JF, NOWAK LM (1990) Mechanisms of blockade of excitatory amino acid receptor channels. *Trends Pharmacol Sci.* 11(4):167-72.
- MALENKA RC, NICOLL RA (1993) NMDA-receptor-dependent synaptic plasticity: multiple forms and mechanisms. *Trends Neurosci.* 16(12):521-7. Review.
- MANGLIK A, KRUSE AC, KOBILKA TS, THIAN FS, MATHIESEN JM, SUNAHARA RK, PARDO L, WEIS WI, KOBILKA BK, GRANIER S (2012) Crystal structure of the μ -opioid receptor bound to a morphinan antagonist. *Nature* 485(7398):321-6.
- MANSOUR A, FOX CA, BURKE S, MENG F, THOMPSON RC, AKIL H, WATSON SJ (1994) Mu, delta, and kappa opioid receptor mRNA expression in the rat CNS: an in situ hybridization study. *J Comp Neurol.* 350(3):412-38.
- MANZKE T, GUENTHER U, PONIMASKIN EG, HALLER M, DUTSCHMANN M, SCHWARZACHER S, RICHTER DW (2003) 5-HT₄(a) receptors avert opioid-induced breathing depression without loss of analgesia. *Science* 301(5630):226-9.
- MARINA N, ABDALA AP, TRAPP S, LI A, NATTIE EE, HEWINSON J, SMITH JC, PATON JF, GOURINE AV (2010) Essential role of Phox2b-expressing ventrolateral brainstem neurons in the chemosensory control of inspiration and expiration. *J Neurosci.* 30(37):12466-73.

MASON P (2001) Contributions of the medullary raphé and ventromedial reticular region to pain modulation and other homeostatic functions. *Annu. Rev. Neurosci.* 24:737-77.

MATSUDA K, KAMIYA Y, MATSUDA S, YUZAKI M (2002) Cloning and characterization of a novel NMDA receptor subunit NR3B: a dominant subunit that reduces calcium permeability. *Brain Res Mol Brain Res.* 100(1-2):43-52.

MATTHES HW, MALDONADO R, SIMONIN F, VALVERDE O, SLOWE S, KITCHEN I, BEFORT K, DIERICH A, LE MEUR M, DOLLÉ P, TZAVARA E, HANOUNE J, ROQUES BP, KIEFFER BL (1997) Loss of morphine-induced analgesia, reward effect and withdrawal symptoms in mice lacking the mu-opioid-receptor gene. *Nature* 383(6603):819-23.

MATTHES HW, SMADJA C, VALVERDE O, VONESCH JL, FOUTZ AS, BOUDINOT E, DENAVIT-SAUBIÉ M, SEVERINI C, NEGRI L, ROQUES BP, MALDONADO R, KIEFFER BL (1998) Activity of the delta-opioid receptor is partially reduced, whereas activity of the kappa-receptor is maintained in mice lacking the mu-receptor. *J. Neurosci.* 18(18):7285-95.

MAYER DJ, PRICE DD (1976) Central nervous system mechanisms of analgesia. *Pain* 2(4):379-404.

MCCLUNG JR, GOLDBERG SJ (1999) Organization of motoneurons in the dorsal hypoglossal nucleus that innervate the retrusor muscles of the tongue in the rat. *Anat. Rec.* 254(2):222-30.

MCCLUNG JR, GOLDBERG SJ (2000) Functional anatomy of the hypoglossal innervated muscles of the rat tongue: a model for elongation and protrusion of the mammalian tongue. *Anat. Rec.* 260(4):378-86.

MCGILLIARD K, TAKEMORI AE (1978) Antagonism by naloxone of narcotic-induced respiratory depression and analgesia. *J. Pharmacol. Exp. Ther.* 207,494.

MCKAY LC, JANCZEWSKI WA, FELDMAN JL (2005) Sleep-disordered breathing after targeted ablation of preBötzinger complex neurons. *Nat Neurosci.* 8(9):1142-4.

MEGURO H, MORI H, ARAKI K, KUSHIYA E, KUTSUWADA T, YAMAZAKI M, KUMANISHI T, ARAKAWA M, SAKIMURA K, MISHINA M (1992) Functional characterization of a heteromeric NMDA receptor channel expressed from cloned cDNAs. *Nature* 357(6373):70-4.

MELLEN NM, JANCZEWSKI WA, BOCCHIARO CM, FELDMAN JL (2003) Opioid-induced quantal slowing reveals dual networks for respiratory rhythm generation. *Neuron* 37(5):821-6.

- MERRILL EG (1970) The lateral respiratory neurones of the medulla: their associations with nucleus ambiguus, nucleus retroambiguus, the spinal accessory nucleus and the spinal cord. *Brain Res.* 24, 11-28.
- MERRILL EG, LIPSKI J, KUBIN L, FEDORKO L (1983) Origin of the expiratory inhibition of nucleus tractus solitarius inspiratory neurones. *Brain Res.* 263(1):43-50.
- MERRILL EG, FEDORKO L (1984) Monosynaptic inhibition of phrenic motoneurons: a long descending projection from Bötzing neurons. *J. Neurosci.* 4(9):2350-3.
- MILLER DJ (2004) Sydney Ringer; physiological saline, calcium and the contraction of the heart. *J. Physiol.* 555(Pt 3):585-7.
- MIRONOV SL (2008) Metabotropic glutamate receptors activate dendritic calcium waves and TRPM channels which drive rhythmic respiratory patterns in mice. *J. Physiol.* 586(Pt 9): 2277–2291.
- MITCHELL RA, BERGER AJ (1977) Neural regulation of respiration. *Int. Anesthesiol. Clin.* Summer; 15(2):59-79.
- MONTANDON G, QIN W, LIU H, REN J, GREER JJ, HORNER RL (2011) PreBotzinger complex neurokinin-1 receptor-expressing neurons mediate opioid-induced respiratory depression. *J. Neurosci.* 31(4): 1292-301.
- MONTEAU R, PTAK K, BROQUÈRE N, HILAIRE G (1996) Tachykinins and central respiratory activity: an *in vitro* study on the newborn rat. *Eur. J. Pharmacol.* 314(1-2):41-50.
- MORGADO-VALLE C, FELDMAN JL (2007) NMDA receptors in preBötzing complex neurons can drive respiratory rhythm independent of AMPA receptors. *J. Physiol.* 582(Pt 1):359-68.
- MORIN-SURUN MP, GACEL G, CHAMPAGNAT J, DENAVIT-SAUBIE M, ROQUES BP (1984A) Pharmacological identification of delta and mu opiate receptors on bulbar respiratory neurons. *Eur. J. Pharmacol.* 98(2):241-7.
- MORIN-SURUN MP, BOUDINOT E, GACEL G, CHAMPAGNAT J, ROQUES BP, DENAVIT-SAUBIE M (1984B) Different effects of mu and delta opiate agonists on respiration. *Eur. J. Pharmacol.* 98(2):235-40.
- MORIYOSHI K, MASU M, ISHII T, SHIGEMOTO R, MIZUNO N, NAKANISHI S (1991) Molecular cloning and characterization of the rat NMDA receptor. *Nature* 354, 31-37.

- MULKEY DK, HENDERSON RA 3RD, OLSON JE, PUTNAM RW, DEAN JB (2001) Oxygen measurements in brain stem slices exposed to normobaric hyperoxia and hyperbaric oxygen. *J Appl Physiol.* 90(5):1887-99.
- MULKEY DK, STORNETTA RL, WESTON MC, SIMMONS JR, PARKER A, BAYLISS DA, GUYENET PG (2004) Respiratory control by ventral surface chemoreceptor neurons in rats. *Nat. Neurosci.* 7(12):1360-9.
- MURAKOSHI T, SUZUE T, TAMAI S (1985) A pharmacological study on respiratory rhythm in the isolated brainstem-spinal cord preparation of the newborn rat. *Br. J. Pharmacol.* 86(1):95-104.
- NAGARAJAN N, QUAST C, BOXALL AR, SHAHID M, ROSENMUND C (2001) Mechanism and impact of allosteric AMPA receptor modulation by the ampakine CX546. *Neuropharmacology* 41(6):650-63.
- NATTIE E (1999) CO₂, brainstem chemoreceptors and breathing. *Prog. Neurobiol.* 59:299-33.
- NATTIE EE (2001) Central chemosensitivity, sleep, and wakefulness. *Respir Physiol.* 129(1-2):257-68.
- NATTIE EE, LI A (2001) CO₂ dialysis in the medullary raphé of the rat increases ventilation in sleep. *J. Appl Physiol.* 90(4):1247-57.
- NATTIE EE, LI A (2002) CO₂ dialysis in nucleus tractus solitarius region of rat increases ventilation in sleep and wakefulness. *J. Appl. Physiol.* 92: 2119–2130.
- OERTEL BG, FELDEN L, TRAN PV, BRADSHAW MH, ANGST MS, SCHMIDT H, JOHNSON S, GREER JJ, GEISLINGER G, VARNEY MA, LÖTSCH J (2010) Selective antagonism of opioid-induced ventilatory depression by an ampakine molecule in humans without loss of opioid analgesia. *Clin Pharmacol Ther.* 87(2):204-11.
- OGIER M, WANG H, HONG E, WANG Q, GREENBERG ME, KATZ DM (2007) Brain-derived neurotrophic factor expression and respiratory function improve after ampakine treatment in a mouse model of Rett syndrome. *J. Neurosci.* 27(40):10912-7.
- OKADA Y, MÜCKENHOFF K, HOLTERMANN G, ACKER H, SCHEID P (1993) Depth profiles of pH and PO₂ in the isolated brain stem-spinal cord of the neonatal rat. *Respir Physiol.* 93(3):315-26.
- ONIMARU H, ARATA A, HOMMA I (1990) Inhibitory synaptic inputs to the respiratory rhythm generator in the medulla isolated from newborn rats. *Pflugers Arch.* 417(4):425-32.

- ONIMARU H, ARATA A, HOMMA I (1995) Intrinsic burst generation of preinspiratory neurons in the medulla of brainstem-spinal cord preparations isolated from newborn rats. *Exp. Brain Res.* 106(1):57-68.
- ONIMARU H, HOMMA I (1987) Respiratory rhythm generator neurons in medulla of brainstem-spinal cord preparation from newborn rat. *Brain Res.* 403(2):380-4.
- ONIMARU H, HOMMA I (2003) A novel functional neuron group for respiratory rhythm generation in the ventral medulla. *J. Neurosci.* 23(4):1478-86.
- ONIMARU H, HOMMA I (2005) Developmental changes in the spatio-temporal pattern of respiratory neuron activity in the medulla of late fetal rat. *Neuroscience* 131(4):969-77.
- ONIMARU H, IKEDA K, KAWAKAMI K (2008) CO₂-sensitive preinspiratory neurons of the parafacial respiratory group express Phox2b in the neonatal rat. *J. Neurosci.* 28(48):12845-50.
- ONIMARU H, KUMAGAWA Y, HOMMA I (2006) Respiration-related rhythmic activity in the rostral medulla of newborn rats. *J. Neurophysiol.* 96(1):55-61.
- ONIMARU H, SHAMOTO A, HOMMA I (1998) Modulation of respiratory rhythm by 5-HT in the brainstem-spinal cord preparation from newborn rat. *Pflugers Arch.* 435(4):485-94.
- PAARMANN I, FRERMANN D, KELLER BU, HOLLMANN M (2000) Expression of 15 glutamate receptor subunits and various splice variants in tissue slices and single neurons of brainstem nuclei and potential functional implications. *J. Neurochem.* 74(4):1335-45.
- PAARMANN I, FRERMANN D, KELLER BU, VILLMANN C, BREITINGER HG, HOLLMANN M (2005) Kinetics and subunit composition of NMDA receptors in respiratory-related neurons. *J. Neurochem.* 2005 93(4):812-24.
- PACE RW, MACKAY DD, FELDMAN JL, DEL NEGRO CA (2007A) Role of persistent sodium current in mouse preBötzinger Complex neurons and respiratory rhythm generation. *J. Physiol.* 580(Pt. 2):485-96.
- PACE RW, MACKAY DD, FELDMAN JL, DEL NEGRO CA (2007B) Inspiratory bursts in the preBötzinger complex depend on a calcium-activated non-specific cation current linked to glutamate receptors in neonatal mice. *J. Physiol.* 582(Pt 1):113-25.
- PACE RW, DEL NEGRO CA (2008) AMPA and metabotropic glutamate receptors cooperatively generate inspiratory-like depolarization in mouse respiratory neurons *in vitro*. *Eur. J. Neurosci.* 28(12):2434-42.

- PAGLIARDINI S, REN J, GREER JJ (2003) Ontogeny of the pre-Bötzinger complex in perinatal rats. *J. Neurosci.* 23(29):9575-84.
- PAGLIARDINI S, ADACHI T, REN J, FUNK GD, GREER JJ (2005) Fluorescent tagging of rhythmically active respiratory neurons within the pre-Bötzinger complex of rat medullary slice preparations. *J. Neurosci.* 25(10):2591-6.
- PAGLIARDINI S, JANCZEWSKI WA, TAN W, DICKSON CT, DEISSEROTH K, FELDMAN JL (2011) Active expiration induced by excitation of ventral medulla in adult anesthetized rats. *J. Neurosci.* 31(8):2895-905.
- PANAITESCU B, RUANGKITTISAKUL A, BALLANYI K (2009) Silencing by raised extracellular Ca^{2+} of pre-Bötzinger complex neurons in newborn rat brainstem slices without change of membrane potential or input resistance. *Neurosci Lett.* 456(1):25-9.
- PAN YX, XU J, BOLAN E, ABBADIE C, CHANG A, ZUCKERMAN A, ROSSI G, PASTERNAK GW (1999). Identification and characterization of three new alternatively spliced mu opioid receptor isoforms. *Mol. Pharmacol.* 56: 396–403.
- PAN YX, XU J, BOLAN E, CHANG A, MAHURTER L, ROSSI G, PASTERNAK GW (2000) Isolation and expression of a novel alternatively spliced mu opioid receptor isoform, MOR-1F. *FEBS Lett.* 466: 337–40.
- PAN YX, XU J, MAHURTER L, BOLAN E, XU M, PASTERNAK GW (2001) Generation of the mu opioid receptor (MOR-1) protein by three new splice variants of the Oprm gene. *Proc Natl Acad Sci USA*; 98: 14084–9.
- PAN YX, XU J, BOLAN E, MOSKOWITZ HS, XU M, PASTERNAK GW (2005) Identification of four novel exon 5 splice variants of the mouse mu-opioid receptor gene: functional consequences of C-terminal splicing. *Mol. Pharmacol.* 68(3):866-75.
- PANTALEO T, MUTOLO D, CINELLI E, BONGIANNI F (2011) Respiratory responses to somatostatin microinjections into the Bötzing complex and the pre-Bötzing complex of the rabbit. *Neurosci. Lett.* 498(1):26-30.
- PAPE HC (1996) Queer current and pacemaker: the hyperpolarization-activated cation current in neurons. *Annu Rev Physiol.* 58:299-327.
- PARTRIDGE LD, SWANDULLA D (1988) Calcium-activated non-specific cation channels. *Trends Neurosci.* 11(2):69-72.

- PARTRIDGE LD, VALENZUELA CF (1999) Ca²⁺ store-dependent potentiation of Ca²⁺-activated non-selective cation channels in rat hippocampal neurones *in vitro*. *J. Physiol.* 521 Pt 3:617-27
- PASTERNAK GW (1993) Pharmacological mechanisms of opioid analgesics. *Clin. Neuropharmacol.* 16(1):1-18.
- PASTERNAK GW (2004) Multiple opiate receptors: déjà vu all over again. *Neuropharmacology.* 47 Suppl 1:312-23.
- PATEL YC (1999) Somatostatin and its receptor family. *Front. Neuroendocrinol.* 20(3):157-98.
- PATTINSON KT (2008) Opioids and the control of respiration. *Br. J. Anaesth.* 100(6):747-58.
- PAZOS A, FLÓREZ J (1984) A comparative study in rats of the respiratory depression and analgesia induced by mu- and delta-opioid agonists. *Eur. J. Pharmacol.* 99(1):15-21.
- PEEVER JH, SHEN L, DUFFIN J (2002) Respiratory pre-motor control of hypoglossal motoneurons in the rat. *Neurosci.* 110:711-722.
- PEÑA F, PARKIS MA, TRYBA AK, RAMIREZ JM (2004) Differential contribution of pacemaker properties to the generation of respiratory rhythms during normoxia and hypoxia. *Neuron* 43(1):105-17.
- PEÑA F, RAMIREZ JM (2002) Endogenous activation of serotonin-2A receptors is required for respiratory rhythm generation *in vitro*. *J. Neurosci.* 22(24):11055-64.
- PEÑA F, RAMIREZ JM (2004) Substance P-mediated modulation of pacemaker properties in the mammalian respiratory network. *J. Neurosci.* 24(34):7549-56.
- PEREZ-OTANO I, SCHULTEIS CT, CONTRACTOR A, LIPTON SA, TRIMMER JS, SUCHER NJ, HEINEMANN SF (2001) Assembly with the NR1 subunit is required for surface expression of NR3A-containing NMDA receptors. *J. Neurosci.* 21(4):1228-37.
- PIERANI A, MORAN-RIVARD L, SUNSHINE MJ, LITTMAN DR, GOULDING M, JESSELL TM. (2001) Control of interneuron fate in the developing spinal cord by the progenitor homeodomain protein Dbx1. *Neuron* 29(2):367-84.
- PILLI J, KUMAR SS (2012) Triheteromeric N-methyl-d-aspartate receptors differentiate synaptic inputs onto pyramidal neurons in somatosensory cortex: Involvement of the GluN3A subunit. *Neuroscience* 222:75-88.

- PIÑA-CRESPO JC, TALANTOVA M, MICU I, STATES B, CHEN HS, TU S, NAKANISHI N, TONG G, ZHANG D, HEINEMANN SF, ZAMPONI GW, STYS PK, LIPTON SA (2010) Excitatory glycine responses of CNS myelin mediated by NR1/NR3 "NMDA" receptor subunits. *J. Neurosci.* 30(34):11501-5.
- PTAK K, KONRAD M, DI PASQUALE E, TELL F, HILAIRE G, MONTEAU R (2000A) Cellular and synaptic effect of substance P on neonatal phrenic motoneurons. *Eur. J. Neurosci.* 12(1):126-38.
- PTAK K, HUNT SP, MONTEAU R (2000B) Substance P and central respiratory activity: a comparative *in vitro* study in NK1 receptor knockout and wild-type mice. *Pflugers Arch.* 440(3):446-51.
- PTAK K, YAMANISHI T, AUNGST J, MILESCU LS, ZHANG R, RICHERSON GB, SMITH JC (2009) Raphé neurons stimulate respiratory circuit activity by multiple mechanisms via endogenously released serotonin and substance P. *J. Neurosci.* 29(12):3720-37.
- RAFFA RB, MARTINEZ RP, CONNELLY CD (1994) G-protein antisense oligodeoxyribonucleotides and mu-opioid supraspinal antinociception. *Eur J Pharmacol.* 258(1-2):R5-7.
- RAMAN IM, TRUSSELL LO (1995) The mechanism of alpha-amino-3-hydroxy-5-methyl-4-isoxazolepropionate receptor desensitization after removal of glutamate. *Biophys. J.* 68(1):137-46.
- RAMANANTSOA N, HIRSCH M-R, THOBY-BRISSEON M, DUBREUIL V, BOUVIER J, RUFFAULT P-L, MATROT B, FORTIN G, BRUNET J-F, GALLEGU J, GORIDIS C (2011) Breathing without CO₂ Chemosensitivity in Conditional Phox2b Mutants. *J. Neurosci.* 31(36):12880-12888.
- RAMIREZ JM, QUELLMALZ UJ, WILKEN B, RICHTER DW (1998) The hypoxic response of neurones within the *in vitro* mammalian respiratory network. *J. Physiol.* 507 (Pt 2):571-82.
- RAMIREZ JM, SCHWARZACHER SW, PIERREFICHE O, OLIVERA BM, RICHTER DW (1998) Selective lesioning of the cat pre-Bötzinger complex *in vivo* eliminates breathing but not gasping. *J. Physiol.* 507 (Pt 3):895-907.
- RAMIREZ JM, TELGKAMP P, ELSER FP, QUELLMALZ UJ, RICHTER DW (1997) Respiratory rhythm generation in mammals: synaptic and membrane properties. *Respir Physiol.* 110(2-3):71-85.
- RAY RS, CORCORAN AE, BRUST RD, KIM JC, RICHERSON GB, NATTIE E, DYMECKI SM (2011) Impaired respiratory and body temperature control upon acute serotonergic neuron inhibition. *Science* 333(6042):637-42.

- REKLING JC, CHAMPAGNAT J, DENAVIT-SAUBIÉ M (1996A) Electroresponsive properties and membrane potential trajectories of three types of inspiratory neurons in the newborn mouse brain stem *in vitro*. *J. Neurophysiol.* 75(2):795-810.
- REKLING JC, CHAMPAGNAT J, DENAVIT-SAUBIÉ M (1996B) Thyrotropin-releasing hormone (TRH) depolarizes a subset of inspiratory neurons in the newborn mouse brain stem *in vitro*. *J. Neurophysiol.* 75(2):811-9.
- REKLING JC, FELDMAN JL (1997A) Calcium-dependent plateau potentials in rostral ambiguous neurons in the newborn mouse brain stem *in vitro*. *J. Neurophysiol.* 78(5):2483-92.
- REKLING JC, FELDMAN JL (1997B) Bidirectional electrical coupling between inspiratory motoneurons in the newborn mouse nucleus ambiguus. *J. Neurophysiol.* 78(6):3508-10.
- REN J, DING X, FUNK GD, GREER JJ (2009) Ampakine CX717 protects against fentanyl-induced respiratory depression and lethal apnea in rats. *Anesthesiology* 110(6):1364-70.
- REN J, GREER JJ (2006) Modulation of respiratory rhythmogenesis by chloride-mediated conductances during the perinatal period. *J. Neurosci.* 26(14):3721-30.
- REN J, POON BY, TANG Y, FUNK GD, GREER JJ (2006) Ampakines alleviate respiratory depression in rats. *Am. J. Respir. Crit. Care Med.* 174(12):1384-91 14.
- RICHERSON GB (1995) Response to CO₂ of neurons in the rostral ventral medulla *in vitro*. *J. Neurophysiol.* 73(3):933-44.
- RICHERSON GB (2004) Serotonergic neurons as carbon dioxide sensors that maintain pH homeostasis. *Nat. Rev. Neurosci.* 5: 449-461.
- RICHTER DW (1982) Generation and maintenance of the respiratory rhythm. *J. Exp. Biol.* 100:93-107.
- RICHTER DW, HEYDE F (1974) Reciprocal innervation of medullary inspiratory and expiratory neurons. *Pflugers Arch.* 347, R39.
- RICHTER DW, MANZKE T, WILKEN B, PONIMASKIN E (2003) Serotonin receptors: guardians of stable breathing. *Trends Mol Med.* 9(12):542-8.
- RINGER S (1883) A further Contribution regarding the influence of the different Constituents of the Blood on the Contraction of the Heart. *J. Physiol.* 4(1):29-42.3.

ROBINSON D, ELLENBERGER H (1997) Distribution of N-methyl-D-aspartate and non-N-methyl-D-aspartate glutamate receptor subunits on respiratory motor and premotor neurons in the rat. *J Comp Neurol.* 389(1):94-116.

ROSE MF, REN J, AHMAD KA, CHAO HT, KLISCH TJ, FLORA A, GREER JJ, ZOGHBI HY (2009) Math1 is essential for the development of hindbrain neurons critical for perinatal breathing. *Neuron* 64(3):341-54.

RUANGKITTISAKUL A, PANAITESCU B, BALLANYI K (2011) K(+) and Ca²⁺(+) dependence of inspiratory-related rhythm in novel "calibrated" mouse brainstem slices. *Respir Physiol Neurobiol.* 175(1):37-48.

RUANGKITTISAKUL A, SCHWARZACHER SW, SECCHIA L, POON BY, MA Y, FUNK GD, BALLANYI K (2006) High sensitivity to neuromodulator-activated signaling pathways at physiological [K⁺] of confocally imaged respiratory center neurons in on-line-calibrated newborn rat brainstem slices. *J. Neurosci.* 26(46):11870-80.

RUANGKITTISAKUL A, SCHWARZACHER SW, SECCHIA L, MA Y, BOBOCEA N, POON BY, FUNK GD, BALLANYI K (2008) Generation of eupnea and sighs by a spatiochemically organized inspiratory network. *J. Neurosci.* 28(10):2447-58.

RUBIN JE, HAYES JA, MENDENHALL JL, DEL NEGRO CA (2009) Calcium-activated nonspecific cation current and synaptic depression promote network-dependent burst oscillations. *Proc. Natl. Acad. Sci. U S A.* 106(8):2939-44.

SAKURADA K, MASU M, NAKANISHI S (1993) Alteration of Ca²⁺ permeability and sensitivity to Mg²⁺ and channel blockers by a single amino acid substitution in the N-methyl-D-aspartate receptor. *J. Biol. Chem.* 268(1):410-5.

SALLERT M, MALKKI H, SEGERSTRÅLE M, TAIRA T, LAURI SE (2007) Effects of the kainate receptor agonist ATPA on glutamatergic synaptic transmission and plasticity during early postnatal development. *Neuropharmacology.* 52(6):1354-65.

SALO LM, CAMPOS RR, MCALLEN RM (2006) Differential control of cardiac functions by the brain. *Clin. Exp. Pharmacol. Physiol.* 33(12):1255-8.

SASAKI YF, ROTHE T, PREMKUMAR LS, DAS S, CUI J, TALANTOVA MV, WONG HK, GONG X, CHAN SF, ZHANG D, NAKANISHI N, SUCHER NJ, LIPTON SA (2002) Characterization and comparison of the NR3A subunit of the NMDA receptor in recombinant systems and primary cortical neurons. *J. Neurophysiol.* 87(4):2052-63.

SCHREIHOFFER AM, STORNETTA RL, GUYENET PG (1999) Evidence for glycinergic respiratory neurons: Botzinger neurons express mRNA for glycinergic transporter 2. *J Comp Neurol.* 407(4): 583-97.

SCHWARZACHER SW, RÜB U, DELLER T (2001) Neuroanatomical characteristics of the human pre-Bötzinger complex and its involvement in neurodegenerative brainstem diseases. *Brain* 134(1): 24-35.

SCHWARZACHER SW, SMITH JC, RICHTER DW (1995) Pre-Bötzinger complex in the cat. *J. Neurophysiol.* 73(4):1452-61.

SIMANTOV R, KUCHAR MJ, UHL GR, SNYDER SH (1977) Opioid peptide enkephalin: immunohistochemical mapping in rat central nervous system. *Proc Natl Acad Sci U S A.* 74(5):2167-71.

SIMMONS DA, REX CS, PALMER L, PANDYARAJAN V, FEDULOV V, GALL CM, LYNCH G (2009) UP-regulating BDNF with an ampakine rescues synaptic plasticity and memory in Huntington's disease knockin mice. *Proc Natl Acad Sci U S A.* 106(12):4906-11.

SMITH JC, ELLENBERGER HH, BALLANYI K, RICHTER DW, FELDMAN JL (1991) Pre-Bötzinger complex: a brainstem region that may generate respiratory rhythm in mammals. *Science* 254(5032):726-9.

SMITH JC, GREER JJ, LIU GS, FELDMAN JL (1990) Neural mechanisms generating respiratory pattern in mammalian brain stem-spinal cord *in vitro*. I. Spatiotemporal patterns of motor and medullary neuron activity. *J. Neurophysiol.* 64:1149-1169.

SMITH JC, MORRISON DE, ELLENBERGER HH, OTTO MR, FELDMAN JL (1989) Brainstem projections to the major respiratory neuron populations in the medulla of the cat. *J. Comp. Neurol.* 281(1):69-96.

SOBOLEVSKY AI, ROSCONI MP, AND GOUAUX E (2009) X-ray structure, symmetry and mechanism of an AMPA-subtype glutamate receptor. *Nature* 462:745–756.

SOLOMON IC, EDELMAN NH, NEUBAUER JA (1999) Patterns of phrenic motor output evoked by chemical stimulation of neurons located in the pre-Bötzinger complex *in vivo*. *J. Neurophysiol.* 81(3):1150-61.

SOMMER B, KEINÄNEN K, VERDOORN TA, WISDEN W, BURNASHEV N, HERB A, KÖHLER M, TAKAGI T, SAKMANN B, SEEBURG PH (1990) Flip and flop: a cell-specific functional switch in glutamate-operated channels of the CNS. *Science* 249(4976):1580-5.

STEIN C, LANG LJ (2009) Peripheral mechanisms of opioid analgesia. *Curr. Opin. Pharmacol.* 9(1):3-8.

- STELLA G (1938) On the mechanism of production, and the physiological significance of "apneusis". *J. Physiol.* 93(1):10-23.
- ST-JOHN WM, LEITER JC (2008) Maintenance of gasping and restoration of eupnea after hypoxia is impaired following blockers of alpha1-adrenergic receptors and serotonin 5-HT2 receptors. *J. Appl. Physiol.* 104(3):665-73.
- STORNETTA RL, ROSIN DL, WANG H, SEVIGNY CP, WESTON MC, GUYENET PG (2003) A group of glutamatergic interneurons expressing high levels of both neurokinin-1 receptors and somatostatin identifies the region of the pre-Bötzinger complex. *J. Comp. Neurol.* 455(4):499-512.
- STORNETTA RL, SCHREIHOFFER AM, PELAEZ NM, SEVIGNY CP, GUYENET (2001) PG. Preproenkephalin mRNA is expressed by C1 and non-C1 barosensitive bulbospinal neurons in the rostral ventrolateral medulla of the rat. *J. Comp. Neurol.* 435(1):111-26.
- STORNETTA RL, SEVIGNY CP, GUYENET PG (2003) Inspiratory augmenting bulbospinal neurons express both glutamatergic and enkephalinergic phenotypes *J Comp Neurol.* 455(1):113-24.
- STUESSE SL (1982) Origins of cardiac vagal preganglionic fibers: a retrograde transport study. *Brain Res.* 236(1):15-25.
- SUZUE T (1984) Respiratory rhythm generation in the *in vitro* brain stem-spinal cord preparation of the neonatal rat. *J. Physiol.* 354:173-83.
- TAKEDA S, ERIKSSON LI, YAMAMOTO Y, JOENSEN H, ONIMARU H, LINDAHL SG (2001) Opioid action on respiratory neuron activity of the isolated respiratory network in newborn rats. *Anesthesiology.* 95(3):740-9.
- TAKITA K, HERLENIUS EA, LINDAHL SG, YAMAMOTO Y (1997) Actions of opioids on respiratory activity via activation of brainstem mu-, delta- and kappa-receptors; an *in vitro* study. *Brain Res.* 778(1):233-41.
- TALLEY EM, LEI Q, SIROIS JE, BAYLISS DA (2000) TASK-1, a two-pore domain K⁺ channel, is modulated by multiple neurotransmitters in motoneurons. *Neuron* 25:399-410.
- TAN W, JANCZEWSKI WA, YANG P, SHAO XM, CALLAWAY EM, FELDMAN JL (2008) Silencing preBötzinger complex somatostatin-expressing neurons induces persistent apnea in awake rat. *Nature Neuroscience* 11(5):538-40.
- TAN W, PAGLIARDINI S, YANG P, JANCZEWSKI WA, FELDMAN JL (2010) Projections of preBötzinger complex neurons in adult rats. *J. Comp. Neurol.* 518(10):1862-78.

TATSUMI H, KATAYAMA Y (1994) Brief increases in intracellular Ca²⁺ activate K⁺ current and non-selective cation current in rat nucleus basalis neurons. *Neuroscience* 58(3):553-61.

TEMPEL A, ZUKIN RS (1987) Neuroanatomical patterns of the mu, delta, and kappa opioid receptors of rat brain as determined by quantitative *in vitro* autoradiography. *Proc Natl Acad Sci U S A.* 84(12):4308-12.

TIAN GF, PEEVER JH, DUFFIN J (1998) Bötzinger-complex expiratory neurons monosynaptically inhibit phrenic motoneurons in the decerebrate rat. *Exp. Brain Res.* 122(2):149-56.

TIAN GF, PEEVER JH, DUFFIN J (1999) Bötzinger-complex, bulbospinal expiratory neurones monosynaptically inhibit ventral-group respiratory neurones in the decerebrate rat. *Exp. Brain Res.* 124(2):173-80.

THOBY-BRISSON M, BOUVIER J, GLASCO DM, STEWART ME, DEAN C, MURDOCH JN, CHAMPAGNAT J, FORTIN G, CHANDRASEKHAR A (2012) Brainstem Respiratory Oscillators Develop Independently of Neuronal Migration Defects in the Wnt/PCP Mouse Mutant looptail. *PLoS One.* 7(2):e31140.

THOBY-BRISSON M, KARLÉN M, WU N, CHARNAY P, CHAMPAGNAT J, FORTIN G (2009) Genetic identification of an embryonic parafacial oscillator coupling to the preBötzinger complex. *Nature Neuroscience* 12(8):1028-35.

THOBY-BRISSON M, RAMIREZ JM (2001) Identification of two types of inspiratory pacemaker neurons in the isolated respiratory neural network of mice. *J. Neurophysiol.* 86(1):104-12.

THOBY-BRISSON M, TELGKAMP P, RAMIREZ JM (2000) The role of the hyperpolarization-activated current in modulating rhythmic activity in the isolated respiratory network of mice. *J Neurosci.* 20(8):2994-3005.

THOMPSON RC, MANSOUR A, AKIL H, WATSON SJ (1993) Cloning and pharmacological characterization of a rat μ opioid receptor. *Neuron* 11(5):903-913.

THOR KB, HELKE CJ (1987) Serotonin- and substance P-containing projections to the nucleus tractus solitarii of the rat. *J. Comp. Neurol.* 265(2):275-93. Review.

TOPPIN VA, HARRIS MB, KOBER AM, LEITER JC, ST-JOHN WM (2007) Persistence of eupnea and gasping following blockade of both serotonin type 1 and 2 receptors in the *in situ* juvenile rat preparation. *J. Appl. Physiol.* 103(1):220-7.

TRYBA AK, PEÑA F, RAMIREZ JM (2006) Gasping activity *in vitro*: a rhythm dependent on 5-HT_{2A} receptors. *J. Neurosci.* 26(10):2623-34.

WALLÉN-MACKENZIE A, GEZELIUS H, THOBY-BRISSESON M, NYGÅRD A, ENJIN A, FUJIYAMA F, FORTIN G, KULLANDER K (2006) Vesicular glutamate transporter 2 is required for central respiratory rhythm generation but not for locomotor central pattern generation. *J. Neurosci.* 26(47):12294-307.

WANG JB, IMAI Y, EPPLER CM, GREGOR P, SPIVAK CE, UHL GR (1993) mu opiate receptor: cDNA cloning and expression. *Proc. Natl. Acad. Sci. U S A.* 90(21):10230-4.

WANG W, PIZZONIA JH, RICHERSON GB (1998) Chemosensitivity of rat medullary raphé neurones in primary tissue culture. *J. Physiol.* 511 (Pt 2):433-50.

WANG H, STORNETTA RL, ROSIN DL, GUYENET PG (2001) Neurokinin-1 receptor-immunoreactive neurons of the ventral respiratory group in the rat. *J. Comp. Neurol.* 434(2):128-46.

WANG SJ, WANG KY, WANG WC (2004) Mechanisms underlying the riluzole inhibition of glutamate release from rat cerebral cortex nerve terminals (synaptosomes). *Neuroscience* 125(1):191-201.

WARD SJ, HOLADAY JW (1982) Relative involvement of mu and delta opioid mechanisms in morphine-induced depression of respiration in rats. *Proc. Soc. Neurosci.* 8,388.

WATERFIELD AA, SMOKCUM RW, HUGHES J, KOSTERLITZ HW, HENDERSON G (1977) *In vitro* pharmacology of the opioid peptides, enkephalins and endorphins. *Eur. J. Pharmacol.* 43(2):107-16.

WESTON MC, STORNETTA RL, GUYENET PG (2004) Glutamatergic neuronal projections from the marginal layer of the rostral ventral medulla to the respiratory centers in rats. *J. Comp. Neurol.* 473(1):73-85.

WHITAKER-AZMITIA PM, DRUSE M, WALKER P, LAUDER JM (1996) Serotonin as a developmental signal. *Behav Brain Res.* 73(1-2):19-29.

WISDEN W, SEEBURG PH (1993) A complex mosaic of high-affinity kainate receptors in rat brain. *J Neurosci.* 13(8):3582-98.

WONG-RILEY MT, LIU Q (2005) Neurochemical development of brain stem nuclei involved in the control of respiration. *Resp. Physiol. Neurobiol.* 149(1-3): 83-98.

WU H, WACKER D, MILENI M, KATRITCH V, HAN GW, VARDY E, LIU W, THOMPSON AA, HUANG XP, CARROLL FI, MASCARELLA SW, WESTKAEMPER RB, MOSIER PD, ROTH BL, CHEREZOV V, STEVENS RC (2012) Structure of the human

κ -opioid receptor in complex with JDTic. *Nature*. doi: 10.1038/nature10939.
[Epub ahead of print]

XU J, XU M, ROSSI GC, PASTERNAK GW, PAN YX (2011) Identification and characterization of seven new exon 11-associated splice variants of the rat μ opioid receptor gene, OPRM1. *Mol. Pain*. 7(1):9.

YAKSH TL (1997) Pharmacology and mechanisms of opioid analgesic activity. *Acta Anaesthesiol Scand*. 41(1 Pt 2):94-111.

YAU HJ, BARANAUSKAS G, MARTINA M (2010) Flufenamic acid decreases neuronal excitability through modulation of voltage-gated sodium channel gating. *J. Physiology* 588(20): 3869-3882.

YING-XIAN P (2005) Diversity and Complexity of Mu opioid receptor gene: alternative pre-mRNA splicing and promoters. *DNA AND CELL BIOLOGY* 24(11): 736-750.

ZHANG, A-Z, PASTERNAK GW (1981) Ontogeny of opioid pharmacology, and receptors: high and low affinity site differences. *European J. Pharmacol*. 73(1):29-40.

CHAPTER 2

MATERIAL AND METHODS

2.1 MATERIAL AND METHODS FOR ELECTROPHYSIOLOGICAL RECORDINGS

2.1.1 BRAINSTEM SPINAL CORD PREPARATION

All experimental procedures were approved by the Faculty of Medicine and Dentistry Animal Welfare Committee of the University of Alberta. Brainstem spinal cord preparations were isolated in cold, saturated artificial cerebrospinal fluid (aCSF) [containing in mM: 128 NaCl, 3 KCl, 1.5 CaCl₂; 1 MgCl₂; 0.5 NaH₂PO₄; 23.5 NaHCO₃, 30 D-Glucose] maintained and equilibrated with carbogen (95% O₂; 5% CO₂) at pH = 7.4. This aCSF solution was used for dissection and perfusion vehicle for all the experiments. Newborn Sprague-Dawley (SD) rats P0 to P5 were anaesthetized via inhalation of isoflurane, decerebrated and the neuraxis isolated. The preparation extended rostrally from the level of the caudal pons to approximately the 7th cervical segment caudally. The preparation was pinned down on a Sylgard resin for removal of the dura and pia mater.

2.1.2 MEDULLARY SLICE PREPARATION

The medullary slice preparation was the main electrophysiological model used in this thesis work. All rhythmic medullary slices were obtained from brainstem spinal cord preparations isolated from neonatal rodents (P0-P5). Medullary slices contained the preBötzinger complex (preBötC), the semi-compact division of the nucleus ambiguus (NAsc), the raphé nucleus obscurus (RNO), inferior olive (IO), part of the nucleus raphé pallidus, part of the NTS, and rostral part of the XII motor nucleus. Robust rhythmic inspiratory-related motor activity could be recorded from rostral XII nerve rootlets for several hours. Medullary slices were prepared as follows. An isolated brainstem spinal cord was pinned down on its dorsal side to a wax chuck. Fine pins were used to hold the brainstem spinal cord in place. The whole chuck was then transferred and securely

fixed to a slicing chamber. The brainstem spinal cord was quickly immersed in cold and carbogenated aCSF. Using a vibratome (Leica, VT1000S, Germany), transverse sequential 100 to 300 μm slices were cut from the rostral to caudal direction and anatomical landmarks of each slice were assessed with a dissecting microscope (Leica, WILD M3C, Germany). Sections were discarded until the appearance of a developed inferior olive (IO) (see newborn rat brainstem atlas in Ruangkittisakul et al., 2006). At this point the final rhythmic slice was cut with a thickness of 700 μm . The rhythmic medullary slice preparation extended from the preBötC on its rostral margin, to a point just caudal to the obex at its caudal end. The rhythmic slice was placed into a glass-bottom recording chamber containing pre-warmed [26 to 27 degrees Celsius ($^{\circ}\text{C}$)] aCSF and mounted on a fixed stage upright Zeiss Axioskop FS Plus microscope (Zeiss, Germany; Fig. 2.1). Nylon threads stretched and glued onto a flattened platinum horseshoe shaped device were used to hold the slice in place in the recording chamber. The carbogenated aCSF circulated at a flow rate of 5 mL/min via a peristaltic minipulse pump (Minipuls 3, Gilson Inc.) and its potassium concentration was raised to 9 mM to enhance long lasting inspiratory activity. Rhythmic inspiratory-related activity was monitored by suction of a XII nerve rootlet into an extracellular glass suction electrode connected to a pre-amplifier (Life Electronics Ltd QT 5c) and extracellular amplifier (Power-One, Bauart Geprüft, D.C. Power supplies). Signals were amplified (X2000), band pass filtered (High pass filter: 0.1Hz - Low pass filter: 3Hz), rectified, integrated, and captured using a Digidata 1322 A/D board (sampling rate of 2–10 kHz, Axon instruments). A fifteen to twenty minute stabilizing period was allowed before starting recording sessions.

2.1.3 WHOLE-CELL PATCH-CLAMP RECORDING TECHNIQUE

Visualized, whole-cell patch-clamp recordings were performed using infrared-differential interference contrast optics (IR-DIC). Targeted preBötC neurons were localized ventral to the NAsc. RNO neurons localized on the edges of either side of the midline and just dorsal to the IO were targeted. Intracellular

pipettes were pulled with a vertical puller (PC-10, Narishige, Japan) and had resistances of 3-7 mega-ohms when filled with internal solution. The same internal solution was used for all whole-cell recordings and contained (in mM): 140 KCl, 1 MgCl₂, 0.3 Na₃GTP, 10 HEPES, 10 EGTA, 2 CaCl₂ and 2 MgATP (pH adjusted at 7.25 with KOH, osmolarity adjusted to 290-310 mOsm). In some experiments, neurobiotin at 0.2% (Vector Laboratories, Burlington, ON) was added to the internal solution immediately prior to the experiment. The patch-clamp pipette was positioned close to the targeted cell under positive pressure (10 to 40 psi) until the appearance of a small meniscus around the patch electrode. Tight seals 1 to 10 giga-Ohms were established in voltage-clamp by very brief suction of the membrane. Once a seal was formed it was ruptured by gentle and brief suction. Both voltage- and current-clamp recordings were made using a NPI amplifier (NPI Electronics GmbH, Germany). Data were filtered (1.3 KHz current filter; 13 KHz potential filter) prior to being acquired using a computer interface (Digidata 1322A) and pClamp 9.2 and 10 software (Molecular Device, Sunnyvale, CA). Switch to the current-clamp configuration was made to identify the impaled cell type based on firing pattern. Typically, inspiratory related neurons that fired action potential bursts in phase with XII nerve motor discharge were selected (Figs.2.2 and 2.3).

Neurons were routinely held in voltage-clamp at -60 mV (-47 mV online for liquid junction potential compensation) except when examining changes in membrane potential. Voltage-clamp recordings were corrected offline for the calculated 13.5 mV liquid junction potential. Recordings of neuronal properties were made immediately after obtaining whole-cell configuration. Cell input resistance (R_N), membrane capacitance (C_M) and membrane time constant (τ) were calculated from small negative voltage responses to hyperpolarizing current steps in current-clamp mode and from current responses to small discontinuous depolarizing voltage steps in voltage-clamp mode. Stability of discharge activity, the holding current and access resistance over a period of at least 5 minutes was a prerequisite prior to the initiation of any experimental manipulation. Recordings of R_N and τ , including an assessment of access resistance, were made prior to

drug application (control), during drug perfusion (lasting approximately 10 to 20 minutes), and at 10 or 20 minutes during the washout period. A slow, positive-going voltage-ramp protocol (18 mV/s, starting at -135 mV to -55 mV) was used to assess changes to the steady-state membrane current-voltage (I-V) relationship.

2.1.4 DRUG APPLICATION

The following drugs were used: [D-Ala², NMe-Phe⁴, Gly-ol⁵]-enkephalin (DAMGO), tetrodotoxin (TTX), alpha-amino-3-hydroxy-5-methyl-4-isoxazolepropionic acid (AMPA), ampakine 1-(1,4-benzodioxan-6-ylcarbonyl) piperidine (CX546), 2,3-Dioxo-6-nitro-1,2,3,4 tetrahydrobenzo[f]quinoxaline-7-sulfonamide (NBQX), N-Methyl-D-aspartic acid (NMDA), L-glutamic acid and glycine were all purchased from Sigma (St Louis, MO). 6-Cyano-7-nitroquinoxaline-2,3-dione (CNQX) and cyclothiazide were purchased from Tocris Biosciences (Bristol, United Kingdom). Forskolin, NKH 477 (the water soluble form of forskolin), naloxone and the specific μ -opoid receptor antagonist Cys-Tyr-D-Trp-Orn-Thr-Pen-Thr-NH₂ (CTOP) were all purchased from Ascent Scientific (Princeton, NJ). All other ampakine compounds (CX614, CX717, CX1763, CX1942 and CX1739) were provided by Cortex Pharmaceuticals Inc (Dr. Mark Varney, CEO, Irvine CA). Stock solutions of ampakines and forskolin were made in DMSO to a final concentration of $\leq 0.02\%$ (bath application) or $\leq 0.4\%$ (local application) and frozen in aliquots. DMSO alone at these concentrations has been previously found to be without effect on baseline inspiratory behavior. Stock solutions of all other drugs were made in standard aCSF and frozen in aliquots. The final concentration of potassium in the drug solutions was matched to that of the perfusing aCSF solution.

Drugs were either applied to the bathing media or locally applied by microinjection with triple-barrel pipettes (tip diameter $\sim 5\text{--}8\ \mu\text{m}$ per barrel O.D.) pulled from borosilicate glass capillaries (World Precision Instruments, Sarasota, FL). For local microinjections, drug pipettes were placed into position under microscope visualization so that the tip was just above the surface of the tissue or

between 100 and 200 μm from the recorded neuron for puff applications to individual neurons. Drug microinjections (~ 10 psi) were controlled via a picospritzer (Dagan Corporation, Minneapolis, USA) triggered by a pulse generator (Master8, A.M.P.I., Jerusalem, Israel). Local injection within the RNO was established by first verifying the region around the midline for the site that gave the maximum inspiratory burst frequency increase in response to a local application of AMPA (Al-Zubaidy et al., 1996; Ptak et al., 2009). Knowing that the concentration of drug decreases exponentially with distance from the pipette tip when performing local application (Nicholson, 1985), the concentration used in local application experiments was 10-fold the concentration that would be used for bath application to produce similar effects (Liu et al., 1990).

2.1.5 DATA ACQUISITION, PROTOCOLS AND STATISTICAL ANALYSIS

2.1.5.1 Respiratory event analysis

Clampex.10 and Axoscope.10 were the two data acquisition modules of pClamp10 used to monitor and record all electrophysiological data. Clampfit.10 was the analysis module of pClamp10 used to process and analyze all electrophysiological data offline.

The effect of locally-applied drugs on inspiratory activity was assessed by applying a threshold search through Clampfit.10 and measuring parameters in recorded XII nerve integrated traces. Mean values of XII burst parameters (frequency, amplitude, area and duration) were calculated pre and post-drug application for a period of 2 minutes for each experimental condition. For delayed effects, burst parameters were calculated during the observed effect of the drug. Recovery values were calculated at least 10 minutes after the end of drug application, over a 2 minutes period

When drugs were applied to the bathing solution, the bathing volume was decreased from 300 mL to 50 mL and the control XII nerve bursting values were assessed in that volume, prior to drug application. Also for bath application

experiments, a larger time window of 4 to 5 minutes was used to estimate the XII nerve burst discharge characteristics or inspiratory input current/depolarization events for each experimental condition.

The effect of drugs on inspiratory synaptic currents in raphé and preBötC neurons was examined by performing a template search through Clampfit.10. The average amplitude, frequency and area of inspiratory synaptic currents were collected on a 2 minute time frame of drug exposure (for local applications) or 5 minute time frame (for bath applications). Data were compared with those obtained for the same time period prior to drug application.

After all electrophysiological data were analyzed with Clampfit 10 and results were exported to Microsoft Excel 2010, SigmaPlot.11 and/or GraphPad Prism.5 for statistical analysis and data plotting. Values were normalized against paired control and expressed as mean \pm standard error of the mean (s.e.m.). For statistical analysis comparing two data groups, statistical significance was tested using paired Student's *t* test and was accepted at *p* values < 0.05. For statistical analysis involving one variable evaluated in more than two groups, an analysis of variance (one-way ANOVA followed by a Tukey's post-test, unless otherwise stated) was performed and significance was accepted when *p* values < 0.05. Note that, when using normalized data, a normality test (Kolmogorov-Smirnov test) was used before the ANOVA.

2.1.5.2 Agonist-induced currents

Using Clampfit.10 analyzer, the agonist-evoked current features (peak amplitude, rise time, rise slope) were automatically detected. The amplitude was determined by subtracting the baseline current averaged over a 5 to 10 sec control period immediately preceding agonist application, from the peak of the agonist-induced current. Data reported were relative to the average value during the control period that immediately preceded drug application. The rise time represents the time required for the current to reach from 10 to 90 % of the peak, and the rise slope represents a measurement of the velocity of the ionic current during that time frame. Additional current characteristics (decay time, decay time

constant, area and duration) were determined by taking into account the end of the agonist-induced current. Specifically, the end of the agonist-induced current was automatically set as being the first value after the peak, equal or above the average current value of the control period. For current area and duration both beginning and end of each current were taken into account. The decay time represents the time required for the current to reach from 90 to 10 % of the peak during the decay phase and the decay time constant was determined by fitting the decay portion of the current with a monoexponential curve.

2.1.5.3 Spontaneous postsynaptic current analysis

Analyses of synaptic events (see Derkach, 2003) were performed automatically using a template search (Clampfit) and the reliability of the detection criteria confirmed via visual inspection. To examine interburst synaptic modulation by the ampakine CX614, spontaneous postsynaptic currents were recorded at resting membrane potential (resulting in inward PSCs) were analyzed. In cases when presynaptic activity was strong, miniature synaptic currents could be recorded in presence of 0.5 μM TTX for gap-free periods of 20 min, under control and one or more experimental conditions, using either Clampex.9.2 or Axoscope.9.2 (Axon Instruments).

Cumulative probability plots were generated in some cases to evaluate the effect of various drugs on the amplitude, decay time constant and inter-event interval distribution of sPSCs. Individual amplitude, decay time constant or inter-event intervals of increasing size were ranked. Rank values were plotted against corresponding amplitude, decay time constant or inter-event interval. For data populations that were identically distributed, a Kolmogorov-Smirnov test was used to compare each distribution of amplitude, decay time constants or inter-event intervals. When data sets were not normally distributed the non-parametric Wilcoxon matched pairs test was used to assess differences between two groups of data sets. For group data graphs relative data were reported as mean \pm s.e.m. Differences between means were assessed on relative data using Student's *t* test.

Differences between means were considered significant when at least $p < 0.05$ (Graphpad Prism 5.2).

2.1.5.4 Input resistance and capacitance measurements

Drug-induced changes in R_N were calculated based on current responses to voltage ramps (from -90 to -40 mV) when cells were recorded under voltage-clamp configuration and inverted voltage responses to hyperpolarizing current steps (-50 pA; 180 ms) when cells were recorded under current-clamp configuration. The protocols were applied on the same cell before, during, and after application of a drug to assess drug-induced R_N changes. R_N was estimated from the inverse slope of the linear portion of the current-voltage (I/V) relationship (in voltage-clamp), or from dividing the resulting potential difference by the current pulse amplitude (in current-clamp).

Cell capacitance (C_M) was determined from analysis of the transient capacitative current evoked from a 10 ms hyperpolarizing step of 20 mV, using the formula $C_M = \tau (1/R_s + 1/R_p)$, where R_s is the estimated series resistance of the recording pipette, R_p is the cell membrane resistance and τ the exponential decay time constant of the current (Gentet et al., 2000). R_s could be measured by placing the pipette filled with internal solution in the bathing medium and analyzing the transient capacitative current evoked from a 10 ms hyperpolarizing step of 20 mV. R_s and R_p were calculated as $R_s = V_{\text{step}}/I_{\text{peak}}$ and $R_p = V_{\text{step}}/I_{\text{ss}} - R_s$, where V_{step} is the amplitude of the voltage step, I_{peak} is the peak amplitude of the current transient and I_{ss} is the steady-state current following the step.

2.1.5.5 Protocols

General conductance protocol

In some instances, under voltage-clamp configuration, ionic currents of the cell being recorded were assessed by applying a voltage step protocol that ranged from -120 mV up to +100 mV, with 10 mV increments and a fixed pulse width of 100 ms duration. The protocol was used before and during drug treatment.

Steady-state currents evoked by the voltage steps were then plotted offline as current-voltage relationship in order to evaluate the effect of the drug on particular ionic currents.

I_h current protocol

To study I_h, a family of hyperpolarizing voltage steps was applied from a holding potential of -55 mV (-65 to -125 mV in 10 mV increments; the initial step lasted 1800 ms, and each subsequent step was successively shortened by a 100 ms increment to prevent damage to the patched cell). The magnitude of I_h at a given potential step was determined as the difference between the initial peak negative current amplitude and the final steady-state current amplitude for each step.

Action potential and voltage threshold analysis

Action potentials (APs) were evoked by applying a series of depolarizing currents steps of varying intensities to a recorded neuron. More specifically, action potential and voltage threshold analysis were evaluated by evoking APs with 500 ms depolarizing current steps of varying intensities; AP frequency was determined using Clampfit. The relationship between AP frequency and intensity of injected current (f-I curve) was characterized for individual neurons. Instantaneous and steady-state AP firing frequencies were measured from the interval between the first and second AP, and the interval between the last two APs elicited during the prolonged depolarizing step, respectively.

2.2 METHODOLOGY FOR IMMUNOHISTOCHEMISTRY AND IMMUNOCYTOCHEMISTRY

2.2.1 IMMUNOHISTOCHEMISTRY OF TRANSVERSE MEDULLARY SLICES

2.2.1.1 Tissue preparation and paraffin sections

Brainstem spinal cord preparations were isolated from neonatal SD rats (P0-P4) and the rostral boundaries were cut with a scalpel under a dissecting microscope (Leica model # WILD M3C). In some cases, freshly isolated brainstem spinal cord preparations were incubated for 30 minutes in μ -opioid agonist (DAMGO, 1 μ M) at 37°C to allow internalization of μ -opioid receptors. The brainstem-spinal cord preparations were then fixed in 4% paraformaldehyde in 0.1 mM phosphate buffer for a minimum of 24 hours at 4°C. The fixed brainstem was then dehydrated in a graded series of ethanol incubations (from 50% to 100% ethanol) and cleared with xylene. The tissue was embedded in melted paraffin wax overnight in an appropriate oven (Precision Science Co., model #16). Tissue blocks were sectioned to obtain serial transverse slices (4 to 8 μ m thick) using a rotary microtome (Lipshaw MFG Co. model # 45, Detroit Michigan). Tissue slices were extended on warm water (Fisher Scientific Co., TISSUEMAT water bath) and mounted on poly-L-lysine coated glass slides. In some experiments, sections were mounted on pairs of slides so that two thin sections mounted on one slide were always followed by two thin sections on the paired slide. This procedure was mainly used when performing DAB staining to ensure that the protein of interest was expressed within the preBötC characterized by higher level of NK1R labeling. Sections were baked overnight, dewaxed with xylene, and rehydrated through a graded series of ethanol washes and rinsed in phosphate buffered saline solution (PBS).

2.2.1.2 Immunolabeling

All sections were pre-incubated for 30 min to 1 hour with 3% donkey serum (DS) in PBS with Triton X-100 (0.3%) and incubated for 24 hours at room temperature with the appropriate primary antibody (See Table 3.1). All primary antibodies were diluted in PBS with 3% DS and 0.3% Triton X-100. The sections were then washed with PBS and left for 60-90 min with a mixture of fluorophore-conjugated secondary antibodies diluted in PBS and 0.1% bovine serum albumin (BSA) or 3% DS. Secondary antibodies were generally used at a 1:200 ratio. In some cases a combination of biotinylated secondary antibody followed by an incubation with streptavidin 488 (Molecular Probes, Eugene, OR) was used. After incubation with the secondary antibody, sections were washed with PBS and coverslipped with fluorosave mounting medium (Calbiochem, San Diego, CA). In cases where two primary antibodies were from the same species [as for example with the rabbit anti-mu-opioid receptor 1a (MOR1A) and the rabbit anti-NK1R], the tyramide signal amplification kit Plus fluorescein was used (PerkinElmer, Boston, MA) and the protocol was followed according to the manufacturer's instructions.

2.2.1.3 Image acquisition

Confocal images were obtained with a laser-scanning confocal microscope (Zeiss; model LSM 150). Alexa Fluor 488, Cy3, and Cy5 were excited at 488, 543, and 633 nm emission wavelengths respectively, and collected using 505 nm, 560 nm and 630 nm filters respectively. Images were acquired and processed with Zeiss Zen Light Edition 2009 system software and presented as single optical sections. Acquired images were exported in JPEG or Bitmap format and image brightness and contrasts were adjusted in Adobe Photoshop or Image J Software.

DAB-immunostained sections were analyzed with a Leica microscope (model # DM5500B) and images captured with a digital microscope camera (model HAMAMATSU CI0600-ORCAR²) connected to a computer running Quorum Analysis Metamorph software (Molecular Devices, Sunnyvale, CA).

Acquired images were exported in TIFF format; brightness and contrast were also adjusted in Image J and/or Adobe Photoshop Software before publication.

In some experiments, neurobiotin-filled neurons were reconstructed. Slices were fixed and rinsed as described above, then pretreated for 30 min with 0.3% H₂O₂ in PBS with 0.3% Triton X-100 (PBS-T). Slices were left in PBS-T for 1 hour and rinsed 3 times for 5 min with PBS. Slices were then incubated overnight at 4°C in an avidin-biotinylated horseradish peroxidase avidin D reagent (Vector Laboratories). Slices were then rinsed with PBS, and reacted with diaminobenzidine (DAB) (DAB kit, Vector Laboratories). Slices were dehydrated, cleared with xylene, mounted in slides, coverslipped, and coated with Permount (Fisher Scientific). Labeled cell bodies were visualized with light microscopy.

For verification of recording sites, fluorescent beads were added to the drug solution used for local application. After recording, slices were placed in phosphate-buffered 4% paraformaldehyde at 4°C for at least 24 hours. The slice was then immersed in agar and sectioned (50 µm) with a vibratome. After wet mounting the slices on glass slides cytoarchitectonic identification of injection sites was done either directly or after counterstaining with cresyl violet.

2.2.2 IMMUNOCYTOCHEMISTRY OF HEK293 CELLS

After transfection, cells were washed with Dulbecco PBS (D-PBS) 3 times, then 4% paraformaldehyde was applied for 15 minutes before being washed again 2 times with PBS and stored at 4°C. To permeabilize the cells and block non-specific protein-protein interactions, cells were left for one hour in 10% DS or left for 30 minutes in 5% BSA. Primary and secondary antibodies were used according to Table 2.1.

2.3 MATERIAL AND METHODS FOR PROTEIN EXPRESSION IN HEK293 CELLS

2.3.1 HEK293 CELL CULTURE

Human embryonic kidney cell lines (HEK 293 and HEK293T) were kindly provided by Dr Warren Gallin (University of Alberta). Cells were grown in 25 cm² flasks (BD Falcon # 353108, Bedford, MA) with Dulbecco's minimal essential medium (DMEM # 11995065, Invitrogen, Carlsbad, CA) supplemented with 10% fetal bovine serum (GIBCO #16000036, Carlsbad, CA), 1% penicillin (100 units/mL) and streptomycin (100 µg/mL) (Invitrogen #15140122, Carlsbad, CA), incubated at 37°C and 5% CO₂ incubation. As soon as they reached 80-90% confluency (typically biweekly), cells were carefully washed with Dulbecco's phosphate buffered saline solution (D-PBS; Hyclone, Logan, UT) and lifted from the dish after 2 to 5 min incubation with 300 µL TrypLE Express (Invitrogen, Carlsbad, CA). 2 mL of culture medium was used to quench TrypLE activity. Cells were resuspended as a single cell suspension by gentle pipetting in order to break up cell clumps. 150 µL of suspension was used for seeding. Culture media was exchanged every 2 days. Cell culture was typically discarded after 19 passages.

One day before plating the cells for transfection, 15 mm circular and sterilized poly-L/D-lysine coated glass coverslips (Biokeystone # GG-15-PLL or # GG-15-PDL, El Monte, CA) were placed onto 60 mm culture dish. Laminin (Sigma # L 2020) was thawed slowly on ice and diluted in Hank's balanced salt solution (HBSS) at 10 µg/mL. 100 µL drop of diluted laminin was put on the centre of the coverslips and left overnight (or at least 5 hours) in a culture incubator at 37°C. The laminin solution was then suctioned and the coverslips were washed with D-PBS (Hyclone, Logan, UT) before being flooded with culture medium and used to plate the cells. 400 µL out of 2 mL suspension was used for seeding before transfection on the following day. In some cases, cells

were plated after transfection and incubated for 5 hours at 37°C to allow single cell attachment to the coverslips for electrophysiological recordings.

2.3.2 HEK293 CELL TRANSFECTION WITH RECOMBINANT RECEPTORS

The rat NMDA receptor subunit cDNAs NR1-1a, NR3A and NR3B were used in the study. The NR1-1a subunit (*Rattus Norvegicus*, Genbank accession number U08261) was subcloned in a pcDNA1.1/Amp vector and this plasmid was kindly provided by Dr. Shigetada Nakanishi (Osaka Bioscience Institute, Japan). The NR3A subunit and NR3B (*Rattus Norvegicus*, Genbank accession number L34938 or U29873, and AF440691 or AF396649 respectively) were each subcloned in a pcDNA3.1(+) vector and were both provided by Dr. Stuart Lipton (Burnham Institute, San Diego, CA; see NR3A and NR3B plasmid map in annex 1 and annex 2). A blanked EGFP plasmid was used (pEGFP-C2 GeneBak number U57606) to evaluate the transfection efficiency. Plasmids were released with Tris-EDTA Buffer for 6 hours at room temperature and DNA concentration was evaluated using spectrophotometry. cDNAs were cloned via transformation using chemical heat shock method of 5-alpha competent E.Coli bacterial host (New England BioLabs). The transformation was made following the New England BioLabs protocol instructions (NEB 5-alpha competent E.coli C2987H). Transformation efficiency of this method ranges between 1 and 3 X 10⁹ transformants/μg of DNA when optimized. Ampicillin (100 μg/mL) was used to select successful DNA plasmid transformants and the QIAGEN Plasmid Midi Kit or the Endo-free Plasmid Maxi Kit (Qiagen) was used for DNA purification.

NR1, NR3A and NR3B plasmids were mixed with the reporter gene EGFP plasmid. We used 2 to 6 μg total per culture dish at a (1:2:2):5 or (1:1:1):10 ratio and transfected into HEK293 cells following manufacturer's instructions using Lipofectamine 2000, Lipofectamine LTX Plus Reagent (Invitrogen, Carlsbad, CA) or X-Treme GENE 9 DNA Transfection Reagent (Roche Applied Sciences).

OPTIMEM I was used as a transfection medium (Invitrogen # 11058021, Carlsbad, CA).

After transfection, the medium was removed by gentle aspiration; cells were carefully washed with D-PBS three times and flooded with warmed culture medium containing glutaMAX (Invitrogen, Carlsbad, CA) rather than glutamine, no sodium pyruvate and no antibiotics. Cells were incubated for at least 24 hours at 28 or 37 °C and 5% CO₂ to allow single cell accumulation of the desired NR1/NR3 ion channels. Cells were recorded 1 to 6 days after transfection.

2.3.3 ELECTROPHYSIOLOGY OF TRANSFECTED HEK293 CELLS

Culture dishes containing transfected cells were taken out of the incubator and the culture medium was replaced by the sterilized HBSS bathing solution. Coverslips were placed in the recording chamber and it was quickly flooded with circulating sterilized HBSS solution at 2 mL/min, oxygenated with 100% oxygen.

As described for work with slices, drug pipettes were prepared prior to electrophysiological recording. Drugs used were glycine (Sigma, CAT), CX717 (Cortex Pharmaceutical), glutamate (Sigma) and D-Serine (Sigma). All drugs were prepared in sterilized HBSS, except for CX717 that was diluted in DMSO.

HBSS contained (in mM): 146 NaCl, 2.5 KCl, 2 CaCl₂, 1 MgCl₂, 20 D-Glucose, 10 HEPES (pH = 7.4 adjusted with NaOH; 310 Osm) or 153 NaCl, 5.4 KCl, 1.8 CaCl₂, 10 D-Glucose, 5 HEPES (pH = 7.4 adjusted with NaOH; 310 Osm). Intracellular solution contained: 140 CsCl, 4 NaCl, 0.5 CaCl₂, 5 EGTA, 10 HEPES, 0.5 NaGTP, 2 MgATP (pH = 7.33 adjusted with CsOH; 315 Osm) or 117 CsGluconate, 9 NaCl, 10 EGTA, 10 HEPES, 2 MgCl₂ (pH = 7.2; 315 Osm).

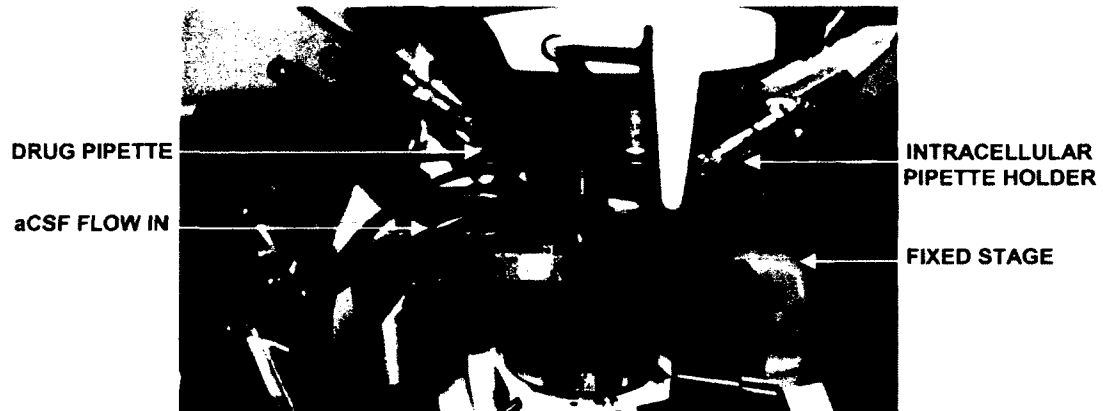


Figure 2.1 Photograph of the electrophysiological chamber used for recording inspiratory activity from a medullary slice preparation.

The slice is held on a chamber, immersed in a circulating flow in and out with an artificial cerebrospinal solution, and fixed on a stage. This set up allows concomitant single-cell visualized intracellular recording, focal injection of specific drugs and extracellular recording from XII nerves.

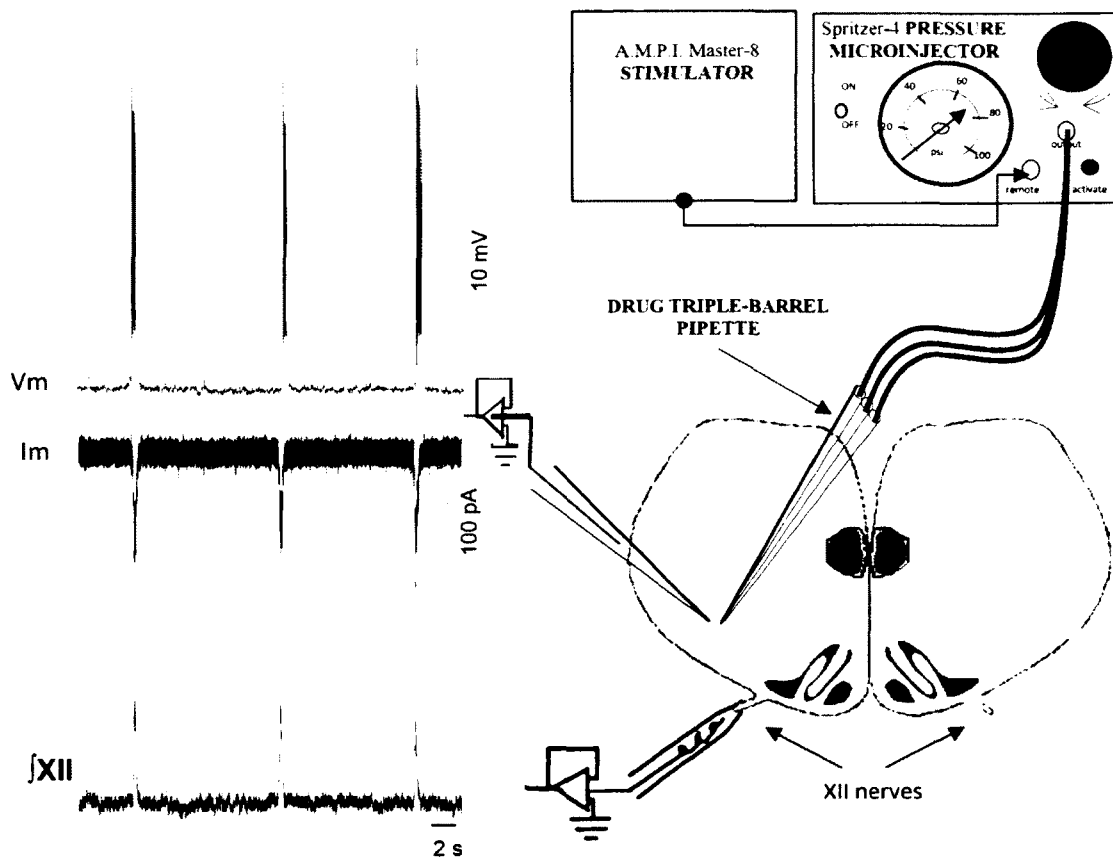


Figure 2.2 Schematic diagram of a rhythmically-active medullary slice preparation used for recordings of preBötC neurons and hypoglossal nerve activity.

PreBötC (light grey circles) inspiratory neuron display spontaneous depolarizing discharges in current-clamp recording and spontaneous rhythmic input currents in voltage-clamp recording. This spontaneous cellular activity of the preBötC inspiratory neuron is synchronized throughout the network and correlates with inspiratory motor output. Hypoglossal (XII) nerve activity is recorded as a reference for inspiratory motor output. Drugs can be added to the bath or locally pressure injected via a triple-barrel drug pipette that can contain up to three different drugs. The pressure injector is controlled by a stimulator. All characteristics of the microinjections (duration, intervals, etc.) can be controlled by the stimulator.

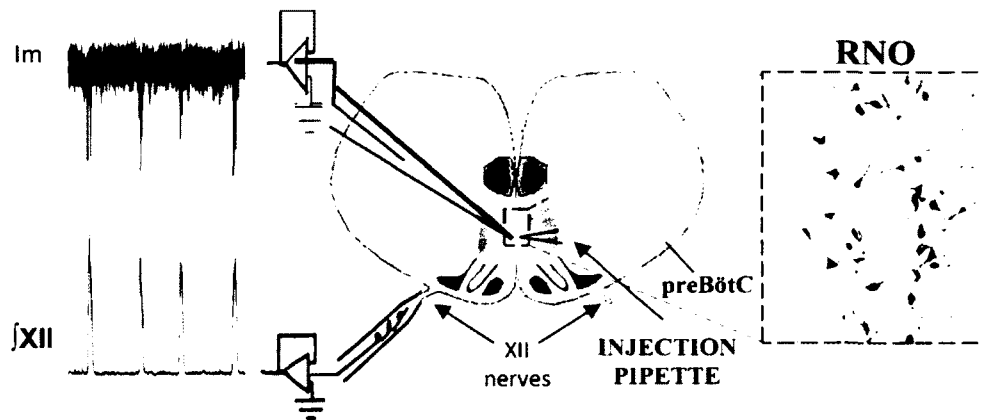


Figure 2.3 Schematic diagram of the medullary slice preparation and the recording of a respiratory neuron of the RNO.

The *in vitro* medullary slice preparation which generates spontaneous rhythm recorded from XII nerve rootlets also contains respiratory-related neurons located close to the midline, within the RNO (raphé nucleus obscurus). Drugs are added directly to the bath or injected with a drug pipette locally into the RNO or the preBötzinger complex (preBötC) to examine drive transmission to hypoglossal motoneurons (XII) and rhythmogenesis. Very thin transverse slices of the medulla can also be used for immunohistochemistry studies. The right picture shows serotonergic neurons of the RNO.

ANTIBODY NAME	Type	Host	Dilution	CAT#	Manufacturer
Opioid Receptor - Mu (MOR) antibody IgG	polyclonal (antigen:384-398)	Rabbit	1:2700	24216	Immunostar
Opioid Receptor - Mu (MOR1A) antibody	(AS 308-409) with sequence LENLEAETAPLP (COOH-terminus) conjugated to KLH	Rabbit	1:8000	OR-600	Biotrend Chemicals
Anti-Serotonin (5HT) IgG	polyclonal	Goat	1:4000	20079	Immunostar
Anti-Choline Acetyltransferase(ChAT) Affinity Purified	polyclonal	Goat	1:600	AB144P-200UL	Chemicon
Anti-GAD67 Purified IgG2a	monoclonal (clone 1G10.2)	Mouse	1:700	MAB5406	Chemicon
Anti-Substance P	monoclonal (clone NC1)	Rat	1:500	MAB356	Chemicon
Anti-Neuronal nuclei (NeuN) Purified IgG1	monoclonal (clone A60)	Mouse	1:500	MAB377	Millipore
Anti-beta Galactosidase (β Gal) Affinity Purified IgY	polyclonal	Chicken	1:2000	AB9361	Abcam
Anti-Neurokinin Receptor 1 (NK1R)	polyclonal	Rabbit	1:2500	AB5060	Chemicon
Anti-NMDAR receptor subunit 1 Purified IgG2a	monoclonal (clone 54.1; amino acids 660-811 of rat NR1)	Mouse	1:200	556308	BD Pharmingen
Anti-NR3A Purified IgG	polyclonal (amino acids 1098-1113 (sequence SRKTELEEYQKT NRTC) of rat NR3A)	Rabbit	1:500 (HEK293) 1:750 (tissue)	07-356(CH)	Chemicon
Anti-NR3B Purified IgG	polyclonal (amino acids 916-930 (C-RRVRRRAVVERE RRVV) of mouse NR3B)	Rabbit	1:500 (HEK293) 1: 750 (tissue)	07-351(CH)	Chemicon

Table 2.1 List of primary antibodies used in immunohistochemistry studies

2.4 REFERENCES

AL-ZUBAIDY ZA, ERICKSON RL, GREER JJ (1996) Serotonergic and noradrenergic effects on respiratory neural discharge in the medullary slice preparation of neonatal rats. *Pflugers Arch.* 431(6):942-9.

DERKACH VA (2003) Silence analysis of AMPA receptor mutated at the CaM-kinase II phosphorylation site. *Biophys J.* 84(3):1701-8.

GENTET LJ, STUART GJ, CLEMENTS JD (2000) Direct measurement of specific membrane capacitance in neurons. *Biophys J.* 79(1):314-20.

LIU G, FELDMAN JL, SMITH JC (1990) Excitatory amino acid-mediated transmission of inspiratory drive to phrenic motoneurons. *J. Neurophysiol.* 64(2):423-36.

NICHOLSON C (1985) Diffusion from an injected volume of a substance in brain tissue with arbitrary volume fraction and tortuosity *Brain Res.* 333(2):325-9.

PTAK K, YAMANISHI T, AUNGST J, MILESCU LS, ZHANG R, RICHERSON GB, SMITH JC (2009) Raphé neurons stimulate respiratory circuit activity by multiple mechanisms via endogenously released serotonin and substance P. *J Neurosci.* 29(12):3720-37.

RUANGKITISAKUL A, SCHWARZACHER SW, SECCHIA L, POON BY, MA Y, FUNK GD, BALLANYI K (2006) High sensitivity to neuromodulator-activated signaling pathways at physiological [K⁺] of confocally imaged respiratory center neurons in on-line-calibrated newborn rat brainstem slices. *J. Neurosci.* 26(46):11870-80.

CHAPTER 3

MODULATION OF RESPIRATORY NEURAL ACTIVITY BY OPIOIDS AND HIGH-IMPACT AMPAKINES

My contribution to this study consisted in the planning, execution and analyses of electrophysiological recordings and anatomical studies. Dr. Wei Zhang provided significant assistance with immunohistochemical procedures.

3.1 ABSTRACT

The cellular mechanisms underlying opioid-induced respiratory depression and subsequent alleviation by ampakines are poorly understood. In this study, the interaction of high-impact ampakines and opioids within the preBötC at the single-cell and network levels was analyzed.

Local injections of the opioid receptor agonist DAMGO within the preBötC significantly depressed inspiratory rhythm and this was reversed by local injections of the μ -opioid receptor (MOR) antagonist naloxone. Immunohistochemical studies demonstrated the expression of the MOR subtype 1a within the preBötC and the colocalization of MOR-1a and neurokinin-1 receptor expression in the preBötC. Whole-cell patch-clamp analysis identified preBötC neurons responsive to DAMGO, which significantly decreased synaptic excitatory inputs in some preBötC neurons while affecting intrinsic membrane properties in others. The ampakine CX614 significantly increased amplitude, area and duration of AMPA-mediated current in all respiratory preBötC neurons tested. This modulation was independent of extracellular calcium. CX614 also induced an increase in inspiratory current amplitude and spontaneous event frequency in baseline conditions, as well as in presence of DAMGO. Another high-impact ampakine (CX546) also increased inspiratory drive in baseline conditions, and increased inspiratory rhythm under conditions of weak endogenous inspiratory drive.

Those results provide the first evidence that ampakines increase AMPA-mediated ionic load in respiratory preBötC neurons. The potentiation of AMPA-mediated conductance by high-impact ampakines underlies the enhancement of endogenous glutamatergic synaptic transmission necessary to counteract central respiratory depression induced by opioid or low extracellular concentration of potassium.

3.2 INTRODUCTION

Opioid analgesics are effective pharmacological agents used to treat acute, postoperative and chronic pain (reviewed in Swarm et al., 2001). However, activation of opioid receptors can also lead to suppression of respiratory drive (reviewed in Keats, 1985 and Shook et al., 1990; Greer et al., 1995; Gray et al., 1999). Thus, there is a clinical need for drug treatment capable of counteracting the depression of central respiratory drive without removing the analgesic effects of opioids. Acute effects of opioids on breathing have recently been studied *in vivo* showing that the preBötzinger complex (preBötC), a kernel of neurons that centrally generates rhythmic inspiratory drive (Smith et al., 1991), is a main target of μ -opioid agonist for inducing respiratory depression (Montandon et al., 2011). Previous work has described the physiological effects of μ -opioid receptor agonists on medullary respiratory neurons (Gray et al., 1999; Takeda et al., 2001; Mellen et al., 2003; Lorier et al., 2008; Ballanyi et al., 2009), but the mechanisms underlying the decrease in inspiratory rhythm are still incompletely understood.

Neuronal synaptic transmission within the preBötC relies primarily on the activity of fast conducting glutamatergic AMPA receptors channels (Greer et al., 1991; Funk et al., 1993, Pace et al., 2008). The synthetic compounds ampakines are potent enhancers of AMPA receptors conductance that allosterically bind to native or recombinant AMPA receptors and slow their deactivation and desensitization rates (Nagarajan et al., 2001; Arai et al., 2002). This positive allosteric modulation of AMPA receptor current can shape endogenous glutamatergic synaptic responses (reviewed in Lynch and Gall, 2006; Black, 2005; Arai et al., 2002; Aria et al., 2000), and enhances glutamatergic neurotransmission in a number of neural systems, such as the hippocampus and the cerebellum (Arai et al., 2004; Xia et al., 2005a, 2005b; Montgomery et al., 2009). By combining *in vitro*, *in situ* and *in vitro* rat models, Ren et al. (2006) demonstrated that the ampakine 1-(1,4-benzodioxan-6-ylcarbonyl) piperidine (CX546; member of the high-impact ampakine drug family) alleviates opioid-induced respiratory depression. Further, an *in vitro* study has shown the efficacy

of yet another high-impact ampakine (pyrrolidino-1,3-oxazinobenzo-1,4-dioxan-10-one; CX614) in potentiating AMPA and glutamate-mediated currents of inspiratory hypoglossal (XII) motoneurons and slowing excitatory postsynaptic current decay kinetics resulting in an increase in their synaptic drive (Lorier et al., 2010).

The goal was two-fold in this study. First, the objective was to extend previous work by investigating how opioids affect synaptic transmission within the heterogeneous population of preBötC neurons and how this may impact the inspiratory rhythm. The second goal was to determine whether or not high-impact ampakines counter opioid-induced respiratory depression by modulating excitatory synaptic transmission within the preBötC. *In vitro* medullary slice preparations isolated from neonatal rats were used to examine the effects of opioid and ampakines at the network and cellular levels. The analysis was restricted to the high-impact ampakines CX614 and CX546 because they increase respiratory activity (Ren et al., 2006; Lorier et al., 2010) and their mechanisms of action on AMPA receptor conductance have been studied in different brain regions and primary cell models (Nagarajan et al., 2001; Jin et al., 2005; Xia et al., 2005). Complimentary data were obtained using cyclothiazide, an allosteric modulator of AMPA receptors that decreases desensitization of AMPA receptors (Partin et al., 1993; Partin et al., 1994; Aria et al., 2004).

3.3 RESULTS

***IN VITRO* MU-OPIOID RECEPTOR ACTIVATION IN THE PREBÖTC**

The first stage of the study was to examine the synaptic modulation of opioids on respiratory neural activity *in vitro*. The specific μ -opioid receptor agonist [D-Ala², NMe-Phe⁴, Gly-ol⁵]-enkephalin (DAMGO) was used as a pharmacological tool to assess the functional expression of μ -opioid receptors in preBötC and to understand the synaptic mechanisms involved in the suppression of rhythmic inspiratory drive.

3.3.1 DAMGO MODULATES INSPIRATORY MOTOR OUTPUT *IN VITRO*

In 6 out of 25 medullary slice preparations, bath application of DAMGO resulted in a complete block of inspiratory activity within 10 minutes of exposure to DAMGO. On the remaining 19 medullary slice preparations, bath application of DAMGO (400 nM) induced a marked decrease in XII nerve burst frequency to 0.48 ± 0.06 fold of control ($n = 19$; $p < 0.001$; paired t test). DAMGO also induced a significant decrease in XII burst duration to 0.83 ± 0.04 of control ($p < 0.001$). No significant effect was found on amplitude (1.01 ± 0.79 of control; $p = 0.96$) or area (0.90 ± 0.96 of control; $p = 0.62$) of XII bursts. Inspiratory activity slowly reversed to control upon 30 minutes of wash out.

To examine whether these responses were mediated by μ -opioid receptor activation within the preBötC, two sets of experiments were performed: local microinjections of DAMGO (4 μ M; 120 s steady duration; $n = 7$) into the preBötC, and local applications of the μ -opioid antagonist naloxone (10 μ M; 60 to 120 s steady duration) into the preBötC during DAMGO delivery (either locally to the preBötC or bath applied; $n = 5$).

To appreciate the extent of the effect of local application of DAMGO, relative mean values of XII burst interevent intervals were plotted against event occurrence (Figure 3.1A), and show an instant and pronounced increase in XII

burst period (inter-event interval). More specifically, one-way analysis of variance (ANOVA) on normalized values of XII discharge parameters shows that DAMGO locally applied to the preBötC significantly decreased XII burst instant frequency to 0.65 ± 0.05 of control ($p < 0.001$) which rapidly recovered to 0.96 ± 0.07 of control ($p < 0.01$; $n = 7$). DAMGO also significantly decreased XII burst duration to 0.70 ± 0.04 ($p < 0.001$) which recovered to 0.94 ± 0.04 of control ($p < 0.001$; $n = 7$). No significant effect of DAMGO was found on the amplitude (0.96 ± 0.07 of control; $n = 7$; $p = 0.80$) nor area (0.81 ± 0.08 of control; $n = 7$; $p = 0.43$) of XII bursts.

Local administration of the μ -opioid antagonist naloxone strongly attenuated DAMGO-mediated effects on XII bursts ($n = 5$; one-way ANOVA; see group data graph in Fig. 3.1B). More specifically, XII burst frequency was significantly reversed by naloxone from 0.55 ± 0.11 of control (in DAMGO) to 0.94 ± 0.09 of control (in DAMGO + naloxone; $p = 0.02 < 0.05$; $n = 5$), but XII burst duration was increased from 0.85 ± 0.04 of control (in DAMGO) to 0.99 ± 0.06 of control (in DAMGO + naloxone) without reaching statistical significance ($p > 0.05$). These responses slowly recovered after 5 minutes following the end of DAMGO application. Note that the amplitude and area of XII bursts (not affected by DAMGO) were not significantly affected by naloxone.

Together those results demonstrated that *in vitro* μ -opioid receptor activation within the preBötC of neonatal rats modulates motor output and markedly decreases inspiratory frequency, consistent with previous studies (Greer et al., 1996; Gray et al., 1999; Lorier et al., 2009).

3.3.2 MU-OPIOID RECEPTOR EXPRESSION IN THE VENTROLATERAL MEDULLA

A specific μ -opioid receptor subunit is expressed in the preBötC of neonatal rats.

There have been difficulties replicating the immunohistochemical demonstration of μ -opioid receptor expression in the preBötC of neonatal rat to

confirm the adult data reported by Gray and colleagues (Gray et al., 1999). However, after evaluating several μ -opioid receptor antibodies under a variety of experimental conditions, it was determined that the use of a rabbit polyclonal antiserum raised against a synthetic peptide corresponding to amino acids 308-409 of the c-terminus of human and rat μ -opioid receptor 1a (MOR1a; Kemp et al., 1996) provided consistent results and improved immunohistochemical detection of MOR1 expressing cells in the rat preBötC. Diaminobenzidine staining of 4 to 7 μ m thick serial transverse sections through neonatal (P0-P4) rat medulla revealed the expression of MOR1a in the preBötC (Fig. 3.2). More specifically MOR1a was expressed on neuronal membranes and fibre arborisations within the preBötC (n = 5). Figures 3.2 A and B illustrate the high concentration of MOR1a positive (MOR1a⁺) cells in the NA region and a more diffused distribution of MOR1a⁺ cells in the preBötC area, which is consistent with data obtained by Gray et al. (1999).

Triple labeling shows that NK1R and MOR1a are co-expressed in the preBötC.

In the rat ventrolateral medulla, preBötC neurons express neurokinin-1 receptors (NK1R; Gray et al., 2001; Pagliardini et al., 2003), and choline acetyl transferase (ChAT) is commonly used as a reference marker for the compact and semi-compact division of the nucleus ambiguus (NA; Pagliardini et al., 2003). Therefore, the expression pattern of MOR1a was investigated using triple fluorescent labeling for ChAT, NK1R and MOR1a (n = 4; see example in figure 3.3). Confocal imaging demonstrated that MOR1a is strongly expressed in the compact division of the nucleus ambiguus (NAc), with strong colocalization with ChAT but no MOR1a labeling in the BötC area. However, at the level of the semi-compact division of the NA (NA_{sc}), ChAT immunolabeling rarely colocalized with MOR1a labeling (see Figs. 3.3E, F and G). In the preBötC, a few scattered ChAT⁺/NK1R⁻ neurons of the external formation of the NA were positive for MOR1a. Importantly, more intense punctated MOR1a labeling was detected in a subset of NK1R⁺/ChAT⁻ cells of the preBötC, although the level of

MOR1a expression in the preBötC appeared significantly lower than in the NAc. Figure 3.3H illustrates MOR1a and NK1R immuno-colocalization pattern at higher magnification. A 40X oil lens magnification was used to acquire confocal images that allow better discrimination of the pattern of MOR1a pattern of expression, at the cellular level (Fig. 33B). The images showed an intense labeling for MOR1a on the neuronal processes and membranes as well as what appeared to be the axon hillock. In the preBötC area, part of the NK1R⁺ cells population was not immunoreactive for MOR1a, but all MOR1a and NK1R labeling was colocalized.

3.3.3 WHOLE-CELL PATCH-CLAMP ANALYSIS OF DAMGO-MEDIATED MODULATION OF RESPIRATORY NEURONS AND SYNAPTIC DRIVE

Effects of DAMGO on membrane properties of respiratory preBötC neurons.

Whole-cell recordings in current- and voltage-clamp configuration were performed in order to examine DAMGO-induced changes of intrinsic and firing properties of respiratory preBötC neurons. None of the 11 expiratory neurons tested responded significantly to DAMGO, although 1 out of 5 expiratory neurons recorded in current-clamp mode displayed a decrease in spiking frequency when exposed to DAMGO.

12 out of 46 (approximately 26%) inspiratory neurons recorded responded to DAMGO with a decrease in R_N accompanied by either a hyperpolarization of their membrane potential in current-clamp configuration and/or a small but observable outward current in voltage-clamp configuration. Figures 3.4A illustrates the current-clamp response to bath application of DAMGO of an inspiratory preBötC neuron that responded with a hyperpolarization of its membrane potential. The average membrane hyperpolarization induced by local application of DAMGO was 10 ± 2 mV ($n = 4$) for recordings made in current-clamp and the average outward current was 42 ± 11 pA ($n = 8$) in voltage-clamp. R_N changes before and during DAMGO application were assessed in current-

clamp by examining potential responses evoked by 50 pA current steps, or in voltage-clamp by calculating the slope of the current-voltage (I/V) relationship. DAMGO application induced a decrease in R_N to 0.76 ± 0.1 of control values, from $253 \pm 24 \text{ M}\Omega$ to $192 \pm 21 \text{ M}\Omega$ ($n = 9$). I/V curve delivery on voltage-clamped neurons showed an inward rectification of the current response and that the intercept of the current-voltage relationships recorded in control and in presence of DAMGO ranged between -65 mV and -80 mV, which is close to the calculated Nernst equilibrium potential for potassium ions of -70.98 mV for the experimental conditions (see bottom of Fig. 3.5A). Thus these data suggested that the change in R_N produced by DAMGO was associated with an increase in K^+ ion conductance.

Current and voltage-clamp recordings showed that 34 out of 46 (74%) inspiratory preBötC neurons did not respond to DAMGO (illustrated in Figs. 3.4C and D) and did not undergo any significant change in R_N or I/V responses (see Fig. 3.5 B).

Effects of DAMGO on inspiratory currents of preBötC neurons.

To evaluate the effect of DAMGO on synaptic transmission of the inspiratory drive within the preBötC, inspiratory currents in preBötC inspiratory cells were analyzed and compared in control and in the presence of bath-applied DAMGO using whole-cell recordings in voltage-clamp configuration.

Results were separated into two groups. A first group included inspiratory cells that displayed a decrease in R_N and/or decrease in holding potential (associated with an outward current) upon exposure to DAMGO. Those cells were categorized as *opioid-sensitive cells*. The second group included inspiratory cells that did not respond to bath application of DAMGO with a hyperpolarization of their membrane potential (current-clamp) or an outward current (voltage-clamp) and were categorized as *opioid-insensitive cells*. Although we realized over the course of this study that this second category of cells could display significant changes in terms of synaptic inputs when exposed to DAMGO, “opioid-

insensitive cells” will refer to cells that did not undergo any significant changes in postsynaptic membrane properties upon DAMGO exposure.

Amplitude, area and duration of the inspiratory currents were examined and compared between control and DAMGO bath application (normalized data shown in figure 3.5). Other parameters were also included in the analysis, as follows. The rise slope (usually expressed in pA/ms) is a measurement of the velocity of propagation of the ionic current on the rising phase of the event and the rise time represents the time required to travel from 10 to 90 % of the amplitude of the event at the rising phase of the event. Conversely the decay time represents the time required to travel from 90 to 10 % of the amplitude of the event at the decay phase of the event.

In opioid-sensitive cells, DAMGO (400 nM) produced no significant effect on the amplitude of inspiratory currents (from -133 ± 10 pA in control to -110 ± 22 pA in DAMGO, $p = 0.17 > 0.05$; $n = 6$; paired t test), nor on their duration (513 ± 113 ms in control to 547 ± 155 ms in DAMGO, $p = 0.69 > 0.05$; $n = 6$; paired t test). The area of inspiratory currents was significantly reduced by DAMGO to 0.64 ± 0.21 of control ($p = 0.04 < 0.05$; $n = 6$). The group data histogram is shown in Fig. 3.5A. The size of s.e.m. values clearly indicates a large variability in the results that may be caused by the changes in R_N induced by DAMGO. Note that there was no significant decrease in the rise time and decay time of input currents with DAMGO but the rise slope was significantly decreased by DAMGO from 1.0 ± 0.2 to 0.60 ± 0.2 of control ($p = 0.006 < 0.01$; $n = 6$; paired t test). Overall these results indicate that DAMGO does not significantly alter the amplitude and duration of inspiratory currents in this category of cells. The fact that the area and rise slope of inspiratory currents were significantly reduced by DAMGO suggests that DAMGO may be affecting the shape of the inspiratory envelope.

Conversely, in opioid-insensitive neurons, DAMGO application caused a significant alteration of most inspiratory current parameters ($n = 8$; paired t test). More specifically DAMGO produced a significant decrease in the amplitude (from -142 ± 10 pA in control to -115 ± 9 pA in DAMGO; $p < 0.001$) and

duration (from 616 ± 72 ms in control to 498 ± 78 ms in DAMGO) of inspiratory currents. Also, the inspiratory charge transfer (area) was significantly decreased by DAMGO to 0.60 ± 0.10 of control values (presented in mean \pm s.e.m. of normalized values; $p = 0.007 < 0.01$). The group data histogram is shown in Fig. 3.5B. Overall these results indicate that in cells referred to as opioid-insensitive neurons, DAMGO significantly diminishes the inspiratory envelope. The fact that the amplitude, duration and area of inspiratory currents are all reduced by DAMGO suggests that DAMGO may not affect the shape of the inspiratory envelope itself, but rather have an overall decreasing effect on inspiratory currents.

Analysis of interburst synaptic event activity on respiratory preBötC neurons.

The integration of synaptic signals underlying the inspiratory rhythmogenesis within the preBötC is hypothesized to primarily rely on excitatory synaptic release activity mediated by glutamatergic receptors (among other excitatory receptors) present at the postsynaptic membrane of respiratory neurons (Ge and Feldman, 1998; Del Negro et al., 2002; Shao et al., 2003; Pace et al., 2007; Pace et al., 2008; Del Negro et al., 2010). A comparison of the frequency and size (amplitude and area) of inward sPSCs before and after bath application of DAMGO represents a comprehensive approach for measuring the degree and weight of tonically active excitatory inputs to respiratory preBötC neurons that occur in the presence of DAMGO. To examine the effect of DAMGO on tonic excitatory synaptic activity in each group of inspiratory preBötC neurons, interburst synaptic events at the somatic level were quantified by analyzing inward sPSCs recorded in voltage-clamp at resting membrane potential. Although experimental conditions (holding potential of -58 mV) yield a positive (outward) driving force for inhibitory synaptic current, inhibitory synaptic conductance cannot be excluded from the analysis of inward events because of the absence of chloride-mediated channels blockers (bicuculline and strychnine) in the bathing medium. It must also be noted that in the foregoing sections reporting tonic

synaptic events analysis, experiments were performed without tetrodotoxin (TTX). Therefore it is important to understand that the present analyses will not allow us to distinguish between an indirect action of DAMGO on spike-dependent synaptic neurotransmission springing from upstream excitatory neurons and a direct action of DAMGO on calcium-independent vesicular release at presynaptic terminals.

Figure 3.6 illustrates the results of a paired *t* test analysis on sPSC parameters obtained for each group from preBötC cells recorded under control conditions versus bath application of DAMGO. Amplitude, frequency, area and duration of sPSCs were examined. For cumulative probability analysis, the interevent interval was taken into account. The interevent interval was automatically measured as the time between the start of one synaptic event and the start of the subsequent synaptic event.

In opioid-sensitive cells (Fig. 3.6A), DAMGO did not significantly affect sPSC frequency (from 1.0 ± 0.9 in control to 0.9 ± 0.1 in DAMGO; paired *t* test; $p > 0.05$; $n = 5$) but significantly decreased sPSCs amplitude (from -52 ± 12 pA in control to -36 ± 9 pA in DAMGO; paired *t* test; $p = 0.045 < 0.05$; $n = 5$). A Kolmogorov-Smirnov test on the cumulative probability distribution of the interevent intervals shows no significant difference between the distribution in control ($n = 952$) versus in the presence of DAMGO ($n = 727$; $p > 0.05$). Although the decrease in sPSCs amplitude induced by DAMGO may suggest a postsynaptic effect of DAMGO, we cannot deny the fact that it may also reflect an artifactual decrease of amplitude due to an overall decrease of neurotransmission release from presynaptic neurons.

In contrast, in opioid-insensitive cells, sPSC amplitude was not significantly changed by DAMGO (-57 ± 10 pA in control, and -48 ± 12 pA in DAMGO; $p = 0.13 > 0.05$ in paired *t* test; $n = 7$) while the frequency of sPSCs was significantly decreased by DAMGO (from 1 ± 0.12 in control to 0.56 ± 0.16 in DAMGO; paired *t* test; $n = 7$; see Fig. 3.6B). A Kolmogorov-Smirnov test on the cumulative probability distribution of the interevent intervals showed a significant difference between the distribution in control ($n = 1550$) and in the presence of DAMGO (n

= 466; $p < 0.05$). This effect indicated that the rate of excitatory neurotransmitter release to opioid-insensitive cells was diminished by DAMGO and may suggest a presynaptic effect of DAMGO in these cells. However, while it is reasonable to link the deceleration of spontaneous release of neurotransmitters from presynaptic terminals with a decrease in intracellular calcium ($[Ca^{2+}]_i$), no inference can be made on the location of the opioid-receptors mediating this effect (presynaptic terminals versus postsynaptic sites of presynaptic neurons). In addition, a direct action of G-protein coupled opioid receptors on quantal release may be occurring. Ideally, an analysis of miniature excitatory currents (mEPSC) in presence of bicuculline and strychnine would have been performed in order to unmask this particular effect of DAMGO. However, due to typically high background noise levels, it was not possible to detect sufficient amount of synaptic events in the presence of TTX (especially during DAMGO bath treatment) for convincing mEPSC analysis.

AMPAKINE MODULATION OF INSPIRATORY NETWORK

The second stage of the study was to apply a high-impact ampakine that partially reversed the respiratory depression induced by opioids *in vitro* and examine its potentiating effects on single respiratory preBötC neurons.

3.3.4 CX614 MODULATES INSPIRATORY MOTOR OUTPUT

CX614 alleviates inspiratory drive depression caused by DAMGO.

First the ability of the ampakine CX614 to modulate the medullary inspiratory network was examined by recording XII nerve activity in rhythmic medullary slices. XII burst frequency that was decreased by DAMGO from 13 ± 3 bursts/min to 7.3 ± 3.4 bursts/min was significantly increased by the addition of CX614 at 20 μ M to 10 ± 3 bursts/min (repeated measures ANOVA, Tukey's multiple test comparison; $p < 0.05$; $n = 7$; see Fig. 3.7). CX614 (20 μ M) modulated the amplitude, duration and area of XII bursts but these effects were not significant ($p > 0.05$; see group data histogram in Fig. 3.7) Note that the 15

min wash out period (used in figure 3.7) was not enough for recovery and that a minimum of 45 minutes of wash-out was required for values to return to control levels (n = 2 / 7).

CX614 acts within the preBötC to alleviate opioid-induced respiratory depression.

To verify that the observed increase of inspiratory frequency was due to a direct effect of CX614 onto the inspiratory rhythmogenic centre, local applications of CX614 (200 μ M) into the preBötC were performed during DAMGO-induced respiratory depression. As illustrated in Figure 3.8, local applications of CX614 (200 μ M) in the preBötC significantly alleviated the DAMGO-induced suppression of inspiratory rhythm (ANOVA with Tukey's multiple test comparison; $p < 0.05$; population data shown in Fig. 3.8).

3.3.5 CX614 POTENTIATES AMPA RECEPTOR CONDUCTANCE ON RESPIRATORY PREBÖTC NEURONS.

CX614 increases inward currents induced by the exogenous application of AMPA in preBötC neurons.

To assess AMPA receptor channel modulation by CX614 on respiratory neurons AMPA puffs (100 μ M; 300-400 ms duration) were delivered onto respiratory preBötC neurons clamped at -58 mV. After obtention of a paired recording with XII outputs to verify inspiratory behaviour of the recorded cell, TTX (0.5 μ M) was applied to the bath and AMPA puffs were delivered (repeated at least 3 times to ensure consistency and steady AMPA-evoked inward currents; see Fig. 3.9A). At least 2 minutes passed between each AMPA puff to allow for recovery from desensitization. Each experiment involved one steady whole-cell recording (up to 90 minutes) of a single preBötC neuron per slice. In both expiratory and inspiratory preBötC cells, exogenous application of AMPA evoked a large inward current, confirming the presence of functional AMPA receptors on

respiratory preBötC neurons (Figs. 3.9A, B and C). Note the data shown in Fig. 3.9A shows data for 1/4 cells for which DAMGO was bath applied after CX614.

Overall, Student's analysis on normalized mean values of AMPA-induced currents produced in 9 preBötC cells (including 7 inspiratory cells and 2 expiratory cells) showed that CX614 caused a significant increase in the amplitude (2.2 ± 0.3 fold of control; $p < 0.01$); area (3.9 ± 0.6 fold; $p < 0.001$); rise slope (2.8 ± 0.6 fold; $p < 0.01$); decay time (3.1 ± 0.7 fold; $p < 0.05$); duration (2.3 ± 0.3 fold; $p < 0.05$). No significant change was found in the decay slope (1.4 ± 0.2 fold; $p > 0.05$) or rise time (1.3 ± 0.2 fold; $p > 0.05$; $n = 9$).

Note that it was not possible to differentiate the CX614 potentiation of AMPA-mediated currents between opioid-sensitive versus -insensitive cells due to the low number of opioid-sensitive cells ($n = 2$).

CX614 increases the AMPA component of the preBötC inspiratory drive.

Pharmacological studies of preBötC inspiratory neurons had previously shown that, while synaptic excitation through postsynaptic glutamatergic receptors has only a small direct contribution to the inspiratory drive itself, it may significantly contribute to the inspiratory drive indirectly via its capacity to evoke the recruitment of endogenous conductances activated by intracellular calcium (Pace et al., 2007; Pace et al., 2008). In particular, the endogenous calcium-activated non-selective cationic current I_{CAN} has been proposed to be an important carrier of the inspiratory conductance capable of promoting rhythmic bursting behaviours in preBötC neurons (Pace and Del Negro, 2008; Rubin et al. 2009, Dunmyre et al., 2011). Thus, since the neuronal inspiratory envelope represents an amplified signal reflecting a heterogenous combination of various synaptic excitations and second messenger pathways (Pace et al., 2007; Mironov et al., 2008), it is impossible to discriminate the portion of potential directly linked to AMPA receptors activation. As a mean to examine how the ampakine CX614 modulates the AMPA component of the inspiratory drive, AMPA-evoked (100 μ M; 100-200 ms duration) depolarizations were generated in preBötC inspiratory neurons in the absence of synaptic inputs or calcium related conductance. The

exogenously triggered depolarization was adjusted (by changing the duration of the AMPA puffs and/or the distance between the drug pipette and the recorded cell) so that its amplitude could repeatedly and consistently match the amplitude of the endogenous spontaneous inspiratory depolarization (see Fig. 3.10A). The cell was then synaptically isolated with TTX (0.5 μ M) and calibrated AMPA puffs were delivered. Subsequently, calcium-activated conductances were blocked by bath application of cadmium ($[Cd^{2+}]_e$; 200 μ M) and AMPA puffs were delivered after sufficient exposure to $[Cd^{2+}]_e$ (at least 10 minutes). AMPA-evoked depolarizations were significantly decreased by $[Cd^{2+}]_e$ ($n = 3$; illustrated in Fig. 3.10B), which confirmed that calcium is a major conducting ion mediating AMPA-evoked depolarizations on inspiratory preBötC neurons (Pace et al., 2007). Because of the presence of the AMPA receptor subunit GluR2, AMPA receptors on respiratory preBötC neurons are thought to have very low calcium permeability (Paarmann et al., 2000; Pace et al., 2007; Pace and Del Negro, 2008). Therefore the electric potential difference (ddp) that had been subtracted by Cd^{2+} had most certainly been activated endogenously (ddp may have been triggered by I_{CAN} ; (Pace and Del Negro, 2008) or by voltage-gated calcium channels) and the AMPA-evoked depolarizations that remained in presence of $[Cd^{2+}]_e$ more likely reflected the full (yet originally masked) AMPA receptor depolarization. Addition of CX614 (20 μ M) to the bathing medium significantly potentiated the residual AMPA-evoked depolarization ($n = 3$; see Fig. 3.10 for example). Those results indicate that in inspiratory neurons, the potentiation in AMPA conductance induced by CX614 had the ability of evoking a substantial depolarization independently of calcium ions.

3.3.6 SYNAPTIC ANALYSIS OF CX614 EFFECT ON PREBÖTC NEURONS

CX614 modulation of respiratory preBötC neuron activity.

The first step was to evaluate the effect of CX614 on its own. Voltage-clamp recordings of respiratory preBötC neurons were performed and spontaneous synaptic events examined under bath application of CX614 (20 μ M).

The effects of CX614 on inspiratory synaptic currents of preBötC neurons were examined (see in Fig. 3.11A). CX614 induced a progressive and reversible increase in the size of inspiratory currents, while the frequency of inspiratory currents reached a significant increase only after 10 minutes of CX614 exposure. Statistical analysis on inspiratory current parameters showed that CX614 significantly and reversibly increases the amplitude of inspiratory currents (2.8 ± 0.7 fold of control values in CX614, reversed to 1.0 ± 0.1 fold of control values during wash out, $p = 0.04 < 0.05$, one way ANOVA, Dunnett's multiple comparison test; $n = 5$). This increase correlated with the increase in the area of the inspiratory currents (2.9 ± 0.7 fold of control values in CX614 and 1.1 ± 0.2 fold of control values during wash out, $p = 0.04 < 0.05$). However, although the steady state frequency of inspiratory currents was statistically increased after 10 minutes of CX614 exposure, it only reached 1.4 ± 0.1 fold of control values in CX614 and 1.2 ± 0.0 fold of control values during wash out ($p = 0.03 < 0.05$; $n = 5$). The group data histogram can be seen in Fig. 3.11. Collectively those data indicate that the high impact ampakine CX614 increase both the size of the inspiratory currents as well as the frequency. However it can be noted that the increase in inspiratory-related charge transfer in preBötC evoked by CX614 is not proportional to the increase in frequency produced by CX614.

In a second stage, the effects of CX614 on interburst inward sPSCs of preBötC neurons were examined. These results include expiratory and inspiratory preBötC neurons because both types of cells have functional AMPA receptors that are modulated by CX614 and they were both seen to undergo large increases in sPSCs during CX614 exposure. Since single-channel recordings from excised-patches and reconstructive lipid bilayers have previously demonstrated that

ampakines can block desensitization, slow deactivation of glutamate responses and increase kinetics of AMPA receptor channels (Arai et al., 2000; Nagarajan et al., 2001; Suppiramaniam et al., 2001; Arai et al., 2002), we hypothesized that the ampakine CX614 would increase the kinetics of synaptic currents in preBötC neurons, similarly to its effects in other neuronal systems (Arai et al., 2004; Lorier et al., 2010). An analysis of the decay time constant (decay tau) of the whole-cell synaptic events was therefore added since it evaluates how effectively each event decays from peak to baseline level and provides a measurement of the kinetic exponential component of the decay phase of the events. Decay time constants were evaluated by fitting the decay phase of each individual sPSC with an exponential curve.

One-way ANOVA followed by Tukey's multiple comparison test analysis of sPSC parameters showed no significant effect of CX614 on sPSC frequency (2.0 ± 0.5 fold of control values in CX614) nor on sPSC amplitude (-39 ± 0.0 pA in control, to -48 ± 0.0 pA in CX614, and -39 ± 0.0 pA in wash out ($p > 0.05$; $n = 5$). However, sPSC decay tau was significantly increased by CX614 (1.6 ± 0.3 of control; one-way ANOVA, Tukey's multiple comparison test; $p < 0.05$; $n = 5$). Comparing the entire distribution of sPSC events between control and CX614 confirmed that CX614 did not have any significant effect on amplitude (Kolmogorov-Smirnov two sample test, $p > 0.05$; $n = 2984$; 5 cells; Fig. 5.11E lower panel), but a significant difference between sPSCs inter-event interval distributions was found (Kolmogorov-Smirnov two sample test, $p < 0.001$; $n = 3088$; 5 cells; see Fig. 5.11E upper panel). This clearly indicates that in preBötC respiratory neurons the number of action potential dependent excitatory synaptic events is increased in presence of CX614. The Kolmogorov-Smirnov test on the cumulative distribution of sPSCs decay tau showed no significant difference between the decay tau of sPSCs recorded in control and that of recorded in the presence of CX614 ($n = 2865$; $p > 0.05$). A Wilcoxon post-test on sPSC decay taus also showed no significant difference ($p = 0.0625 > 0.05$). These data suggested that decay kinetics of AMPA receptors of preBötC respiratory neurons were not affected by CX614 in baseline experimental conditions.

CX614 modulation of respiratory preBötC neuron activity following DAMGO-mediated respiratory depression.

The efficacy of CX614 to modulate spontaneous synaptic events after inspiratory drive depression was examined on preBötC cells already exposed to DAMGO.

First, the effects of CX614 on inspiratory currents of opioid-insensitive cells were examined (see in Fig. 3.12A.). While CX614 significantly increased the frequency of inspiratory currents from 8.9 ± 1.65 inspiratory currents (events)/min in control to 3.1 ± 1.1 events/min in DAMGO and 6.0 ± 1.2 events/min in DAMGO + CX614 (one-way ANOVA; $p < 0.001$), CX614 also increased the charge transfer (area) of inspiratory current to 2.1 ± 0.5 fold of inspiratory current recorded in DAMGO (one-way ANOVA; $p < 0.05$). With the addition of CX614 the amplitude increased to 1.3 ± 0.1 fold of that was measured in presence of DAMGO (130 ± 32 pA in control, 104 ± 21 pA in DAMGO and 140 ± 33 pA in DAMGO + CX614) but this effect was not significant (one-way ANOVA; $p > 0.05$; $n = 5$; see summary histogram in Fig. 3.12C).

The low number of inspiratory cells categorized as opioid-sensitive inspiratory cells ($n = 3$) unables yet a firm conclusion on the effect of CX614 on those cells, but mean values of inspiratory current parameters showed no significant effect of CX614 on amplitude nor the area of inspiratory current ($p > 0.05$; one-way ANOVA; $n = 3$).

Second, the effects of CX614 on interburst sPSCs of preBötC neurons (3 expiratory and 7 inspiratory cells) were examined. Note that this set of experiments only includes cells categorized as opioid-insensitive cells and expiratory cells.

CX614 significantly increased sPSC frequency to 2.4 ± 0.5 of DAMGO ($p < 0.05$; one-way ANOVA). Averaged sPSC amplitude was increased from -69 ± 22 pA in DAMGO to -98 ± 32 pA with addition of CX614 (1.6 ± 0.2 fold increase compared to DAMGO; $n = 10$). While paired t test between sPSCs amplitude in DAMGO and in DAMGO + CX614 showed a significant difference ($p = 0.047 <$

0.05), one-way ANOVA (comparing data in control/ DAMGO/ DAMGO + CX614/ wash out) showed no significant difference between those two groups ($p > 0.05$); see Fig. 3.12C right panel). The entire distributions of sPSC amplitudes and interevent intervals were then compared between DAMGO and DAMGO + CX614 using a Kolmogorov-Smirnov test. As illustrated in Fig. 3.12E, the difference between the two distributions of interevent interval was statistically significant ($p < 0.05$) and the difference between the two distributions of sPSC amplitude was highly significant ($p < 0.01$). We interpreted the increase in amplitude induced by CX614 as further evidence that AMPA receptors can mediate tonic spontaneous synaptic events on preBötC neurons (Shao et al., 2003). Interestingly, since the increase in sPSC amplitude did not occur with CX614 alone, these data also suggest that the efficiency of CX614 to affect tonic synaptic activity is increased in presence of DAMGO.

CX614 did not significantly increase sPSC decay tau (3.0 ± 0.9 fold of decay tau values obtained in DAMGO; $p < 0.05$; one-way ANOVA). The Kolmogorov-Smirnov test on the cumulative distribution of sPSCs decay tau showed no significant difference between the decay tau of sPSCs recorded in DAMGO and that of recorded in the presence of DAMGO + CX614 (7 cells; $n = 2522$; $p > 0.99$). This result was quite surprising because CX614 is known to increase postsynaptic AMPA receptor single channel decay kinetics (Arai et al., 2000) more likely reflected in AMPA receptor-mediated sEPSCs decay kinetics. When examining each single voltage-clamp recording, a very heterogeneous distribution of sPSC decay time constants was noticed: fast and slower inward synaptic currents were observed. Because glutamate-mediated EPSC have much faster decay time constant than other receptor-mediated EPSC, we hypothesized that CX614 would affect EPSC with faster decay time constants. To test this hypothesis in a simpler manner we sought to select cells that display more than 70% of their sPSCs with a decay time constant < 8 ms in baseline conditions. 8 ms was chosen as a cut off decay time constant because it demarcates most fast decay time constant values found for glutamate and AMPA-mediated EPSCs in previous studies (Tian et al; Angulo et al., 1999). 3/7 cells met this criteria and

these cells were selected for further analysis. Student's *t* test on decay taus of sPSC recorded in DAMGO versus DAMGO + CX614 showed a highly significant difference (from 5.66 ± 0.44 ms in DAMGO to 14.12 ± 1.31 ms in DAMGO + CX614; $p < 0.0001$; unpaired *t* test). The cumulative distributions of decay taus in DAMGO versus DAMGO + CX614 showed two distinct curves but no significant difference was found with the Kolmogorov Smirnov test ($p = 0.37$), and the Wilcon post matched pairs test on the raw mean values revealed no significant difference either ($p = 0.125 > 0.05$). Because of the low number of cells, the possibility for CX614 to affect the decay tau of rapid spontaneous events in different cells cannot be ruled out, although the present data suggests that it does not.

Together the results obtained on opioid-insensitive cells suggest that the increase in synaptic excitatory efficacy produced by CX614 is much stronger in presence of DAMGO than in baseline conditions. During DAMGO exposure, CX614 increases the amplitude and the frequency of sPSCs.

3.3.7 OTHER ALLOSTERIC MODULATORS OF AMPA RECEPTORS

CX546 modulates preBötC inspiratory drive.

As mentioned in the introduction, CX546 has been shown to share similar binding properties with CX614, notably to decrease the deactivation rate of AMPA receptors. Whole-cell recording of inspiratory preBötC neurons in voltage and current-clamp were performed and the effect of bath applied CX546 was tested in normal conditions and with weak endogenous drive conditions (by lowering extracellular concentration of potassium). As shown in Figure 3.13, similar to CX614, CX546 increased inspiratory current amplitude, area and duration in baseline conditions. In addition, CX546 significantly increased the frequency and amplitude of inspiratory currents on inspiratory neurons in 3 mM $[K^+]_e$ as seen in Figure 3.14. Note that the potentiation of AMPA-mediated conductance by CX546 evokes larger and longer inspiratory bursts that display action potentials spiking block quickly after the upstroke of the burst. This spiking

block is typical of the development of I_{CAN} (Pace et al., 2007; Pace et al., 2008). The results therefore suggest that signalling cascades synaptically activated by AMPA-receptors may recruit latent postsynaptic currents such as I_{CAN} . However, although the frequency was increased in the inspiratory cell shown on Fig. 3.13, CX546 did not increase the frequency of inspiratory bursts in all medullary slice preparations tested. Moreover, increases in inspiratory current amplitude and area in preBötC neurons were not always proportional to the increase in frequency induced by CX546 application.

Cyclothiazide alleviates DAMGO-mediated respiratory depression *in vitro*.

Cyclothiazide is one of the best studied enhancers of AMPA receptor conductance. In contrast to CX546, the binding of cyclothiazide to the AMPA receptor has been found to be independent of agonist binding (Kessler et al., 1996; Stern-Bach et al., 1998). Further, it preferentially decreases the rate of desensitization of AMPA receptors over their rate of deactivation (Nagarajan et al., 2000), and has a higher affinity for flip splice variants of AMPA receptor subunits. Cyclothiazide has already been tested in *in vitro* medullary slice preparation where it was shown to increase XII bursts frequency and inspiratory currents of inspiratory XII MNs (Funk et al., 1995). First the efficacy of cyclothiazide to counter DAMGO-induced respiratory depression *in vitro* was studied. Cyclothiazide significantly alleviated DAMGO-induced respiratory depression in medullary slice preparations (see Fig. 3.15). The effect of bath application of cyclothiazide (100 μ M) on inspiratory cells was also tested (n = 2). Although cyclothiazide increased the frequency of rhythmic bursts in standard conditions (Funk et al., 1995), somewhat surprisingly, unlike the modulation of XII MNs inspiratory current increase induced by cyclothiazide, no significant effect on the amplitude of inspiratory currents of preBötC neurons in baseline conditions. Those results are preliminary and there is need to study a larger pool of rhythmogenic preBötC neurons. More detailed analysis on all parameters of inspiratory currents should facilitate the understanding the cellular mechanisms involved in inspiratory frequency increase produced by cyclothiazide *in vitro*.

3.4 DISCUSSION

3.4.1 DIFFERENTIAL DISRUPTION OF SYNAPTIC TRANSMISSION AMONG RESPIRATORY PREBÖTC NEURONS BY OPIOIDS

This study describes how the μ -opioid agonist DAMGO differentially affects synapses between preBötC respiratory neurons, how μ -opioid receptors are distributed within the preBötC and how ampakines modulate synaptic activity within the preBötC in order to increase inspiratory frequency.

The first significant result of this study comes from voltage-clamp recordings of respiratory preBötC neurons. Expiratory neurons did not show any response to DAMGO, in agreement with a previous study (Takeda et al., 2001). Inspiratory neurons on the other hand, responded differentially to DAMGO.

26% of recorded inspiratory neurons displayed an outward current accompanied by a decrease in R_N upon DAMGO exposure and were categorized as opioid-sensitive neurons. This is in line with previous work that has demonstrated the existence of neurons responding similarly to opioids (Gray et al., 1999; Takeda et al., 2001), but in contrast to another study that claims no postsynaptic effect of opioid on preBötC neurons (Ballanyi et al., 2010). Two factors may contribute to the discrepancy between our results and Ballanyi et al.'s data. First, our data indicate that not all inspiratory cells happen to respond postsynaptically to DAMGO, but only a restrictive portion of preBötC neurons is sensitive to opioid postsynaptically. In addition, the possibility for some preBötC cells to respond presynaptically to opioid is not excluded. In fact, the dichotomous nature of opioid signalling within the preBötC might represent an essential component of the inspiratory drive depression induced by opioids. Second, our data showed that the postsynaptic effect of opioid may be underlied by a discrete inward rectifying potassium conductance which is known to be exacerbated by higher extracellular concentration of potassium ($[K]_o$) (Hibino et al., 2010). The difference in $[K^+]_o$ used in different experimental settings may therefore very well influence the postsynaptic current size and its detection.

Another interesting point revealed by the data is that neurons in this category of cells (opioid-sensitive) do not necessarily have the amplitude of their inspiratory currents decreased by DAMGO. If this result truly reflected the effect of DAMGO, inspiratory bursts may be less dependent of synaptic transmission and may prominently rely on self-generated conductances such as persistent sodium current and I_{CAN} that have both been reported present in preBötC neurons (Thoby-Brisson and Ramirez, 2001; Del Negro et al., 2002; Peña et al., 2004; Del Negro et al., 2005). This scenario would not be incompatible with previous reports showing that preBötC neurons responding to μ -opioid agonists were characterized as type I neurons (Gray et al., 1999; Takeda et al., 2001), which are neurons with early-inspiratory burst pattern that may hold some pacemaker properties (Rekling et al., 1996). This would thus suggest that the outward potassium conductance and the consequent membrane hyperpolarization resulting from μ -opioid receptor activation increases the driving force for ions that are either carried by background channels (e.g. sodium-leak channels; Lu et al., 2007) or by channels involved in the inspiratory drive *per se* (e.g. calcium-activated non-specific channels (CAN); Del Negro et al., 2005; Pace et al., 2007). However, this interpretation is inconsistent with the fact that both background and inspiratory currents cited have been proposed to promote an increase in rhythmicity as opposed to the decrease in rhythmicity observed with opioid. On the other hand the interburst presynaptic event analysis showed that sPSC amplitude decreased significantly with DAMGO in opioid-sensitive neurons, suggesting a functional postsynaptic effect of μ -opioid receptors activation. The question arises as to whether or not the discrepancy between how opioids impact interburst sPSC amplitude versus inspiratory current amplitude has a functional significance. First, sPSCs may be mainly excitatory and driven by glutamate receptors, as indicated by opioid-insensitive cell sPSC analysis (amplitude significantly increased by CX614) and also proposed by others (Paarmann et al., 2005). In contrast, inspiratory currents are believed to be mainly carried by I_{CAN} (Thoby-Brisson and Ramirez, 2001; Peña et al., 2004), where AMPA and other receptors contribute to its development (Pace et al., 2008). Direct AMPA receptor

conductance is only partially present in inspiratory currents, evaluated to be approximately only ~10% of the total conductance (Pace et al., 2007; Pace et al., 2008). Therefore it is possible that DAMGO decreases inspiratory current amplitude in those neurons (strong tendency of the data) but statistical significance can only be reached with a larger pool of data. Second, one must be cognisant of the fact that the voltage-clamp recording measurements could have suffered from voltage attenuation errors due to poor space-clamp conditions. Because of the discontinuous single-electrode voltage-clamp mode used it is unlikely that errors in measurements of synaptic currents would have been introduced by series resistance. Rather, substantial distortion of synaptic currents may have occurred with synapses located on dendrites (Spruston et al., 1993). Dendritic Ca^{2+} transients are hypothesized to contribute to somatic inspiratory conductances in preBötC neurons (Morgado-Valle et al., 2008) and synaptic recruitment of I_{CAN} for the inspiratory bursts is believed to take place in the dendrites (Pace et al., 2007; Mironov, 2008; Del Negro et al., 2011). Therefore the possibility of unclamped remote synaptic events and consequent occlusion of DAMGO effects at postsynaptic dendritic sites in those neurons cannot be excluded. Third, R_{N} measurements indicated that DAMGO induces a net decrease in R_{N} in those neurons. Therefore compensation for the decrease in R_{N} should unmask a decrease in the inspiratory currents proportional to the decrease in R_{N} .

In opioid-insensitive cells, the finding that DAMGO induces a significant decrease in sPSC frequency but not amplitude suggests a presynaptic effect of DAMGO. Although the exact mechanism of this presynaptic effect remains to be determined, previous reports have demonstrated that μ -opioid receptors are negatively coupled to voltage-gated calcium channels in a variety of neuron types (Rhim and Miller, 1994; Wilding et al., 1995; Connor et al., 1999; Heinke et al., 2011). If DAMGO also decreases the frequency of TTX resistant mPSCs, opioid receptor activation may also regulate vesicle release machinery at presynaptic terminal sites (Heinke et al., 2011). This would be consistent with the immunohistochemical data showing punctate expression of μ -opioid receptors on somata and processes of preBötC neurons. It is therefore possible that μ -opioid

receptors exert their inhibitory action on inspiratory rhythm by suppressing vesicle release and/or presynaptic calcium channel influx in presynaptic terminals of local neurons (opioid-sensitive cells, expiratory neurons or even non-respiratory neurons) or terminals of external inputs (such as raphé obscurus neurons). Also in this category of cells, DAMGO induced a significant decrease of inspiratory current amplitude without significant change in R_N . The observed decrease in the size of inspiratory currents can first be interpreted as a consequence of a decrease in synaptic neurotransmission within the inspiratory network, similarly to the effect of DAMGO observed in inspiratory XII MNs (Lorier et al., 2010). Nevertheless, the possibility of postsynaptic effects of DAMGO on endogenously activated conductances (such as I_{CAN}) cannot be disregarded. In fact, it has been suggested that opioid may inhibit intracellular levels of cyclic adenosine monophosphate (cAMP) in medullary respiratory neurons (Ballanyi et al., 1997; Manzke et al., 2003). The dynamic interaction between intracellular calcium and cAMP may directly or indirectly modulate inspiratory currents in preBötC neurons (Shao et al., 2003; Pace et al., 2007, 2008). The results presented in this study suggest that DAMGO decreases network-mediated synaptic drive in opioid-insensitive cells, but do not exclude a possible postsynaptic action of DAMGO

With respect to the immunohistochemical data, previous work had shown that the most commonly expressed μ -opioid receptor splice variants in the rat CNS were MOR1 and MOR1A (Takida et al., 1997; Colman and Miller, 2001; Oldfield et al., 2008). Therefore the MOR1a subunit was studied and found to be expressed in the preBötC and in the NAc. MOR expression within the NAc had been defined in early pharmacological studies as having a major role in the cardiovascular actions of opioids (Hassen et al., 1984). Importantly, many of the MOR1a⁺ cells in the preBötC were also NK1R positive, which is consistent with previous studies (Gray et al., 1999; Montadon et al., 2011). The data also show that the opioid receptor subtype MOR1a is largely expressed on processes and cellular membrane, consistent with the physiological data indicating both pre- and post-synaptic effects of μ -opioid agonist on preBötC neurons.

3.4.2 CELLULAR MECHANISMS UNDERLYING THE INCREASE OF INSPIRATORY RHYTHM BY AMPAKINES

The *in vitro* medullary slice model allowed us to study the effect of high-impact ampakines on central inspiratory activity. Both ampakines CX614 and CX546 are very effective in alleviating DAMGO-induced respiratory drive depression *in vitro*, even when opioid completely abolishes rhythmic activity. Those results emphasize the important role of excitatory synaptic transmission for preBötC rhythmogenesis. Because ampakines are not agonists, but allosteric modulators, these data also imply that an endogenous glutamatergic release persists in presence of respiratory drive depression and can be modulated by ampakines. High-impact ampakines have the ability to boost respiratory network activity in low or inhibited physiological conditions (opioid-induced respiratory depression and 3 mM $[K^+]$ extracellular conditions). CX546 has been shown to potentiate respiratory drive in presence of opioids (Ren et al., 2006). Here, it was demonstrated that CX546 can also potentiate weak endogenous respiratory drive.

Ampakines can also increase neuronal inspiratory drive in baseline physiological conditions at high enough concentrations. Both inspiratory current amplitudes and sPSC frequency on all inspiratory preBötC neurons recorded were increased by CX614, suggesting pre- and post-synaptic effects of CX614. Despite the lack of miniature postsynaptic event (mPSCs) analysis to complement the sPSC data, the results also leave the possibility of endogenously active AMPA receptors being present at presynaptic terminals. This represents a major contraindication for these specific high-impact ampakines to be considered as suitable therapeutic drugs against drug-induced respiratory depression because of the underlying potential for an undesirable hyperventilation.

Voltage-clamp recordings showed that CX614 can potentiate up to 3-fold the AMPA-mediated charge transfer in preBötC respiratory neurons and potentiate spontaneously active inspiratory currents, which confirms the contribution of AMPA receptors conductance in preBötC inspiratory currents (Pace et al., 2007; Pace et al., 2008), but contrasts with whole-cell recordings of

respiratory hypoglossal motoneurons that have shown no presynaptic effect of CX614 (Lorier et al., 2010).

Current-clamp recordings of preBötC neurons have shown that CX546 and CX614 can also potentiate inspiratory bursts. Pharmacological isolation of the AMPA component of neuronal discharge after blocking synaptic transmission with TTX and calcium-related conductance with Cd^{2+} unmasked the potency of high-impact ampakines: the AMPA-mediated depolarization augmentation directly evoked by CX614 is much larger than the potentiation of the spontaneous inspiratory depolarization induced by CX614 alone. This suggests that ionic AMPA receptor current is only part of the current contributing to the inspiratory drive potential. Further, other endogenous conductance(s) may also act to dampen ampakines' direct increase of bursting depolarization.

3.4.3 AMPA RECEPTOR CONDUCTANCE AND PREBÖTC RHYTHM

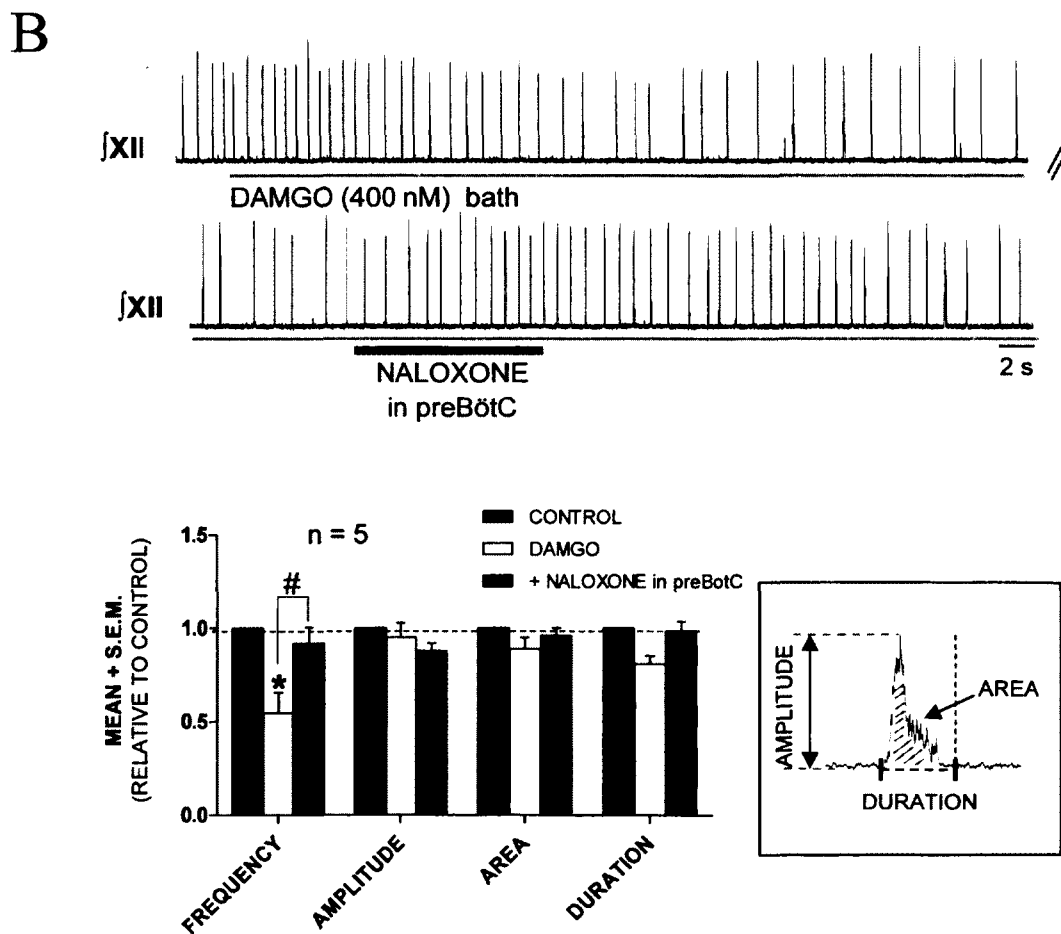
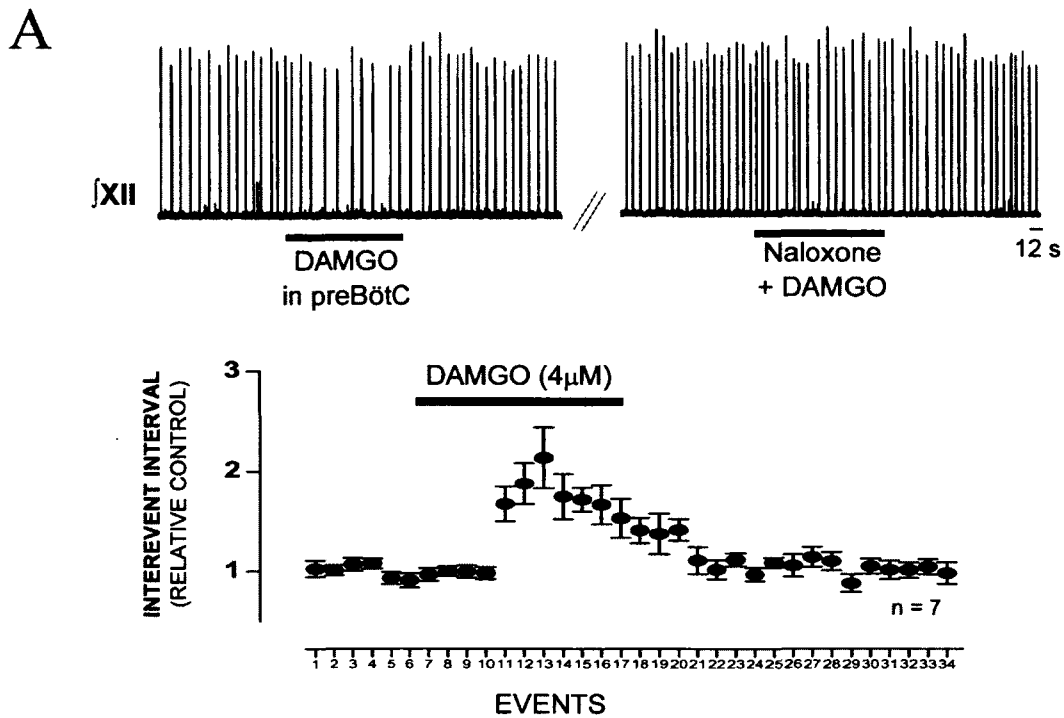
The data demonstrated that high-impact ampakines are capable of enhancing synaptic transmission within the preBötC and increasing the magnitude of single-cell synaptic currents sufficiently to convert sub-threshold activity (caused by DAMGO or low $[\text{K}^+]_e$) into a robust and long-lasting oscillatory activity that propagates throughout the entire neuronal network. More specifically, the frequency of interburst spontaneous events was primarily increased by ampakines which progressively enhanced postsynaptic inspiratory currents, suggesting that the repeated and persistent presynaptic stimulations induced by ampakine may increase synaptic efficacy and strengthen active synapses until producing a network-wide burst of action potentials. This is in line with the "Hebb's concept" which considers integration of synaptic inputs and increase in firing rate among electrically connected neurons as determinant neuronal coding schemes that can elicit synaptic coupling, enhance synaptic efficacy and improve network wiring (Brown et al., 1990).

Nevertheless, it is important to note that the increase in inspiratory conductance induced by ampakines did not result in a proportional increase in

motor output frequency. For example, CX614 increased the amplitude and area of the inspiratory current (2-fold the size of control) at the single-cell level but only increased the frequency to ~ 40% of control in baseline conditions. Also, even when ampakine effectively accelerated inspiratory bursts subsequent to DAMGO-induced respiratory depression, the amplitude and area of inspiratory currents reached values well above control values but yet the frequency stayed below control values. Thus it seems that the charge transfer increase resulting from the potentiation of inspiratory current area and amplitude by ampakine does not necessarily lead to a commensurate increase in rhythm frequency. Those results were quite surprising and rather unpredictable because the inspiratory current has been shown to rely on specific endogenous conductances (mainly calcium-activated types of conductances; Del Negro et al., 2005; Pace et al., 2007; Pace et al., 2008) that are hypothesized to generate rhythmicity (Rubin et al., 2009; Dunmyre et al., 2011). Further, current-clamp data (e.g. Fig. 3.13 and Fig. 3.14) showed that ampakines (CX546 in particular) are capable of triggering mechanisms that can generate very large and long plateau potentials, accompanied by action potential block, two distinct characteristics that strongly support an increase of burst-like generating conductances (such as I_{CAN}).

Thus, this study suggests that, within the preBötC, the change in amplitude of postsynaptic responses may be necessary for promoting inspiratory bursts and for the maintenance of a recurrent and synchronized rhythmic inspiratory activity, but may not be sufficient to affect burst regeneration and the inspiratory rhythm phase itself.

Future work will be directed toward elucidating the effect of ampakines on pacemaker neurons of the preBötC. Inspiratory neurons with autonomous bursting behaviour that persists in the absence of glutamatergic transmission have been reported (Koshiya and Smith, 1999; Peña et al., 2004; Thoby-Brisson and Ramirez, 2001). In these cells, inspiratory bursts do not rely on synaptic transmission, but rather on intrinsic endogenous properties. Therefore it will be interesting to examine how the increase in synaptic transmission gated by AMPA receptors may affect intrinsic bursting behaviour.



Previous Page

Figure 3.1 Local activation of mu-opioid receptors within the preBötzing complex (preBötC) in *in vitro* medullary slice preparation of neonatal rat depresses inspiratory rhythm.

A. Integrated traces of XII nerve bursts in active medullary slice showing a depression of inspiratory burst frequency induced by local application of the mu-opioid agonist DAMGO (4 μ M; 120 sec duration; n = 7) which can be attenuated by naloxone (4 μ M; 30 sec delay and 120 sec duration). The group data graph below shows the instant and pronounced increase in interevent interval induced by local application of DAMGO into the preBötC. **B.** Integrated traces of XII nerve bursts in active medullary slice showing a depression of inspiratory burst frequency induced by bath application of the mu-opioid agonist DAMGO (400 nM). The depressing effect of DAMGO can be attenuated by local application of naloxone in the preBötC (10 μ M; n = 5). The group data graph shows relative values of XII bursting discharge characteristics during DAMGO application and during naloxone locally applied to the preBötC during DAMGO application (* = p < 0.05 significant different from control; # = p < 0.05 significant different from DAMGO; one way ANOVA; n = 5). Average of 5 XII burst integrated traces is used on the right to show XII nerve discharge characteristics that are described in the histogram.

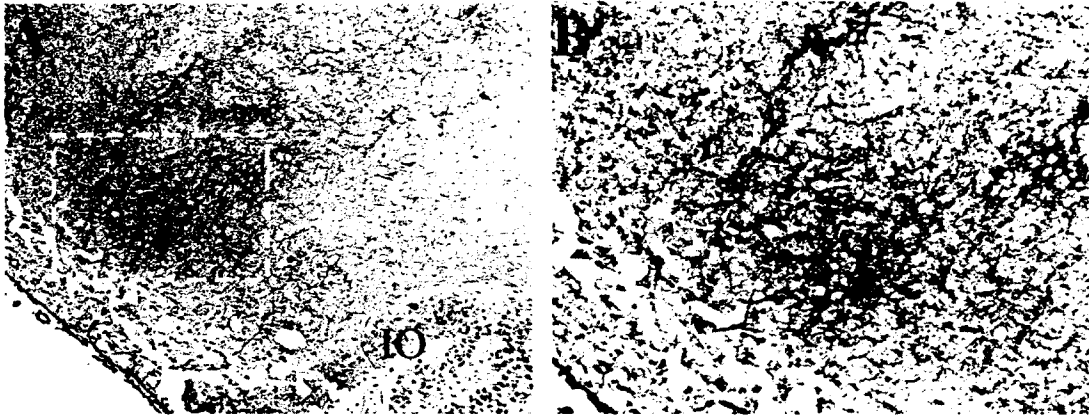
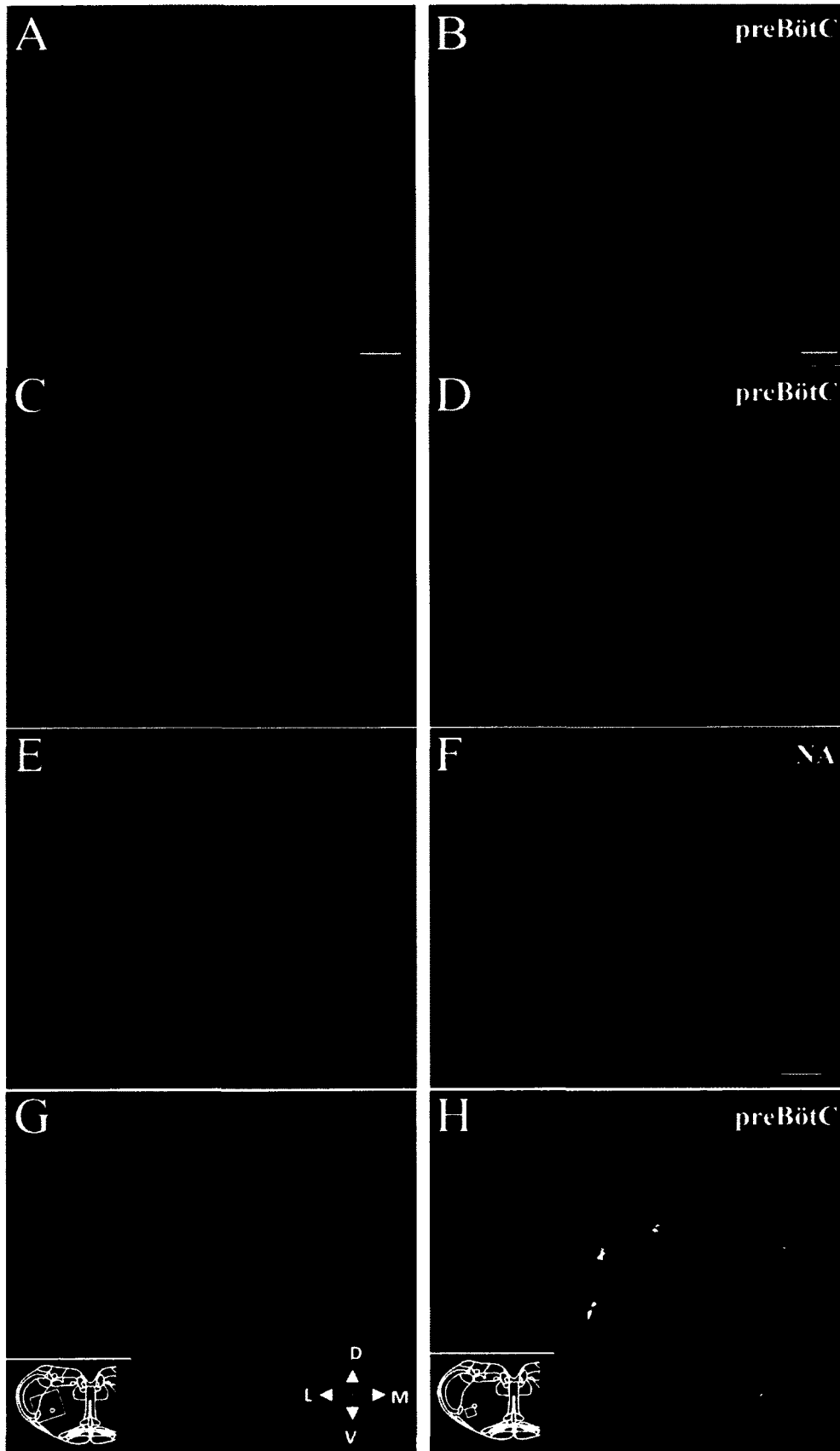


Figure 3.2 Mu-opioid receptor 1a is expressed in the preBötC of new born rat.

Photomicrographs of a transverse section of the medulla show that, ventral to the nucleus ambiguus (NA), some cells and fibres in the preBötzinger complex region are strongly immunoreactive for mu-opioid receptor 1a (MOR1a). MOR1a immunostaining was performed with diaminobenzidine reaction. **A.** MOR1a positive cells are also present in the Inferior Olive (IO). The dashed square represents the approximate area of the preBötC. MOR1a is mostly immunoreactive in fibres and somatic membranes (X10). **B.** The image shows the preBötC area at higher magnification (X20). The hypothesis is that the subpopulation of interneurons expressing MOR1a in the preBötC is responsible for the respiratory depression induced by mu-opioid agonist microinjection within the preBötC (n = 5).



Previous Page

Figure 3.3 Expression of MOR1a, NK1R, and ChAT in a transverse section of the medulla in neonatal rat.

A. MOR1a (in red) is expressed in cells located in the compact formation of the NA and in the preBötC area. **C.** Neurokinin receptors 1 (NK1R, in green) is expressed in the NA and preBötC. **E.** The semi-compact formation of the NA is assessed by the expression of choline acetyltransferase (ChAT, in blue) in motoneurons of the NA. **G.** Overlay of MOR1a, NK1R and ChAT labeling. In the preBötC, MOR1a colocalizes with NK1R in a subpopulation of NK1R⁺ cells and with ChAT in few motoneurons of the external formation of the nucleus ambiguus. However in the NA area, note the absence of MOR1a labeling in the semi-compact formation of the NA (seen at higher magnification in **F**). Scale bar for **A, C, E** and **G** is 50 μm . **B, D, H.** High magnification (X40) images within the preBötC are shown in **B** (MOR1a), **D** (NK1R) and **H** (overlay) where the colocalization pattern is seen in yellow. MOR1a colocalizes with NK1R in a subpopulation of NK1R⁺ cells on neuronal processes and cell membranes. **F.** High magnification (X40) image within the NA showing the co existence of both compact (red) and semi-compact (blue) divisions in this picture. Scale bar for **B, D, H** is 20 μm and 25 μm for **F**. n = 4.

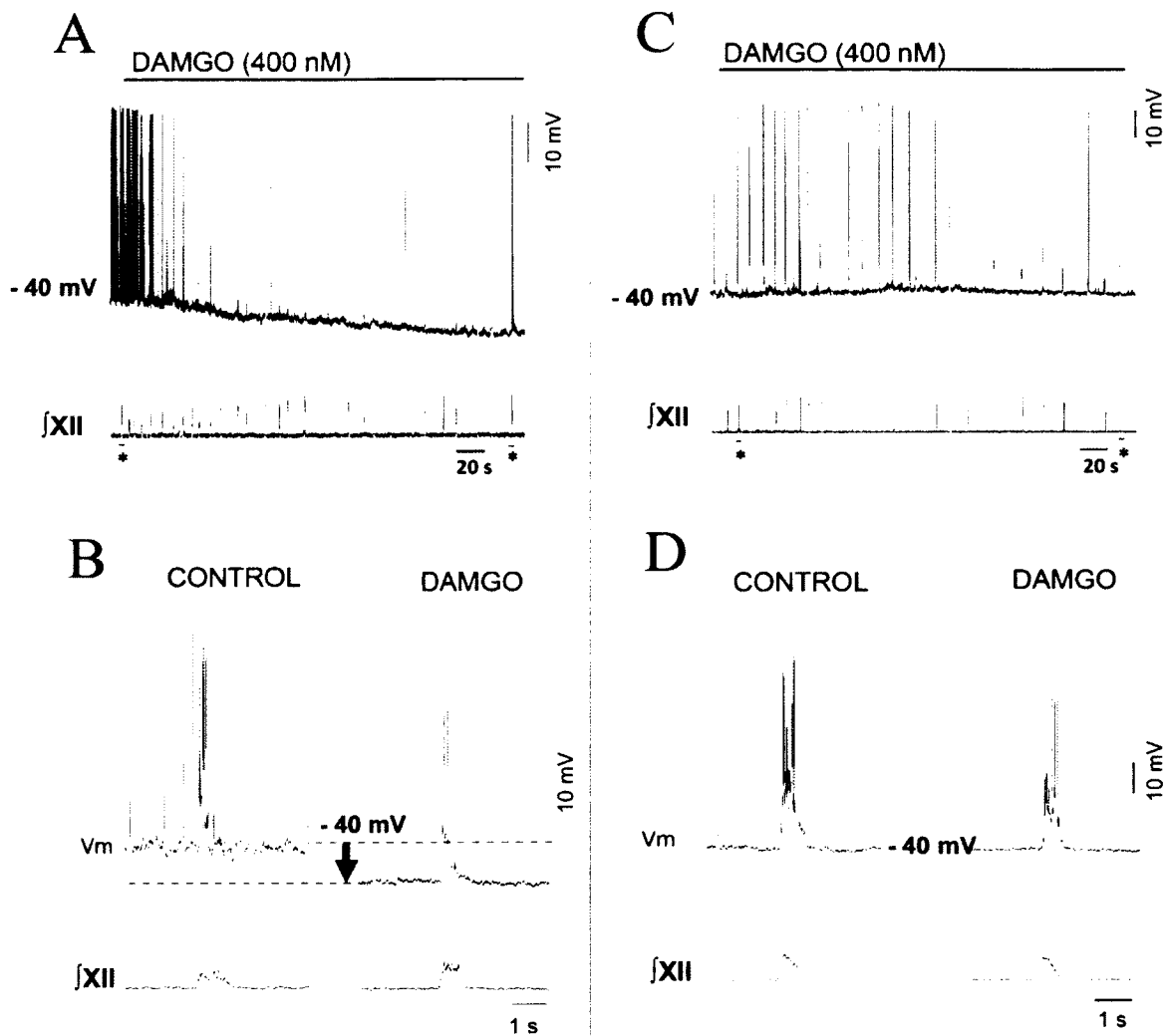
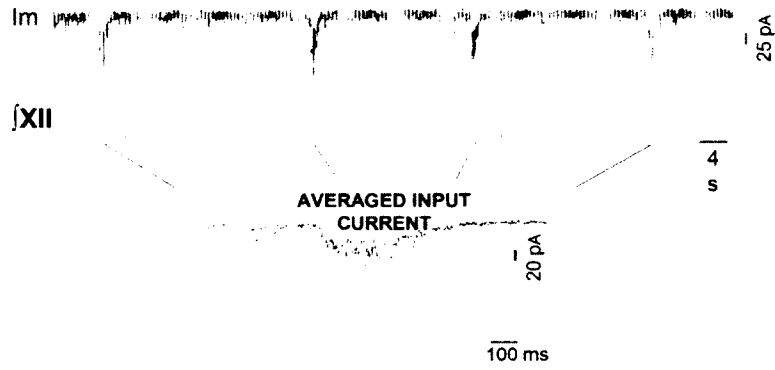


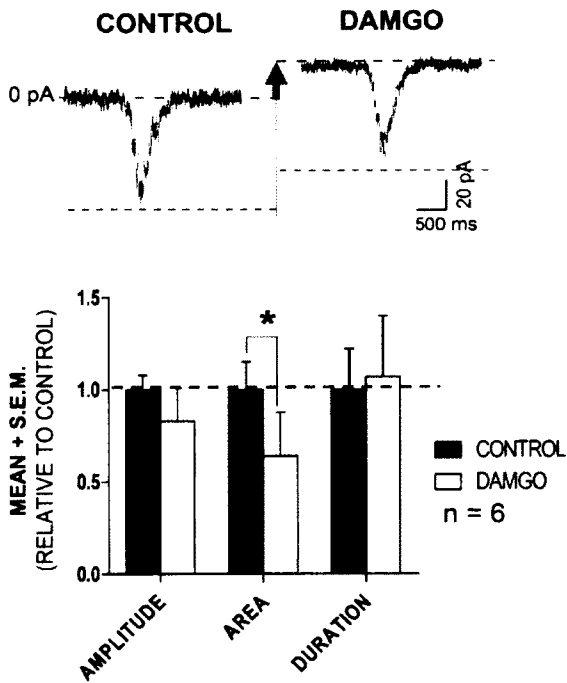
Figure 3.4 DAMGO differentially affects respiratory neurons of preBötC in *in vitro* medullary slice preparation of neonatal rats.

A, C. The upper traces show whole-cell current-clamp recordings of inspiratory preBötC neuron under bath application of DAMGO (400 nM). The bottom traces are suction electrode recordings of XII nerve activity concomitant to the intracellular recording showing a decrease of inspiratory drive frequency induced by DAMGO. Asterisks on the bottom of figure A and C mark the bursts highlighted in figure B and D. **B, D.** Membrane potential and inspiratory drive potential with corresponding XII nerve bursts integrated trace are compared just before and during DAMGO bath application effect. The blue arrow points out the membrane potential hyperpolarization induced by DAMGO.



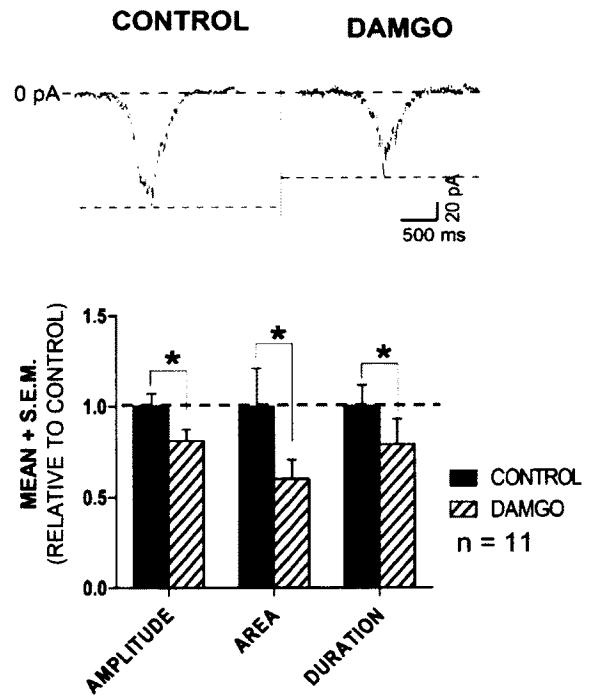
A

OPIOID SENSITIVE CELLS



B

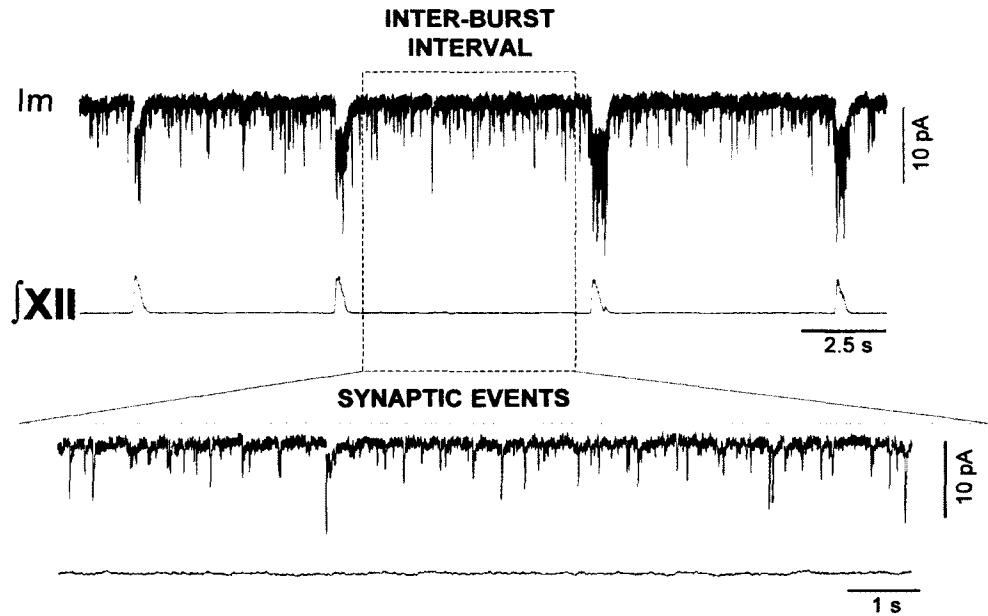
OPIOID INSENSITIVE CELLS



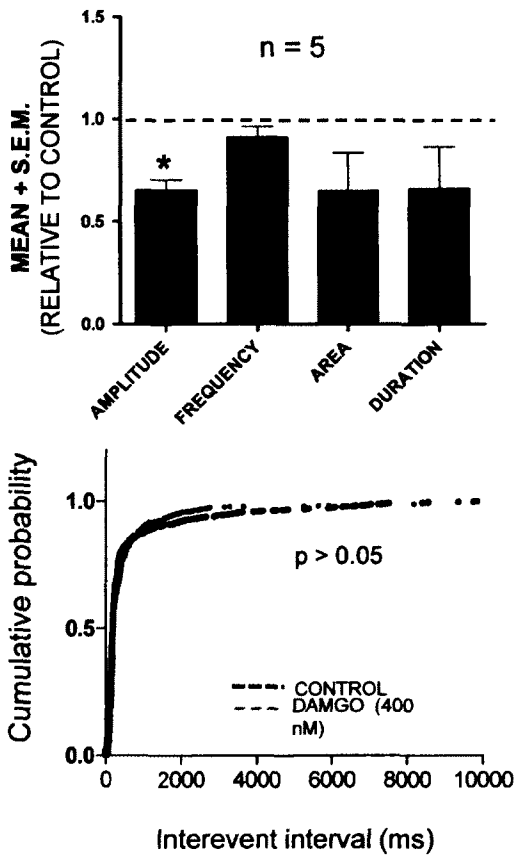
Previous Page

Figure 3.5 Differential effects of DAMGO on inspiratory currents of preBötC neurons.

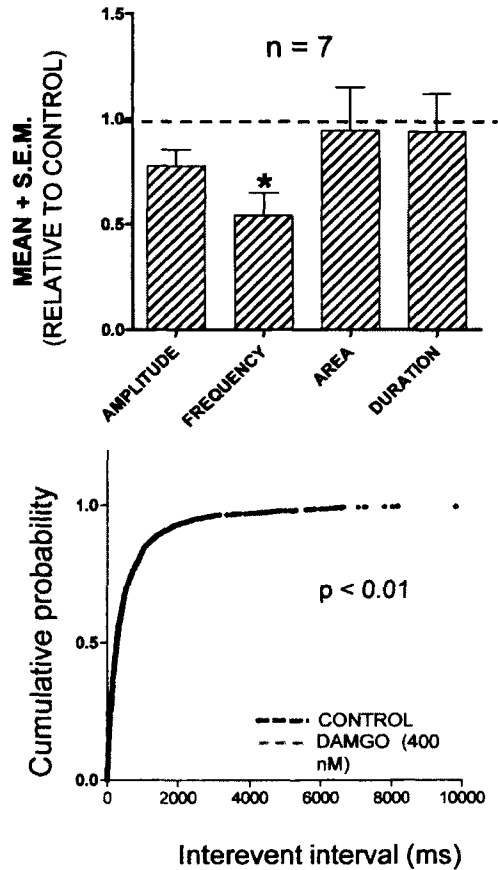
Upper trace is a representative trace of an inspiratory input current obtained from a voltage-clamp recording of an inspiratory preBötC neuron in basic physiological conditions. **A, B.** First traces are representative traces of the average of 10 postsynaptic events before (left: control) and during (right: DAMGO) bath application of DAMGO, in an inspiratory cell categorized as “opioid-sensitive” cell (**A**) and in a inspiratory cell categorized as a “opioid-insensitive” cell (**B**). Each group data histogram is shown below its corresponding representative trace. Group data graphs show normalized values of area, amplitude and duration analyzed in inspiratory input currents recorded during DAMGO bath application (white for opioid-sensitive cell group or stripes for opioid-insensitive cell group). Note that in **A**, group data show statistic difference only for the area ($p > 0.05$), whereas in **B** statistical significance is reached for all 3 parameters. * represents p value < 0.05 for mean values obtained in DAMGO compared to mean values obtained in control in a paired Student’s t test. Below, whole-cell I/V relationships obtained before (control trace in black) and during bath application of DAMGO (grey trace) in an inspiratory preBötC opioid sensitive cell (**A**) or opioid-insensitive cell (**B**).



A OPIOID SENSITIVE CELLS



B OPIOID INSENSITIVE CELLS



Previous Page

Figure 3.6 Differential effect of DAMGO on interburst synaptic events in inspiratory neurons of the preBötC.

Example of interburst sPSCs recorded in inspiratory preBötC neurons in voltage-clamp configuration. Figure A shows group data of sPSCs recorded in “opioid-sensitive” cells and figure B shows group data of sPSCs recorded in “opioid-insensitive” cells. Group data graphs show relative values of different parameters of the sPSCs recorded during DAMGO bath application (black for opioid-sensitive cells group or stripes for opioid-insensitive cells group). * represent a p value < 0.05 for a Student’s *t* test. Graphs below represent cumulative distribution plots of the sPSCs interevent interval recorded in opioid-sensitive cells (left) and opioid insensitive cells (right). Note how sPSC interevent interval distribution skews toward larger interevent interval in opioid insensitive cells. Statistical comparison of the two distribution was done with Kolmogorov-Smirnov two sample test ($p = 0.0013 < 0.01$ significance).

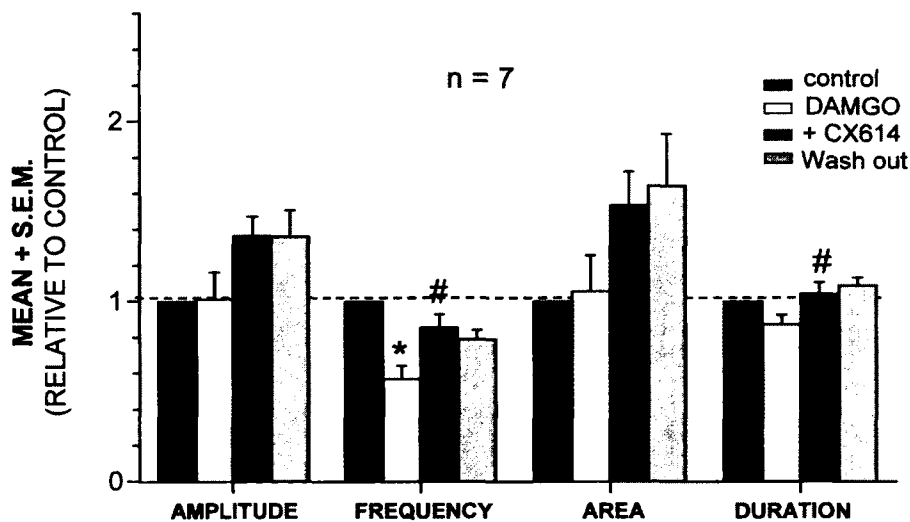
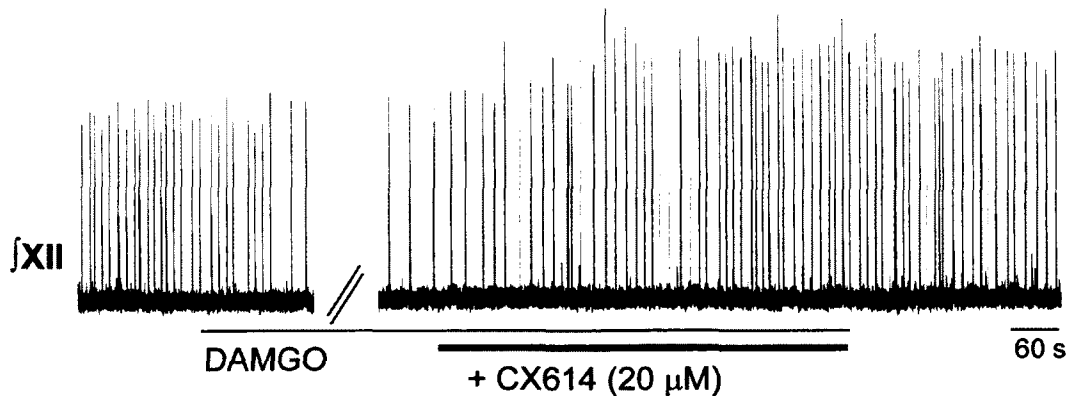


Figure 3.7 Bath application of CX614 alleviates DAMGO-induced inspiratory drive frequency depression in in vitro rat medullary slice preparation.

A. Integrated traces of XII nerve bursts in active medullary slice showing a depression of inspiratory burst frequency induced by bath application of DAMGO (400 nM) and subsequent increase in frequency and amplitude of inspiratory drive. **B.** The group data graph show relative values of XII bursting discharge characteristics in 4 conditions: control; DAMGO (400 nM); DAMGO (400 nM) + CX614 (20 μM); wash out (* = $p < 0.05$ significant different from control; # = $p < 0.05$ significant different from DAMGO, repeated-measures ANOVA).

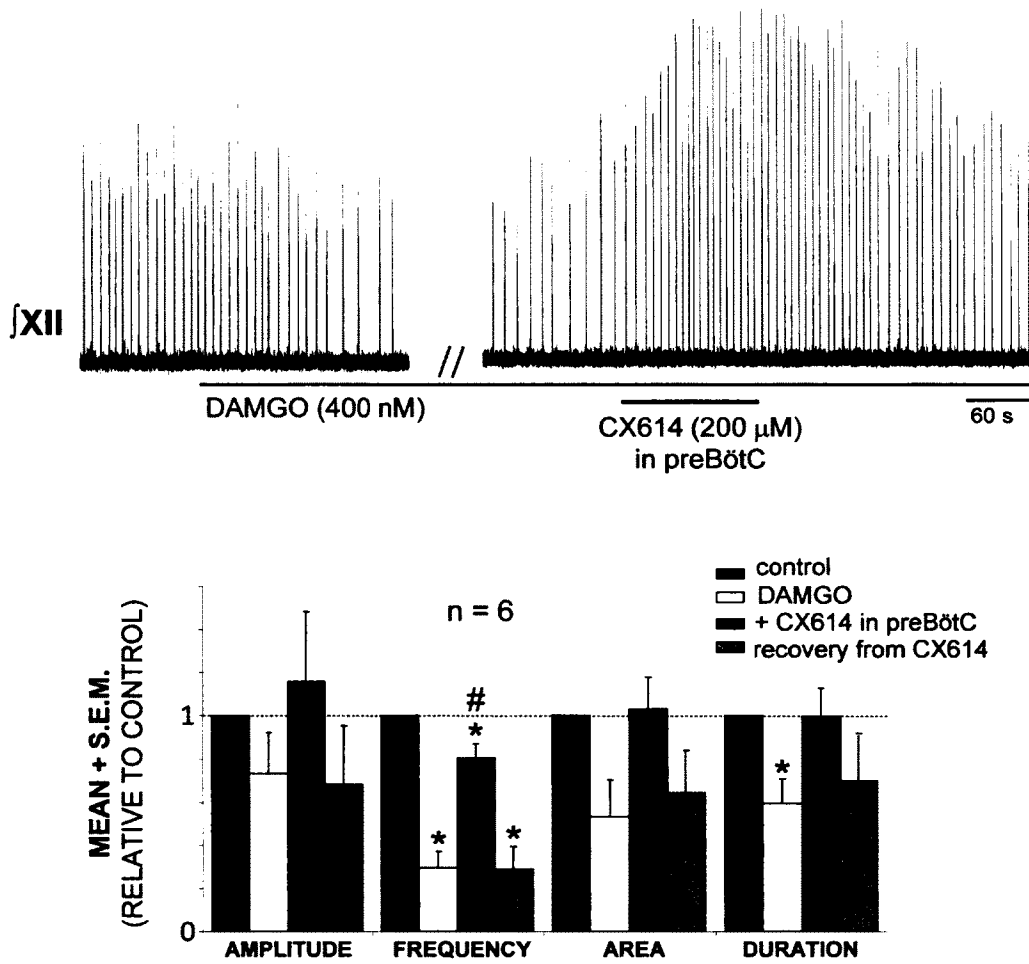


Figure 3.8 Local application of CX614 into the preBötC alleviates opioid-induced inspiratory rhythm depression.

The upper trace shows integrated XII nerve bursts recorded from a medullary slice preparation in presence of bath-applied DAMGO and subsequent CX614 local application into the preBötC. The group data below shows normalized values of XII burst parameters under different experimental conditions. * = p values < 0.05 significantly different from control; # = p values < 0.05 significantly different from DAMGO.

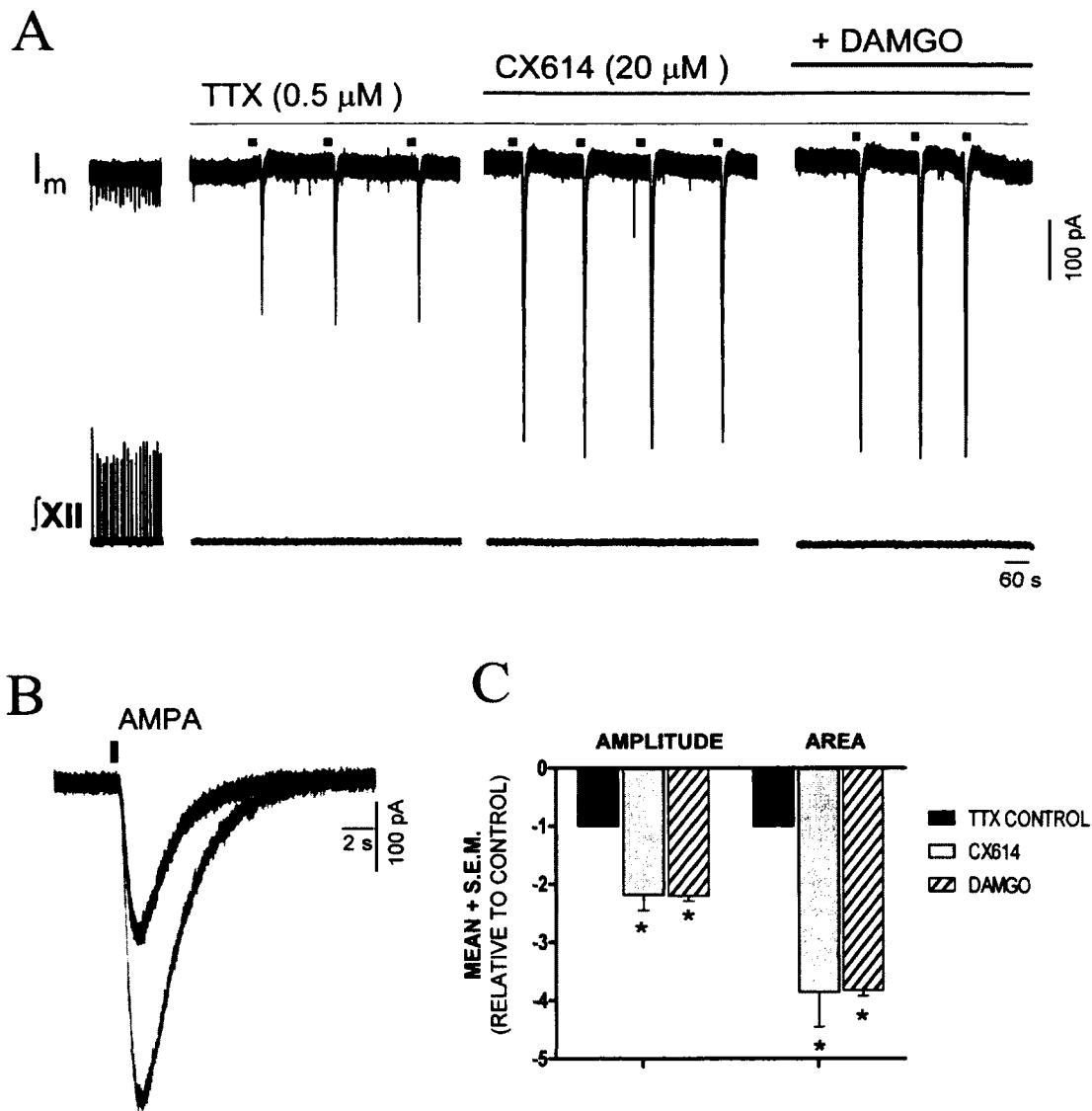


Figure 3.9 AMPA-mediated current load is increased by CX614 in respiratory preBötC neurons.

A. Voltage-clamp recording of an inspiratory neurons of the preBötC in presence of TTX showing that currents evoked by local application of AMPA (400 ms) are increased in the presence of CX614 (bath); those currents are not affected by subsequent bath application of DAMGO. **B.** Currents evoked by AMPA puff (400 ms; 100 μ M) in control (black) and in the presence of bath- applied CX614, 20 μ M (grey) **C.** Histogram summary of group data (n = 9 (CX614); n = 4 (DAMGO)) showing relative current amplitude and area. (* = p values significantly different from control).

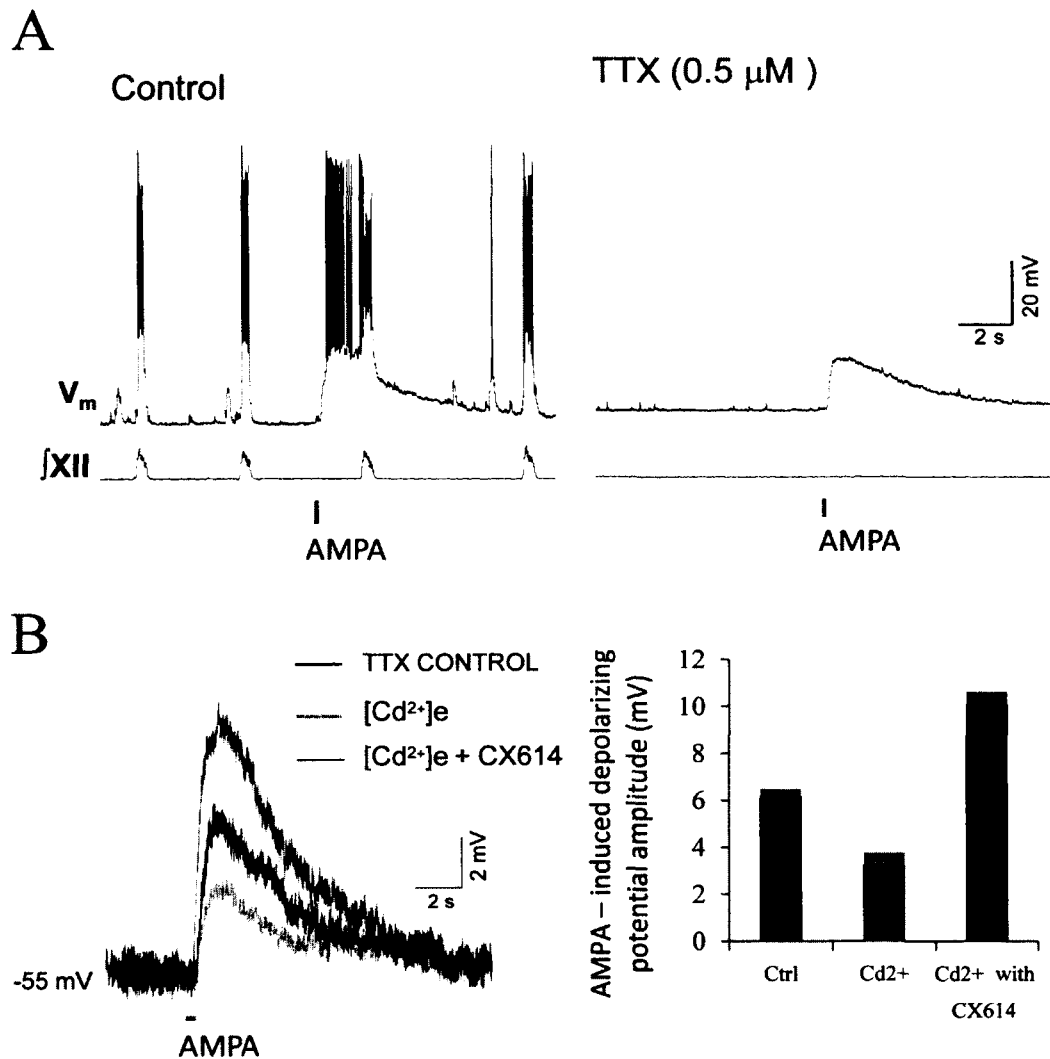
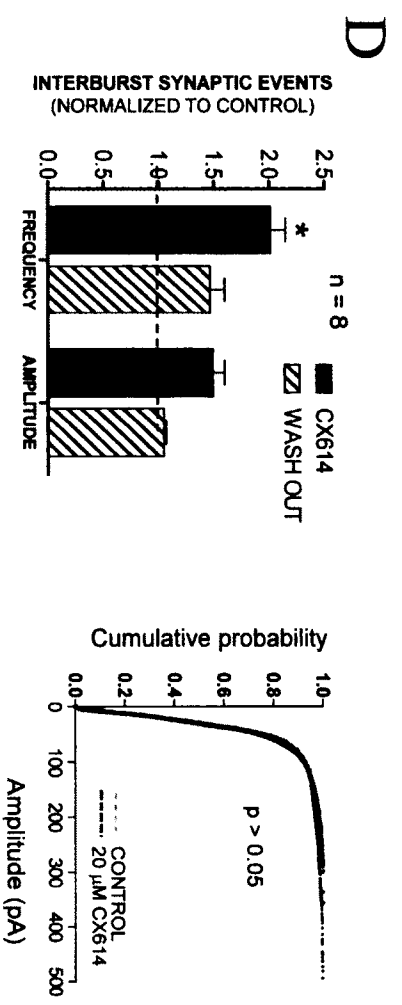
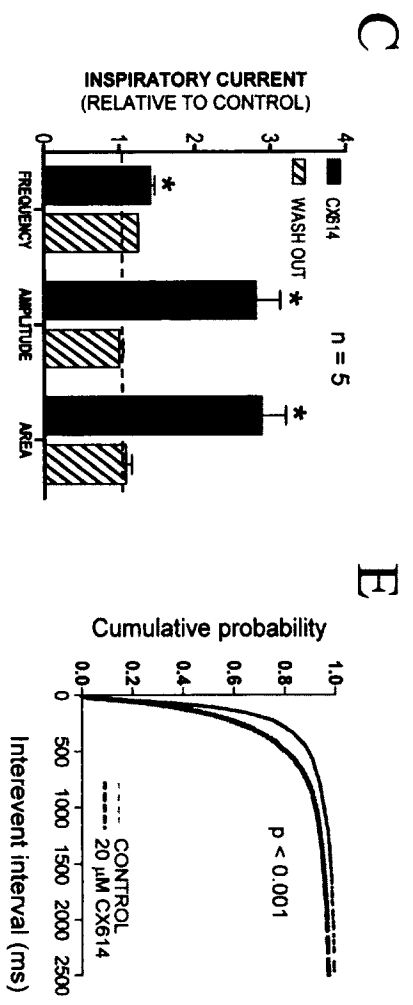
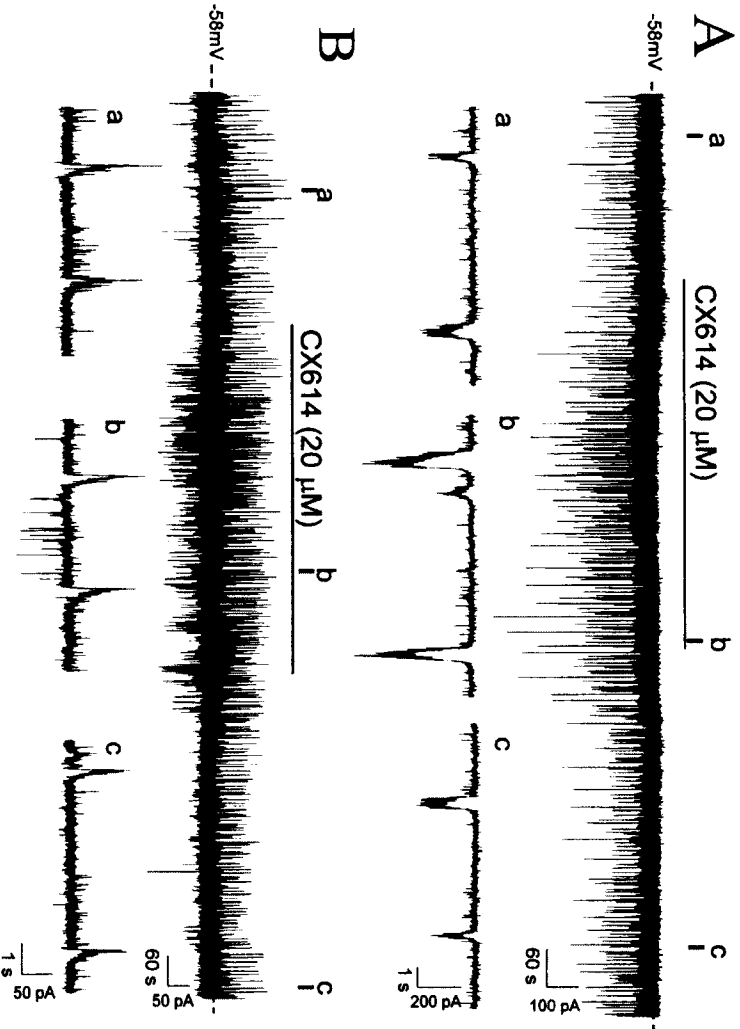


Figure 3.10 CX614 increases the AMPA component of preBötC inspiratory drive potentials independently of external calcium.

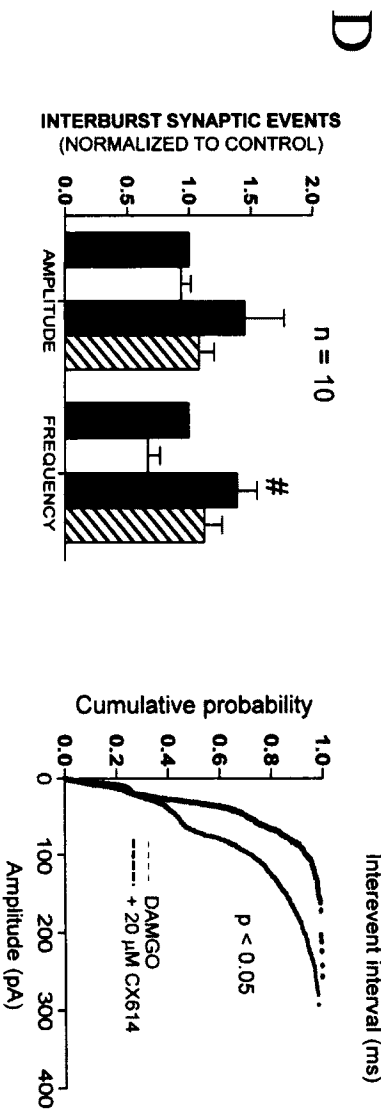
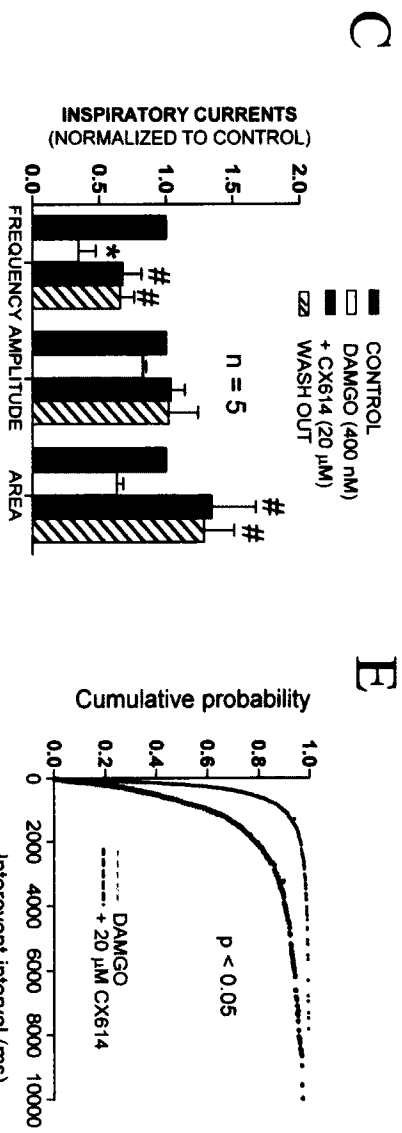
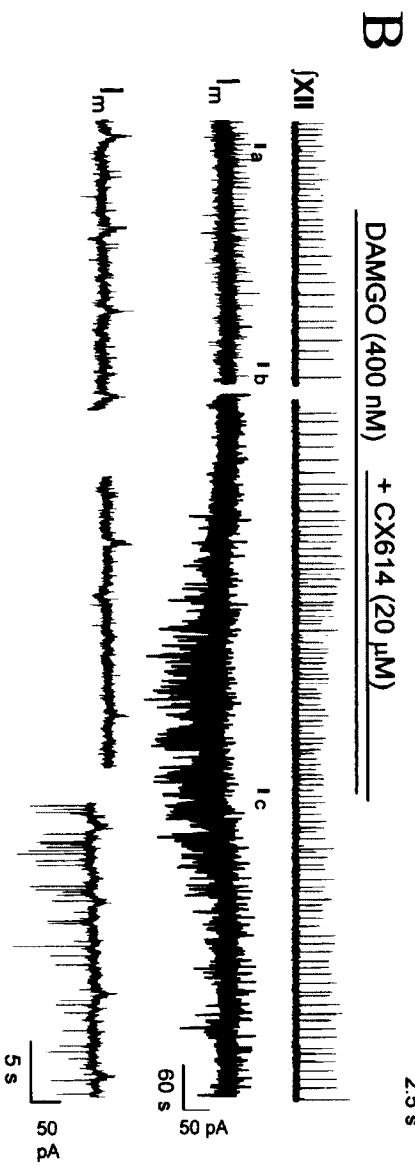
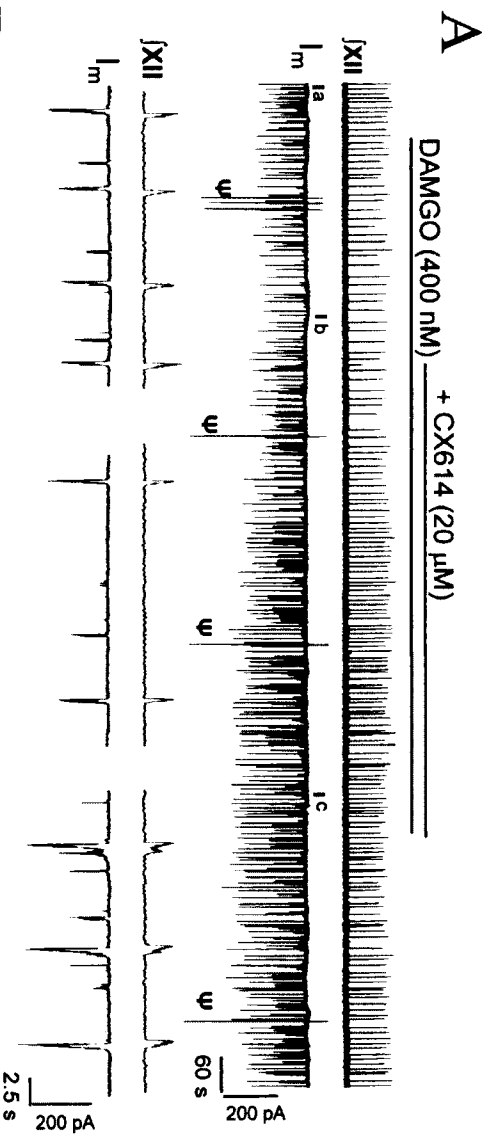
A. Voltage-clamp recording of an inspiratory neuron of the preBötC in control and in presence of TTX showing depolarization evoked by local application of AMPA (100 μM ; 200 ms duration). AMPA-evoked depolarization amplitude was matched to that of spontaneous inspiratory depolarizing potentials. **B.** AMPA-evoked depolarizations are first decreased by extracellular Cd^{2+} and subsequently increased by CX614 (bath). Histogram summary of repeated AMPA depolarization amplitudes obtained in different conditions (**B**) are shown on the right.



Previous Page

Figure 3.11 CX614 alone augments excitatory currents on respiratory preBötC neurons and increasing inspiratory frequency.

A. Representative trace of a whole-cell recording of an inspiratory neuron of the preBötC in voltage-clamp configuration showing the increase in inspiratory input currents induced by bath application of CX614. **B.** Representative trace of a voltage-clamp recording of an expiratory neuron of the preBötC under bath application of CX614 (20 μ M). Note that while the expiratory-related outward currents are not affected by CX614, the excitatory postsynaptic current amplitude and frequency are largely increased by CX614. **C.** Group data showing inspiratory input current parameters modulated by CX614. * = different from control, $p < 0.05$; one-way ANOVA and Tukey's post test. **D.** Group data showing tonic spontaneous postsynaptic current parameters modulated by CX614. * = different from control, $p < 0.05$; one-way ANOVA and Tukey's post test. **E.** Cumulative distribution plots of the sPSCs interevent interval (upper) and amplitude (lower) recorded in respiratory cells (Kolmogorov-Smirnov two sample test ($p < 0.05$ significance)).



Previous Page

Figure 3.12 CX614 effect on preBötC neuronal postsynaptic activity subsequent to DAMGO-induced suppression of inspiratory drive.

A. Voltage-clamp recording of a preBötC inspiratory neuron showing suppression of inspiratory input current by DAMGO and the subsequent reversal after CX614 application. The Ψ on each figure shows current-voltage responses for input resistance measurements. **B.** Representative trace of a voltage-clamp recording of an expiratory neuron of the preBötC under bath application of DAMGO and subsequent addition of CX614 to the bathing medium. Note the large increase in the size of sPSCs induced by CX614. **C.** Histogram of group relative data showing the increase in inspiratory current frequency and area induced by CX614 ($n = 5$; only opioid-insensitive cells were taken for this graph. * = p values < 0.05 significant different from control; # = p values < 0.05 significant different from DAMGO). **D.** Histogram of group relative data showing sPSC frequency and amplitude induced by CX614 ($n = 10$; # = p values < 0.05 significant different from DAMGO). **E.** Cumulative distribution plots of the sPSC interevent interval (upper) and amplitude (lower) recorded in respiratory cells. Note how sPSC amplitude distribution skews towards larger amplitude with addition of CX614 in the bathing medium (Kolmogorov-Smirnov test; $p < 0.05$).

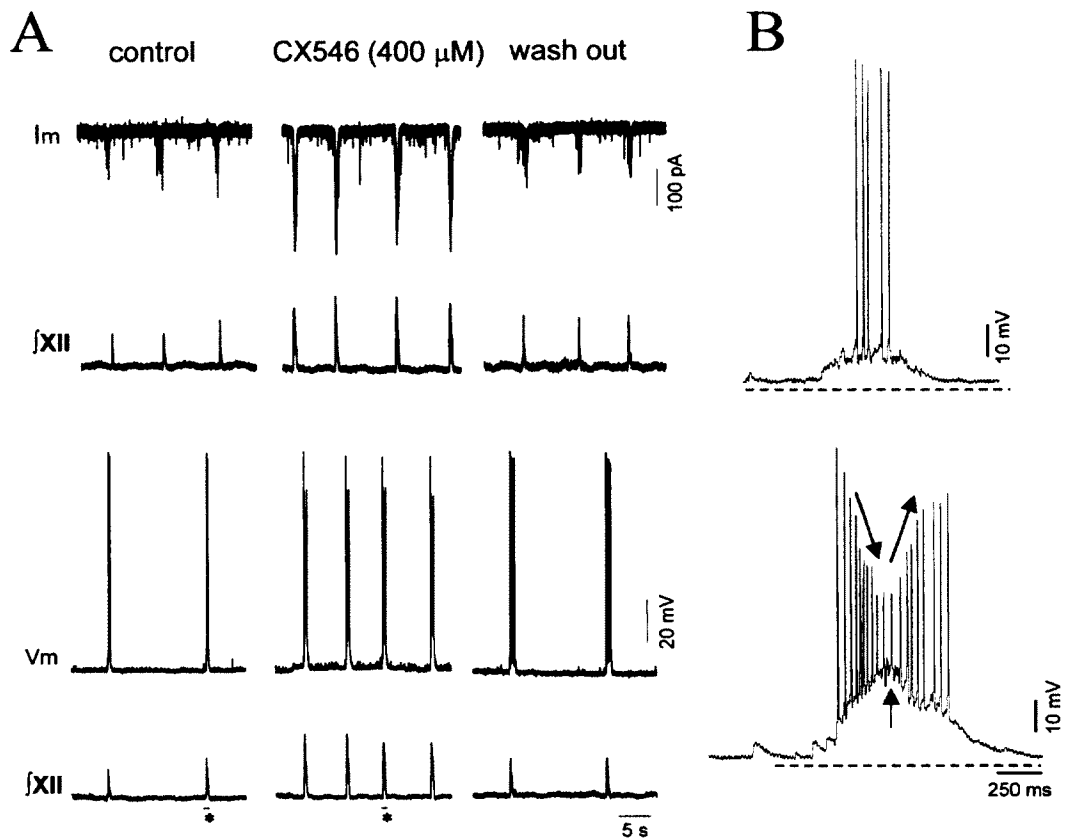
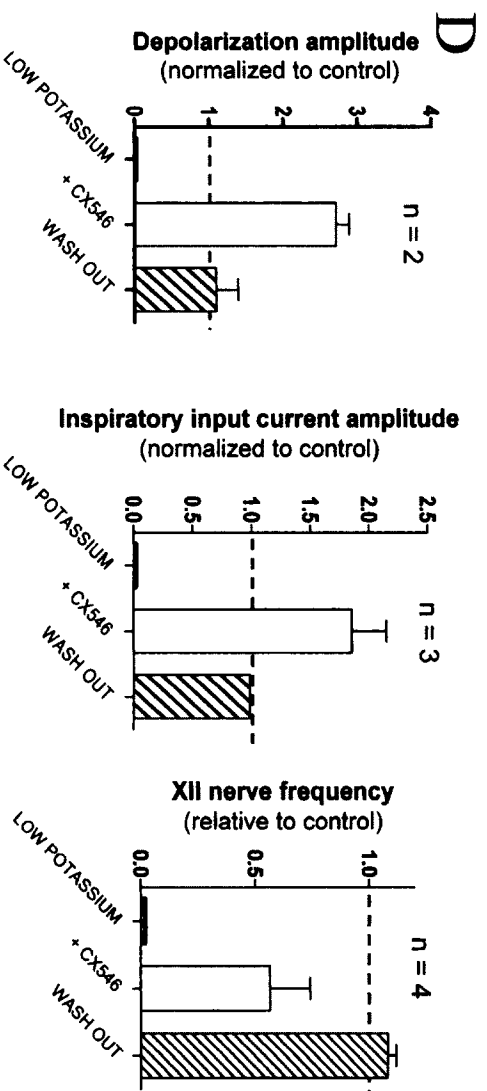
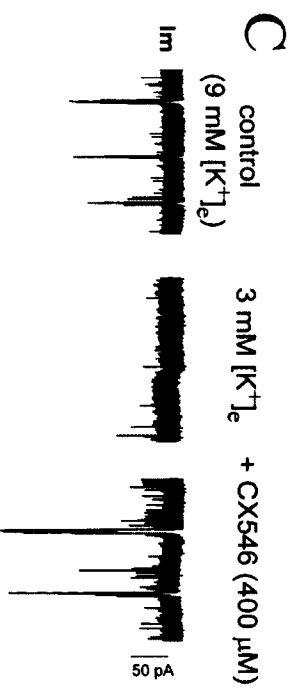
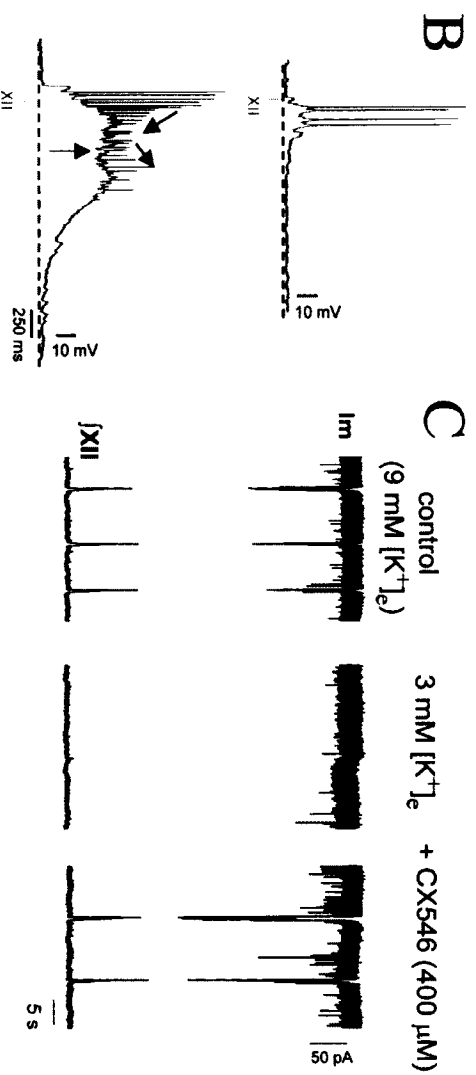
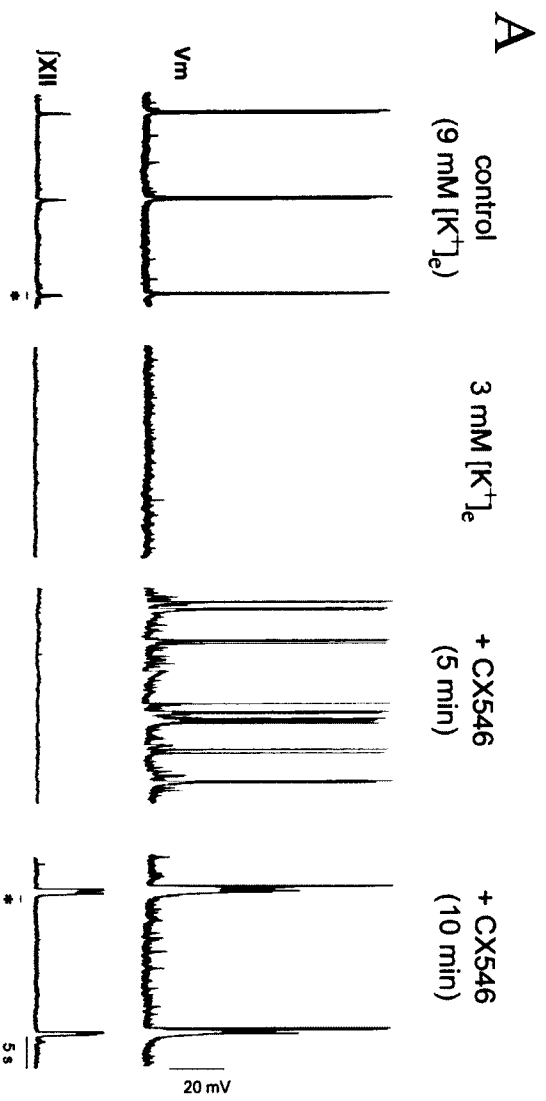


Figure 3.13 Allosteric modulation of AMPA receptors by the high impact ampakine CX546 increases inspiratory envelope of preBötC neurons in basic physiological conditions.

A. Voltage-clamp (upper trace) and current-clamp (lower trace) recording of inspiratory neurons of the preBötC showing inspiratory drive depolarizations and input currents increased by the high impact ampakine CX546 in baseline physiological conditions. The asterisks indicate the inspiratory bursts reproduced at higher magnification in figure B.

B. At the same membrane potential, CX546 enhanced inspiratory-coupled depolarization (from 7.6 mV in control to 26 mV in CX546) accompanied by superimposed high frequency spikes. Black arrows indicate the period of rapid spiking during the depolarizing upstroke followed by a phase of spike attenuation. This spiking block is transient and the cell resumes tonic spiking with larger amplitude until burst termination



Previous Page

Figure 3.14 Ampakine CX546 increases inspiratory currents in weak endogenous inspiratory drive.

A. Current-clamp recording of an early-type of inspiratory preBötC cell in which inspiratory drive depolarizations and paired inspiratory network activity completely suppressed by low extracellular concentration of potassium (3 mM $[K^+]_e$). Both can largely be increased by adding CX546 to the bathing medium. Note that CX546 increases ectopic bursting behavior at the cellular level before inducing phase-locked bursts synchronized with network rhythmic activity assessed by XII burst activity pattern. The asterisks indicate the exact inspiratory bursts reproduced at higher magnification in **B**. The grey bars denote the onset of the paired XII nerve burst. Both bursts were recorded at the exact same membrane potential (-60 mV). CX546 elicits a rapid ramp-like depolarizations in 3mM $[K^+]_e$. **C.** Voltage-clamp recording of an inspiratory preBötC neuron shows that the inspiratory current is increased by CX546 in 3 mM $[K^+]_e$. Note that the inspiratory currents (**C**) and inspiratory drive depolarizing bursts (**A**) have their amplitude and duration increased by CX546, which results in an increase in charge transfer in inspiratory cells. **D.** Group data graphs showing the degree of potentiation induced by CX546 at the cellular level (left and middle panel), as well as the network level (right panel) in 3 mM $[K^+]_e$.

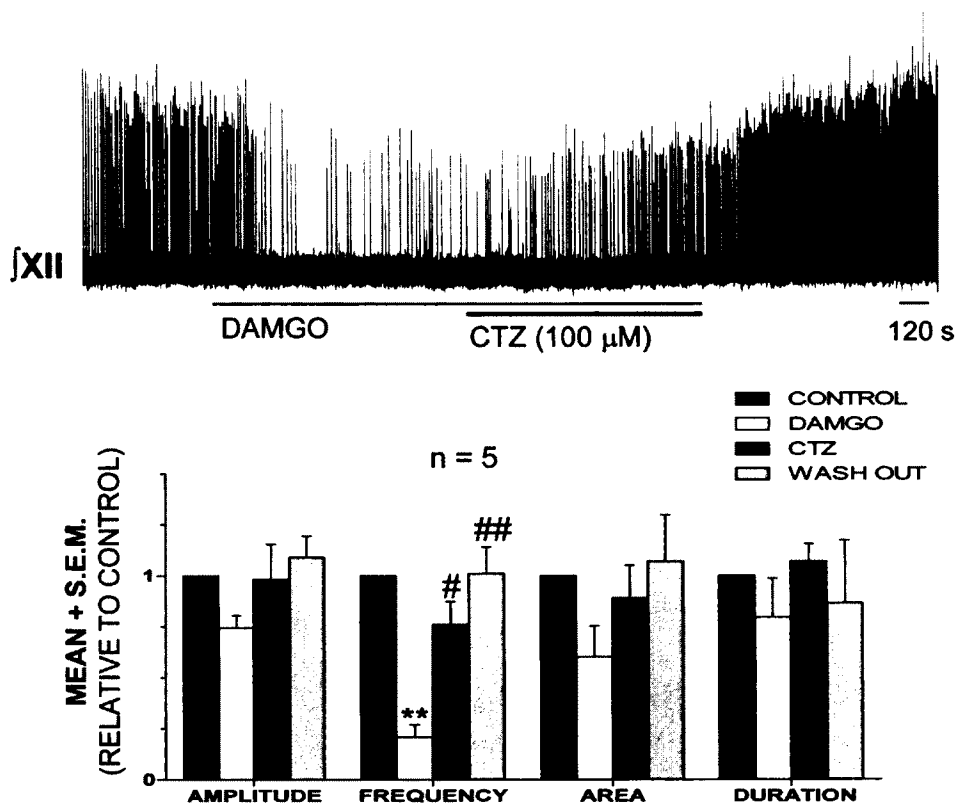


Figure 3.15 Cyclothiazide reverses DAMGO-induced inspiratory drive depression in *in vitro* medullary slice of neonatal rat.

The upper trace is a representative example of the XII bursts nerve recording during DAMGO (400 nM) and subsequent bath application of cyclothiazide (100 μM). The lower histogram is a group data graph representing relative values of XII nerve characteristics under the different experimental conditions (n = 4). Note the significant increase in XII burst frequency produced by cyclothiazide (# = p < 0.05 compared to DAMGO; ## = p < 0.01 compared to DAMGO; ** = p < 0.01 compared to CONTROL; one-way ANOVA with Tukey's post test).

3.5 REFERENCES

ANGULO MC, ROSSIER J, AUDINAT E (1999) Postsynaptic glutamate receptors and integrative properties of fast-spiking interneurons in the rat neocortex. *J Neurophysiol.* 82(3):1295-302.

ARIA A, KESSLER M., ROGERS G, LYNCH G (2000) Effect of the potent ampakines CX614 on Hippocampal and Recombinant AMPA receptors: Interaction with cyclothiazide and GYKI 52466. *Molecular Pharmacology* 58:802-813.

ARAI A, XIA Y-X, ROGERS G, LYNCH G, KESSLER M (2002) Benzamide-type AMPA Receptor Modulators Form Two Subfamilies with Distinct Modes of Action. *Journal of Pharmacology and Experimental Therapeutics* 303:1075-1085.

ARAI AC, XIA Y-F, SUZUKI E (2004) Modulation of AMPA receptor kinetics differentially influences synaptic plasticity in the hippocampus. *Neuroscience* 103:1075-1024.

ARMSTRONG N, JASTI J, BEICH-FRANDBEN M, GOUAUX E (2006) Measurement of conformational changes accompanying desensitization in an ionotropic glutamate receptor. *Cell* 127(1):85-97.

BALLANYI K, LALLEY PM, HOCH B, RICHTER DW (1997) cAMP-dependent reversal of opioid- and prostaglandin-mediated depression of the isolated respiratory network in newborn rats. *J Physiol.* 504 (Pt 1):127-34.

BALLANYI K, PANAITESCU B, RUANGKITTISAKUL A (2010) Indirect opioid actions on inspiratory pre-Bötzinger complex neurons in newborn rat brainstem slices. *Adv Exp Med Biol.* 669:75-9.

BALLANYI K, RUANGKITTISAKUL A, ONIMARU H (2009) Opioids prolong and anoxia shortens delay between onset of preinspiratory (pFRG) and inspiratory (preBötC) network bursting in newborn rat brainstems. *Pflugers Arch.* 458(3):571-87.

BLACK MD (2005) Therapeutic potential of positive AMPA modulators and their relationship to AMPA receptor subunits: a review of preclinical data. *Psychopharmacology* 179:154-163.

BROWN TH, KAIRISS EW, KEENAN CL (1990) Hebbian synapses: biophysical mechanisms and algorithms. *Annu Rev Neurosci.* 13:475-511.

BUTERA RJ, RINZEL L AND SMITH JC (1999) Models of respiratory rhythm generation in the preBotzinger complex I. Bursting pacemaker neurons. *Journal of Neurophysiology* 82: 382-97.

- COLMAN AS, MILLER JH (2001) Modulation of breathing by mu1 and mu2 opioid receptor stimulation in neonatal and adult rats. *Respir Physiol.* 127(2-3):157-72.
- CONNOR M, SCHULLER A, PINTAR JE, CHRISTIE MJ (1999) MU-opioid receptor modulation of calcium channel current in periaqueductal grey neurons from C57B16/J mice and mutant mice lacking MOR-1. *Br J Pharmacol.* 126(7):1553-8.
- DEL NEGRO CA, HAYES JA, PACE RW, BRUSH BR, TERUYAMA R, FELDMAN JL (2010) Synaptically activated burst-generating conductances may underlie a group-pacemaker mechanism for respiratory rhythm generation in mammals. *Prog Brain Res.* 187:111-36.
- DEL NEGRO CA, HAYES JA, REKLING JC (2011) Dendritic calcium activity precedes inspiratory bursts in preBotzinger complex neurons. *J. Neurosci.* 31(3):1017-22.
- DEL NEGRO CA, MORGADO-VALLE C, FELDMAN JL (2002) Respiratory rhythm: an emergent network property? *Neuron.* 34(5):821-30.
- DEL NEGRO CA, MORGADO-VALLE C, HAYES JA, MACKAY DD, PACE R.W, CROWDER EA, FELDMAN JL (2005) Sodium and calcium currents-mediated pacemaker neurons and respiratory rhythm generation. *Journal of Neuroscience* 25:446-453.
- DENG L AND CHEN G (2003) Cyclothiazide potently inhibits gamma-aminobutyric acid type A receptors in addition to enhancing glutamate responses. *PNAS* 100(22):13025-29.
- DUNMYRE JR, DEL NEGRO CA, RUBIN JE (2011) Interactions of persistent sodium and calcium-activated nonspecific cationic currents yield dynamically distinct bursting regimes in a model of respiratory neurons. *J. Comput Neurosci* .31(2):305-28.
- FUNK GD, SMITH JC, FELDMAN JL (1993) Generation and transmission of respiratory oscillations in medullary slices: role of excitatory amino acids. *Journal of Neurophysiology* 90(4): 1497-515.
- FUNK GD, SMITH JC, FELDMAN JL (1995) Modulation of neural network activity *in vitro* by cyclothiazide, a drug that blocks desensitization of AMPA receptors. *Journal of Neuroscience* 15(5): 4046-4056.
- GE Q, FELDMAN JL (1998) AMPA receptor activation and phosphatase inhibition affect neonatal rat respiratory rhythm generation. *J Physiol.* 509 (Pt 1):255-66.

GONZALEZ J, DU M., PARAMESHWARAN K, SUPPIRAMANIAM V, JAYARAMAN V (2010) Role of dimer interface in activation and desensitization in AMPA receptors. *Proc Natl Acad Sci U S A* 107(21):9891-6.

GRAY PA, JANCZEWSKI WA, MELLEN N, MCCRIMMON DR, FELDMAN JL (2001) Normal breathing requires preBötzinger complex neurokinin-1 receptor-expressing neurons. *Nature Neuroscience* 4: 927-30.

GRAY PA, REKLING JC, BOCCHIARO CM, FELDMAN JL (1999) Modulation of respiratory frequency by peptidergic input to rhythmogenic neurons in the preBötzinger complex. *Science* 286:1566-1568.

GREER JJ, CARTER J, AL-ZUBAIDY ZA (1995) Opioid depression of respiration in neonatal rats. *Journal of Physiology* 437: 727-749.

GREER JJ, SMITH JC, FELDMAN JL (1991) Role of excitatory amino acids in the generation and transmission of respiratory drive in neonatal rat. *Journal of Physiology* 485: 845-855.

HAYES JA, MENDENHALL JL, BRUSH BR, DEL NEGRO CA. (2008) 4-Aminopyridine-sensitive outward currents in preBötzinger complex neurons influence respiratory rhythm generation in neonatal mice. *J. Physiol.* 586(7):1921-36.

HAMPSON RE, ESPAÑA RA, ROGERS GA, PORRINO LJ, DEADWYLER SA (2009) Mechanisms underlying cognitive enhancement and reversal of cognitive deficits in nonhuman primates by the ampakine CX717. *Psychopharmacology (Berl)*. 202(1-3):355-69.

HASSEN AH, FEUERSTEIN G, FADEN AI (1984) Selective cardiorespiratory effects mediated by mu opioid receptors in the nucleus ambiguus. *Neuropharmacology* 23(4):407-15.

HEINKE B, GINGL E, SANDKÜHLER J (2011) Multiple targets of μ -opioid receptor-mediated presynaptic inhibition at primary afferent A δ - and C-fibers. *J. Neurosci.* 31(4):1313-22.

HIBINO H, INANOBE A, FURUTANI K, MURAKAMI S, FINDLAY I, KURACHI Y (2010) Inwardly rectifying potassium channels: their structure, function, and physiological roles. *Physiol Rev.* 90(1):291-366.

ITO I, TANABE S, KOHDA A, SUGIYAMA H (1990) Allosteric potentiation of quisqualate receptor by a nootropic drug aniracetam. *Journal of Physiology* 424:533-543.

JANCZEWSKI WA, ONIMARU H, HOMMA I, FELDMAN JL (2002) Opioid-resistant respiratory pathway from the preinspiratory neurones to abdominal muscles: *in vivo* and *in vitro* study in the newborn rat. *Journal of Physiology* 545: 1017–1026.

JIN R, CLARK S, WEEKS AM, DUDMAN JT, GOUAUX E AND PARTIN K (2005) Mechanism of positive allosteric modulators acting on AMPA receptors. *Journal of Neuroscience* 25(39): 9027-9036.

JOHNSON SM, SMITH JC, FUNK GD, FELDMAN JL (1994) Pacemaker behavior of respiratory neurons in medullary slices from neonatal rat. *Journal of Neurophysiology* 72(6): 2598-608

KEATS AS (1985) The effect of drugs on respiration in man. *Annual Review of Pharmacological Toxicology* 25:41-65.

KELLER BU, BLASCHKE M, RIVOSECCHI R, HOLLMANN M, HEINEMAN SF, KONNERTH A (1993) Identification of a subunit-specific antagonist AMPA/Kainate receptor channels. *Proceeding of the National Academy of Sciences* 90:605-609.

KEMP T, SPIKE RC, WATT C, TODD AJ (1996) The mu-opioid receptor (MOR1) is mainly restricted to neurons that do not contain GABA or glycine in the superficial dorsal horn of the rat spinal cord. *Neuroscience* 75(4):1231-8.

KESSLER M, ARAI AC (2006) Use of [H]fluorowillardiine to study properties of AMPA receptor allosteric modulators. *Brain Research* 1076:25-41.

KOSHIYA N, SMITH JC (1999) Neuronal pacemaker for breathing visualized *in vitro*. *Nature* 400(6742):360-3.

LIU YY, JU G, WONG-RILEY MT (2001) Distribution and colocalization of neurotransmitters and receptors in the preBotzinger complex of rat. *Journal of applied Physiology* 91(3):1387-95

LORIER AR, FUNK GD, GREER JJ (2010) Opiate-induced suppression of rat hypoglossal motoneuron activity and its reversal by ampakine therapy. *PLoS One*. 5(1):e8766.

LU B, SU Y, DAS S, LIU J, XIA J, REN D (2007) The neuronal channel NALCN contributes resting sodium permeability and is required for normal respiratory rhythm. *Cell* (2):371-83.

LYNCH G, GALL CM (2006) Ampakines and the threefold path to cognitive enhancement. *Trends in Neuroscience* 29(10):554-62.

MANZKE T, GUENTHER U, PONIMASKIN EG, HALLER M, DUTSCHMANN M, SCHWARZACHER S, RICHTER DW (2003) 5-HT₄(a) receptors avert opioid-induced breathing depression without loss of analgesia. *Science*. 301(5630):226-9.

MIRONOV SL (2008) Metabotropic glutamate receptors activate dendritic calcium waves and TRPM channels which drive rhythmic respiratory patterns in mice. *J. Physiol*. 586(9):2277-91.

MONTANDON G, QIN W, LIU H, REN J, GREER JJ, HORNER RL (2011) PreBötzinger complex neurokinin-1 receptor-expressing neurons mediate opioid-induced respiratory depression. *J. Neurosci*. 31(4):1292-301.

MONTGOMERY KE, KESSLER M, ARAI AC (2009) Modulation of agonist binding to AMPA receptors by 1-(1,4-benzodioxan-6-ylcarbonyl)piperidine (CX546): differential effects across brain regions and GluA1-4/transmembrane AMPA receptor regulatory protein combinations. *J. Pharmacol. Exp. Ther*. 331(3):965-74.

MORGADO-VALLE C, BELTRAN-PARRAZAL L, DIFRANCO M, VERGARA JL, FELDMAN JL (2008) Somatic Ca²⁺ transients do not contribute to inspiratory drive in preBötzinger Complex neurons. *J. Physiol*. 586(Pt 18):4531-40.

NAGARAJAN N., QUAST C, BOXALL A.L., SHAHID M., ROSENMUND C (2001) Mechanism and Impact of allosteric AMPA receptor modulation by the Ampakine CX546. *Neurpharmacology* 41:650-663.

OLDFIELD S, BRAKSATOR E, RODRIGUEZ-MARTIN I, BAILEY CP, DONALDSON LF, HENDERSON G AND KELLY E (2008) C-terminal splice variants of the mu-opioid receptor: existence, distribution and functional characteristics. *J. Neurochem*. 104(4):937-45.

ONIMARU H AND HOMMA I (2003) A novel functional neuron group for respiratory rhythm generation in the ventral medulla. *Journal of Neuroscience* 23: 1478–1486.

ONIMARU H, KUMAGAWA Y, HOMMA I (2006) Respiration-related rhythmic activity in the rostral medulla of newborn rats. *Journal of Neurophysiology* 96: 55–61.

PAARMANN I, FRERMANN D, KELLER BU, VILLMANN C, BREITINGER HG, HOLLMANN M (2005) Kinetics and subunit composition of NMDA receptors in respiratory-related neurons. *J Neurochem*. 93(4):812-24.

PACE RW, DEL NEGRO CA (2008) AMPA and metabotropic glutamate receptors cooperatively generate inspiratory-like depolarization in mouse respiratory neurons *in vitro*. *Eur. J. Neurosci*. 28(12):2434-42.

- PACE RW, MACKAY DD, FELDMAN JL, DEL NEGRO CA (2007) Inspiratory bursts in the preBötzing complex depend on a calcium-activated non-specific cation current linked to glutamate receptors in neonatal mice. *J. Physiol.* 582(Pt 1):113-25.
- PAARMANN I, FRERMANN D, KELLER BU, HOLLMANN M (2000) Expression of 15 glutamate receptor subunits and various splice variants in tissue slices and single neurons of brainstem nuclei and potential functional implications. *Journal of Neurochemistry* 74: 1335-1345.
- PARTIN KM, PATNEAU DK, MAYER ML (1994) Cyclothiazide differentially modulates desensitization of alpha-amino-3-hydroxy-5-methyl-4-isoxazolepropionic acid receptor splice variants. *Mol Pharmacol.* 46(1):129-38.
- PARTIN KM, PATNEAU DK, WINTERS CA, MAYER ML, BUONANNO A (1993) Selective modulation of desensitization at AMPA versus kainate receptors by cyclothiazide and concanavalin A. *Neuron* 11(6):1069-82.
- PEÑA F, PARKIS MA, TRYBA AK, RAMIREZ JM (2004) Differential contribution of pacemaker properties to the generation of respiratory rhythms during normoxia and hypoxia. *Neuron* 43(1):105-17.
- PORRINO LJ, DAUNAIS JB, ROGERS GA, HAMPSON RE, DEADWYLER SA (2005) Facilitation of task performance and removal of the effects of sleep deprivation by an ampakine (CX717) in nonhuman primates. *PLoS Biol.* 3(9):e299.
- REN J, POON BY, TANG Y, FUNK GD, GREER JJ (2006) Ampakines alleviates respiratory depression in rats. *American Journal Respiratory Critical Care Medicine* 174(12):1384-91
- RHIM H, MILLER RJ (1994) Opioid receptors modulate diverse types of calcium channels in the nucleus tractus solitarius of the rat. *J. Neurosci.* 14(12):7608-15.
- RUANGKITISAKUL A, SCHWARZACHER SW, SECCHIA L, POON BY, MA Y, FUNK GD, BALLANYI K (2006) High sensitivity to neuromodulator-activated signaling pathways at physiological $[K^+]$ of confocal imaged respiratory center neurons in online-calibrated newborn rat brainstem slices. *Journal of Neuroscience* 26(46):11870-11880.
- RUBIN JE, HAYES JA, MENDENHALL JL, DEL NEGRO CA (2009) Calcium-activated nonspecific cation current and synaptic depression promote network-dependent burst oscillations. *Proc Natl Acad Sci U S A.* 106(8):2939-44.
- SHAO XM, GE Q, FELDMAN JL (2003) Modulation of AMPA receptors by cAMP-dependent protein kinase in preBötzing complex inspiratory neurons regulates respiratory rhythm in the rat. *J Physiol.* 547(Pt 2):543-53.

SHOOK JE, WATKINS WD, CAMPORESI EM (1990) Differential roles of opioid receptors in respiration, respiratory disease, and opiate-induced respiratory depression. *Am Rev Respir Dis.* 142(4):895-909. Review.

SMITH JC, HELLENBERG HH, BALLANYI K., RICHTER DW, FELDMAN JL (1991) Pre-Bötzing complex: a brainstem region that may generate respiratory rhythm in mammals. *Science* 254(5032):726-6.

SPRUSTON N, JAFFE DB, WILLIAMS SH, JOHNSTON D (1993) Voltage- and space-clamp errors associated with the measurement of electrotonically remote synaptic events. *J. Neurophysiol.* 70(2):781-802.

SUPPIRAMANIAM V, BAHR BA, SINNARAJAH S, OWENS K, ROGERS G, YILMA S, VODYANOV V (2001) Member of the Ampakine class of memory enhancers prolongs the single channel open time of reconstituted AMPA receptors. *Synapse.* 40(2):154-8.

SUZUE T (1984) Respiratory rhythm generation in the *in vitro* brain stem-spinal cord preparation of the neonatal rat. *Journal of Physiology* 354:173-83.

SWARM RA, KARANIKOLAS M, KALAUOKALANI D (2001) Pain treatment in the perioperative period. *Curr Probl Surg.* 38(11):835-920.

TAKEDA S, ERIKSSON LI, YAMAMOTO Y, JOENSEN H, ONIMARU H, LINDHAL SGE (2001) Opioid action on respiratory neuron activity of the isolated respiratory network in newborn rats. *Anesthesiology* 95:740-9.

TAKITA K, HERLENIUS EA, LINDAHL SG, YAMAMOTO Y (1997) Actions of opioids on respiratory activity via activation of brainstem mu-, delta- and kappa-receptors; an *in vitro* study. *Brain Res.* 778(1):233-41.

THOBY-BRISSON M AND RAMIREZ JM (2001) Identification of two types of inspiratory pacemaker neurons in the isolated respiratory neural network of mice. *Journal of Neurophysiology* 86:104-12.

TIAN N, HWANG TN, COPENHAGEN DR (1998) Analysis of excitatory and inhibitory spontaneous synaptic activity in mouse retinal ganglion cells. *J. Neurophysiol.* 80(3):1327-40.

WILDING TJ, WOMACK MD, MCCLESKEY EW (1995) Fast, local signal transduction between the mu opioid receptor and Ca²⁺ channels. *J Neurosci.* 15(5 Pt 2):4124-32.

XIA YF, ARAI AC (2005a) AMPA receptor modulators have different impact on hippocampal pyramidal cells and interneurons. *Neuroscience.* 135(2):555-67.

XIA YF, KESSLER M, ARAI AC (2005b) Positive alpha-amino-3-hydroxy-5-methyl-4-isoxazolepropionic acid (AMPA) receptor modulators have different impact on synaptic transmission in the thalamus and hippocampus. *J Pharmacol Exp Ther.* 313(1):277-85.

ZHOU Z, CHAMPAGNAT J, POON C-S (1997) Phasic and Long Term Depression in brainstem nucleus tractus solitarius neurons: differing roles of AMPA receptor desensitization. *Journal of Neuroscience* 17(14): 5349-5356.

CHAPTER 4

OPIOID-MEDIATED RESPIRATORY DEPRESSION VIA ACTIONS IN THE RAPHE NUCLEUS

My contribution to this study consisted in the planning, execution and analyses of electrophysiological recordings as well as the planning and analyses of the anatomical results. Immunohistochemical study reported in this chapter was performed by Dr. Wei Zhang.

4.1 ABSTRACT

Respiratory depression is a serious adverse effect associated with opioid pain treatment but the mechanisms mediating breathing vulnerability to opioid are still poorly understood. Medullary raphé nuclei are known to contain μ -opioid receptors (MOR) that are targeted by endogenous opioids to relieve pain. Data from recent *in vitro* studies have suggested the existence of inherently active excitatory connections between the raphé nucleus and the preBötzinger complex (preBötC; Al-Zubaidy et al., 1996; Ptak et al., 2009). It remains unknown to what extent opioid, either endogenously or exogenously delivered to the raphé, can affect inspiratory drive generated by the preBötC. To investigate this issue, *in vitro* rhythmically active medullary slice preparations containing the RNO, the preBötC and hypoglossal nerve roots to record inspiratory drive motor activity were used. Local injections of the μ -opioid agonist DAMGO in the RNO induced a significant decrease in inspiratory frequency to 0.61 ± 0.04 of control. Immunohistochemical data revealed that a high density of serotonin and substance P positive neurons express MOR in the most ventral part of the RNO, which is also the most sensitive area for the DAMGO-induced inspiratory depression. More striking was the presence of MOR on almost all substance P positive RNO neurons. Whole-cell patch-clamp recordings showed functional MOR and AMPA receptors on RNO neurons that receive direct inputs from and project to the preBötC; it was shown that DAMGO decreases excitability in respiratory-related RNO neurons. Further, increasing AMPA receptor conductance within the RNO using the ampakine CX614 significantly alleviated DAMGO-induced inspiratory depression. In conclusion, independent MOR activation within the RNO can induce a significant inspiratory drive depression *in vitro*. Cellular mechanisms underlying this effect can include inhibition of excitatory 5HT⁺/SP⁺ neuron excitability, which may result in impairments of synaptic strength in the “RNO-preBötC loop”. Since the action of serotonin release is known to play a major role during sleep state, the higher risk of sleep apnea detected with the use of opioid might be associated with activation of opioid receptors within RNO.

4.2 INTRODUCTION

Opioid treatment for pain can result in severe, and on occasion, fatal respiratory depression. The opioid receptors are present in several important respiratory nuclei including the preBötzinger complex (preBötC), the compact nucleus ambiguus and the nucleus tractus solitarius (Hassen et al., 1982; Hassen et al., 1984; Ding et al., 1996; Gray et al., 1999). The causes of respiratory depression induced by opioids are believed to be multifactorial and may combine inhibition of respiratory chemoreflexes (Zhang et al., 2009a; 2009b), decrease in airways patency (Lorier et al., 2009), inhibition of cortical inputs to brainstem respiratory centres (Pattinson et al., 2009) and depression of inspiratory rhythm generating network (Manzke et al., 2003; Montandon et al., 2011). The group of medullary raphé nuclei is a potential opioid target since it contains neurons associated with chemosensitive properties and chemoreflexes (Wang et al., 1998; Bradley et al., 2002; reviewed in Hodges and Richerson, 2010; DePuy et al., 2010), neurons that project to respiratory motoneurons (Manaker and Tischler, 1993; Lalley et al. 1997; Ptak et al., 2009; Depuy et al., 2010; reviewed in Barker et al., 2009), as well as neurons that act endogenously via projections to the preBötC (Ptak et al., 2009; Kobayashi et al., 2010; DePuy et al., 2010). Raphé nuclei are classically known to be part of the pain descending signalling pathway and contain μ -opioid receptors (MOR) that are targeted by endogenous opioids to relieve pain. Abundant expression of MOR in medullary raphé nuclei has been repeatedly confirmed (Ding et al., 1996; Zhang et al., 2009a) and while some raphé neurons are inhibited, others are stimulated by opioids (Anderson et al., 1977; Chiang and Pan, 1985; Heinricher et al., 1994). Nevertheless, the exact distribution of functional opioid receptors among the very diverse population of medullary raphé remains unknown. To this end, because MOR of medullary raphé neurons are involved in the pain descending pathway towards spinal cord pain centres (reviewed in Milan, 2002), recent retrograde labeling and electrophysiological experiments appropriately described opioid receptor distribution among raphé neurons that project to the spinal cord (Marinelli et al.,

2002; Pedersen et al., 2011). Yet medullary raphé neurons that project to respiratory centres have not been systematically studied.

The hypothesis that opioids may induce respiratory depression via the raphé is not novel. Microinjections of μ -opioid agonists in the raphé magnus induces a decrease of breathing and cardiac rate (Hellman et al., 2009; Phillips et al., 2012) and attenuates hypoxic ventilator responses (Zhang et al., 2009) in rodents through unknown mechanisms. On the other hand, studies in cats have suggested that raphé magnus stimulation could induce respiratory inhibition via gamma-aminobutyric acid (GABA) signalling (Lalley et al., 1986; Song and Aoki, 2001; Cao et al., 2006a, b).

The raphé nuclei are the main source of serotonin (5HT) in the brain but depending on the type of receptor it binds to, 5HT may exert an inhibitory or excitatory effect on its targets. Hence, it has been proposed that stimulation of raphé neurons belonging to the raphé nucleus obscurus (RNO) could abolish phrenic nerve activity via Bötzing complex expiratory neurons (Yu et al., 2011) through inhibitory 5HT₁ receptors (Lalley et al., 1997; Manzke et al., 2009). Other studies have shown that RNO stimulation facilitates inspiratory drive via excitatory connections with the preBötC (Al-Zubaidy and Greer, 1995; Ptak et al., 2009); 5HT and substance P released from RNO neurons have been proposed to mediate these excitatory effects (Al-Zubaidy and Greer, 1995; Ptak et al., 2009). Further, respiratory neurons have been identified within the RNO and were found to receive direct projections from the preBötC (Ptak et al., 2009), which led to the hypothesis of an endogenous recurrent excitatory pathway that could be referred to as the “RNO-preBötC loop”.

Here, we hypothesized that activation of MOR located in the RNO can affect inspiratory drive *in vitro*, independently of MOR located within the rhythm generation centre. The present study was designed to i) extend preliminary work by examining the modulation of the endogenous excitatory loop between the RNO and the preBötC ii) determine mechanisms by which opioids can decrease inspiratory activity, and iii) examine the effects of opioids on individual respiratory neurons in the RNO.

4.3 RESULTS

4.3.1 MU-OPIOID RECEPTOR ACTIVATION IN THE RAPHE NUCLEUS OBSCURUS CAN DEPRESS INSPIRATORY DRIVE *IN VITRO*

Independent action of μ -opioid receptors agonist in the RNO induces a delayed inspiratory drive depression *in vitro*.

To explore the possible action of MOR of the RNO on inspiratory drive, a reduced *in vitro* brainstem slice model isolated from neonatal rats ranging from postnatal day zero (P0) to P6 was used. The acute rhythmically active slice preparation contains the RNO, the spontaneously active preBötC, and hypoglossal (XII) nerve roots for recording online inspiratory drive activity. The specific μ -opioid receptor agonist [D-Ala (2), N-MePhe (4), Gly-ol]-enkephalin (DAMGO) was locally applied to the RNO in medullary slice preparations and inspiratory XII nerves discharges were recorded. An analysis of variance (ANOVA) on relative mean values of XII burst parameters shows that DAMGO induced a significant decrease in XII burst frequency to 0.61 ± 0.04 of control values ($p < 0.01$, $n = 7$; see Fig. 4.1), which corresponds to a decrease of 39.5%. No significant effect of DAMGO on XII burst amplitude was found (see Figs. 4.1.A and C). The inhibitory effect of DAMGO on inspiratory frequency was only observed when DAMGO was applied to the same sensitive area that induced a significant increase of the inspiratory drive after a 5 sec microinjection of AMPA (100 μ M): 2.2 ± 0.3 ($p < 0.05$, $n = 7$) of control values (see Figs. 4.1B, C and D). Further, the RNO area most sensitive to local applications of AMPA and DAMGO was specifically confined within the ventral side of the RNO. The diagram in figure 4.1B illustrates XII burst interevent interval against event occurrence and eases the comparison between data obtained before, during and after local injections of DAMGO into the ventral RNO versus dorsal RNO. As a negative control, artificial cerebrospinal fluid solution was microinjected locally at the same site of drug injections and no significant change in any of the XII nerve burst characteristics (frequency, amplitude, area, duration) was found. In

some experiments, a solution containing fluorescent beads was included in the microinjection pipette to monitor the relative spread of injected solution. The onset of the inspiratory frequency increase evoked by AMPA microinjections in the RNO started within 5 sec after the beginning of the injection. In contrast, the decrease in inspiratory drive frequency following DAMGO microinjection was significantly delayed (see Fig. 4.1B). This delay could vary, spanning from 20 to 240 sec after the end of the microinjection. In the same rhythmic slice preparations, local applications of DAMGO within the preBötC were also performed and induced a large decrease in XII burst frequency (0.60 ± 0.09 of control values; $n = 7$). However, the decrease in inspiratory burst frequency occurred simultaneously with DAMGO microinjections (see Fig. 4.1.A).

To ensure that the inspiratory frequency decrease was evoked by action of DAMGO at the site of injection and not after a diffusion of DAMGO to the preBötC, control experiments were performed by injecting DAMGO at an equivalent distance of RNO to preBötC. This control site was located dorso laterally from the preBötC of the medullary slice preparation, and no XII motor output changes were found during and after local injection DAMGO into the control site (120 s; 1 μ M). This result confirmed that the inspiratory drive frequency depression was due to the action of DAMGO within the RNO high sensitive area.

DAMGO-induced inspiratory depression is specifically due to μ -opioid receptors activation.

To verify the contribution of μ -opioid receptor activation to the observed inspiratory depression, the opioid receptor antagonist naloxone was administrated. Local applications of DAMGO into the RNO ventral area in presence of bath applied naloxone (1 μ M) were performed. XII burst frequency depression by DAMGO was significantly attenuated by naloxone ($n = 5$; $p < 0.05$; see Fig. 4.1C), although XII burst irregularity remained after the DAMGO injection., Bath application of naloxone (1 μ M) did not significantly change the baseline XII burst frequency and amplitude, suggesting no alteration in serotonin release at the

preBötC. Moreover, an alternative selective μ -opioid receptor antagonist Cys-Tyr-D-Trp-Orn-Thr-Pen-Thr-NH₂ (CTOP) was administered in a second set of experiments and the results were similar to those obtained with naloxone. Concurrent microinjection of DAMGO and CTOP in the ventral side of the RNO significantly occluded the DAMGO effect on inspiratory rhythmic motor output recorded from XII nerve rootlets (0.68 ± 0.10 of control frequency after DAMGO local application, and 0.94 ± 0.08 of control frequency after CTOP + DAMGO local application; $n = 4$; $p < 0.05$; repeated measures ANOVA), consistent with DAMGO specific activation of MOR within the RNO.

4.3.2 DISTRIBUTION OF MU-OPIOID RECEPTORS AMONG EXCITATORY AND INHIBITORY RNO NEURONS

RNO distribution of μ -opioid receptors amongst 5HT versus GABAergic neurons in the ventral RNO.

Immunohistochemical studies were performed on 4 to 8 μm thin transverse sections of the medulla in order to assess the distribution of μ -opioid receptor (MOR) among RNO neurons. The more ventral side of the RNO was the focus because it was the most sensitive area of the RNO for eliciting inspiratory frequency decrease with DAMGO. Based on previous immunohistochemical and electrophysiological work, both GABA (gamma-aminobutyric acid) and 5HT (serotonin) are established molecular markers of medullary raphé nuclei (Marinelli et al., 2002; Cao et al., 2006b). To identify inhibitory GABAergic neurons, the antibody against the GABA-synthesizing enzyme (GAD) was used (see Chapter 2 section 2.2.1 for details on the methodology). Figure 4.2 shows representative confocal images of sections triple labeled for MOR, 5HT and GAD within the ventral RNO. This region of the RNO contained a high number of 5HT positive (5HT⁺) neurons, and less GAD positive (GAD⁺) neurons. Unlike previous immunohistochemical reports from human tissue (Broadbelt et al., 2009), there was no colocalization of 5HT and GAD, suggesting that 5HT⁺ and GAD⁺ neurons are two distinct neuronal populations in the neonatal rat ventral RNO.

Immunolabeling for MORs was apparent. Based on visual inspection of both population of neurons (5HT⁺ and GAD⁺ cells), a higher density of MOR⁺/GAD⁺ cells was observed at a more dorsal level of the RNO, and a higher density of MOR⁺/5HT⁺ cells was present in the most ventral side of the RNO.

SP⁺ neurons represent a subpopulation of 5HT⁺ neurons in the ventral RNO.

Because some RNO neurons express the neuropeptide substance P (SP; Holtman and Speck, 1994; Ptak et al., 2009), the distribution of SP⁺ cells in the medullary raphé region was assessed. To evaluate the level of the medulla relative to the preBötC, immunolabeling of neurokinin 1 receptors (NK1R), a partial surrogate marker for preBötC neuron (Gray et al., 1999; Guyenet et al., 2002; Pagliardini et al., 2003) was examined in medullary transverse slices between the compact formation of the nucleus ambiguus and the semi-compact division of the nucleus ambiguus. Transverse sections of the medulla were serially collected and immunoreacted with SP, 5HT and NK1R (n = 3). Figure 4.3 shows a selection of confocal images taken at different levels of the medulla acquired at an interval of $50 \pm 10 \mu\text{m}$ from each other, and illustrates the strong correlation between the level of SP⁺ expression within the RNO and NK1R expression in the ventrolateral medulla. Visual inspection of series of medullary sections rostral to caudal to the preBötC depicted a high density of NK1R positive cells in the preBötC that correlates with a high density of SP⁺ cells in the RNO. Those data are consistent with RNO SP⁺ neurons being a source of endogenous SP to preBötC neurons. A significant portion of neurons in the ventral part RNO were SP⁺/5HT⁺ (see Fig. 4.3). Further, SP⁺ neurons likely represent a subset of 5HT⁺ neurons because there was no detection of any SP⁺ neuron without 5HT expression when examining transverse slices double stained for 5HT and SP.

Distribution of μ -opioid receptors amongst 5HT versus SP neurons in the ventral RNO.

Because SP⁺ RNO neuronal population appeared to correlate with the preBötC, the expression of MOR among SP⁺ RNO cells was examined. Figure 4.4

illustrates the triple labeling MOR/SP/5HT (n = 4). ~89% of SP⁺ cells within the RNO co-expressed MOR. MOR was also expressed in few 5HT⁻/SP⁻ neurons but ~76% of MOR⁺ neurons were SP⁺. Therefore it is hypothesized that the physiological effect of local injections of DAMGO in the RNO was a consequence of a combined inhibition of 5HT and SP endogenous release by RNO neurons to the preBötC.

4.3.3 DAMGO MODULATES RESPIRATORY RNO NEURONS

RNO respiratory neuronal passive properties.

Previous studies have suggested that RNO neurons may exhibit some endogenous bursting conductances influence inspiratory drive (Pace et al, 2008; Milescu et al., 2010). This hypothesis was verified by examining intrinsic and spontaneous electrical properties of respiratory-related RNO neurons. As shown in Figure 4.5, respiratory RNO neurons have excitatory input currents and bursts of action potentials that are cyclic, occurring in a phase locked manner and synchronized with XII nerve output activity, consistent with previous finding (Ptak et al., 2009). Cell capacitance measurements showed an average of 68 ± 6 pF (n = 19). In 6 out of 11 respiratory RNO neurons tested, the current response to a voltage ramp elicited a large inward rectification, which was abolished by bath application of tetrodotoxin (TTX; 0.5 μ M), typical of a persistent sodium current (I_{NaP} ; see Fig. 4.5D for illustration of the subtracted leak NaP conductance). However, respiratory neurons that were depolarized with injection of DC current did not burst, but rather fired tonically (Fig. 4.5B). A potassium outward rectification and a hyperpolarizing inward current (I_h) current (see Fig. 4.5E) were observed on 1 out of 5 respiratory RNO cells tested.

Effect of DAMGO on intrinsic properties of respiratory RNO cells.

It was observed during voltage-clamp recordings that non-inactivating outward currents present in respiratory RNO neurons could be increased by local application DAMGO (data not shown because no quantitative analysis could be

made). However, potassium conductance assessed in voltage-clamp by a series of voltage-steps of 10 mV incrementing amplitude up to 150 mV showed varying responses among respiratory RNO neurons. Some neurons displayed a delayed outward rectifying potassium conductance (which may or may not be an artifact of the patch-clamp recording), while other cells displayed a non-inactivating potassium conductance of variable amplitude. This variability in current responses made it difficult to determine potassium conductance modulation by DAMGO. This would have required using specific potassium channel blockers and/or outside-out patch-clamp recordings that allow for a better clamp.

Current-clamp recordings of respiratory RNO cells showed that bath application of DAMGO induced a loss of action potential firing and a hyperpolarization of the membrane potential (4.9 ± 0.7 mV ; $n = 3$; see figure 4.6A). Voltage responses to current injections of -100 to +150 pA in 50 pA increments were examined to evaluate action potential firing rates and changes in voltage threshold in the presence of DAMGO. The voltage threshold was defined as the first point of the upstroke of the first action potential (rising rate exceeding 50 mV/ms; Anderson et al., 1987). Responses to negative current injections were analyzed to determine changes in R_N between control and DAMGO conditions. Responses to suprathreshold current stimulations were analyzed to compare voltage threshold and firing (instantaneous and steady state firing frequency) in control versus in DAMGO. As shown in figure 4.6, in presence of bath applied DAMGO (400 nM), responsive RNO neurons had a depolarized voltage threshold. At comparable repetitive voltage threshold, a RNO neuron displayed lower firing frequencies in presence of DAMGO than in control conditions (see example in figure 4.6C). The lowered R_N (decreased to 0.66 ± 0.16 of control; from 364 ± 84 M Ω to 239 ± 58 M Ω) and increased voltage threshold (-34 ± 3 mV in control versus -29 ± 3 mV; $n = 3$) induced by DAMGO in respiratory RNO neurons indicate that DAMGO induces a decrease in excitability in respiratory RNO neurons. This effect could partially be reversed by the addition of naloxone to the bathing medium (1 μ M; see Fig. 4.6C left graph). Examination of instantaneous (first two action potential frequency) and steady-state (last action

potential frequency) firing rates in the different experimental conditions also showed that maximum firing rate was reached at lower injected current in presence of DAMGO compared to control or DAMGO + naloxone conditions. Furthermore, DAMGO limited the range of steady-state spiking responses that RNO sensitive neurons could generate, with a loss of steady state spiking at +150 pA current injection (Fig. 4.6B lower plot). This effect could be reversed by the addition of naloxone in the bath.

DAMGO elicits an outward current in RNO cells.

Whole-cell recordings of respiratory-related RNO neurons showed that 6 out of 8 respiratory RNO neurons recorded in voltage-clamp were sensitive to local application of DAMGO. As illustrated in Figures 4.7A and B, voltage-clamp recordings of respiratory RNO neurons showed that local application of DAMGO induces an outward current of 44 ± 13 pA ($n = 6$). A net outward current of 33 ± 7 pA ($n = 4$) was also recorded in the presence of tetrodotoxin ($0.5 \mu\text{M}$ TTX; see figure 4.7B) when DAMGO was briefly ($4 \mu\text{M}$; 10 s) applied to the recorded cell, indicating a postsynaptic effect of DAMGO. DAMGO was also tested on randomly patched RNO cells that were non-respiratory related. Note that those experiments were not confirmed in TTX. 12 out of 25 non-respiratory RNO cells displayed a response to DAMGO either by an outward current in voltage-clamp configuration or small hyperpolarization in current-clamp configuration. The remainder of the non-respiratory cells showed no response or a depolarization upon DAMGO application. In total, when combining results from current and voltage-clamp configuration recordings, 11 out of 19 respiratory RNO cells responded to DAMGO, with a decrease of R_N of 35% with DAMGO, a synaptic current of 44 ± 13 pA, or a hyperpolarization of 4.9 ± 0.7 mV.

Characterization of RNO neuron response to DAMGO.

In an attempt to characterize neuronal types (presumably 5HT, SP or GAD positive cells) that were sensitive to opioids, neurobiotin (0.2%) was included in the intracellular solution. The difficulty in this set of experiments was to target

respiratory RNO neurons from the first single-cell recording attempt and perform local applications of DAMGO before fixing the slice in paraformaldehyde. Three inspiratory RNO neurons in 3 different slice preparations were recorded. Immunohistochemistry showed no single-neuron labeled with neurobiotin. Rather a cluster of several interconnected cells was labeled with avidin D (see figure 4.5F for example). This may indicate that recorded respiratory raphé neurons were electrically coupled with surrounding neurons. Therefore, we could not be certain that the recorded respiratory cells displaying an outward current upon DAMGO were excitatory ($5HT^+$ and/or SP^+) or inhibitory ($GABA^+$) neurons due to the potential of gap junction-mediated effects.

4.3.4 AMPAKINE MODULATION OF RNO RESPIRATORY NEURONS AND NETWORK

Ampakine CX614 modulates AMPA-mediated currents on respiratory RNO neurons.

Whole cell recordings of respiratory RNO neurons in voltage-clamp configuration were performed. TTX ($0.5 \mu M$) was added to the bath after identification of the patched neuron as a respiratory RNO cell. The ampakine CX614 was used to test the functionality of AMPA receptors on respiratory RNO neurons and their sensitivity to the drug. As illustrated in figure 4.8 the results show a significant increase in AMPA-evoked current size by bath application of CX614 ($20 \mu M$). Specifically, AMPA-induced current amplitude was increased to 2.4 ± 0.4 of control values ($p < 0.05$; $n = 4$) and AMPA-induced current duration was increased to 1.86 ± 0.22 ($p < 0.05$; $n = 4$). These results demonstrate the presence of functional AMPA receptors on respiratory RNO neurons and indicate that AMPA receptors on these neurons are sensitive to the high-impact ampakine CX614.

Local application of ampakines into the RNO elevates inspiratory drive frequency in presence of DAMGO.

The fact that local application of AMPA into the raphé obscurus increases inspiratory frequency (Al-Zubaidy et al., 1996) supports the hypothesis that endogenous synaptic glutamatergic release within the RNO could influence endogenous excitation of the preBötC. XII nerve recordings of active medullary slice preparations were performed and the high-impact ampakine CX614 (200 μ M) was applied locally within the RNO. The local injections were specifically made where AMPA could produce a marked increase in inspiratory motor output frequency, in the ventral side of the RNO. Statistical analysis of XII bursts showed that, while AMPA induced a large increase in burst frequency (one-way ANOVA, $p < 0.001$), no significant increase of inspiratory XII burst frequency or amplitude (one-way ANOVA, $p > 0.05$; see Fig. 4.9). The effect of endogenous glutamate release was assessed using the competitive blocker of AMPA receptors. Local application of 6-cyano-7-nitroquinoxaline-2,3-dione (CNQX; 200 μ M) into the raphé did not have an effect on inspiratory drive (amplitude nor frequency), whereas the same application into the preBötC induced a large decrease in frequency of inspiratory activity recording from the XII nerves, similar to previous report (Funk et al., 1993). Although this does not rule out the possibility of an endogenous release of glutamate into the RNO, the results suggest that endogenous glutamatergic release within the RNO may not play any role on the inspiratory network in the specific *in vitro* conditions used. These data raised the possible interpretation that AMPA receptors are expressed on both inhibitory (GABAergic) neurons and excitatory (5HT) RNO neurons, and that their effects are cancelled.

To test whether ampakine action within the RNO could reduce DAMGO-induced inspiratory drive depression the experiment was repeated in the presence of bath applied DAMGO. As shown in Figure 4.9B, local applications of CX614 in presence of DAMGO induced no change in XII burst amplitude. However, CX614 produced a significant increase in frequency when applied to the RNO (3.6 ± 0.4 burst/min in DAMGO versus 6.6 ± 0.7 bursts/min during CX614

injection)($n = 7$; $p < 0.05$). In the same preparations CX614 also produced a significant increase in burst frequency when it was applied to the preBötC (3.5 ± 0.1 bursts/min during DAMGO bath application versus 8.4 ± 1.0 bursts/min during CX614 injection). The amplitude was not increased by CX614. Although the potentiation of inspiratory burst frequency by CX614 seemed stronger than the one induced by CX614 injected in the preBötC (frequency (CX614 in PBC) was not different from control frequency, whereas frequency (CX614 in RNO) was), there was no significant difference between frequency (CX614 in RNO) and frequency (CX614 in PBC) ($p > 0.05$).

4.4 DISCUSSION

The main finding of this study was that μ -opioid receptor activation within the raphé nucleus obscurus (RNO) results in a significant depression of inspiratory rhythm *in vitro*. This strengthens the case for the RNO being an important site contributing to opiate-induced respiratory depression. The immunohistochemical data demonstrates that μ -opioid receptors are expressed on processes and somatic membranes of RNO neurons. Importantly, a majority of μ -opioid receptor positive (MOR^+) neurons of the RNO are excitatory neurons that co-express 5HT and substance P. MOR^+ neurons are located in the ventral part of the RNO, which is the RNO most sensitive site to DAMGO injection.

Whole-cell recordings demonstrated that respiratory RNO neurons receiving inputs from the preBötC contain functional μ -opioid receptors, which may underlie the observed respiratory depression by DAMGO. Mechanistically, activation of MOR on respiratory RNO neurons induces a post-synaptic outward current, a decrease in R_N and a decrease in excitability.

4.4.1 MODULATION OF THE RNO-PREBÖTC LOOP BY MU-OPIOID RECEPTORS

The electrophysiological evidence provided in the present work demonstrate that DAMGO- and AMPA- receptor mediated regulations of inspiratory drive by the raphé are restricted primarily to the ventral part of the RNO. Those data are consistent with previous studies showing that while stimulation of the raphé magnus and dorsal part of the RNO inhibit inspiratory motor output activity, stimulation of raphé pallidus and ventral part of the RNO facilitate it (Lalley et al., 1986; Song and Aoki, 2001; Cao et al., 2006a, b). Therefore, collectively the data support the idea that within the heterogeneous neuronal population of the RNO, a functional compartmentalization may exist between the dorsal and the ventral region.

Immunohistochemical staining of MOR showed a predominance of somatic expression of MOR within 5HT⁺/SP⁺ raphé neurons located at the same transverse plane of the medulla as the preBötC. The data support the presence of MOR on peptidergic neurons which has also been reported in previous studies (Hokfelt et al., 1977). Previous work by Ptak and collaborators demonstrated that 5HT_{2A/C}, 5HT_{4A} and NK1R antagonists significantly suppress the frequency and amplitude increases of inspiratory XII bursts induced by stimulation of the raphé obscurus; both in the *in vitro* medullary slice and *in situ* preparations (Ptak et al., 2009). Collectively those findings emphasize the important modulatory role of SP and 5HT on inspiratory drive and strongly support the idea that opioids may inhibit 5HT and SP release from the RNO neurons that project to the preBötC. Similarly, opioids suppress SP release from primary sensory terminals to spinal nociceptors (Beaudry et al., 2011; Brodin et al., 1983; Jessell and Iversen, 1977; Kondo et al., 2005). If the decrease in SP and 5HT release is the primary cause of the indirect inspiratory drive depression by DAMGO, then these data also support the idea that SP and 5HT release may counter or at least offset the inhibitory effect of DAMGO. This is consistent with a previous study showing that opioid-induced respiratory depression was alleviated by 5HT in rodent models (Manzke et al., 2003).

Electrophysiological recordings of XII nerve activity demonstrated that the specific decrease in inspiratory motor output frequency induced by local injections of DAMGO in the RNO was delayed. In contrast, no delayed response was observed when applying AMPA to the same injection sites. One interpretation could be that, while AMPA can induce a direct release of excitatory neurotransmitters to the preBötC, DAMGO might affect presynaptic excitatory neurotransmitter released within the RNO. In fact, although part of the RNO neuronal projections have been reported to reach XII motor pool (Manaker and Trischler, 1993; Peever et al., 2001; Ptak et al., 2009), the DAMGO injections performed in the experiments did not yield any significant effect on XII burst amplitude. It is noteworthy that there has been no report of feedback projections from XII motoneurons to the RNO, whereas there are for axonal projections from

preBötC to the RNO (Zagon, 1993; Ptak et al., 2009). Thus, inhibition of feedback excitatory synapses from the preBötC to the RNO (Li and Bayliss; 1998) may represent an additional mechanism of opioid action. Analysis of miniature excitatory postsynaptic event through voltage-clamp recordings of respiratory RNO neurons in presence of TTX would help address this question.

One alternative explanation regarding the observed delay in DAMGO-induced response would be the presence of a “multiple synapse loop”. In fact, in some experiments, neurobiotin was added to the internal solution for *post-hoc* verification of localization of patched cell and multiple stained cell bodies (data not shown) within the RNO were observed. Although those experiments did not serve the purpose of this study, they do suggest that RNO neurons might be electrically interconnected. The RNO-preBötC loop might involve multiple synapses within the RNO before projecting to the preBötC, and presumably opioid sensitive cells of the RNO may not project directly to the preBötC.

4.4.2 POTENTIAL POSTSYNAPTIC EFFECTS OF DAMGO ON RESPIRATORY RAPHE NEURONS UNDERLYING RESPIRATORY DEPRESSION

Evidence was provided that opioids can depress inspiratory rhythm through the RNO *in vitro* and has demonstrated functional μ -opioid receptors on respiratory neurons of the RNO. Two postsynaptic mechanisms are here proposed to be involved in respiratory depression induced by μ -opioid receptors activation of raphé neurons.

The first mechanism involves activation of G-protein coupled inward potassium (GIRK) channels induced by $G_{i/o}$ protein coupled to the μ -opioid receptor. The data show that DAMGO induces a post-synaptic outward current in respiratory RNO neurons. This leads to a hyperpolarization of respiratory-related neurons of the raphé which may in turn decrease the release of neurotransmitters at the preBötC.

The second proposed mechanism of DAMGO action involves the activation of a second messenger signalling cascade that would be triggered by the

activation of μ -opioid receptors and would directly modulate excitatory receptors mediating the inspiratory drive. It was noted that excitatory respiratory inputs on respiratory raphé neurons were smaller during the DAMGO-induced outward current, but could not examine this effect in detail because of small amplitude of respiratory input currents in control conditions. Thus, respiratory input currents might be depressed by opioid through an inhibition of intracellular cascade signalling following activation of μ -opioid receptors (such as adenylyl cyclase activation).

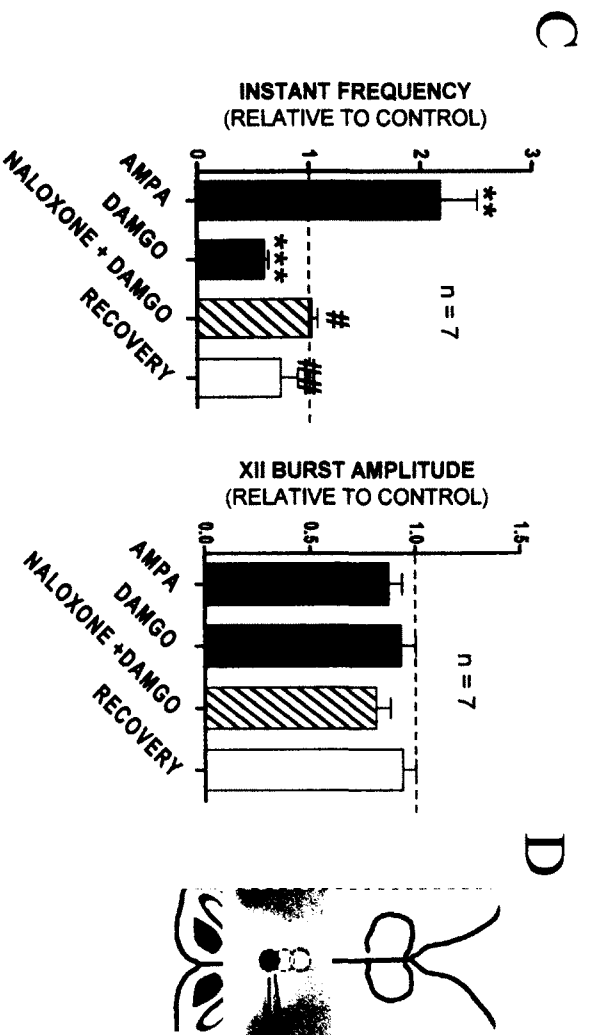
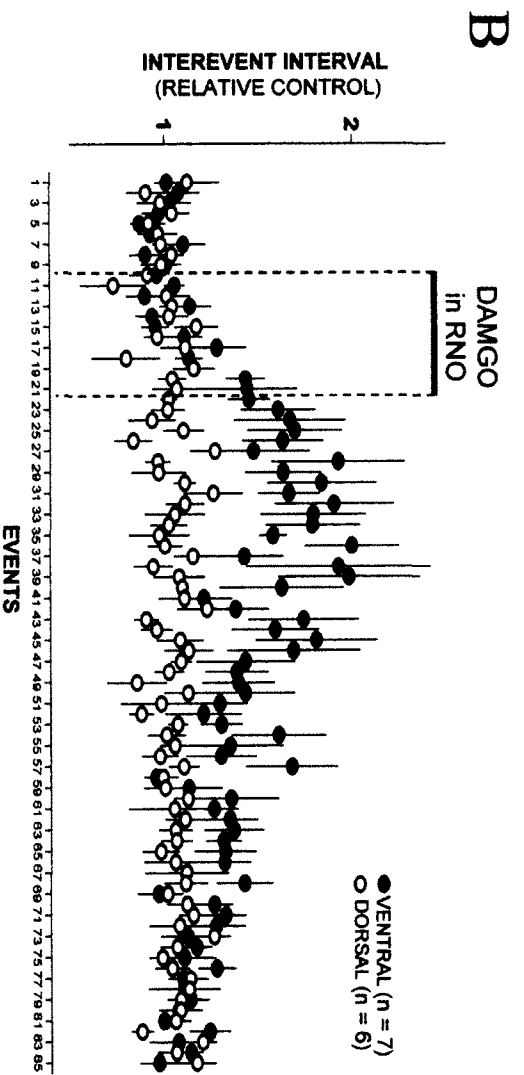
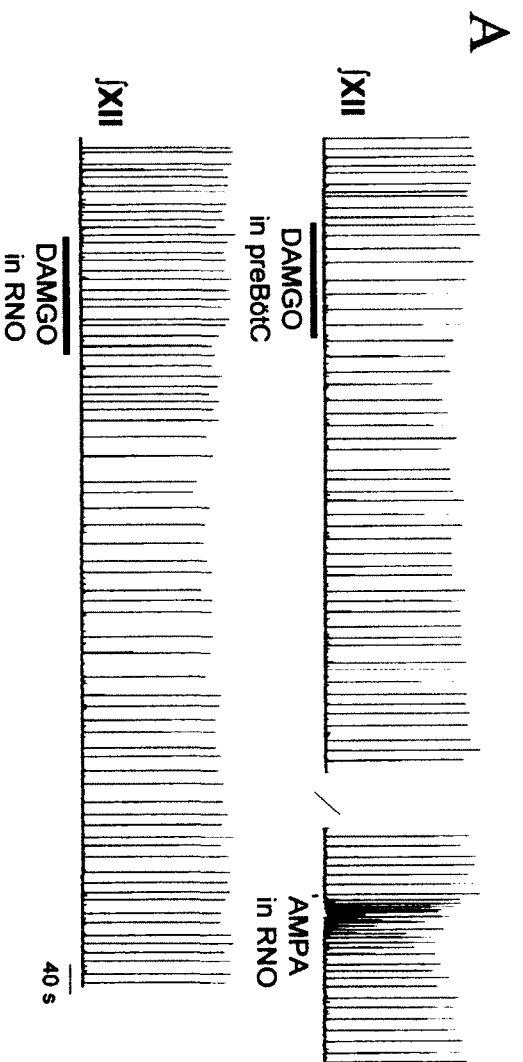
This hypothesis was tested in a separate set of experiments examining the effect of forskolin local microinjections to AMPA-mediated currents in voltage-clamp recordings of respiratory neurons in presence of TTX. Brief local injections of forskolin (10 s) led to an increase in the amplitude of AMPA-mediated currents, but brief applications of DAMGO (1 μ M) into respiratory RNO cells in voltage-clamp mode caused a decrease in AMPA-mediated current amplitude. Interpretation of the data were difficult because of the substantial decrease of R_N induced by DAMGO, and the fact that continuous R_N measurements during AMPA local applications were lacking. Non- K^+ channel effects, such as changes in phosphorylation of ligand-gated receptor/channel complexes have already been reported in the literature (Martin et al., 1997), but longer exposure with the opioid agonist was used. An *in vivo* study using high doses of short acting μ -opioid agonist exposure has recently shown an inhibitory effect of opioid on phosphorylation states of AMPA receptors in spinal C-fiber synapses (Drdla-Schutting et al., 2012). Replacing local applications of DAMGO with similar strategic pharmacological agents in order to further analyze AMPA-mediated responses in RNO neurons might help demonstrate these additional effects.

An I_h current was present in a few RNO cells (but only one respiratory cell). A study examining ganglionic neurons has shown that I_h activation depended on forskolin-induced adenylyl cyclase activation and that opioids could reverse the effect of forskolin on I_h (Ingram and Williams, 1994). Also in rats, opioids were also shown to modulate I_h on hippocampal neurons (Svoboda and Lupica, 1998) and raphé magnus neurons through kappa-opioid receptors (Pan, 2003). It would

be interesting to examine whether or not μ -opioid receptor activation can modulate I_h current on RNO neurons and if this potential effect would play a role in the inhibition of inspiratory drive induced by opioids within the RNO.

4.4.3 SUMMARY

Collectively, these data provide evidence for additional cellular mechanisms underlying opioid-induced respiratory depression. It was demonstrated that opioids may indirectly depress inspiratory rhythm via the ventral RNO *in vitro*. Specifically, immunohistochemical and electrophysiological data can be interpreted as demonstrating an opioid-induced inhibition via the “RNO-preBötC loop” resulting in a decrease of SP and 5HT excitatory synaptic drive to the preBötC.



Previous Page

Figure 4.1 Local injection of the mu-opioid agonist DAMGO in the most ventral part of the RNO decreases inspiratory motor output rhythm in *in vitro* neonatal rat medullary slice.

A. Representative traces of integrated recordings from XII nerve rootlets during local application of DAMGO into the preBötC, followed by an injection of AMPA (100 μ M) in the RNO and DAMGO (1 μ M) in the RNO, in the same experimental slice. **B.** Interevent interval means (mean \pm s.e.m) are plotted against XII burst occurrence. Two data groups are presented in this graph: XII burst interevent intervals obtained for local application of DAMGO injected in the more dorsal sides of the RNO (open circles; n = 6), and interevent intervals obtained for local applications of DAMGO injected in the most ventral side of the RNO (black filled dots; n = 7). Note the effect of DAMGO peaks after the termination of the injection. **C.** Histogram of group relative data (n = 7) showing a significant increase of XII nerve burst instant frequency in response to AMPA and a significant decrease of XII burst frequency induced by DAMGO local injections within the RNO (** p < 0.001 compared to control, *** p < 0.0001; # p < 0.05 compared to DAMGO; ## p < 0.001 compared to DAMGO; one-way ANOVA with Tukey's post test comparison on raw values). Note that in presence of naloxone (1 μ M) in the bathing medium, the effect of local injections of DAMGO in the ventral RNO is significantly reduced. **D.** Schema of the middle part of a slice preparation seen from its rostral side indicating drug-stimulation sites (in red). RNO area of high sensitivity to AMPA and DAMGO is located in the most ventral part of the RNO (shown in red filled dot). Injections made at more dorsal levels of the RNO showed little to no response to either AMPA or DAMGO (red open circles).

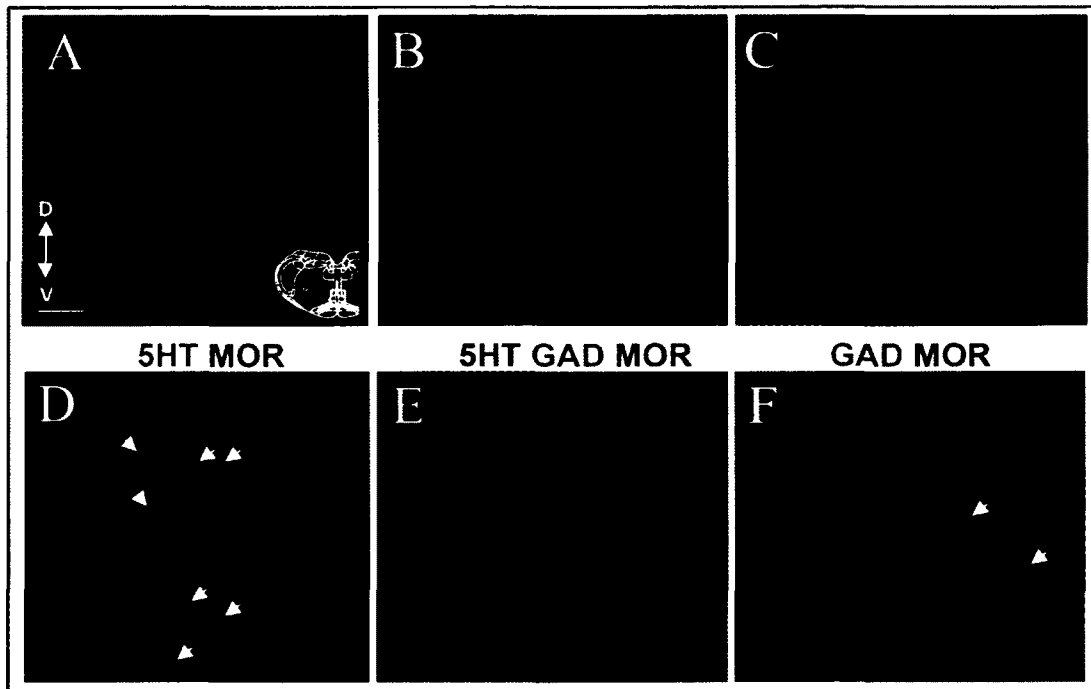


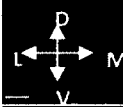



Figure 4.2 Mu-opioid receptors (MOR)-expressing neurons of the RNO highly co-localize with serotonin (5HT)-expressing neurons in the RNO of P2 rat transverse medullary slice.

The RNO contains 5HT (A), GAD (B) and MOR (C) expressing cells. The ventral part of the RNO shows a high density of neurons co-expressing 5HT and MOR (arrowheads), seen on the lower left picture. The ventral part of the RNO also shows some neurons co-expressing GAD and MOR (F). D. Note that for this picture 5HT is shown in red in order to appreciate colocalization between 5HT and MOR. Scale = 50 μ m. Note that in figure F, 5HT labeling is shown in red to have a better appreciation of 5HT/MOR colocalization (n = 3).

5HT / SP		5HT	SP	NK1R	
A		B	C	D	NAc
			 	 	
E		F	G	H	BötC
I		J	K	L	preBötC
M		N	O	P	preBötC

Previous Page

Figure 4.3 Transverse sections of the medulla of P2 rat immunostained for 5HT, substance P (SP) and NK1R at different rostral (upper end) to caudal (lower end) levels.

A, E, I, M: Overlay of triple labeling of 5HT (red), SP (green) and NK1R (blue) in the ventral RNO. Note the high density of colocalization between 5HT and SP particularly in figures **I** and **M** showing the appearance of a subpopulation of 5HT⁺ RNO neurons that also expresses SP. Figures **C, G, K, O** show SP positive neurons within the RNO. **A-C, E-G, I-K, M-O:** The number of 5HT⁺/SP⁺ RNO neurons increases in sections with a higher density of NK1R labeling; corresponding to the level of the preBötzing Complex (preBötC). 5HT⁺ RNO neurons are distributed along the midline. In figure **D** the NK1R labeling depicts the compact formation of the NA (white), while in the ventrolateral region NK1R labeling of figure **H, L, P** defines the Bötzing Complex (BötC) and the preBötC. Note that RNO neurons do not contain NK1R. Figures **D, H, L, P** show rostral to caudal NK1R labeling within the ventrolateral medulla and provide for an anatomical demarcation of the preBötC. Each picture was taken in the same slice corresponding to the RNO picture on the left. * are blood vessels artifacts. Scale bar is 50 μm . n = 3.

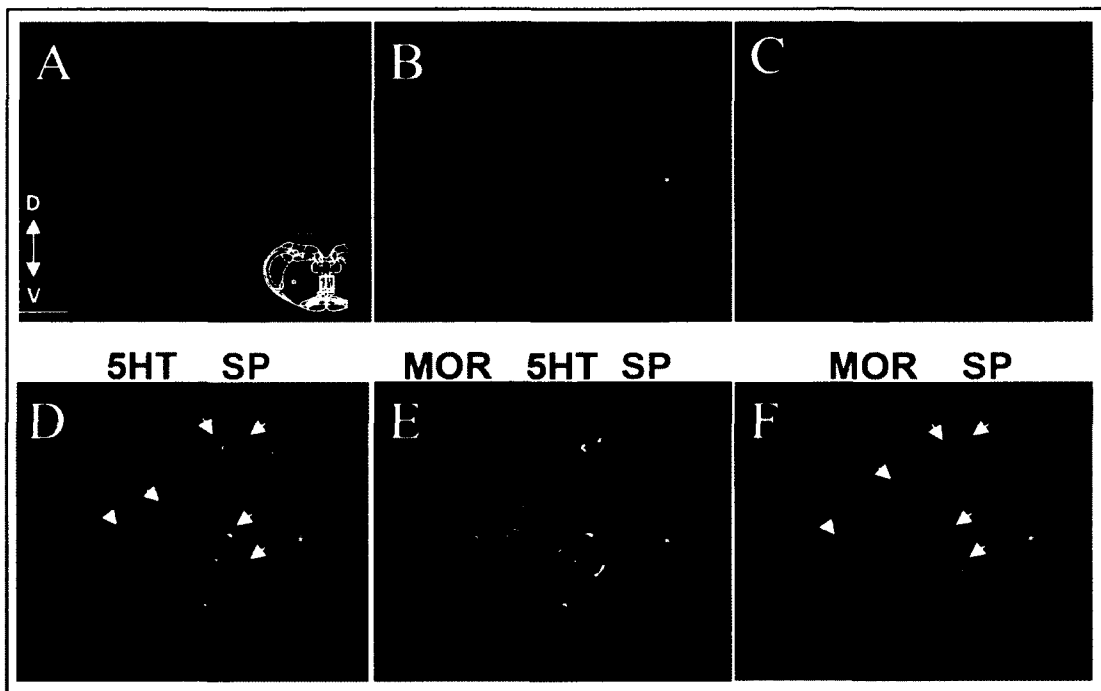
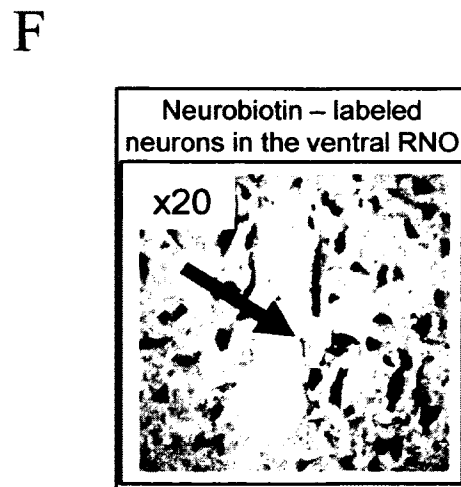
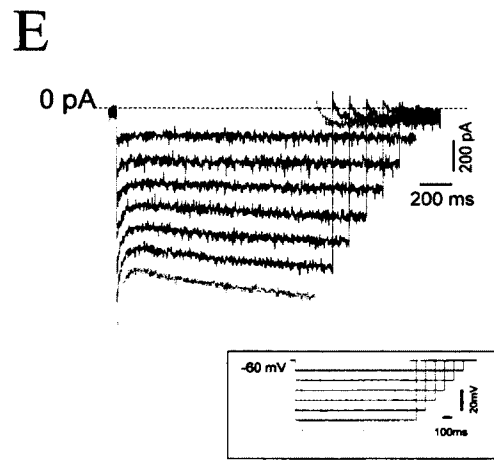
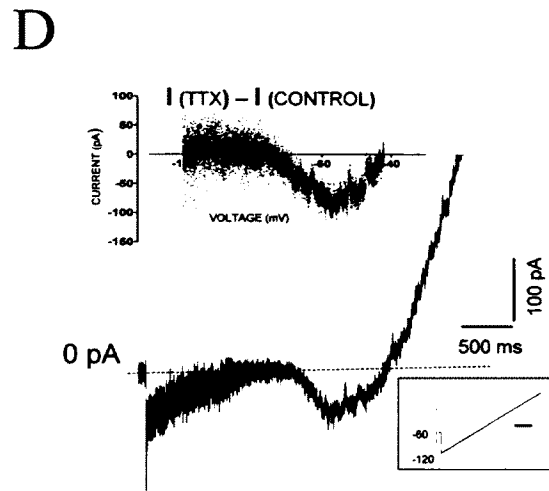
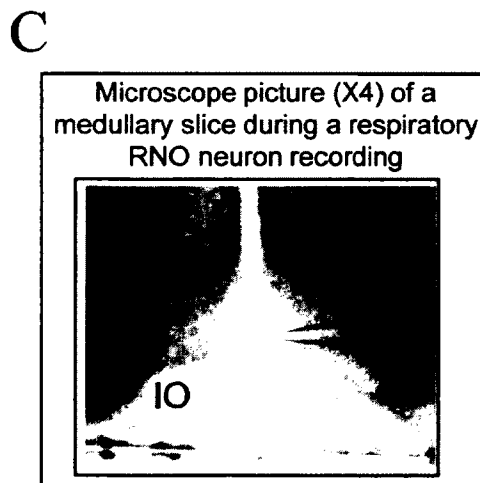
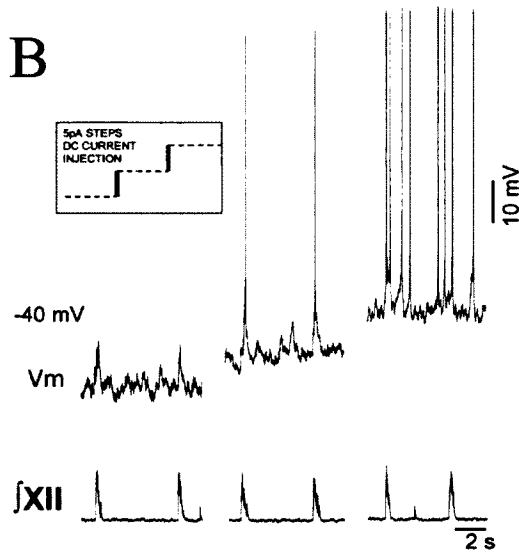
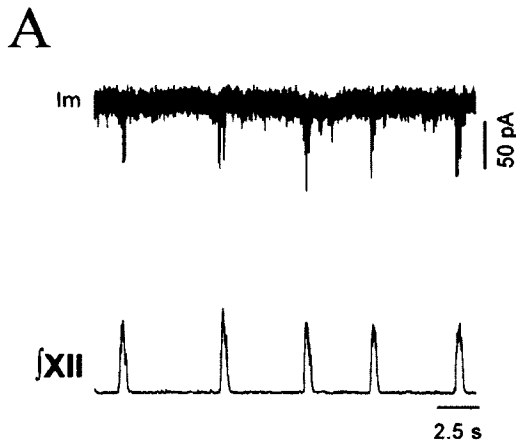


Figure 4.4 A subpopulation of serotonergic neurons in the ventral RNO expresses both SP and MOR.

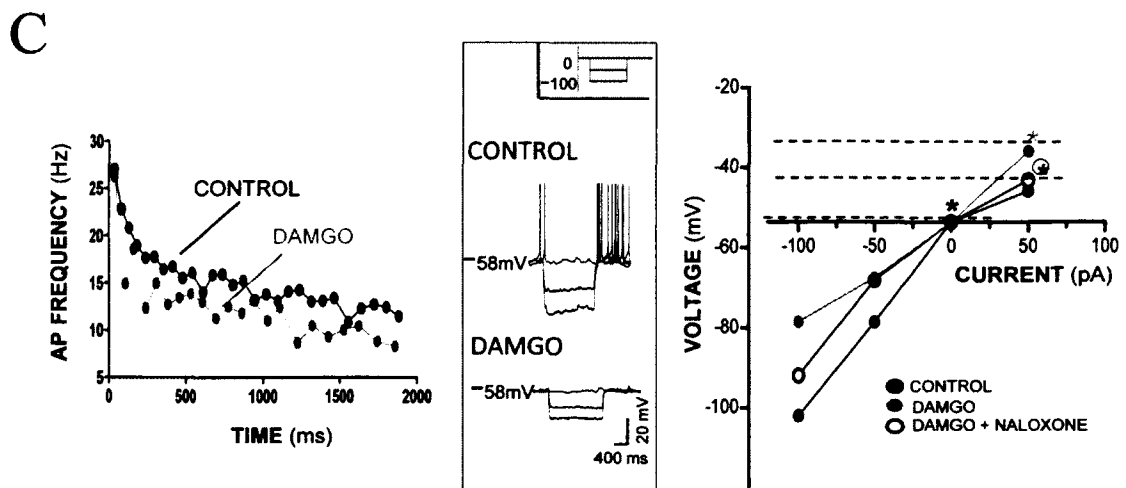
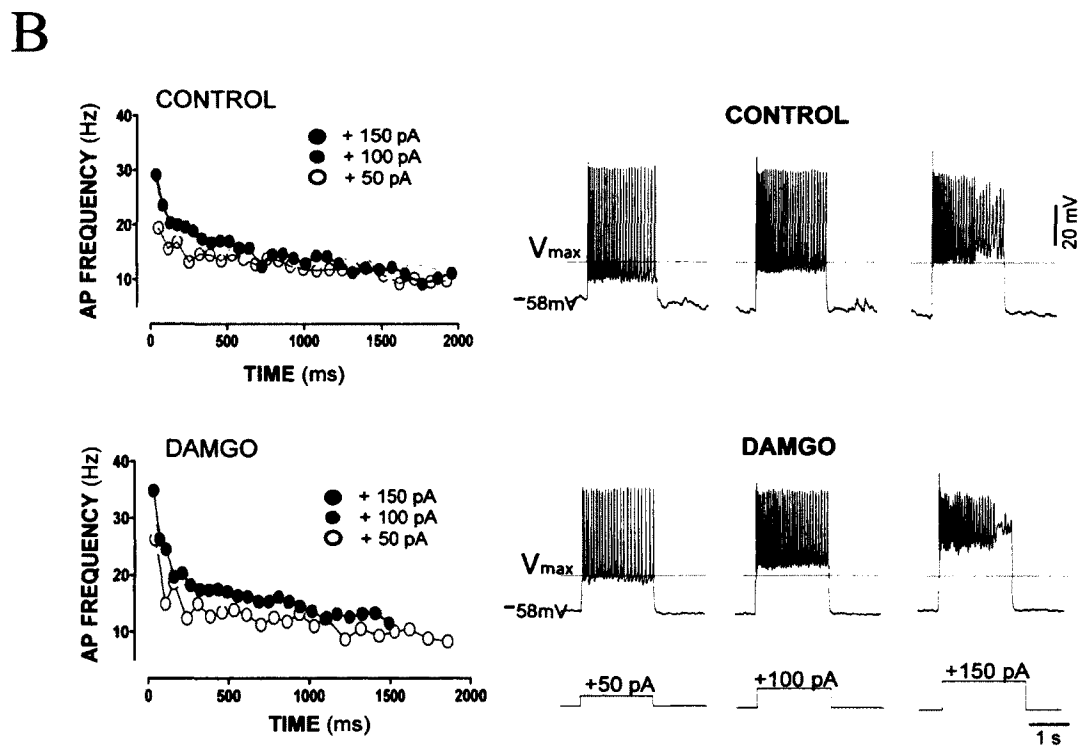
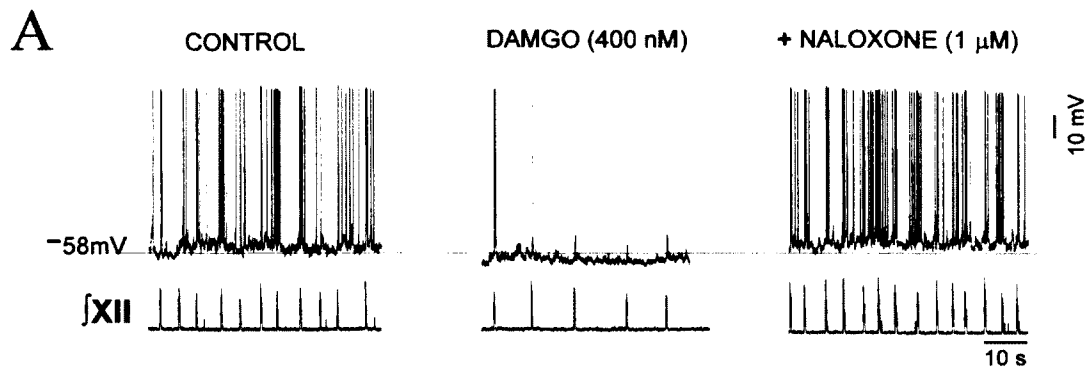
Transverse sections of the ventral medulla immunostained for serotonin (5HT; **A**), substance P (SP; **B**) and μ -opioid receptor (MOR; **C**). **D**. Note that for this picture 5HT is shown in green in order to appreciate colocalization between 5HT and SP. **E**. Overlay of triple labeling 5HT/SP/MOR. 5HT⁺/SP⁺ neurons (**D**) are almost all positive for MOR (**F**). * = blood vessels. Scale = 50 μ m.



Previous Page

Figure 4.5 Characteristics of respiratory neurons of the RNO in medullary slice preparation.

Voltage-clamp (A) and current-clamp (B) recording of a respiratory neuron of the raphé. C. Photomicrograph of the patch pipette impaled on a respiratory RNO neuron, located on the ventral part of the RNO, just dorsal to the inferior olive (IO) and very close to the midline. D. The trace shows a current elicited by voltage ramp command (see framed protocol on the top left of the graph) from a holding potential corresponding to resting membrane potential under regular *in vitro* conditions. Note the presence of a rectifying inward conductance. Bath application of tetrodotoxin (TTX 0.5 μ M) was used to detect TTX-sensitive persistent sodium conductance (I_{NaP}) shown in grey. E. Hyperpolarization-activated inward current (I_h) isolated by hyperpolarizing steps (bottom framed protocol) delivery. F. Post-hoc anatomical photomicrograph obtained after electrophysiological recording of a respiratory neuron of the RNO filled with neurobiotin. Note multiple neurobiotin-filled neurons (coupled with avidin D and reacted with diaminobenzidine) after one single intracellular recording.



Previous Page

Figure 4.6 DAMGO decreases excitability of respiratory-related RNO neurons.

A. Whole-cell current-clamp recording of a respiratory related RNO neuron in control, DAMGO bath application (400 nM) and with added naloxone (1 mM) to bathing medium. **B.** The respiratory RNO neuron was kept at their resting membrane potential and depolarizing steps were evoked by brief current steps (see respective current steps on the bottom of the figure). The traces show depolarizations elicited by current steps under control conditions (upper) in presence of DAMGO (lower). V_{max} corresponds to the maximum voltage threshold reached by that particular neuron in control. Note the voltage threshold widening in presence of DAMGO. On the left, graphs show action potential (AP) firing frequency plotted against time during the sustained depolarizing current injection based on data shown on the right. Note the alteration of instantaneous suprathreshold excitability produced by DAMGO. In the presence of DAMGO the cell is loosing capability to produced steady-state action potentials during high (+150 pA current injection) sustained depolarization. **C.** First graph (left) shows lower firing frequencies obtained in the same neuron during sustained depolarizing step at comparable voltage threshold in control (black) versus DAMGO (grey). Graph on the right shows subthreshold membrane polarizations plotted as a function of the injected currents. Note the decrease in the curve slope associated with the R_N change induced by DAMGO, and its partial reversal by naloxone. The * indicates when the firing threshold had been attained (black for control; grey for DAMGO; circle for DAMGO + NALOXONE). Note the increase in voltage threshold induced by DAMGO which is subsequently attenuated by naloxone. The voltage responses to negative current steps are shown in the middle panel.

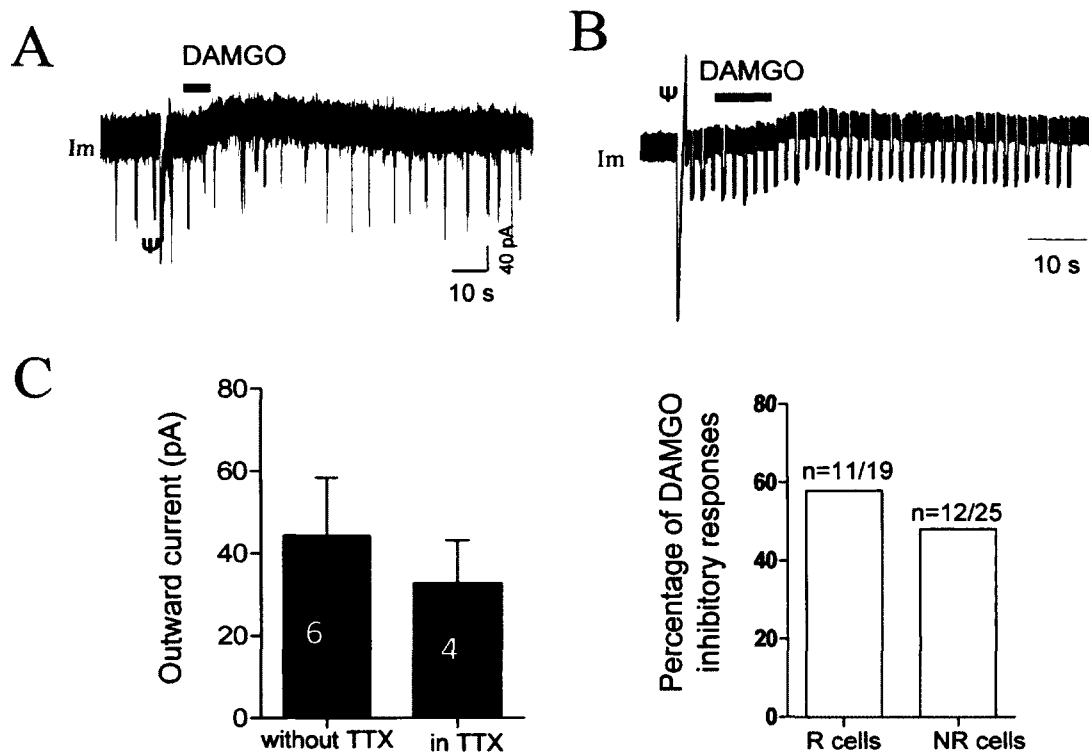


Figure 4.7 Postsynaptic effect of DAMGO on RNO neurons.

A. Representative trace of a voltage-clamp recording of a RNO respiratory neuron and its current response to a local application of DAMGO (1 μM ; 10 s; $n = 6$). Mu-opioid receptor activation by DAMGO leads to a reversing outward current. Note the decrease in respiratory input current amplitude upon DAMGO suggesting an additional inhibitory effect of DAMGO on excitatory postsynaptic events. **B.** Representative trace of a voltage-clamp recording of a respiratory neuron in presence of TTX (0.5 μM). DAMGO-induced outward current is reproduced in TTX ($n = 4$). Hyperpolarizing voltage steps were given at the same time. The Ψ on each figure shows current-voltage responses for input resistance measurements. **C.** Summary histograms of the outward current amplitude obtained from respiratory RNO neurons with and without the presence of TTX in the bathing medium. The histogram on the right shows a summary of total number of recorded RNO cells (R = respiratory; NR = non-respiratory) that responded to DAMGO either by an outward current in voltage-clamp recording, or a membrane hyperpolarization in current-clamp.

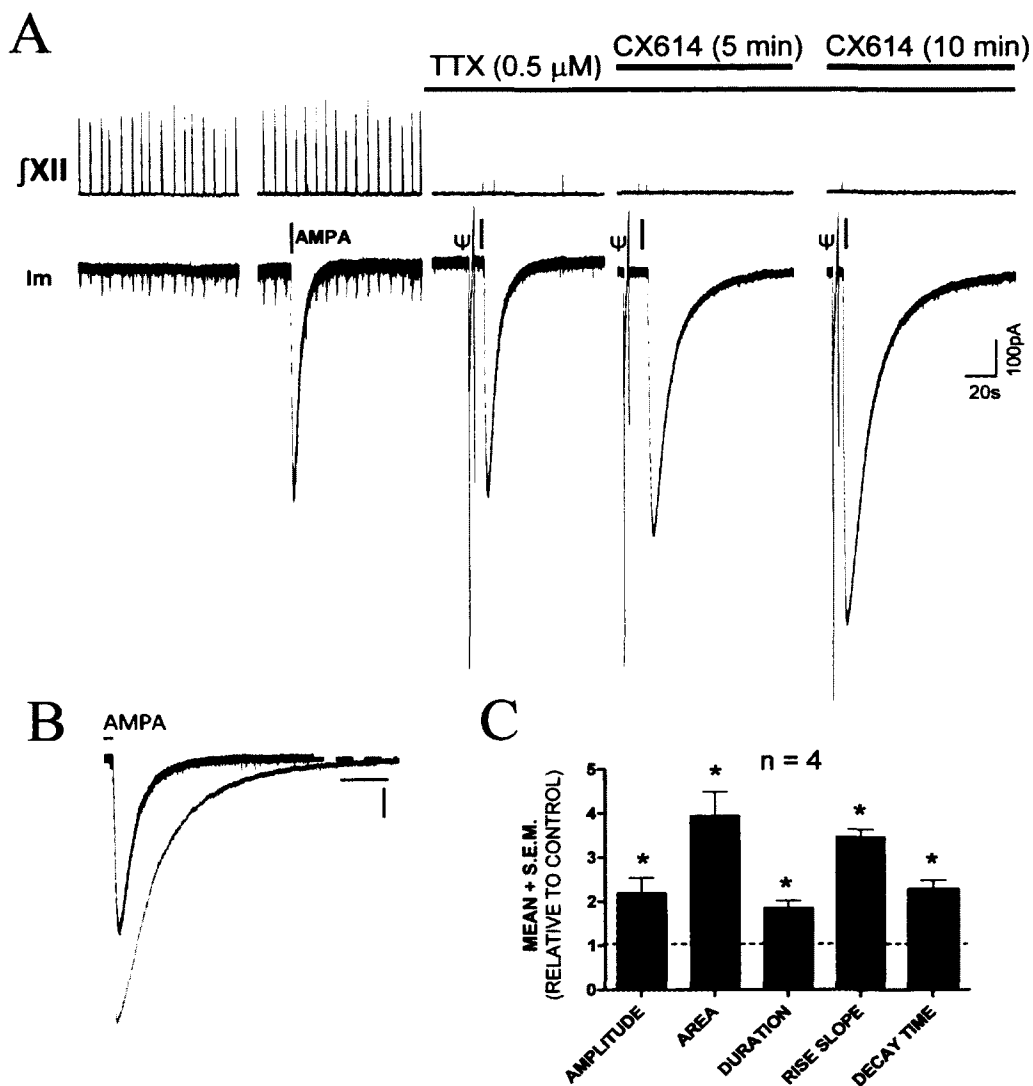
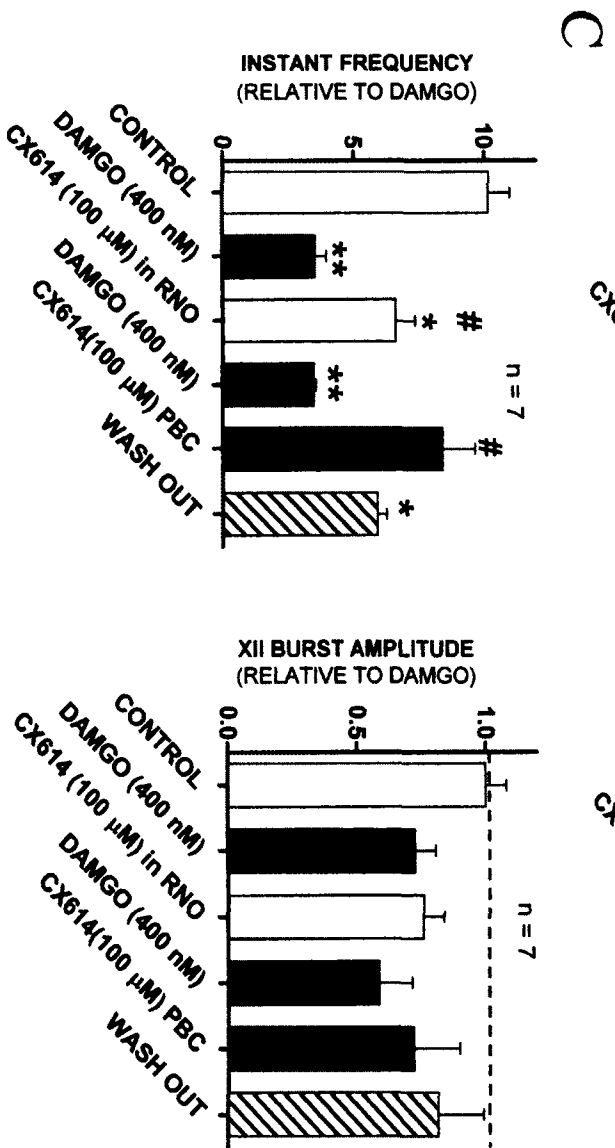
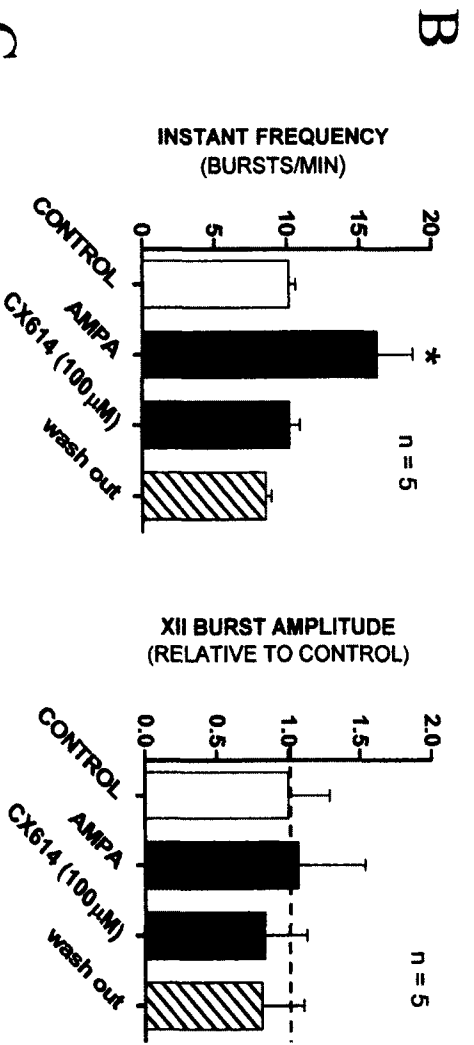
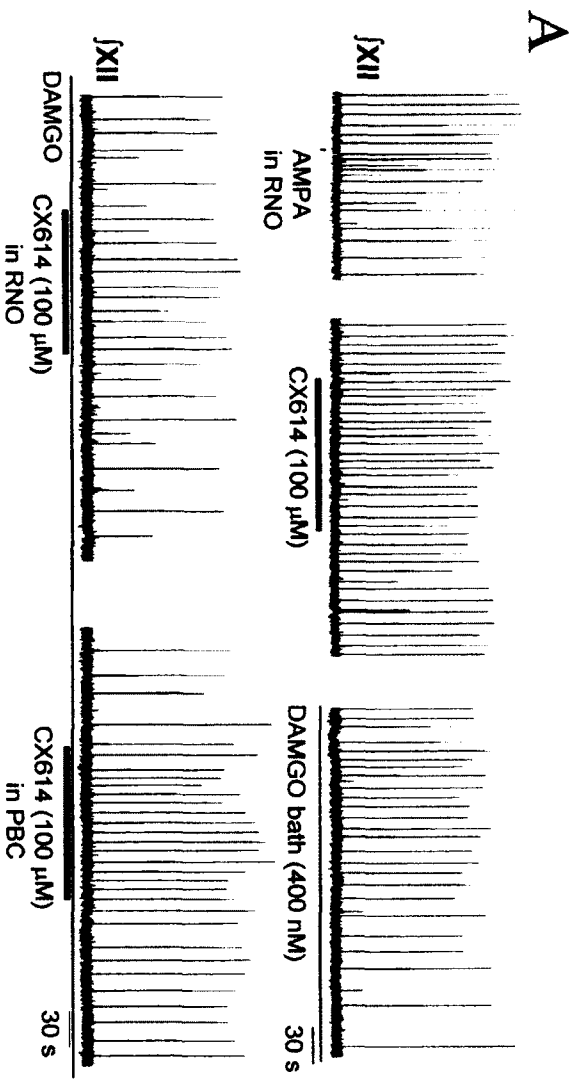


Figure 4.8 Respiratory raphé neurons contain functional AMPA receptors which conductance can be modulated by the high-impact ampakine CX614.

A. Whole-cell recording in voltage-clamp configuration in presence of TTX (0.5 μ M) shows the presence of functional AMPA receptors in respiratory neuron of the RNO. Repeated AMPA puffs (black arrows) were given to the same neuron. The AMPA-mediated currents were increased by bath application of CX614 (20 μ M). The effect of CX614 on AMPA-mediated currents starts only 5 min after CX614 exposure and is greater after 10 min exposure. **B.** AMPA-mediated current responses in control (black) and in presence of CX614 (grey) are superposed. **C.** Group data graph shows AMPA-induced current parameters that were significantly increased in respiratory neurons of the RNO (n = 4). ψ are transients resulting from delivery of I/V ramp for input resistance measurements. * = significantly difference from control.



Previous Page

Figure 4.9 Independent action of the ampakine CX614 within the RNO sensitive area can increase inspiratory drive frequency in presence of DAMGO.

Integrated traces of XII nerve motor output recorded in a medullary slice preparation are shown in different conditions. **A.** Local application of CX614 into the RNO does not affect respiratory drive. Bath application of DAMGO induces a decrease in respiratory frequency. Lower trace shows XII nerve activity during bath application of DAMGO. Local application of CX614 into the RNO (left trace) is compared to local application of CX614 into preBötC. **B.** Group data showing that CX614 locally applied to the RNO does not change respiratory motor output instant frequency, nor amplitude in baseline conditions (one-way ANOVA; * = significantly different from control ($p < 0.05$); ns = non significant with $p > 0.05$; $n = 5$). **C.** Group data showing the increase in respiratory motor output instant frequency when CX614 is locally applied to the ventral side of the raphe obscurus (RNO) versus preBötC (PBC) ($n = 7$). * = significantly different from control (one-way ANOVA; $p < 0.05$); ** = $p < 0.01$; # = significantly different from DAMGO (one-way ANOVA; $p < 0.05$). Note that there was no significant difference between frequency recorded in CX614 (RNO injection) and frequency recorded in CX614 (preBötC injection; $p > 0.05$).

4.5 REFERENCES

AL-ZUBAIDY ZA, ERICKSON RL, GREER JJ (1996) Serotonergic and noradrenergic effects on respiratory neural discharge in the medullary slice preparation of neonatal rats. *Pflugers Arch.* 431 (6):942-949.

ANDERSON SD, BASBAUM AI, FIELDS HL (1977) Response of medullary raphe neurons to peripheral stimulation and to systemic opiates. *Brain Res.* 123(2):363-8.

ANDERSON P, STORM J, WHEAL HV (1987) Thresholds of action potentials evoked by synapses on the dendrites of pyramidal cells in the rat hippocampus in vitro. *J Physiol.* 383:509-26.

BADAWY AA, EVANS M, PUNJANI NF, MORGAN CJ (1983) Does naloxone always act as an opiate antagonist? *Life Sci.* 33 Suppl 1:739-42.

BARKER JR, THOMAS CF, BEHAN M (2009) Serotonergic projections from the caudal raphe nuclei to the hypoglossal nucleus in male and female rats. *Respir Physiol Neurobiol.* 165(2-3):175-84.

BRADLEY SR, PIERIBONE VA, WANG W, SEVERSON CA, JACOBS RA, RICHERSON GB (2002) Chemosensitive serotonergic neurons are closely associated with large medullary arteries. *Nat Neurosci.* 5(5):401-2.

BROADBELT KG, PATERSON DS, RIVERA KD, TRACHTENBERG FL, KINNEY HC (2010) Neuroanatomic relationships between the GABAergic and serotonergic systems in the developing human medulla. *Auton Neurosci.* 154(1-2):30-41. E

BRODIN E, GAZELIUS B, PANOPOULOS P, OLGART L (1983) Morphine inhibits substance P release from peripheral sensory nerve endings. *Acta Physiol Scand.* 117(4):567-70.

BROWN EN, PURDON PL, VAN DORT CJ (2011) General anesthesia and altered states of arousal: a systems neuroscience analysis. *Annu Rev Neurosci.* 34:601-28.

BRUCE D. CARTER AND FEDOR MEDZIHRADESKY (1993) μ Mediates the Coupling of the μ Opioid Receptor to Adenylyl Cyclase in Cloned Neural Cells and Brain. *Proceedings of the National Academy of Sciences of the United States of America* 90(9):4062-4066.

BUCHANAN GF, RICHERSON GB (2010) Central serotonin neurons are required for arousal to CO₂. *Proc Natl Acad Sci U S A.* 107(37):16354-9.

CAO Y, FUJITO Y, MATSUYAMA K, AOKI M (2006A) Effects of electrical stimulation of the medullary raphe nuclei on respiratory movement in rats. *J Comp Physiol A Neuroethol Sens Neural Behav Physiol.* 192(5):497-505.

CAO Y, MATSUYAMA K, FUJITO Y, AND AOKI M (2006B) Involvement of medullary GABAergic and serotonergic raphé neurons in respiratory control: Electrophysiological and immunohistochemical studies in rats. *Neurosci. Research* (56): 322–331.

CHIANG CY, PAN ZZ (1985) Differential responses of serotonergic and non-serotonergic neurons in nucleus raphe magnus to systemic morphine in rats. *Brain Res.* 37(1):146-50.

DEPUY SD, KANBAR R, COATES MB, STORNETTA RL, GUYENET PG (2011) Control of breathing by raphé obscurus serotonergic neurons in mice. *J. Neurosci.* 31(6):1981-90.

DRDLA-SCHUTTING R, BENRATH J, WUNDERBALDINGER G, SANDKÜHLER J (2012) Erasure of a spinal memory trace of pain by a brief, high-dose opioid administration. *Science.* 335(6065):235-8.

DUNCAN JR, PATERSON DS, HOFFMAN JM, MOKLER DJ, BORENSTEIN NS, BELLIVEAU RA, KROUS HF, HAAS EA, STANLEY C, NATTIE EE, TRACHTENBERG FL, KINNEY HC (2010) Brainstem serotonergic deficiency in sudden infant death syndrome. *JAMA* 303(5):430-7.

ERLICHMAN JS, BOYER AC, REAGAN P, PUTNAM RW, RITUCCI NA, LEITER JC (2009) Chemosensory responses to CO₂ in multiple brain stem nuclei determined using a voltage-sensitive dye in brain slices from rats. *J. Neurophysiol.* 102(3):1577-90.

GUYENET PG, SEVIGNY CP, WESTON MC, STORNETTA RL (2002) Neurokinin-1 receptor-expressing cells of the ventral respiratory group are functionally heterogeneous and predominantly glutamatergic. *J. Neurosci.* 22(9):3806-16.

HASSEN AH, FEUERSTEIN G, FADEN AI (1982) Mu Receptors and opioid cardiovascular effects in the NTS of rat. *Peptides* 3(6):1031-7.

HASSEN AH, FEUERSTEIN G, FADEN AI (1984) Selective cardiorespiratory effects mediated by mu opioid receptors in the nucleus ambiguus. *Neuropharmacology* 23(4):407-15.

HELLMAN KM, MENDELSON SJ, MENDEZ-DUARTE MA, RUSSELL JL, MASON P (2009) Opioid microinjection into raphé magnus modulates cardiorespiratory function in mice and rats. *AJP Regul Integ Comp Physiol* 297: R1400–R1408.

HEINRICHER MM, MORGAN MM, TORTORICI V, FIELDS HL (1994) Disinhibition of off-cells and antinociception produced by an opioid action within the rostral ventromedial medulla. *Neuroscience* 63:279–288

HODGES MR, RICHERSON GB (2010) The role of medullary serotonin (5-HT) neurons in respiratory control: contributions to eupneic ventilation, CO₂ chemoreception, and thermoregulation. *J. Appl. Physiol.* 108(5):1425-32. Review.

HODGES MR, WEHNER M, AUNGST J, SMITH JC, RICHERSON GB (2009) Transgenic mice lacking serotonin neurons have severe apnea and high mortality during development. *J. Neurosci.* 29(33):10341-9.

HÖKFELT T, LJUNGDAHL A, TERENIUS L, ELDE R, NILSSON G (1977) Immunohistochemical analysis of peptide pathways possibly related to pain and analgesia: enkephalin and substance P. *Proc Natl Acad Sci U S A.* 74(7):3081-5.

HOLTMAN JR, SPECK DF (1994) Substance P immunoreactive projections to the ventral respiratory group in the rat. *Peptides* 15(5):803-8.

JACOBS BL, MARTÍN-CORA FJ, FORNAL CA (2002) Activity of medullary serotonergic neurons in freely moving animals. *Brain Res Brain Res Rev.* 40(1-3):45-52.

JESSELL TM, IVERSEN LL (1977) Opiate analgesics inhibit substance P release from rat trigeminal nucleus. *Nature* 268 (5620):549-5.

JOLAS J, NESTLER EJ, AGHAJANIAN GK (1999) Chronic morphine increases GABA tone on serotonergic neurons of the dorsal raphe nucleus: association with an up-regulation of the cyclic AMP pathway. *Neuroscience* 95(2):433-443.

KOBAYASHI S, FUJITO Y, MATSUYAMA K, AOKI M (2010) Raphe modulation of the pre-Bötzinger complex respiratory bursts in *in vitro* medullary half-slice preparations of neonatal mice. *J. Comp. Physiol.A Neuroethol. Sens. Neural Behav. Physiol.* 196(8):519-28.

KONDO I, MARVIZON JC, SONG B, SALGADO F, CODELUPPI S, HUA XY, YAKSH TL (2005) Inhibition by spinal mu- and delta-opioid agonists of afferent-evoked substance P release. *J. Neurosci.* 25(14):3651-60.

LALLEY PM (1986) Responses of phrenic motoneurons of the cat to stimulation of medullary raphe nuclei. *J. Physiol.* 380:349-71.

LALLEY PM, BENACKA R, BISCHOFF AM, RICHTER DW (1997) Nucleus raphe obscurus evokes 5HT-1A receptor-mediated modulation of respiratory neurons. *Brain Res.* 747(1):156-9.

- LARKMAN PM, KELLY JS, TAKAHASHI T (1995) Adenosine 3':5'-cyclic monophosphate mediates a -hydroxytryptamine-induced response in neonatal rat motoneurons. *Pflugers Arch.* 430(5):763-9.
- LI YW, BAYLISS DA (1998) Presynaptic inhibition by 5-HT_{1B} receptors of glutamatergic synaptic inputs onto serotonergic caudal raphe neurons in rat. *J. Physiol.* 510 (Pt 1):121-34.
- LIU G, FELDMAN JL, SMITH JC (1990) Excitatory amino acid-mediated transmission of inspiratory drive to phrenic motoneurons. *J. Neurophysiol.* 64, 423-436.
- MANAKER S, TISCHLER LJ (1993) Origin of serotonergic afferents to the hypoglossal nucleus in the rat. *J. Comp. Neurol.* 334(3):466-76.
- MANZKE T, DUTSCHMANN M, SCHLAF G, MÖRSCHER M, KOCH UR, PONIMASKIN E, BIDON O, LALLEY PM, RICHTER DW (2009) Serotonin targets inhibitory synapses to induce modulation of network functions. *Philos Trans R Soc Lond B Biol Sci.* 364(1529):2589-602.
- MANZKE T, GUENTHER U, PONIMASKIN EG, HALLER M, DUTSCHMANN M, SCHWARZACHER S, RICHTER DW (2003) 5-HT₄(A) receptors avert opioid-induced breathing depression without loss of analgesia. *Science* 301, 226-229.
- MARINA N, ABDALA AP, TRAPP S, LI A, NATTIE EE, HEWINSON J, SMITH JC, PATON JF, GOURINE AV (2010) Essential role of Phox2b-expressing ventrolateral brainstem neurons in the chemosensory control of inspiration and expiration. *J. Neurosci.* 30(37):12466-73.
- MARINELLI S, VAUGHAN CW, SCHNELL SA, WESSENDORF MW, CHRISTIE MJ (2002) Rostral ventromedial medulla neurons that project to the spinal cord express multiple opioid receptor phenotypes. *J. Neurosci.* 22(24):10847-55.
- MILESCU LS, YAMANISHI T, PTAK K, SMITH JC (2010) Kinetic properties and functional dynamics of sodium channels during repetitive spiking in a slow pacemaker neuron. *J. Neurosci.* 30(36):12113-27.
- MONTANDON G, QIN W, LIU H, REN J, GREER JJ, HORNER RL (2011) PreBötzinger complex neurokinin-1 receptor-expressing neurons mediate opioid-induced respiratory depression. *J. Neurosci.* 31(4):1292-301.
- NATTIE EE (2001) Central chemosensitivity, sleep, and wakefulness. *Respir. Physiol.* 129(1-2):257-68. Review.
- NICHOLSON C (1985) Diffusion from an injected volume of a substance in brain tissue with arbitrary volume fraction and tortuosity. *Brain Res.* 333: 325-329.

NIJSSEN PC, SEXTON T, CHILDERS SR (1992) Opioid-inhibited adenylyl cyclase in rat brain membranes: lack of correlation with high-affinity opioid receptor binding sites. *J. Neurochem.* 59(6):2251-62.

GRAY PA, JANCZEWSKI WA, MELLEN N, MCCRIMMON D, FELDMAN JL (2001) Normal breathing requires preBötzinger complex neurokinin-1 receptor-expressing neurons. *Nat. Neurosci.* 4(9): 927–930.

PACE RW, MACKAY DD, FELDMAN JL, DEL NEGRO CA (2007) Role of persistent sodium current in mouse preBötzinger Complex neurons and respiratory rhythm generation. *J. Physiol.* 580(Pt. 2):485-96.

PAGLIARDINI S, REN J, GREER JJ (2003) Ontogeny of the pre-Bötzinger complex in perinatal rats. *J. Neurosci.* 23(29):9575-84.

PAN ZZ (2003) Kappa-opioid receptor-mediated enhancement of the hyperpolarization-activated current (I_h) through mobilization of intracellular calcium in rat nucleus raphe magnus. *J. Physiol.* 548(Pt 3):765-75.

PATTINSON KT, GOVERNO RJ, MACINTOSH BJ, RUSSELL EC, CORFIELD DR, TRACEY I, WISE RG (2009) Opioids depress cortical centers responsible for the volitional control of respiration. *J. Neurosci.* 29 (25):8177-86.

PEDERSEN NP, VAUGHAN CW, CHRISTIE MJ (2011) Opioid receptor modulation of GABAergic and serotonergic spinally projecting neurons of the rostral ventromedial medulla in mice. *J. Neurophysiol.* 106(2):731-40.

PEEVER JH, NECAKOV A, DUFFIN J (2001) Nucleus raphe obscurus modulates hypoglossal output of neonatal rat *in vitro* transverse brain stem slices. *J Appl Physiol.* 90(1):269-79.

PHILLIPS RS, CLEARY DR, NALWALK JW, ARTTAMANGKUL S, HOUGH LB, HEINRICHER MM (2012) Pain-facilitating medullary neurons contribute to opioid-induced respiratory depression. *J Neurophysiol.* 2012 Sep 5. [Epub ahead of print]

PTAK K, YAMANISHI T, AUNGST J, MILESCU LS, ZHANG R, RICHERSON GB, SMITH JC (2009) Raphé neurons stimulate respiratory circuit activity by multiple mechanisms via endogenously released serotonin and substance P. *J. Neurosci.* 29(12):3720-37.

SHAO XM, GE Q, FELDMAN JL (2003) Modulation of AMPA receptors by cAMP-dependent protein kinase in preBötzinger complex inspiratory neurons regulates respiratory rhythm in the rat. *J. Physiol.* 1; 547(Pt 2):543-53.

SONG G, AOKI M (2001) Projections from brainstem GABAergic neurons to the phrenic nucleus. *Adv Exp Med Biol.* 499:107-11.

SVOBODA KR, LUPICA CR (1998) Opioid inhibition of hippocampal interneurons via modulation of potassium and hyperpolarization-activated cation (I_h) currents. *J. Neurosci.* 18(18):7084-98.

WANG W, PIZZONIA JH, RICHERSON GB (1998) Chemosensitivity of rat medullary raphe neurones in primary tissue culture. *J Physiol.* 511 (Pt 2):433-50.

WU G, LU ZH, ALFINITO P, LEDEEN RW (1997) Opioid Receptor and Calcium Channel Regulation of Adenylyl Cyclase, Modulated By GM1, in NG108-15 Cells: Competitive Interactions. *Neurochemical Research* 22(10):1281-1289.

ZAGON A (1993) Innervation of serotonergic medullary raphe neurons from cells of the rostral ventrolateral medulla in rats. *Neuroscience* 55(3):849-67.

ZHANG Z, XU F, ZHANG C, LIANG X (2009) Opioid mu-receptors in medullary raphe region affect the hypoxic ventilation in anesthetized rats. *Respir Physiol Neurobiol.* 168(3):281-8.

CHAPTER 5

CELLULAR MECHANISMS UNDERLYING THE ALLEVIATION OF RESPIRATORY DEPRESSION BY LOW-IMPACT AMPAKINES

My contribution to this study consisted in the planning, execution and analyses of electrophysiological recordings and anatomical results. I initiated and provided the rationale for the transfection project in collaboration with Lipton group. I performed the transformation and transfection experiments with the assistance of Dr. Wei Zhang in collaboration with the Persad Lab. Immunohistochemical and immunocytochemical experiments were performed by Dr. Wei Zhang.

5.1 ABSTRACT

The ampakine CX717 belongs to the low-impact ampakine family of compounds and increases synaptic transmission in diverse brain regions. In particular, CX717 is very efficient at alleviating opioid-induced respiratory depression and apneas in rodents as well as in humans. Although several lines of evidence have suggested that CX717 may act centrally by increasing inspiratory drive, the exact cellular mechanisms underlying its mode of action are still unknown. In order to test CX717 *in vitro* and define its potential targets, we studied spontaneously generate inspiratory activity in neonatal rat medullary slice preparations containing the preBötC.

While having no effect on its own, CX717 either bath applied or locally applied to the preBötC significantly reversed opioid-induced respiratory depression, mimicking *in vivo* data. Whole-cell recordings of inspiratory preBötC neurons showed that CX717 regulation of inspiratory currents and postsynaptic events was absent or minimal in baseline conditions. However, when inspiratory activity was depressed by DAMGO, CX717 significantly increased inspiratory synaptic current amplitude and area. Analysis of postsynaptic AMPA-induced currents in the presence of tetrodotoxin showed no significant regulation of AMPA-mediated current parameters by CX717 with the exception of an increase in charge transfer. Interestingly, CX717 potentiated NMDA-evoked depolarizations previously decreased by glycine. Immunohistochemical data revealed that the specific NMDA receptor subunit that initiates excitatory glycinergic currents is expressed in the preBötC and colocalizes in part with neurokinin-1 positive neurons. Glycinergic NMDA receptor expression experimental model combined with whole-cell patch-clamp measurements can be used to determine the exact physiological substrate underlying CX717 action. Collectively, those results provide the foundation for testing a new mechanism of inspiratory frequency potentiation induced by the ampakine CX717.

5.2 INTRODUCTION

CX717 is one of the first low-impact ampakines developed for clinical use. CX717 received particular interest because it showed efficacy as a potential cognitive enhancer in studies using rodent and primate models (Porrino et al., 2005; Wesenstein et al., 2007; Boyle et al., 2011; Zheng et al., 2011). After showing the efficacy of the high-impact ampakine CX546 in counteracting opioid-induced respiratory depression (Ren et al., 2006), Ren and colleagues extended their systematic study on young and adult rats using CX717. They demonstrated that CX717 counteracted severe opiate-induced respiratory depression without suppressing analgesia when delivered pre-, concomitant with, or post-opioid administration (Ren et al., 2009). This led to a collaborative clinical study demonstrating that CX717 could prevent opioid-induced respiratory depression without affecting analgesia in humans (Oertel et al., 2010), establishing proof of concept for considering CX717 as a safe and selective alleviator of respiratory depression.

It has been reported that CX717 may act postsynaptically on AMPA and glutamate mediated currents in respiratory XII motoneurons of neonatal rodent slices (Lorier et al., 2010) and in isolated hippocampal synaptosomes of adult rodents (Parameshwaran et al., 2006; Kariharan et al., 2008). However, insights derived from experimental work describing the exact cellular mechanisms involved in the CX717-induced increase of inspiratory rhythm *per se* are still lacking. Ultimately, the identification of cellular mechanisms underlying ampakine potentiation will help further develop relevant pharmacological interventions to alleviate respiratory depression and apneas. We hypothesized that the effect of CX717 on inspiratory rhythm was due to its direct action on the inspiratory rhythm generator, the preBötzinger complex (preBötC; Smith et al., 1991) and therefore focused the analysis of CX717 mechanisms of action on the preBötC, with the objectives of i) determining where CX717 acts, ii) identifying what type of receptor(s) it binds to in order to exert its effect, iii) understanding how it modulates inspiratory drive.

The ampakines CX1763 and CX1739 belong to the third generation of low-impact ampakines, which are more potent and safer than previous ampakine compounds. CX1739 has been recently protected under US Patent and is currently in Phase II clinical development. Therefore, CX1763 and CX1739 were included in the experiments to verify their efficacy in counteracting opioid-induced respiratory depression *in vitro*. CX1942 is the ester pro-drug of CX1763 and was designed by Cortex Pharmaceuticals as an ampakine with increased water solubility (for intravenous administration). Whether CX1942 can increase central inspiratory drive after it has crossed the blood brain barrier was tested by assessing its effect *in vitro* in the active medullary slice preparation and compared it with its pharmacological active form CX1763.

5.3 RESULTS

5.3.1 LOW-IMPACT AMPAKINES ALLEVIATE DAMGO-INDUCED RESPIRATORY DEPRESSION *IN VITRO*

Low-impact ampakines counter respiratory depression *in vitro*.

The effects of bath application of several low-impact ampakines (CX717; CX1763, CX1942; CX1739) subsequent to a sustained respiratory depression induced by bath application of the μ -opioid agonist D-Ala (2), N-MePhe (4), Gly-ol]-enkephalin (DAMGO; 400 nM) were examined using P0-4 medullary slice preparations. Figures 5.1A, 5.13A and 5.16A show representative examples of the effect of bath applications of CX717, CX1763 and CX1739 on the XII rhythmic inspiratory activity. Population data generated from medullary slice preparations are shown in Figure 5.13B for CX1763 and Figure 5.16B for CX1739. For CX717, XII burst frequency relative values were plotted against time in order to evaluate the time course of CX717-induced potentiation of inspiratory rhythm, compared to the time course of respiratory depression induced by DAMGO alone (see Fig. 5.1B). The increase in inspiratory frequency induced by the introduction of CX717 in the bathing medium occurred within minutes of CX717 exposure and led to an enhancement of frequency reaching up to 0.85 ± 0.35 of control ($n = 8$) after 15 minutes of CX717 exposure. Conversely, the decrease in inspiratory frequency induced by DAMGO alone reached 0.35 ± 0.03 of control after 30 minutes of DAMGO exposure ($n = 6$). The CX717 effect diminished within a minute of wash out with inspiratory frequency slowly recovering to control within approximately 30 minutes. A minimum of 50 μ M CX717 was required to induce a sustained increase in inspiratory frequency, while newer low-impact ampakines only required 25 μ M (CX1763) or 40 μ M (CX1739). More specific to CX717, the net increase of inspiratory frequency could vary markedly depending on the degree of DAMGO-induced respiratory depression. Interestingly, CX717-induced net increase of inspiratory activity was more potent (and therefore required a

lesser dose) when DAMGO-induced respiratory depression was more pronounced (leading to a complete silencing of inspiratory activity).

CX717 acts in the preBötC to counter respiratory depression *in vitro*.

Figure 5.2 shows a representative example of the effect of local application of CX717, as well as the population data generated from recordings of 5 medullary slice preparations (Fig. 5.2B). For this set of experiments, DAMGO was first included in the bathing medium at 400 nM to induce a sustained respiratory rhythm depression. CX717 (1 mM) was then directly applied to the preBötC via steady pressure injection for 120 sec (see section 1 of Chapter 2 for details in methodology). Local applications of artificial cerebrospinal fluid (aCSF) were performed before or after the local application of each ampakine and did not induce a significant change in inspiratory burst frequency. A minimum period of 10 minutes passed between local applications in order to allow recovery. As seen in Figure 5.2B, CX717 microinjections within the preBötC area induced a significant increase in XII motor output frequency compared to DAMGO ($p < 0.05$), although the frequency at 0.61 ± 0.12 of control stayed significantly below control values ($p < 0.05$; $n = 5$).

5.3.2 MODULATION OF RESPIRATORY NEURAL CIRCUITRY BY CX717 IN BASELINE CONDITIONS

Effect of CX717 bath application on respiratory motor output activity.

The effect of CX717 on baseline endogenous respiratory rhythmic activity was examined *in vitro*. Analysis of XII nerve discharge obtained from 10 rhythmic medullary slice preparations in 9 mM $[K^+]_e$ showed no significant change in frequency nor amplitude of the bursts when adding CX717 to the bathing medium ($n = 10$; see relative values histogram in Fig. 5.3A; one-way ANOVA and Tukey's post test comparison on raw values). For a complete examination of CX717 *in vitro*, the brainstem spinal cord model was included in this set of experiments due to the fact that the preparation contains more

excitatory inputs that could possibly be targeted by CX717, and it displays a robust respiratory activity in low extracellular potassium concentration (3 mM $[K^+]_e$). Similarly to results obtained with medullary slice preparations, the statistical analysis of respiratory nerve output (C1 and C4) obtained from 7 brainstem spinal cord preparations showed no significant change in frequency nor amplitude ($n = 7$; one-way ANOVA; $p > 0.05$; see Fig. 5.3B). Note that CX717 was used at a high concentration (200 μ M).

Collectively, these results demonstrated that CX717 does not have any significant effect on respiratory frequency or amplitude under baseline conditions *in vitro*.

Whole-cell patch-clamp analysis of respiratory preBötC neuron activity in presence of CX717.

Next, it was determined whether CX717 could modulate single cell conductance in standard conditions, independently of the fact that CX717 did not appear to have any effect on the frequency of the preBötC oscillatory outputs. Figure 5.4A shows a representative example of a voltage-clamp recording of an inspiratory preBötC neuron with bath application of increasing doses of CX717 (50 μ M to 100 μ M). Population data obtained from 4 inspiratory preBötC cells showed no significant effect on amplitude, area or duration of inspiratory input currents (Fig. 5.4B). Further, R_N measurements did not show any significant effect of CX717.

To verify the possibility of an action on tonic synaptic activity and/or transmitter release process, the effect of CX717 on interburst sPSCs was analyzed. Note that because those experiments were done in the absence of any inhibitory receptor blockers (such as bicuculline and strychnine) and without tetrodotoxin in the bathing medium, it cannot be determined whether inward synaptic events included in this set of data were excitatory, nor that they reflect calcium-independent neurotransmission release. Statistical analysis on the mean values of sPSC parameters of 4 inspiratory preBötC neurons showed no significant difference between control and CX717 for none of the parameters

(amplitude, area, frequency, decay time constant; one-way ANOVA; $p > 0.05$; $n = 4$). As illustrated by cumulative distribution plots in Figure 5.4C, D and E, CX717 did not have any significant effect on interevent interval of sPSCs (Kolmogorov-Smirnov two sample test, $p = 0.43 > 0.05$; $n = 5926$) or decay time constant of sPSCs (Kolmogorov-Smirnov two sample test, $p > 0.99$; $n = 6415$), but the cumulative sPSC amplitude distributions were significantly different (Kolmogorov-Smirnov two sample test, $p < 0.0001$; $n = 6451$). Wilcoxon post-test on sPSC amplitude and interevent interval means showed no significant difference between control ($- 47 \pm 5$ pA amplitude; 308 ± 78 ms inter-event interval; 16 ± 1 ms decay time constant) and CX717 ($- 47 \pm 8$ pA amplitude ($p = 1 > 0.05$); 229 ± 61 ms inter-event interval ($p = 0.155 > 0.05$); 15 ± 1 ms decay time constant ($p = 0.125 > 0.05$); $n = 4$). These data suggest that CX717 does not significantly modulate tonic synaptic activity on inspiratory preBötC neurons on its own.

We also observed that 4 out of 6 expiratory neurons of the preBötC responded to CX717 with an increase in interburst inward synaptic currents. As illustrated by cumulative distribution plots in Figure 5.5, CX717 had a significant effect on interevent interval of sPSCs (Kolmogorov-Smirnov two sample test, $p = 0.036 < 0.05$; $n = 1341$; 3/4 cells) and the amplitude of sPSCs (Kolmogorov-Smirnov two sample test, $p = 0.0005 < 0.05$; $n = 1132$; 3/4 cells), but the sPSC decay time constant distributions were not significantly different (Kolmogorov-Smirnov two sample test, $p = 0.14 > 0.05$; $n = 1315$). Note that no significant effect of CX717 was found on expiratory current (outward inhibitory) frequency ($n = 6$). Wilcoxon post-test on sPSC amplitude and decay time constant means showed no significant difference between control ($- 11 \pm 3$ pA amplitude; 16 ± 5 ms decay time constant) and CX717 ($- 13 \pm 3$ pA amplitude ($p > 0.05$); decay time constant 20 ± 4 ms ($p > 0.05$; $n = 3/4$ cells). However the interevent interval mean was significantly decreased by bath addition of CX717 (1539 ± 115 ms interevent interval in control versus 974 ± 29 ms inter-event interval in presence of CX717; $p < 0.05$). These data suggest that CX717 alone may modulate tonic synaptic activity in preBötC neurons other than inspiratory neurons, although not all expiratory neurons were found to respond similarly.

5.3.3 SINGLE-CELL ANALYSES OF CX717 MODULATION OF PREBÖTC NEURON ACTIVITY FOLLOWING DAMGO-INDUCED RESPIRATORY DEPRESSION

Analysis of inspiratory currents in respiratory preBötC neurons under bath application of CX717 following DAMGO-induced respiratory depression.

The effect of bath-applied CX717 on inspiratory input current parameters following DAMGO-induced frequency depression was examined. Figure 5.6 shows representative examples of voltage-clamp recording traces obtained from two inspiratory preBötC neurons after bath application of DAMGO (400 nM) and subsequent bath addition of CX717 (100 μ M). Note that these data include cells that responded to DAMGO with a slow outward current (2/6 cells), as well as cells “insensitive” to DAMGO (4/6 cells). Repeated-measures ANOVA (followed by Tukey’s post test and using raw data) on inspiratory current parameters showed that in the presence of DAMGO, bath application of CX717 significantly increases frequency and amplitude of inspiratory currents but that the area of inspiratory currents was not significantly increased. More specifically, as illustrated in Figure 5.6C, the amplitude attained an average of 0.64 ± 0.07 of control in DAMGO versus 0.92 ± 0.13 of control in DAMGO + CX717 ($n = 6$; $p < 0.05$) and the frequency attained an average of 0.21 ± 0.08 of control in DAMGO versus 0.62 ± 0.09 of control in DAMGO + CX717 ($n = 6$; $p < 0.05$). The area attained an average of 0.44 ± 0.14 (DAMGO) and 0.83 ± 0.18 (DAMGO + CX717) of control values ($p > 0.05$). Those data include cells for which DAMGO suppressed the inspiratory currents to zero. Interestingly, it was observed that the increase in amplitude of inspiratory currents produced by the addition of CX717 tended to be greater when DAMGO completely abolished rhythmic activity (as illustrated in Fig. 5.6A) compared to when DAMGO partially decreased activity (as seen in Fig. 5.6B). The low number of cells recorded with a complete loss of activity during DAMGO prevented a meaningful statistical analysis. But a paired t test between DAMGO and DAMGO + CX717 data for which DAMGO values were measurable (DAMGO partially decreased inspiratory activity) showed a significant increase in the amplitude and frequency

of inspiratory currents (amplitude increased from 141 ± 34 pA in DAMGO to 176 ± 25 pA in DAMGO + CX717; $p = 0.035 < 0.05$; frequency increased from 2.9 ± 0.7 inspiratory currents (events)/min in DAMGO to 4.87 ± 0.94 events/min in DAMGO + CX717; $p < 0.001$; $n = 4$). Again no significant effect of CX717 was found for the area of inspiratory currents ($p = 0.07 < 0.05$; $n = 4$). Those results are consistent with a potentiation of the inspiratory amplitude and frequency by CX717 when inspiratory preBötC neurons are pre-exposed to DAMGO. However, because the area of inspiratory currents was not significantly increased by CX717 (as opposed to data obtained in Chapter 3 on high impact ampakine CX614 which significantly increased the area but not the amplitude of inspiratory currents), those data suggest that CX717 potentiation may involve mechanisms that differ from the mechanisms underlying CX614 potentiation.

Analysis of interburst synaptic activity of inspiratory preBötC neurons during CX717 reversal of DAMGO-induced respiratory depression.

To test the possibility of a CX717 action on tonic synaptic activity in presence of DAMGO, one-way ANOVA on the mean amplitude and mean frequency of sPSCs on 5/7 inspiratory preBötC neurons recorded in voltage-clamp in different experimental conditions was performed (control; DAMGO; DAMGO + CX717; washout; see Fig. 5.6D). No significant effect was found on any of the parameters ($p > 0.05$). Comparing the entire distribution of sPSC amplitude and interevent interval using a Kolmogorov-Smirnov test showed no significance between DAMGO and DAMGO + CX717 ($p = 0.99 > 0.05$ for interevent interval and $p = 0.32 > 0.05$ for amplitude, see Fig. 5.6E). Post-test analysis with a Wilcoxon paired test on mean of raw amplitude and interevent interval showed no significant difference between DAMGO and DAMGO + CX717 ($n = 5$; $p > 0.05$; see Fig. 5.6E). Those results suggest that tonic synaptic activity did not contribute to CX717-induced potentiation of inspiratory rhythm in inspiratory preBötC neurons. Note that once again, those experiments were done in the absence of TTX, bicuculline or strychnine. Therefore action-potential independent mechanisms were not assessed in this set of experiments.

CX717 effects on AMPA-mediated currents.

AMPA receptor conductance plays a major role in rhythmic synaptic transmission in the preBötC (Funk et al., 1993; Funk et al., 1995; Shao et al., 2003) and mediates part of the inspiratory drive to inspiratory preBötC neurons (Pace et al., 2007; Pace and Del Negro, 2008). Because CX717 has been reported to modulate some characteristics of AMPA receptor conductance kinetics in previous studies (Parameshwaran et al., 2006; Kariharan et al., 2008; Lorier et al., 2010), we examined how CX717 modulates AMPA receptor conductance in preBötC neurons. Voltage-clamp recordings of respiratory preBötC neurons held at -58 mV in the presence of TTX (0.5 μ M) were performed and focal puffs of AMPA (100 μ M; 400 ms duration puffs) delivered close to the cell to induce systematic AMPA-mediated current responses, and the effects of bath application of CX717 (100 μ M) on postsynaptic AMPA-induced currents obtained from 7 respiratory preBötC neurons were examined. Figure 5.6A shows a representative trace of AMPA-induced currents on a respiratory preBötC neuron in control and in presence of CX717. The group data (n = 7) analysis on means of AMPA-mediated current parameters showed no significant alteration in any of the parameters of the AMPA-mediated currents (duration_(CX717) = 1.2 ± 0.2 of control; amplitude_(control) = -326 ± 39 pA versus amplitude_(CX717) = -351 ± 48 pA; rise slope_(control) = -179 ± 46 pA/s versus rise slope_(CX717) = -150 ± 47 pA/s; decay slope_(control) = 30 ± 9 pA/s versus decay slope_(CX717) = 31 ± 11 pA/s; paired *t* test; *p* < 0.05), except for the area, which showed a significant increase to 1.2 ± 0.1 of control values with a *p* = 0.0011 < 0.01 (paired *t* test; see histogram in Fig. 5.7B). Those results suggest that CX717 may have an effect on AMPA receptor conductance in respiratory preBötC neurons, but that this effect remains minimal on the whole-cell scale of synaptic current induced by AMPA puffs. Outside-out patch-clamp recordings of preBötC neurons might determine with better precision a potential CX717 regulation of AMPA receptors conductance.

5.3.4 MODULATION OF NMDA RECEPTOR CONDUCTANCE BY CX717

Block of NMDA receptors interferes with the CX717 reversal of opioid-induced respiratory depression.

NMDA receptors have been shown to drive inspiratory activity in 3 mM $[K^+]$ in medullary slice preparations independent of AMPA receptors (Morgado-Valle and Feldman, 2007). Therefore, effects of CX717 were examined using similar strategies. First, CX717 in 3 mM $[K^+]$ was examined. XII nerve activity in medullary slice preparation was completely suppressed when the extracellular concentration of potassium of the bathing solution was lowered from 9 mM to 3 mM. Subsequent bath application of CX717 (100 μ M) re-established inspiratory activity frequency and amplitude in 3/5 medullary slice preparations. Then, XII nerve recordings were made in medullary slice preparations bathed with an aCSF solution containing 9 mM $[K^+]$ but no $[Mg^{2+}]$ and with increasing concentration of the AMPA receptor specific antagonist 2,3-dihydroxy-6-nitro-7-sulphamoylbenzo(F)quin-oxaline (NBQX; 2-50 μ M) in the bath prior to adding CX717. Surprisingly, despite the presence of NBQX, CX717 (100 μ M) produced a substantial increase of XII nerve amplitude (0.20 ± 0.04 of control in NBQX to 0.44 ± 0.12 of control in NBQX + CX717) and frequency (10 ± 2 bursts/min in control, 8.3 ± 1.0 bursts/min in NBQX; 11 ± 1 bursts/min in NBQX + CX717; $n = 3$). However, NBQX at 50 μ M bathing concentration eventually led to a complete loss of inspiratory activity and the potentiation on inspiratory activity by CX717 was only transient in 2 out of 3 preparations.

Thus the strategy of examining the CX717 alleviation of DAMGO-induced respiratory depression in the presence of bath-application of the non-competitive NMDA antagonist dizocilpine (MK801; 20 to 50 μ M) was applied. Figure 5.8 illustrates the results obtained from 7 medullary slice preparations.

MK801 bath applied at 100 μ M had a minimal effect on XII nerve activity on its own. More specifically, one-way ANOVA on XII burst parameters (in control/ MK801/ wash out) showed that MK801 (100 μ M) bath application had

no effect on amplitude, area, duration or frequency of the bursts ($n = 7$). Paired t test analysis between control and MK801 XII bursts parameters showed a significant decrease in area and amplitude of XII nerve (area_(MK801) = 0.66 ± 0.1 of control; amplitude_(MK801) = 0.75 ± 0.05 of control; $p < 0.05$; $n = 7$), but MK801 had no effect on the frequency nor duration of the XII bursts (frequency_(MK801) = 0.86 ± 0.07 ; duration_(MK801) = 0.88 ± 0.08 of control; $p > 0.05$; $n = 7$). Those results are consistent with previous reports (Funk et al., 1993; Morgado-Valle and Feldman, 2007), which showed that blocking NMDA receptors has little to no effect on baseline inspiratory drive *in vitro*.

The group data histogram shown in Figure 5.8B illustrates how CX717 potentiates inspiratory activity when MK801 is used to block NMDA receptors ($n = 7/9$ slices tested). CX717 significantly reversed inspiratory frequency without affecting duration, amplitude or area of XII bursts. The fact that it was difficult to obtain robust activity after wash-out when using the cocktail MK801 + DAMGO indicated that the combinatorial action of DAMGO and MK801 may have had non-specific effects on XII nerve inspiratory activity. Importantly, the bath-applied cocktail of DAMGO (400 nM) + MK801 (50 μ M) led to a complete suppression of inspiratory activity in 2 out of 9 preparations and subsequent application of CX717 (100 μ M) failed to increase inspiratory activity at all in those 2 cases, indicating that MK801 may interfere with CX717 ability to reverse severe respiratory depression.

Effect of CX717 on NMDA-elicited depolarizations in preBötC neurons.

The effect of CX717 on NMDA-induced depolarizing potentials in preBötC neurons was examined. Current-clamp recordings of preBötC neurons were performed in conjunction with application of NMDA-puffs (100 to 200 ms duration; 500 μ M) to induce depolarizing potentials. CX717 alone induced no change in NMDA-induced responses. However, in 4 out of 9 neurons tested, bath application of glycine (20 to 40 μ M) prior to bath application of CX717 (100 μ M) significantly decreased the amplitude of NMDA responses (see example in Fig. 5.9B). In these conditions, the addition of CX717 to the bathing medium

significantly increased the amplitude of NMDA-elicited depolarizing potentials, specifically at hyperpolarized basal membrane potential ($V_m < -50$ mV). Figure 5.9D illustrates NMDA-evoked depolarization amplitudes obtained from a current-clamp recording of a single preBötC neuron, plotted against different holding potentials and obtained in different experimental conditions (control, glycine, and glycine + CX717). Conversely, in the remaining 5/9 cells whose NMDA responses amplitude were not diminished by glycine, the addition of CX717 did not produce any change in NMDA responses (see NMDA responses plot Fig. 5.9C). Figure 5.9C illustrates the NMDA-elicited depolarization amplitudes obtained at different holding potential in a cell that did not respond to CX717. In one experiment, voltage-clamp of an inspiratory preBötC neuron was used to examine NMDA-evoked currents. At hyperpolarized holding potentials and in presence of glycine (40 μ M), CX717 (100 μ M) significantly increased NMDA-induced currents. Note that those experiments were done in the absence of TTX, no change in $[Mg^{2+}]_e$ was made and 2 out of 9 cells tested were inspiratory neurons (the remainder of the cells were non-respiratory neurons). Further, it is interesting to note that, while CX717 does not change inspiratory activity in baseline conditions, analysis of XII nerve activity exposed to glycine and CX717 showed a significant increase in inspiratory frequency by CX717 to 2.0 ± 0.5 compared to glycine values ($n = 6$; $p = 0.02 < 0.05$; one-way ANOVA with Tukey's post test on raw data; see relative data graph in Fig. 5.8A).

Conventional NMDA receptors require the release of Mg^{2+} (via depolarization) to function. To date, the only NMDA receptor subtype identified as being independent of the holding potential and insensitive to Mg^{2+} block is the NMDA receptor subunit NR3 (Sasaki et al., 2002). This NMDA subunit forms a functional receptor when dimerized with the subunit NR1 (Chatterton et al., 2002). The NR1/NR3 functional receptor binds glycine and/or D-serine and elicits a depolarizing current at resting membrane potentials (Piña-Crespo et al., 2010). Thus local puffs of glycine (500 μ M; 400 ms) and D-serine (500 μ M; 300 to 1000 ms) were applied directly on respiratory preBötC neurons. No responses were obtained with D-serine applications and only strychnine (20 μ M)-sensitive

hyperpolarizing responses were observed with glycine. This confirmed the presence of strychnine-sensitive glycine receptors on preBötC neurons and more importantly indicated that, if NR1/NR3 is indeed present, it must not be expressed under a homo-tetramerized form but rather be assembled or co-expressed with NR2 subunit(s) which prevents it from responding to glycine (Chatterton et al., 2002). This is consistent with a previous study that showed a very heterogeneous composition of NMDA subunit mRNA present in respiratory preBötC neurons (Paarmann et al., 2005).

NR3A is expressed in the preBötC.

Single-cell reverse transcription polymerase chain reaction study has demonstrated the expression of NR3A subunit gene in respiratory neurons of the preBötC (Paarman et al., 2005). NR3A subunit protein expressed in the ventrolateral medulla was examined. Diaminobenzidine staining of NR3A showed a high density of NR3A-expressing cells in the preBötC region (n = 4), as illustrated in Figure 5.10. More specifically, intense NR3A expression within the preBötC appears on somata and neurites of fusiform cells. NR3A⁺ neurons are small and their neurites are orientated in the dorsoventral axis similarly to NK1R labeling pattern (Pagliardini et al., 2003). NR3A staining was also intense in the inferior olive. Triple labeling of transverse medulla sections with acetylcholine esterase (ChAT), neurokinin-1 receptor (NK1R; a well-established marker of the preBötC region) and NR3A confirmed that NR3A is expressed in the preBötC region (n = 3). As seen in Figure 5.11, NR3A⁺ cells highly colocalize with NK1R⁺ cells within the preBötC. NR3A was also expressed in other medullary structures. For example NR3A is present in XII motoneurons and premotoneurons and more rostrally, NR3A⁺ staining could be observed in the compact formation of the nucleus ambiguus as well as in the facial nucleus. NR3A staining of the CA1 region of the hippocampus served as a positive control (Ciabarra et al., 1995; see Figs. 5.10C and D). These data support the hypothesis that the subpopulation of neurons expressing NR3A in the preBötC represents a functional core of

distinctive neurons important for the modulation of inspiratory drive in the developing and young rodent.

CX717 effects on recombinant glycinergic NMDA receptor currents.

The expression of recombinant protein(s) in primary mammalian cells is a common technique used to evaluate the effect of a particular modulator on specific receptor subtypes. Since preBötC neurons possess a very heterogenous population of NMDA receptors subtypes, HEK293 cells were used to specifically express the glycinergic NMDA excitatory receptors that have proven functionality when both NMDA receptor 1 (NR1) and NMDA receptors 3 (NR3) subtypes are co-expressed (Smothers and Woodward, 2007; 2009). We performed immunocytochemical studies of HEK293 cells transfected with each NR1/NR3A/NR3B subunit cDNA to verify the expression of each protein (NR1, NR3A and NR3B). Confocal images obtained from transfected cells expressing NR1 and NR3A are shown in figure 5.12. Electrophysiological study assessing the functionality of NR1/NR3A/NR3B receptors via whole-cell voltage-clamp recordings of successfully transfected HEK293 cells showed repeated inward currents in response to glycine puffs (300 to 500 μ M; 100 to 300 ms duration) of variable amplitude but no response to glutamate puffs (50 μ M to 100 μ M; 100 ms duration; $V_m = -58$ mV; $n = 31$). While local application of CX717 (1 mM; 10 to 60 s duration) prior to or during glycine puffs did not change glycine-induced currents, data from one transfected cell showed a net decrease in the duration of the glycine-induced currents during bath application of CX717 (100 μ M; $n = 1$). However this effect seemed to be mainly imparted by a large outward current elicited by glycine puffs. Because those results could not be observed using a CsCl base internal solution, the outward conductance might be carried by potassium ions. Further experiments using bath application of CX717 need to be conducted in order to i) repeat and evaluate CX717 effect on glycine-evoked current kinetics using K-Gluconate base intracellular solution ii) determine the physiological conditions required for the effect to take place, iii) ensure that the effect is directly due to CX717 and not due to CX717 diluent (DMSO).

5.3.5 IN VITRO ANALYSES OF THE ALLEVIATION OF OPIOID-INDUCED RESPIRATORY DEPRESSION BY OTHER LOW-IMPACT AMPAKINES

Comparison between CX1942 and CX1763.

Other low-impact ampakines *in vitro*, including CX1763, were examined (see Fig. 5.13). CX1763 is more potent than CX717 since it counters respiratory depression *in vitro* with at least 2 fold less concentration (25 to 50 μM instead of 50 to 100 μM for CX717). The low-impact ampakine CX1942, which is the pro-drug of the ampakine CX1763, was also tested. CX1942 has been designed to have increased water solubility for clinical application purposes. The first step was to determine whether or not CX1942 could counter respiratory depression after it has crossed the blood brain barrier. Spontaneous rhythmic inspiratory activity from XII nerves was recorded from medullary slice preparations and the effects of CX1942 in counteracting DAMGO-induced respiratory depression examined. Figure 5.14A illustrates one experiment where XII motor output frequency was increased by bath application of CX1942 at 25 μM , and further increased at 50 μM following DAMGO-induced rhythmic depression. Population analysis showed that XII burst frequency was significantly increased from 0.28 ± 0.04 of control in DAMGO to 0.64 ± 0.06 of control in DAMGO + CX1942 (50 μM), which stays however significantly lower than control. To compare CX1942 with its active form CX1763, average relative values of XII burst frequency were plotted against time (Fig. 5.15). The slope of potentiation induced by CX1763 was higher than the one induced by CX1942. Overall the inspiratory rhythm enhancement induced by CX1942 was delayed compared to the one induced by CX1763. Because of this delay, respiratory depression induced by opioid was more pronounced and lasted longer when using CX1942.

Modulation of *in vitro* inspiratory rhythmic activity by the ampakine CX1739.

CX1739 is the most recent low-impact ampakine to be tested in clinical trials. As illustrated in Figure 5.16, the population data showed a significant

increase in XII discharge instant frequency by CX1739 (Fig. 5.16B). Whole-cell voltage-clamp recordings of preBötC neurons were performed in conjunction with local application of AMPA to evaluate the modulation of CX1739. As seen in group data histogram of Figure 5.16C ($n = 5$), CX1739 significantly increased the area of AMPA-mediated currents to 1.185 ± 0.04 of control values (paired t test on raw values; $p = 0.0054 < 0.01$). The decay time of AMPA-mediated currents was also increased to 1.185 ± 0.25 of control values although statistical significance was not reached ($p = 0.24 > 0.05$). None of the other parameters of AMPA-mediated currents showed any significant difference compared to control mean values. Further recordings and analysis of the CX1739 potentiation of respiratory neuron activity and preBötC synaptic transmission are needed to confirm those data. Alternatively, it would be interesting to know if CX1739 can also affect other type of glutamatergic currents, such as kainate or NMDA receptor conductance.

5.4 DISCUSSION

The main finding of the present study is the potential for an unexpected action of the low ampakine CX717 on NMDA conductance of preBötC neurons. On the basis of the electrophysiological results, it is proposed that the CX717 potentiation of NMDA conductance may be the underlying mechanism by which it alleviates opioid-induced respiratory depression.

5.4.1 LOW-IMPACT AMPAKINES AND AMPA RECEPTORS

In contrast to the initial expectations, the data suggest that CX717 has little to no effect on AMPA receptor conductance in respiratory preBötC neurons, at least under whole-cell recording conditions. Those results are in contrast to the results obtained by Lorier et al., 2010 from XII motoneurons (MNs). That study examined CX717 reversal of opioid-induced XII MNs activity depression. CX717 was shown to have a significant effect on AMPA-mediated current area and duration. This disparity of results might be explained by the fact that glutamate receptor subunit expression may be different between XII MNs and preBötC neurons (Ireland et al., 2008). It is possible that CX717 differentially affects AMPA receptors subunits and may specifically target AMPA subunits that are expressed in XII MNs but absent in preBötC neurons. The second possible explanation is that, as it has been proposed before (Morgado-Valle and Feldman, 2007), the ratio of AMPA/NMDA receptors might be higher in XII MNs than in the preBötC. If this is the case, the macroscopic whole-cell modulation of AMPA receptors kinetics by CX717 might be more prominent and thus measurable in XII MNs than in preBötC neurons. Although CX717 has been employed in numerous models as a potential therapeutic tool (Porrino et al., 2005; Wesenstein et al., 2007; Ren et al., 2009; Boyle et al., 2011; Zheng et al., 2011), it should be noted that there have been very few efforts to consolidate knowledge on its putative functional interaction and modulation of AMPA receptor subunit kinetics. Recombinant expression of AMPA receptor subunits in appropriate models and

evaluation of the effect of CX717 on different AMPA subtype conductance are clearly lacking to fully address and understand this issue.

Previous work also examined the mechanisms of CX717 potentiation of synaptic transmission in other brain regions and CX717 effect was analyzed using calcium wave measurements in rat hippocampal slices (Hampson et al., 2009). Interestingly, NMDA-mediated calcium release was found to be significantly increased by CX717. The authors concluded that there was an indirect effect from AMPA receptor modulation to NMDA receptor regulation (Hampson et al., 2009). Because NR3 subunits are also expressed in the rat hippocampus (Ciabarra et al., 1995), an alternative interpretation of their results could be considered, in accordance with a resulting significant increase of NMDA conductance by CX717.

A noteworthy observation is that NR3A and AMPA receptors do share some genetic and physiological similarities. NR3A shares approximately 23% of sequence homology with AMPA receptor genes, while sharing 27% identity with NMDA receptor genes (Ciabarra et al., 1995). Also, both AMPA and NR3A conductance have very fast kinetics and have intracellular binding partners that participate to their trafficking to the cellular membrane (Dingledine et al., 1999; Perez-Otaño et al., 2006). Further, 6-cyano-7-nitroquinoxaline-2, 3-dione (CNQX) is a pharmacological blocker common to the two receptor types (Honoré et al., 1988; Yao and Mayer, 2006; Piña-Crespo et al., 2010). All of these similarities lend the possibility of any given allosteric ligand (such as CX717) designed to bind one receptor type (e.g. AMPA receptor), to interact with the other (presumably NR3 subunit).

5.4.2 CX717 AND NMDA RECEPTOR CONDUCTANCE

Our study indicated that CX717 strongly potentiates NMDA-elicited responses in preBötC neurons, specifically at hyperpolarized membrane potentials. This increase is thought to reflect an enhancement of NMDA conductance due to an allosteric negative modulation of NR3 receptor subunit by

CX717. First, it must be realized that those experiments were not done in the presence of TTX; and secondly, there has not yet been a demonstration that CX717 indeed increases NMDA-mediated currents in respiratory preBötC neurons. Therefore further whole-cell recordings in voltage-clamp mode are needed in order to clarify the postsynaptic effect of CX717. Conventional NMDA receptors do not conduct current at hyperpolarized potentials because of their inherent ion channel block by Mg^{2+} . For those reasons, the NR3 NMDA receptor subunit is a strong candidate for the potential CX717 modulation target and glycinergic NMDA receptors may be key neurotransmitters capable of regulating inspiratory drive (most probably via intracellular calcium regulation). In addition, data from the immunohistochemical study showed that NR3A is strongly expressed in the preBötC region and confirmed the exact position of NR3A expression in the preBötC by showing its partial colocalization with NK1R labeling, which is consistent with RT-PCR measurements of NMDAR subunits in respiratory neurons of the preBötC that demonstrated that preBötC neurons contain the NR3A gene (Paarmann et al., 2005). Immunohistochemical studies to determine how NR3A expression relates with other important markers such as somatostatin, somatostatin receptor 2a and Dbx1 in the murine model (Gray et al., 2010) are currently being pursued.

The NR3A subunit is the most recently cloned NMDA subunit (Sucher et al., 1995; Ciabarra et al., 1995) and its physiological significance has only started to emerge (Piña-Crespo et al., 2010). Pharmacological studies have shown that NR1/NR3A functional receptors are sensitive to glycine, but not NMDA (Chatterton et al., 2002). More striking is the dominant-negative influence of NR3A on NMDA receptors: co-expression of NR3A in *Xenopus* oocytes expressing NR1/NR2 functional NMDA receptors leads to a decrease in NMDA-induced conductance (Das et al., 1998). The depolarizing responses to NMDA obtained from current-clamp recordings of preBötC neurons could be decreased by glycine (presumably targeting NR1/NR3 subunits) and subsequently be restored closer to control values by CX717 at membrane potentials between -50 and -65 mV. However, it was noticed that at more hyperpolarized membrane

potentials the amplitude of the depolarizing NMDA responses went beyond control values with CX717, which might indicate a very complex interaction between NR3 and other NMDA receptor subunit(s) at hyperpolarized potentials.

Because of the heterogeneity of NMDA subunits expression within preBötC neurons (Paarman et al., 2005; Liu and Wong-Riley., 2010), it was difficult to directly test CX717 on glycinergic-mediated excitatory NMDA receptors. Thus, mammalian model of human embryonic kidney cells (HEK293) that functionally express recombinant NR1/NR3 proteins was used. cDNA plasmids of NR1, NR3A and NR3B were used that yield sufficient measurable currents induced by glycine (Smothers and Woodward, 2007). HEK293 cells were successfully transfected with NR1/NR3 subunits and repeatable glycinergic currents obtained. However the modulation of the currents by CX717 was not successfully characterized. A first potential problem was with the electrophysiological set up that is optimized for single-cell recordings in brain slice preparations but not ideal for the recordings of dissociated cells. More importantly, the fast exchange drug application set-up usually used for those types of experiments might be determinant in obtaining fast desensitizing glycinergic currents (Chatterton et al., 2002; Smothers and Woodward, 2007; Piña-Crespo et al., 2010). Second, the NR1 cDNA used was the subunit NR1-1a, which is the NR1 subunit that yields less current when expressed with NR3A (Smothers and Woodward, 2009). Therefore it might be beneficial to use the subunit NR1-4 instead of NR1-1a in order to obtain larger glycine-induced currents which may help discriminate the potential effect of CX717. Two additional effects of CX717 were noticed during the voltage-clamp experiments of HEK293 transfected cells. CX717 bath application often induced a slow and sustained outward current. Moreover, glycine puffs induced substantial outward currents just after the inward current induced by NR1/NR3 activation. Although classical glycinergic receptors have been found to be endogenously expressed in HEK293 cells, it seems unlikely that CX717 would be acting through those receptors. Rather, the observed outward currents might be the results of an off-target human-ether-a-go-go (hERG) channel activity, quite similar to off-targets side effects already reported in

allosteric modulators of NMDA receptors (Kawai et al., 2007; Mosley et al., 2009).

5.4.3 A STATE-DEPENDENT POTENTIATION OF INSPIRATORY RHYTHM GENERATION BY CX717

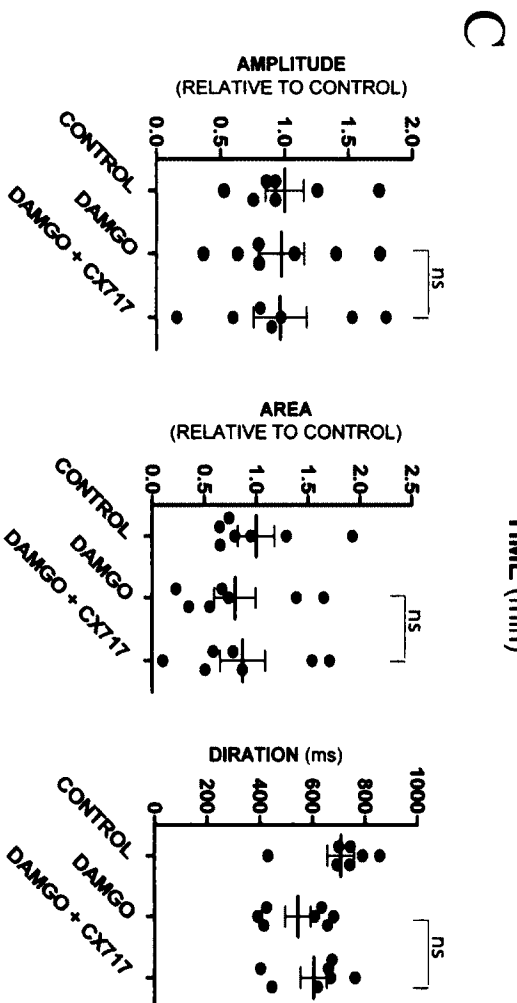
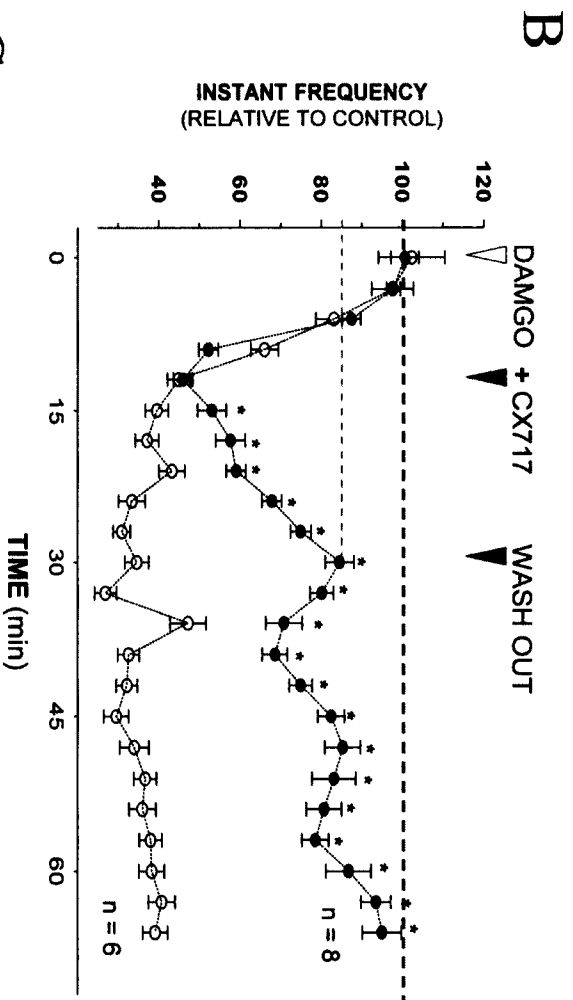
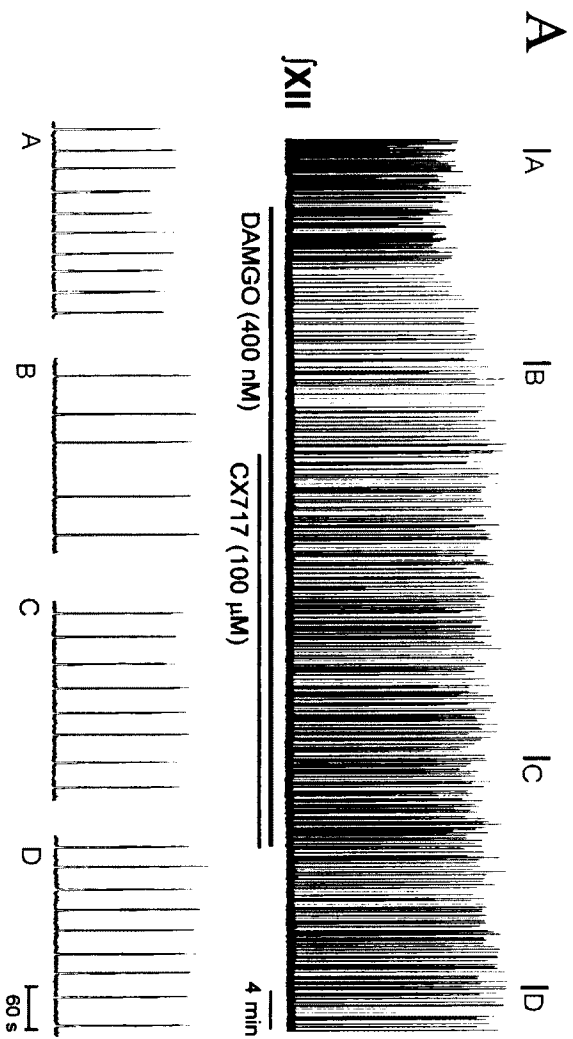
It was demonstrated that CX717 reversed opioid-induced respiratory depression *in vitro* by means of the acute medullary slice preparation. Local applications of CX717 into the preBötC demonstrated that CX717 is acting in the preBötC region to exert its potentiation effect on inspiratory frequency. Interestingly, CX717 does not change baseline inspiratory activity. Rather, its action seems to be specifically prominent when inspiratory frequency is strongly suppressed by opioids conditions. Single-cell analysis of CX717 modulation showed that CX717 does not affect inspiratory drive on rhythmogenic inspiratory cells in baseline conditions. In contrast, inspiratory drive currents were significantly increased by CX717 after DAMGO exposure. Moreover CX717 could also in some cases increase weak endogenous inspiratory drive induced by low extracellular potassium concentration. Together those data indicate that CX717 is particularly sensitive to low level of activity which strongly suggests a type of “state-dependent potentiation” for CX717.

5.4.4 BEHIND THE SCENES: THE PRESENCE OR THE INDUCTION OF A GLYCINERGIC SIGNAL?

Another point that deserves further elaboration is the activation of NR3A itself. According to the data, CX717 counteracts the action of glycine by inducing an increase in NMDA receptors conductance. If CX717 negatively modulates NR3A it implies that NR3A must already be active for CX717 potentiation to occur. How is opioid promoting NR1/NR3A delivery on neuronal membrane? NR1/NR3A functional receptors are known to be very fast desensitizing receptors and to be internalized at rest (Perez-Otaño et al., 2006). One of the interesting features of this receptor is that its endocytosis has been shown to be activity-

dependent and it undergoes less endocytosis when synaptic activity is at its lowest (Perez-Otaño et al., 2006). Thus, DAMGO-induced respiratory rhythm depression may condition NR3A to be more active. This also supports the data because CX717 did not change inspiratory activity at rest, when the putative candidate for CX717 target (NR3A receptor) would mostly be internalized.

Further, the electrophysiological data from examining NMDA-elicited responses on preBötC neurons showed that CX717 potentiation depended on the presence of glycine. In fact, the more pronounced inhibition of NMDA-elicited responses obtained by bath-applied glycine, the higher potentiation induced by CX717. Thus, glycine seems to be a very important component of CX717 activation, suggesting that in the reversal of DAMGO-induced depression by CX717, endogenous glycine must play a critical role in allowing activation of glycinergic NMDA receptors. Because glycinergic neurons do not colocalize with NK1R positive cells in the preBötC (Morgado-Valle et al., 2010) but NK1R and μ -opioid receptors do (data in Chapter 1 of this thesis; Montandon et al., 2010) there are reasons to propose that DAMGO does not affect glycine release (Montandon et al., 2011), but this is clearly a matter that deserves further investigation.



Previous Page

Figure 5.1 Bath application of CX717 alleviates DAMGO-induced depression of inspiratory frequency in *in vitro* medullary slice preparation.

A. Integrated trace of recording from XII nerve rootlets during bath application of CX717 and DAMGO. **B.** Group data graph shows relative values of XII burst frequency against time. DAMGO (400 nM) was given to the bath at 0 minutes. In one data group, DAMGO is left in the bath for 90 minutes ($n = 6$). Open circles show average instant XII nerve frequency with DAMGO treatment only. The other data group shows frequency responses to addition of CX717 (100 μ M) to the bath from 12 minutes and to wash out with bathing solution from 30 minutes ($n = 8$; filled circles). * = significant difference between the two data groups (DAMGO versus DAMGO + CX717), unpaired t test with $p < 0.05$. The alleviation of DAMGO depression by CX717 is associated with a significant increase of inspiratory drive frequency that can reach up 84.68 ± 3.52 percent (relative mean \pm s.e.m.) of control (grey dotted line). **C.** Data group graphs showing amplitude, area and duration of XII bursts do not change with the addition of CX717 (100 μ M) to the bath (one-way ANOVA; $p > 0.05$; $n = 7$). Each filled circle represents the mean value obtained in each preparation. The overall mean for each data group is presented in mean \pm s.e.m.

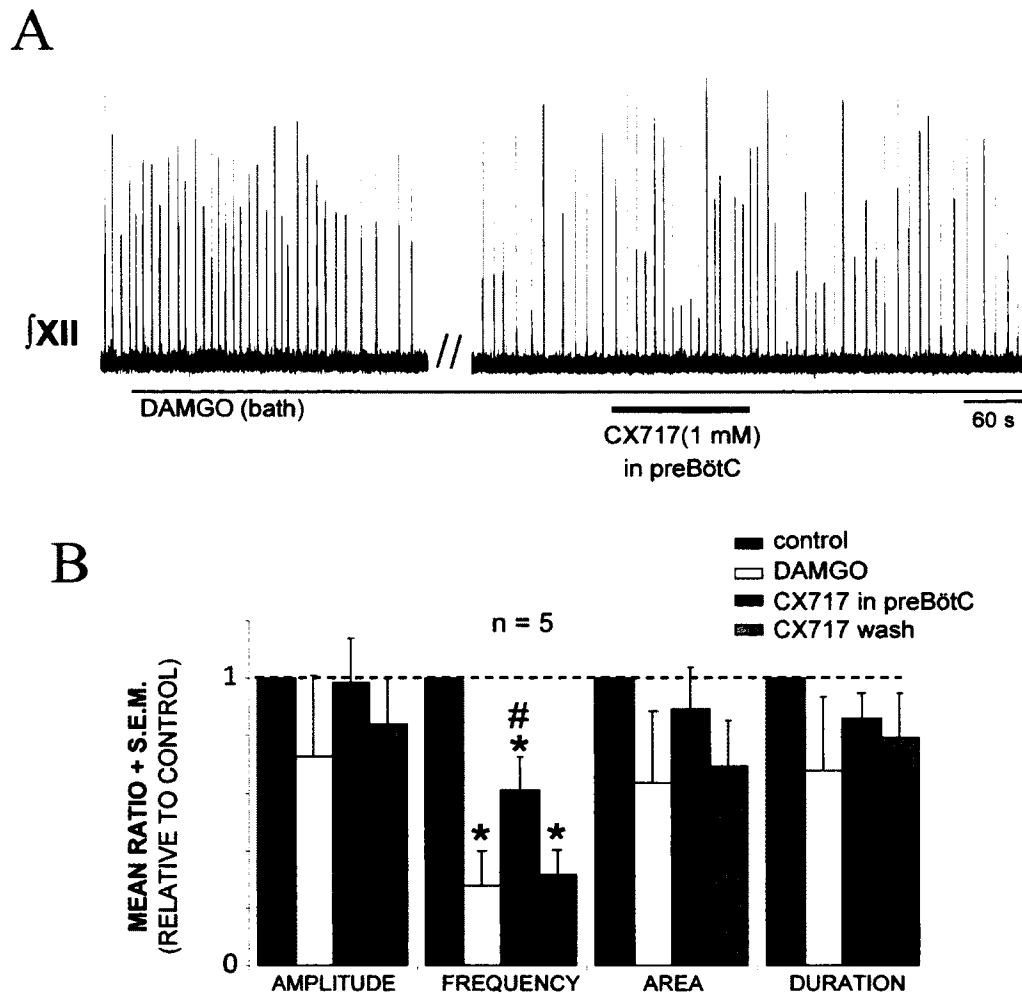
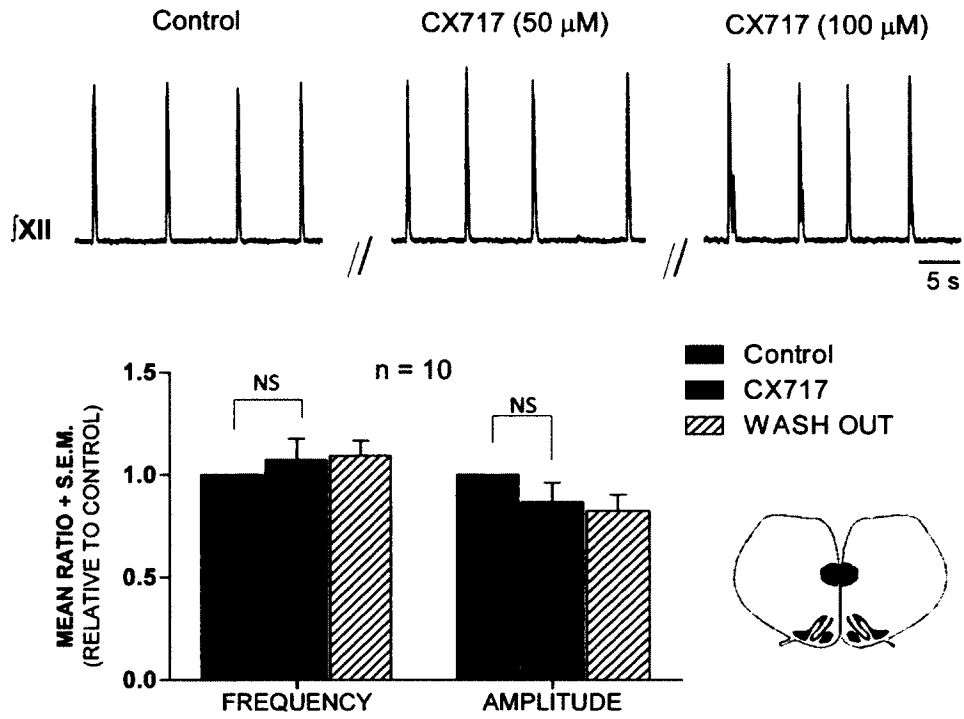


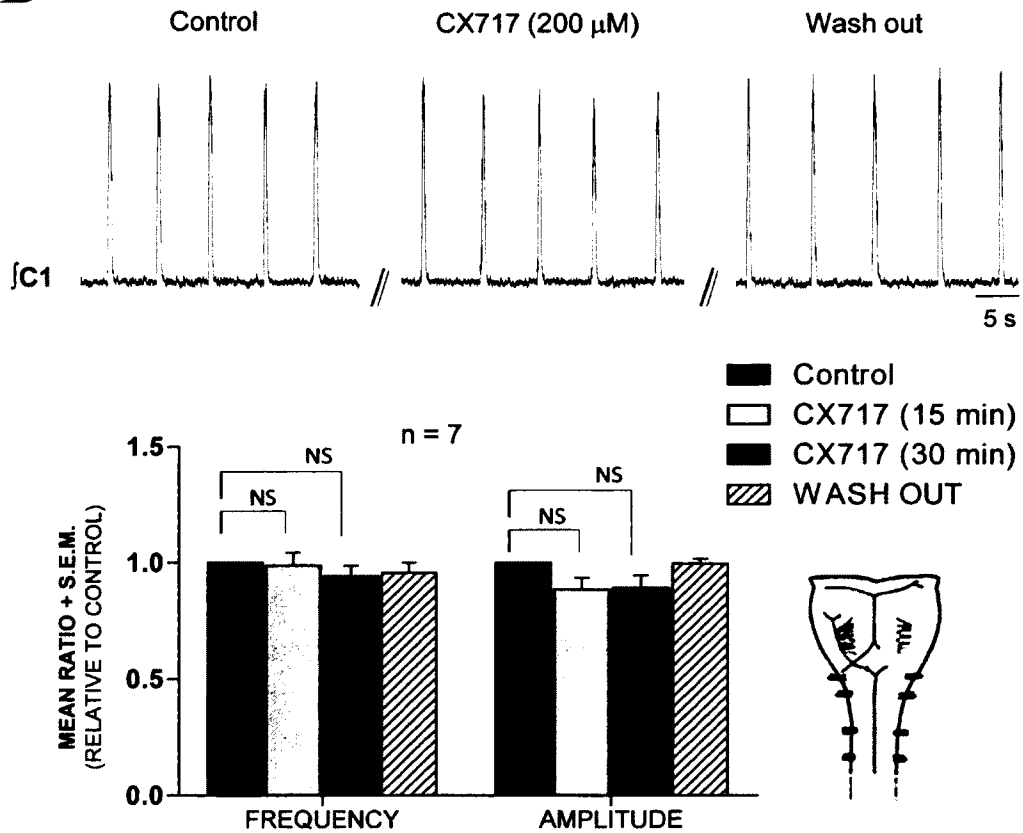
Figure 5.2 Local application of CX717 into preBötC counters respiratory drive inhibition induced by DAMGO.

A. Integrated trace of hypoglossal motor output recorded during DAMGO bath application and subsequent local application of the ampakine CX717 (1 mM) into the preBötC. **B** Group data showing the effect of DAMGO and CX717 on different characteristics of respiratory motor output. CX717 locally applied to the preBötC significantly increases XII burst frequency (* = significantly different from control ; # = significantly different from DAMGO; $p < 0.05$, $n = 5$).

A



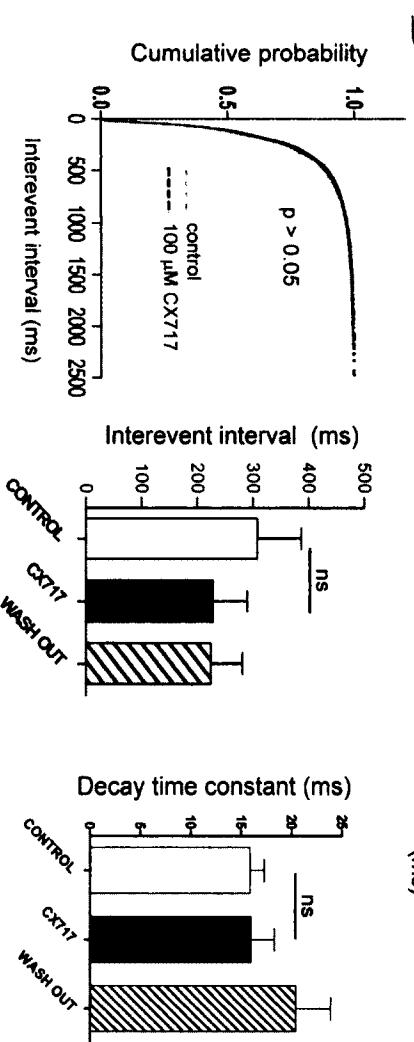
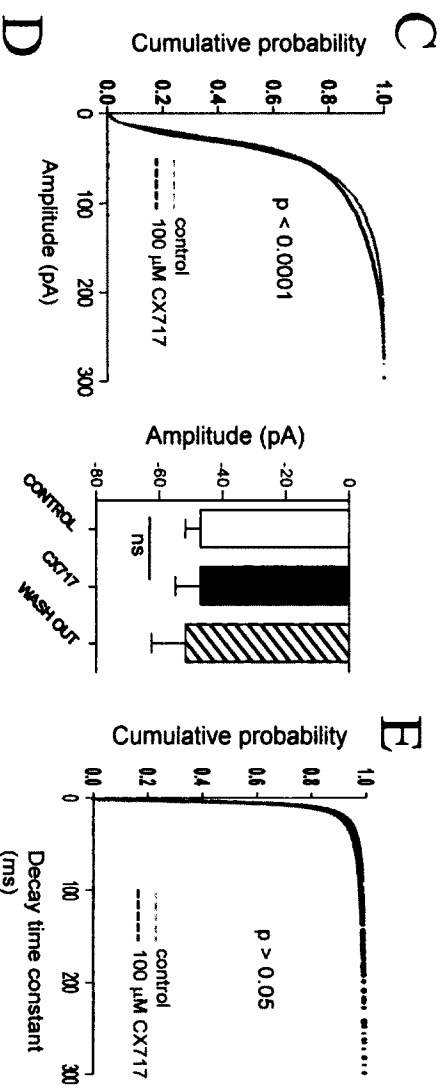
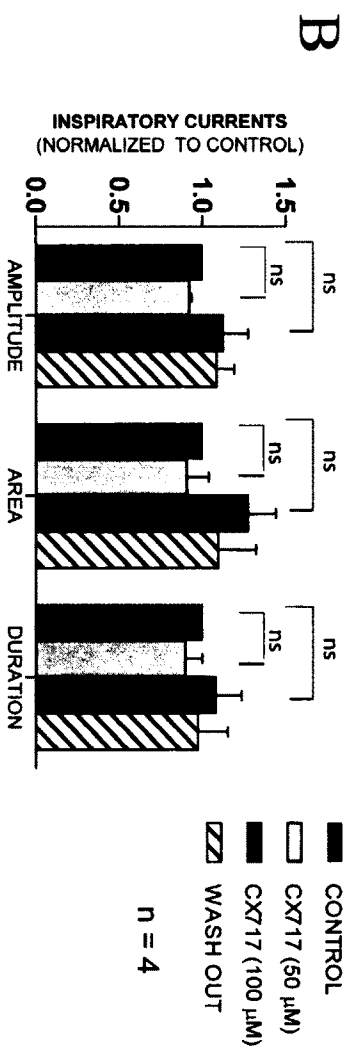
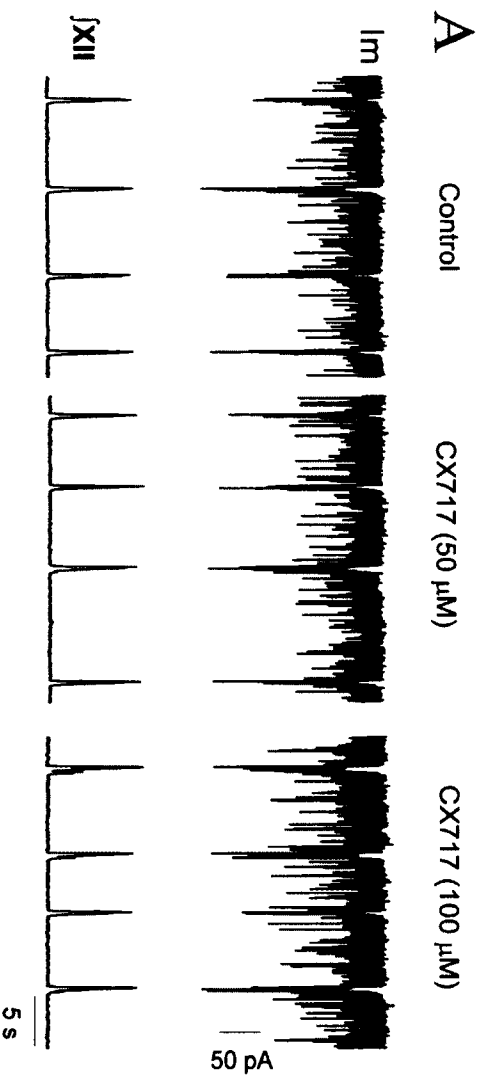
B



Previous Page

Figure 5.3 Bath application of CX717 does not change baseline inspiratory activity in *in vitro* neonatal rat models.

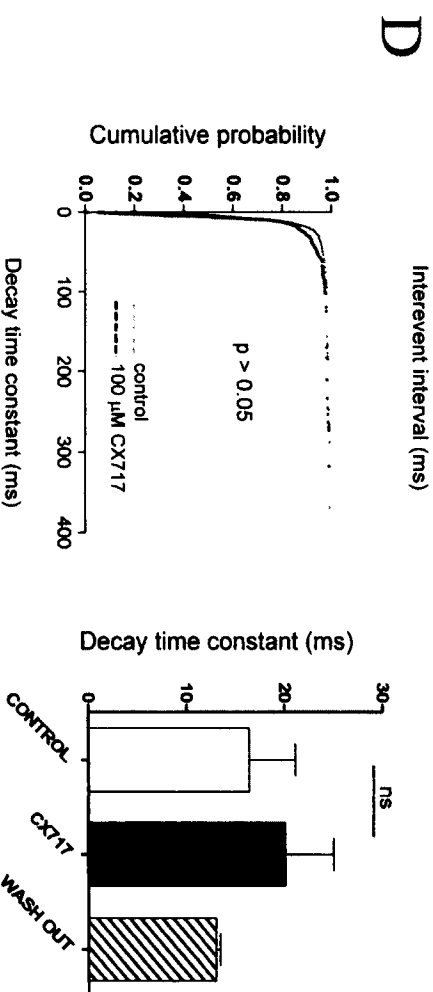
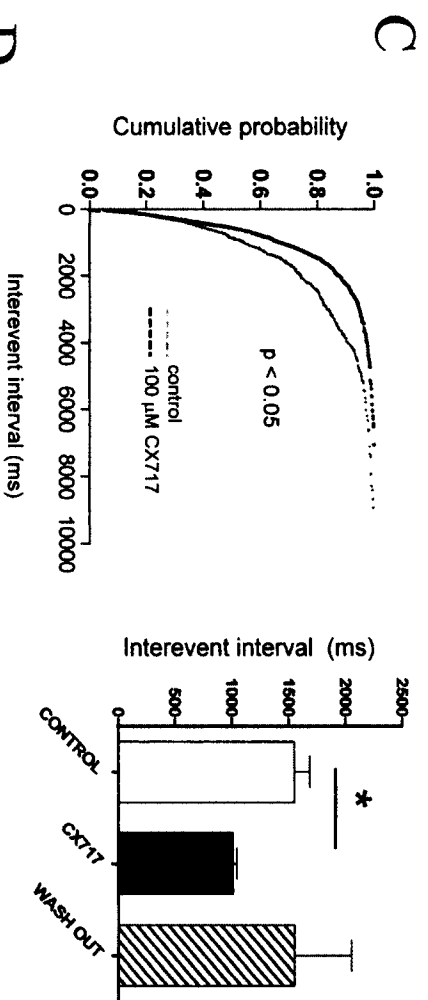
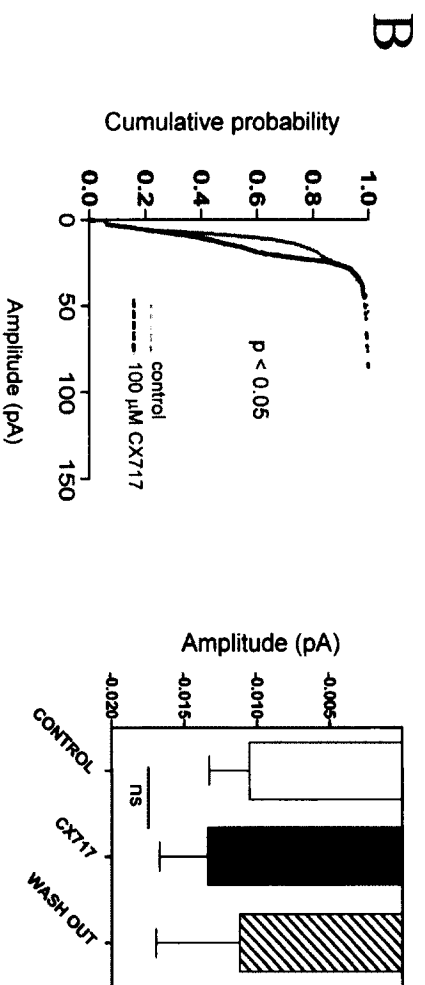
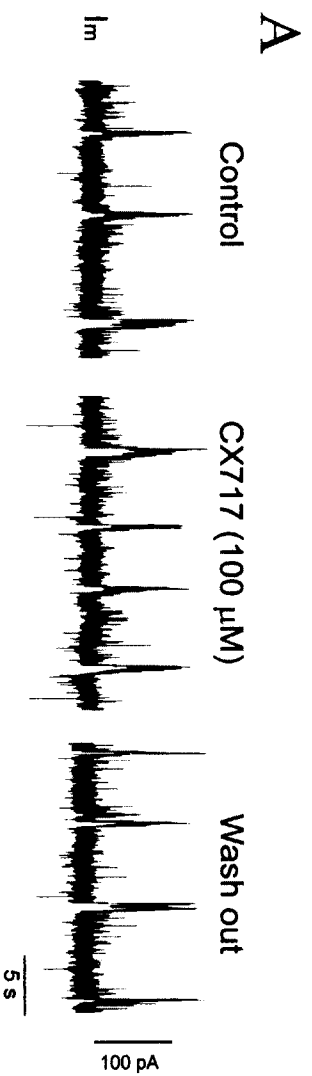
A. Effect of CX717 bath application in medullary slice preparations. Integrated trace of a XII nerve recording showing typical responses to increasing bath concentrations of CX717. Group data obtained from medullary slice preparations ($n = 10$) showing that CX717 does not have any significant effect on frequency or amplitude of XII nerve activity (one-way ANOVA; $p > 0.05$). **B.** Effect of CX717 bath applications in brainstem spinal cord preparations. Integrated C1 nerve recording representative of a typical response to high concentration of CX717 (200 μM) bath applied in brainstem spinal cord preparation. Group data obtained for brainstem spinal cord preparations ($n = 7$) showing that CX717 does not significantly affect frequency or amplitude of C1/4 activity (one-way ANOVA; $p > 0.05$).



Previous Page

Figure 5.4 CX717 alone does not change synaptic input current size nor decay kinetics on inspiratory preBötC neurons.

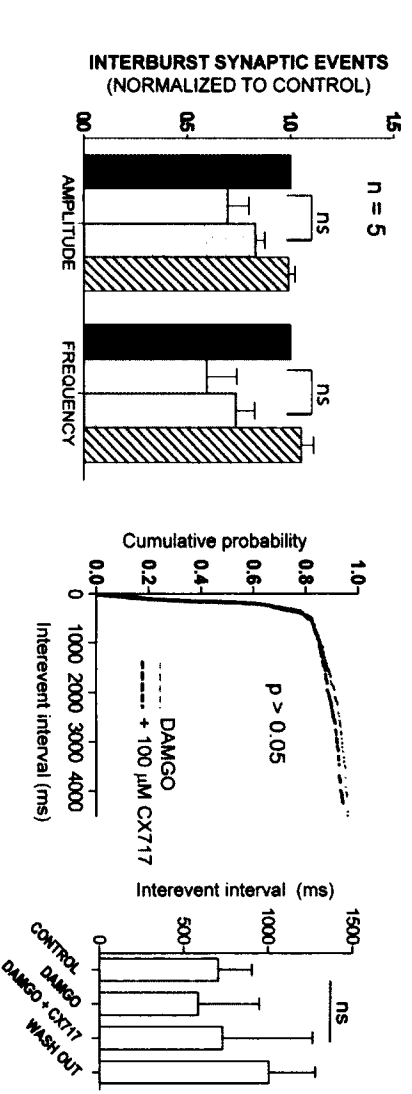
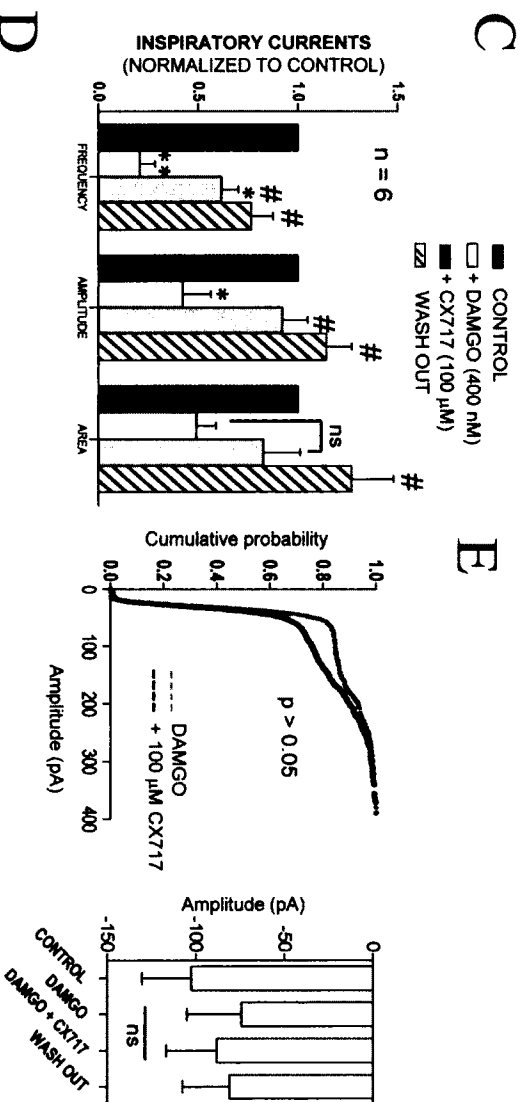
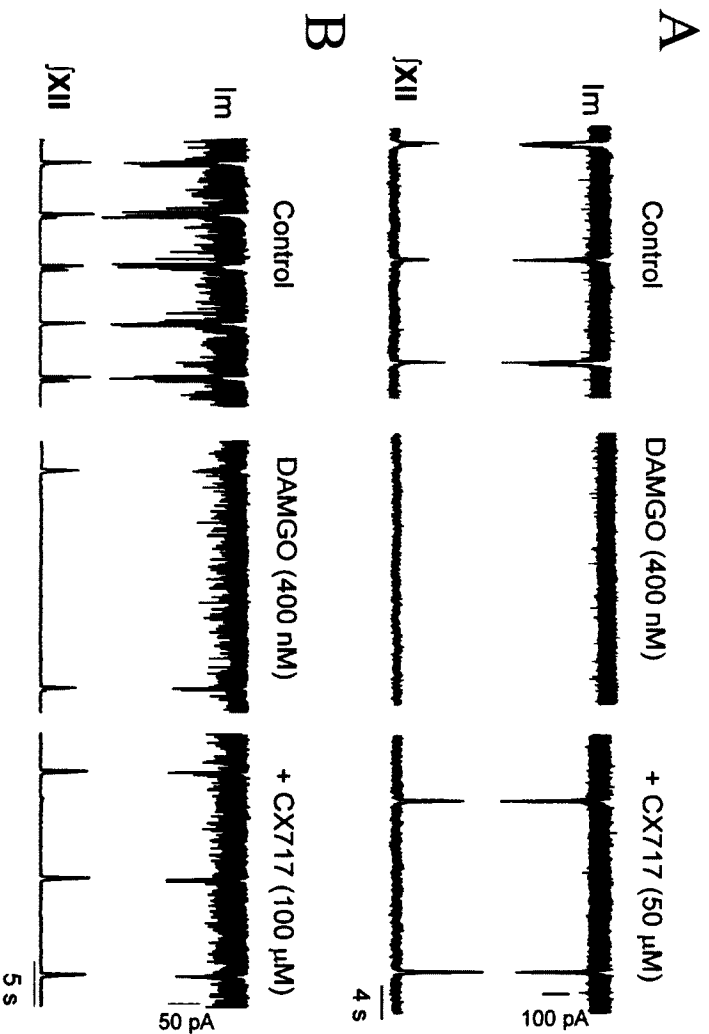
A. Effect of CX717 bath application in medullary slice preparation. The upper trace shows a voltage-clamp recording of an inspiratory neuron of the preBötC at resting membrane potential, upon bath application of increasing concentrations of CX717: CX717 does not affect inspiratory drive in control conditions; the lower trace represents the concomitant recording of the XII nerve output. **B.** Group data ($n = 4$) showing postsynaptic inspiratory drive current parameters in different experimental conditions. There was no significant difference between groups. Cumulative distribution plots of the sPSC amplitude (**C**) interevent interval (**D**) and decay time constant (**E**) recorded in inspiratory cells (Kolmogorov-Smirnov two sample test; significance at $p < 0.05$). Group data graph of spontaneous synaptic event amplitude and interevent interval means are shown on the right of the cumulative distribution, and shown below the cumulative distribution for the decay time constant. No significant difference between control and CX717 was found for any of the 3 parameters of sPSCs (Wilcoxon matched-pairs test; $p > 0.05$; * = $p < 0.05$).



Previous Page

Figure 5.5 CX717 alone can change excitatory synaptic input currents on expiratory preBötC neurons.

A. Effect of CX717 bath application on inward synaptic events. The trace shows a voltage-clamp recording of an expiratory neuron of the preBötC at resting membrane potential, upon bath application of CX717 (100 μ M). Note that no significant effect of CX717 was found on expiratory current frequency ($n = 6$), but a significant effect of CX717 on inward synaptic event (interburst sPSC) frequency was found in 3 out of 6 expiratory cells. Cumulative distribution plots of the spontaneous postsynaptic currents (sPSCs) amplitude (**B**) interevent interval (**C**) and decay time constant (**D**) were analyzed for the 3 responsive expiratory cells (Kolmogorov-Smirnov two sample test; significance at $p < 0.05$). Group data graph of sPSC mean amplitude, interevent interval and decay time constant are shown on the right of the cumulative distribution. No significant difference was found between control and CX717 for the decay time constant or the amplitude of sPSCs (**B**, **D**, Wilcoxon matched pairs test ($p > 0.05$)). However the interevent interval distributions were significantly different between control and CX717 (**C**; Kolmogorov-Smirnov two sample test showed significance ($p < 0.05$; left panel) and Wilcoxon matched pairs test ($p < 0.05$; right histogram)).



Previous Page

Figure 5.6 Ampakine CX717 augments inspiratory currents suppressed by DAMGO on preBötC neurons.

A. Voltage-clamp recording of an inspiratory neuron of the preBötC showing a complete suppression of inspiratory drive upon bath application of DAMGO followed by subsequent partial reversal of frequency and complete reversal of amplitude of inspiratory currents by bath application of CX717. **B.** Voltage-clamp recording of an inspiratory preBötC neuron at resting membrane potential showing a partial suppression of inspiratory drive upon bath application of DAMGO and subsequent increase of inspiratory rhythm by CX717. On both figures the lower trace represents the paired recording of XII nerve activity. **C.** Group data graph ($n = 7$) showing significant decrease in amplitude and area of inspiratory currents by DAMGO and their significant reversal induced by subsequent bath application of CX717. **D.** Summary bar graph of mean ratio for the spontaneous postsynaptic current (sPSCs) amplitude and instant frequency (* = significantly different from control; # = significantly different from DAMGO; $n = 5$; one-way ANOVA). **E.** Cumulative distribution plots of the sPSCs amplitude (upper) and interevent interval (lower) recorded in inspiratory cells, in presence of DAMGO, and subsequent application of CX717. Statistical analysis of sPSCs shows that CX717 do not significantly affect presynaptic activity in inspiratory preBötC neurons after DAMGO-induced respiratory depression.

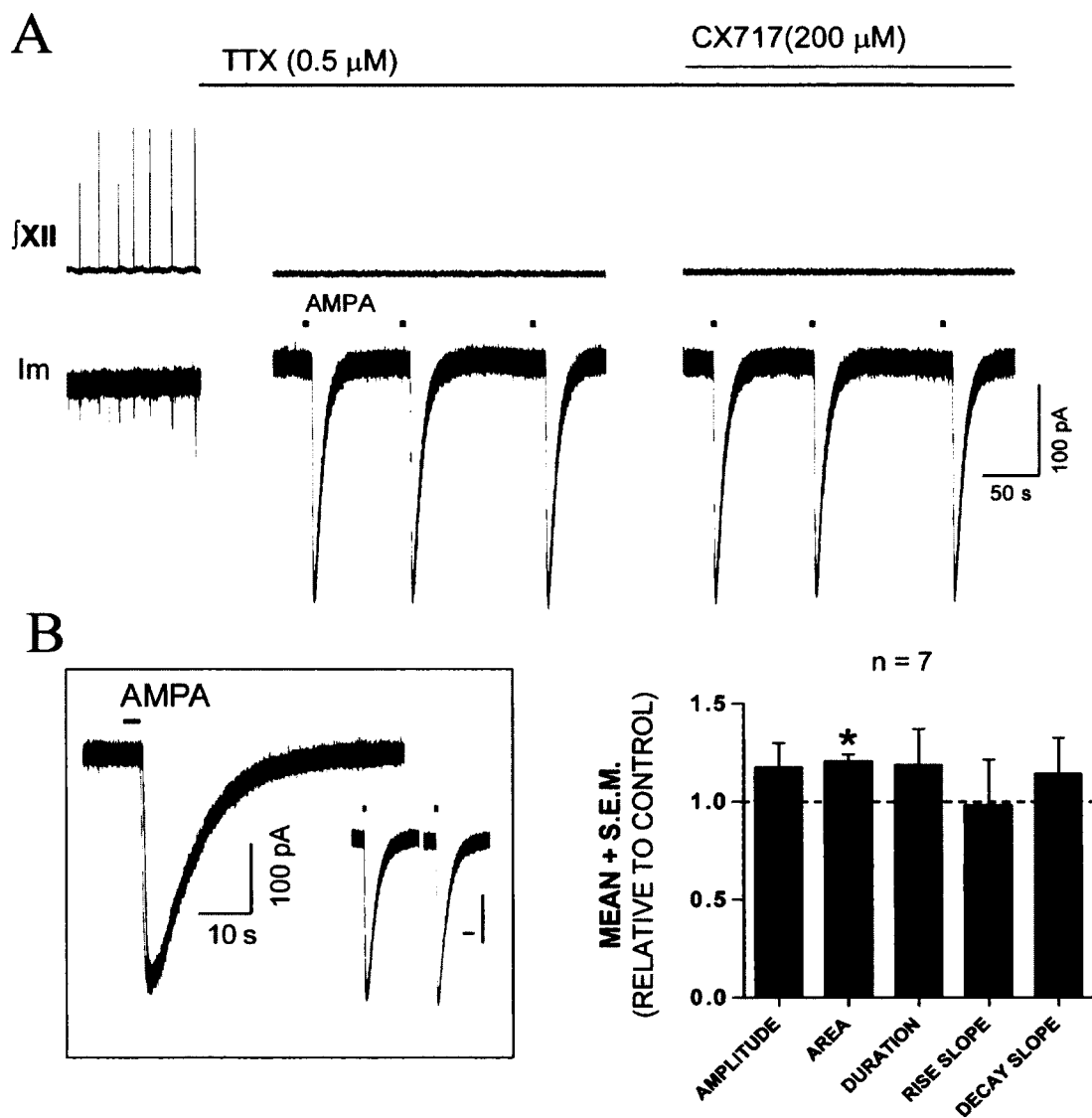


Figure 5.7 CX717 action on AMPA-mediated currents on respiratory preBötC neurons.

A. Whole-cell voltage-clamp recording of a respiratory neuron of the preBötC is shown in control conditions. Repeated AMPA-induced current responses are then shown in presence of TTX (0.5 μ M bath) and in presence of CX717 (200 μ M) in the bathing solution **B.** Superposition of a recorded trace of AMPA-induced current in presence of TTX (0.5 μ M bath; black) with a recorded trace of AMPA-induced current in presence of CX717 (100 μ M to 200 μ M) in the bathing solution (grey). Scale bars are 10 s and 100 pA for **B.** The histogram on the right shows group data (n = 7) of relative values for AMPA-mediated currents parameters. * = significantly different from control; $p < 0.01$; Student's *t* test.

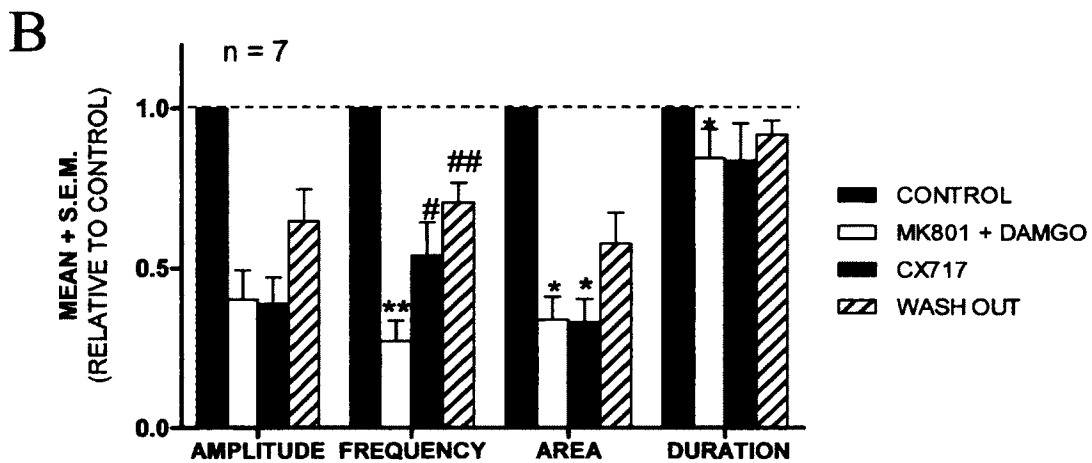
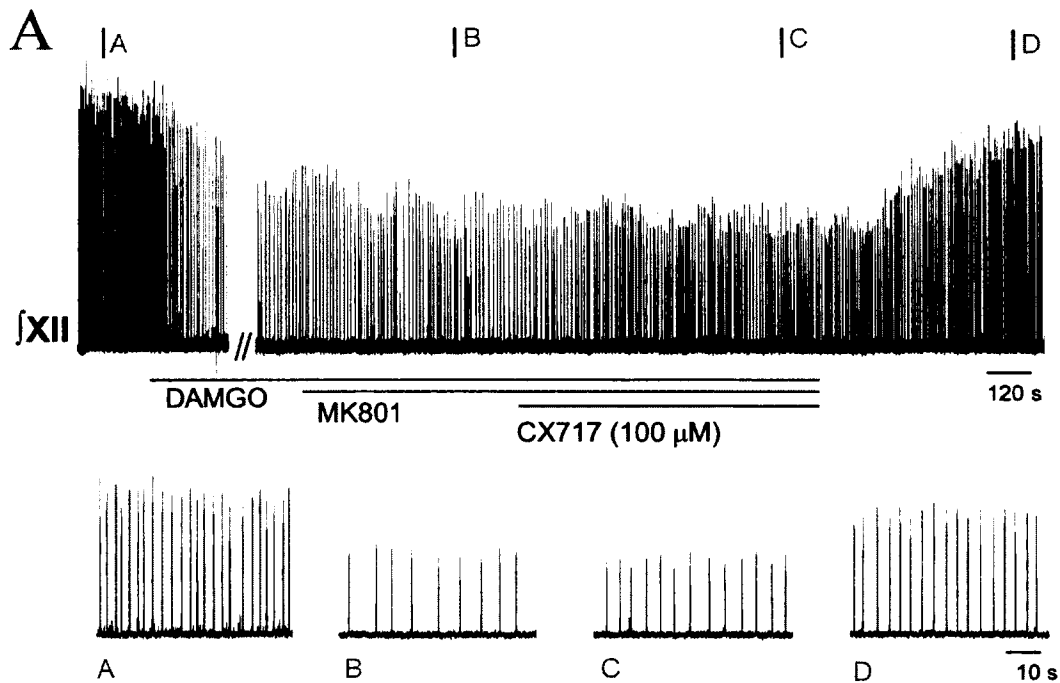


Figure 5.8 Effect of CX717 on respiratory activity after DAMGO-induced respiratory depression and in presence of the NMDA receptor blocker MK801.

A. Representative integrated recordings from XII nerve rootlets during bath application of CX717 following bath application of a cocktail of DAMGO (400 nM) and MK801 (50 μ M). **B.** Group data histogram ($n = 7$) showing that, in the presence of the NMDA receptors blocker MK801, CX717 does not significantly alleviate respiratory drive frequency decrease induced by DAMGO (one-way ANOVA on raw values; * = significantly different from control; * $p < 0.05$; ** $p < 0.01$, # $p < 0.05$; ## $p < 0.01$).

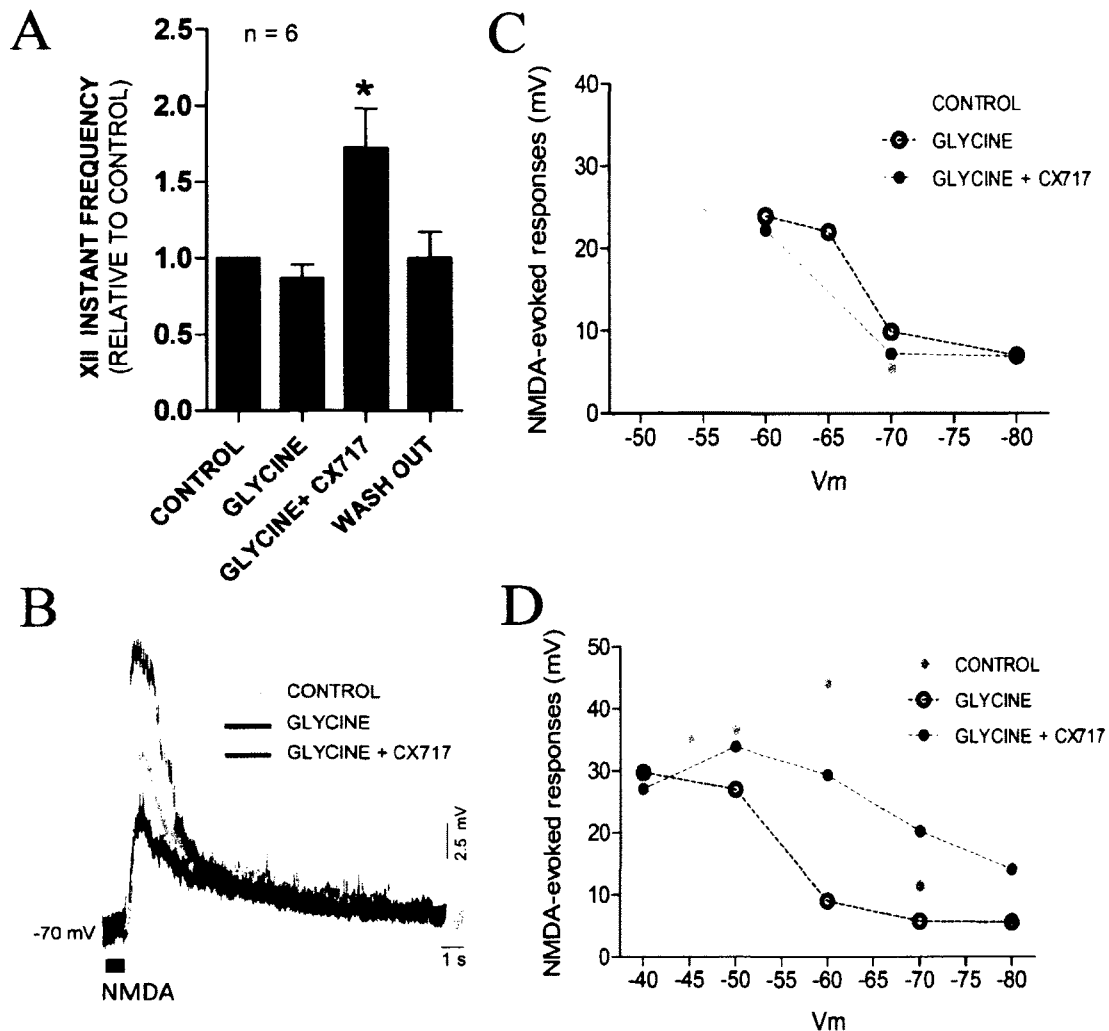


Figure 5.9 NMDA-mediated depolarizing responses are increased by CX717 following glycine exposure in some preBötC neurons.

A. Group data histogram showing mean ratios (relative to control) of XII nerve frequency obtained from 6 medullary slice preparations. In presence of glycine (20 μ M bath application) bath application of CX717 (100 μ M) significantly increases respiratory drive frequency. (* = significantly different from glycine; $p < 0.05$; one-way ANOVA). **B.** Whole-cell current-clamp recording of a preBötC neuron. The figure represents a superposition of depolarizing responses to a NMDA puff (500 μ M; 100 ms duration) obtained at -70 mV holding membrane potential in 3 different conditions: control condition (black trace), in the presence of glycine (20 μ M bath; grey trace); and in the presence of combined glycine (50 μ M bath) + CX717 (100 μ M bath) in red. **C, D.** NMDA-induced potential differences obtained from 2 different single-cell recordings are plotted against the holding potential for the 3 experimental conditions. There was a depolarizing shift in NMDA-evoked responses when CX717 was added to the bath following glycine bath application (C). This shift did not occur when NMDA responses were not significantly diminished by glycine (D).

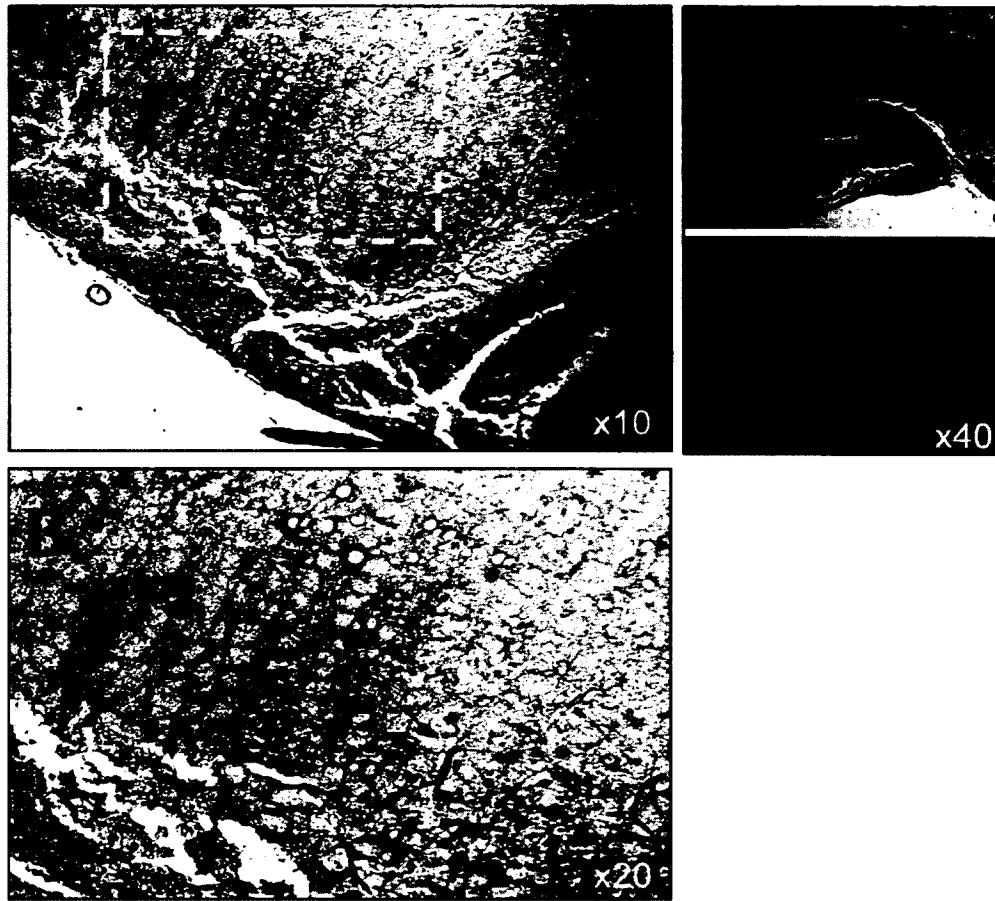
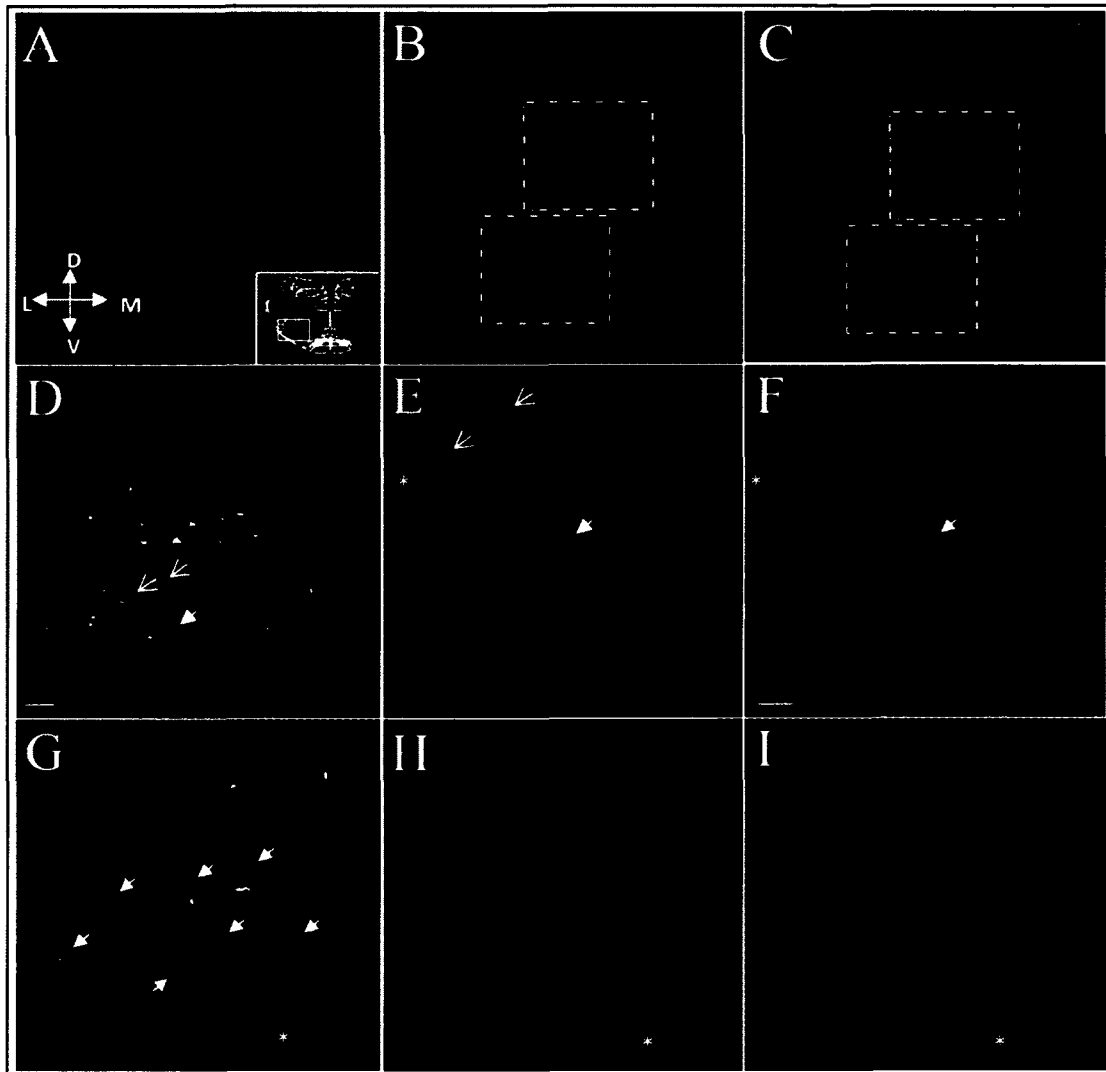


Figure 5.10 NR3A receptor is expressed in the ventrolateral medulla of newborn rats.

A, B. Figure A shows a bright field picture of a transverse section of the ventrolateral medulla. The white box highlights, ventral to the nucleus ambiguus, a cluster of cells and fibers that are strongly immunoreactive for NR3A in the preBötC region. NR3A⁺ cells are also present in the Inferior Olive. The dashed square in figure A demarcates the approximate preBötC region enlarged at higher magnification (X20) on figure B for a better distinction of the NR3A expression pattern. NR3A positive cells are small sized fusiform neurons. Notice the dendritic NR3A staining orientated in dorsoventral axis reminiscent of the NK1R labeling. **C, D.** Microphotographs of NR3A immunoreactivity within the hippocampal formation of P3 rat. Dense NR3A labeling can be seen in pyramidal layer of the cornu ammonis (CA1).



Previous Page

Figure 5.11 Colocalization of NR3A and NK1R is prominent in the preBötC of perinatal rat.

A-D. Immunoreactivity for ChAT (**A**), NK1R (**B, E, H**) and NR3A (**C, F, I**) is shown in 5 μm thin transverse sections of the medulla at the level of the semi-compact division of the NA. The preBötC contains a high density of neurons co-expressing NK1R and NR3A (filled arrowheads; **G**). **D** and **G** are overlay images. Note the absence of neuronal co-expression between ChAT and NR3A. **D-F.** High magnification X40 oil lens images show NK1R staining that does not colocalize with NR3A. **G-I.** NK1R labeling (neurites and cellular membrane; **H**), NR3A labeling (cell bodies; **I**) and the overlay ChAT/NK1R/NR3A. **G.** Double-labeled cells appear yellow. Scale bars are 50 μm for **A - D**; and 20 μm for **E - I**. * pinpoint blood vessels.

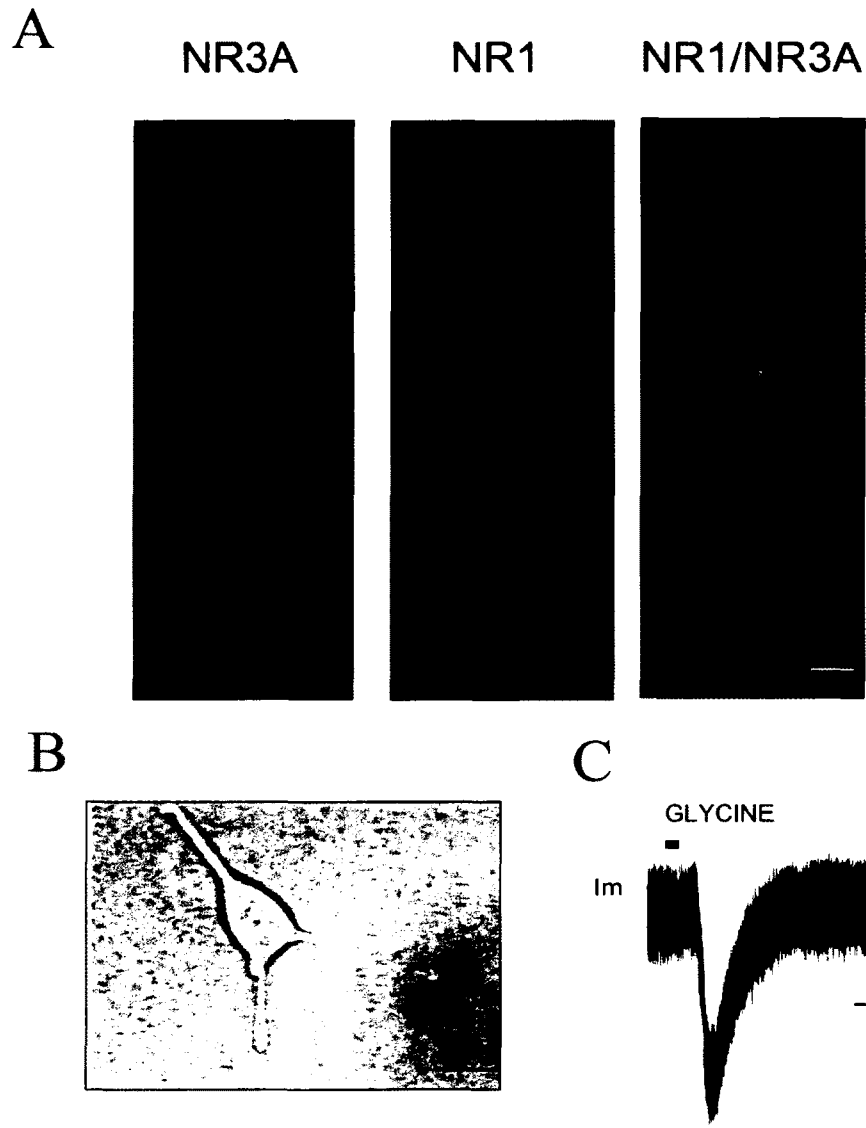


Figure 5.12 HEK293T cells transfected with NR1/NR3A display excitatory inward currents in response to glycine puff.

A. HEK293 cells were transfected with NR1 and NR3A cDNAs . Confocal images of successfully transfected cells that express both NR1 and NR3A were taken 18 hours after transfection. Scale = 10 μm . **B.** IR-DIC picture of a typical single healthy transfected HEK293 cell that was chosen for whole-cell recording (48 hours after transfection). Scale = 15 μm **C.** Whole-cell recording in voltage-clamp configuration on a successfully transfected HEK293 cell with NR1/NR3A plasmids can show an inward current under puff of glycine. Scale bar vertical = 20 pA; scale bar horizontal = 2 sec.

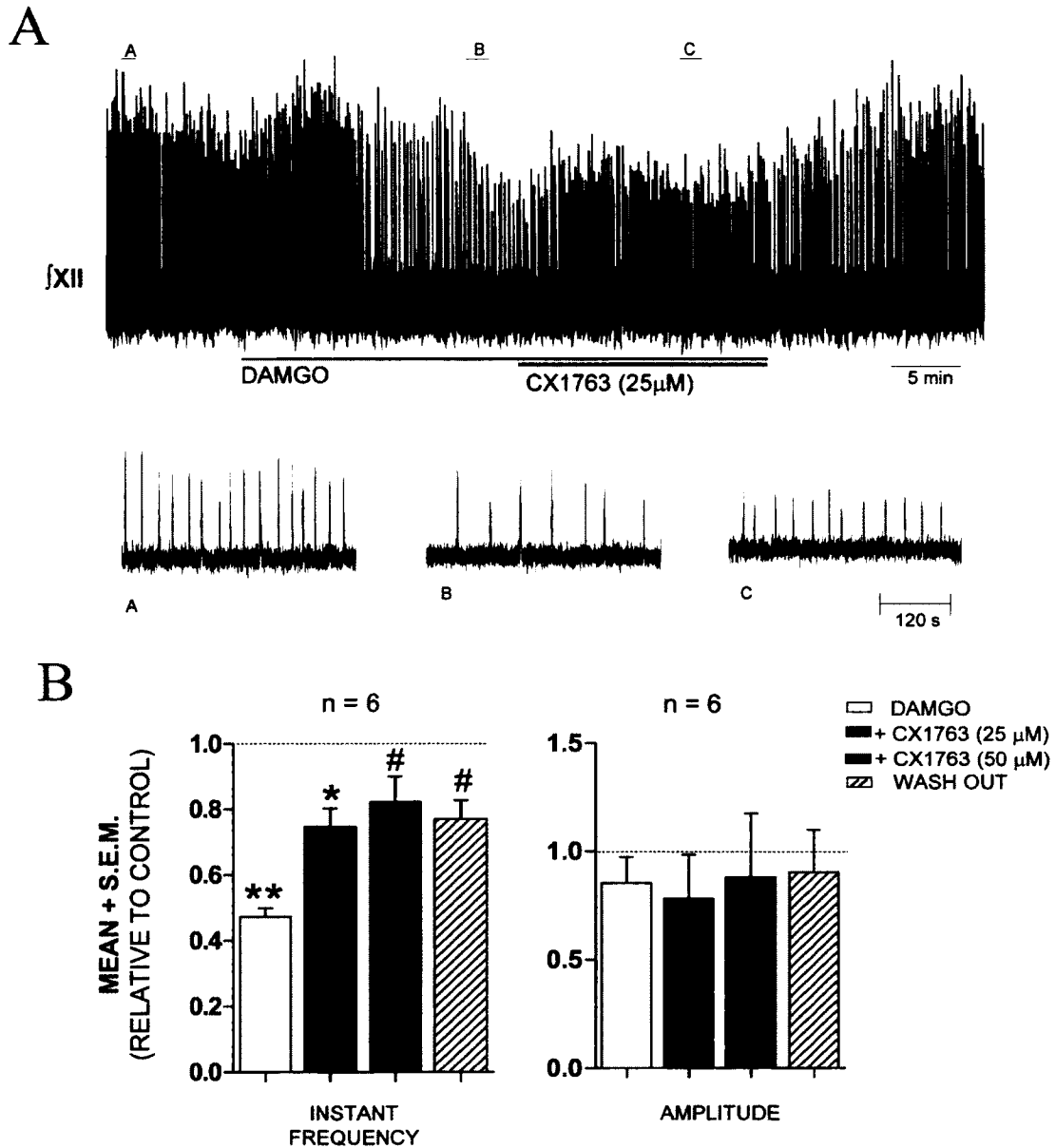


Figure 5.13 CX1763 can alleviate DAMGO-induced suppression of respiratory frequency.

A. Integrated recordings from XII nerve rootlets during bath application of CX1763 following DAMGO bath application. **B.** Histograms of group relative data ($n = 6$) graph showing the alleviation of DAMGO depression frequency by CX1763 (one-way ANOVA on raw values; * = significant difference from control, $p < 0.05$; ** $p < 0.01$; # = significant difference from DAMGO).

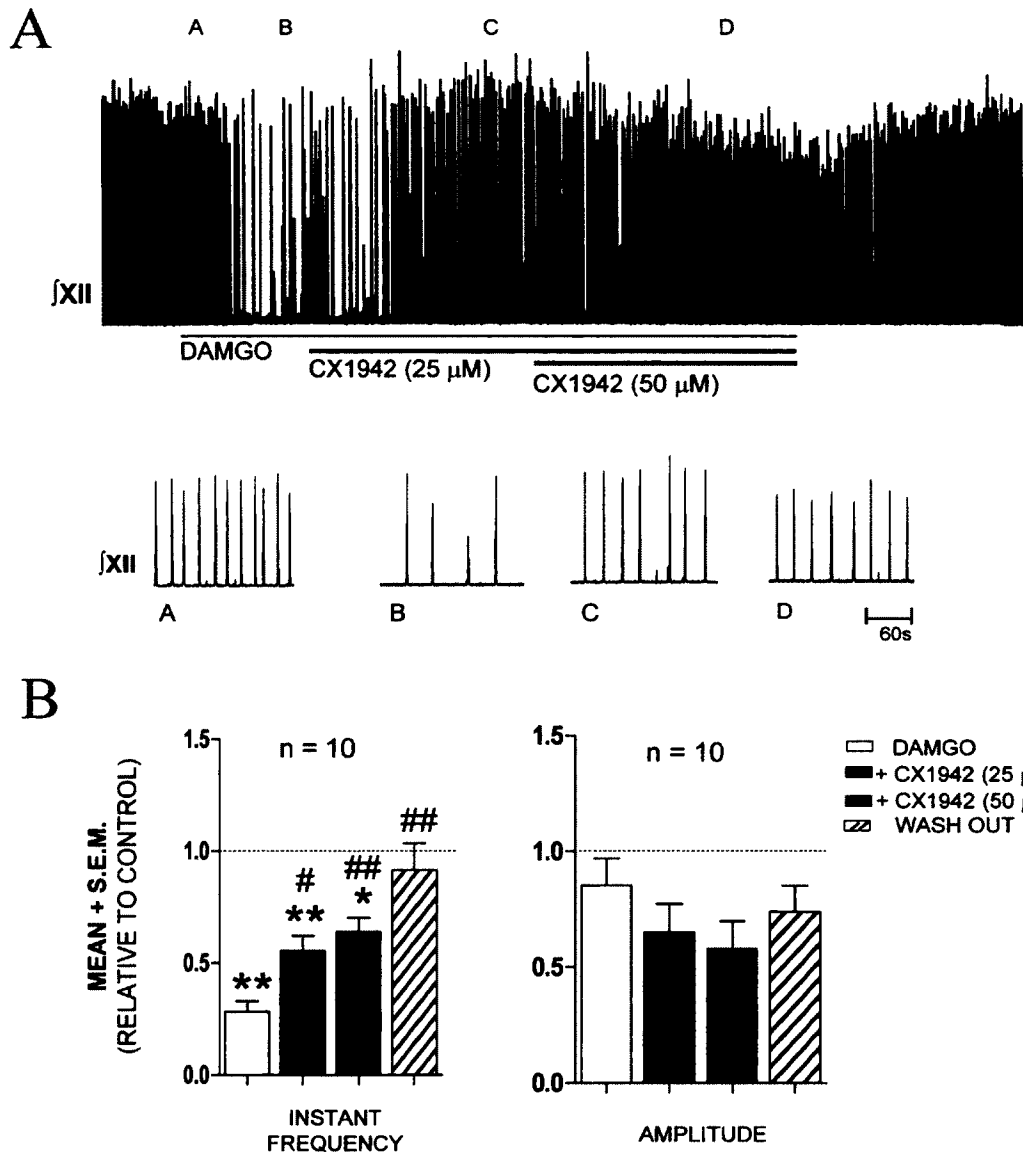


Figure 5.14 CX1942 can alleviate DAMGO-induced suppression of respiratory frequency.

A. Representative example of an integrated recordings from XII nerve rootlets during bath application of CX1942 following DAMGO bath application. **B.** Histograms of group relative data (n = 10) showing the alleviation of DAMGO-induced decrease in frequency by CX1942. Note that the XII burst amplitude stays significantly impaired even in presence of CX1942 at 50 μM (one-way ANOVA on raw values; * = significantly different from control; \bullet p < 0.05; ** p < 0.01, # p < 0.05; ## p < 0.01).

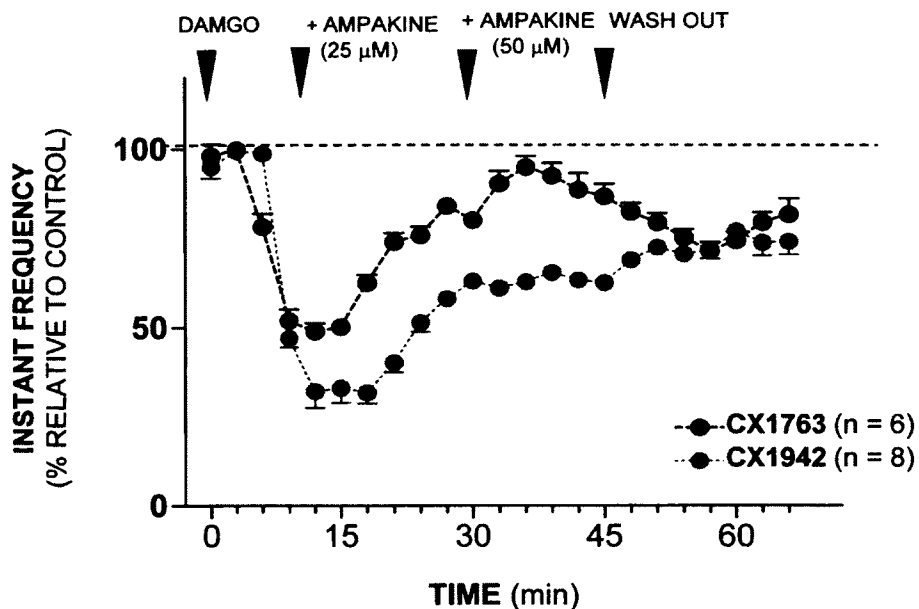
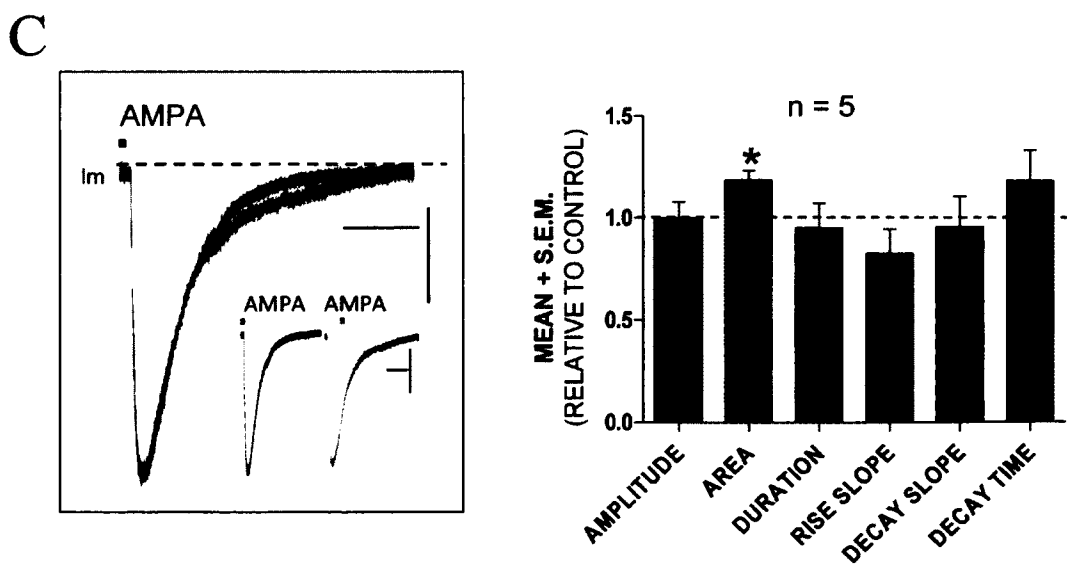
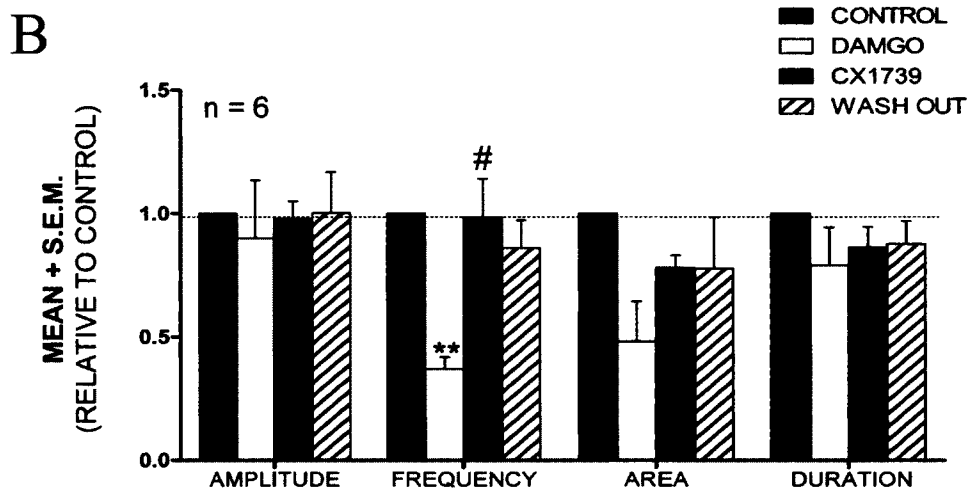
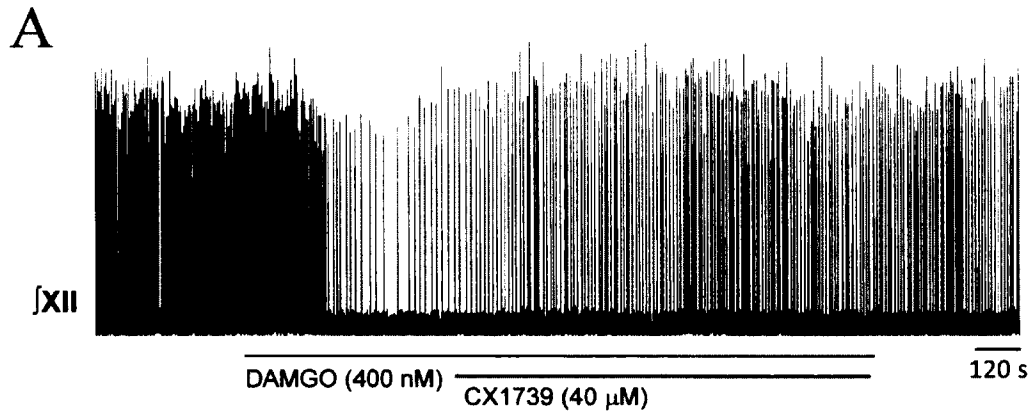


Figure 5.15 Comparison between CX1942 and CX1763 counteractions of DAMGO-induced inhibition of respiratory rate *in vitro*.

This graph shows relative values of XII bursts frequency plotted against time during the course of an *in vitro* experiment. DAMGO bath application (400 nM) effect starts very quickly; for each group the ampakine is added at 25 μM to the DAMGO application after 10 minutes of DAMGO exposure. 20 minutes after, the ampakine concentration was increased to 50 μM. Wash out with normal bath aCSF starts at 45 minutes. Note that the ampakine CX1763 quickly blocks the depressing effect of DAMGO and reverse respiratory bursts frequency up to values close to those obtained in control. CX1942 reversal of respiratory depression is delayed compared to its active form CX1763.



Previous Page

Figure 5.16 CX1739 can alleviate DAMGO-induced suppression of inspiratory frequency.

A. Integrated recordings from XII nerve rootlets during bath application of CX1739 following DAMGO bath application. **B.** Group data graph ($n = 6$) shows the histogram of group relative data showing the alleviation of DAMGO depression by CX1739 (one-way ANOVA; * = significant difference from control, # = significant difference from DAMGO). **C.** Whole-cell recording of an inspiratory cell of the preBötC in presence of TTX ($0.5 \mu\text{M}$). AMPA-mediated currents were compared in control (black) and in presence of CX1739 ($40 \mu\text{M}$) in the bathing medium. CX1739 significantly increased the area of AMPA-mediated currents of recorded cells. Scale bars are 10 s and 100 pA for **B**. The histogram on the right shows group data ($n = 5$) of relative values for AMPA-mediated currents parameters. (* = significantly different from control ($p < 0.05$; Student's t test)).

5.5 REFERENCES

BOYLE J, STANLEY N, JAMES LM, WRIGHT N, JOHNSEN S, ARBON EL, DIJK DJ (2011) Acute sleep deprivation: the effects of the AMPAKINE compound CX717 on human cognitive performance, alertness and recovery sleep. *J. Psychopharmacol.* [Epub ahead of print].

CHATTERTON JE, AWOBULUYI M, PREMKUMAR LS, TAKAHASHI H, TALANTOVA M, SHIN Y, CUI J, TU S, SEVARINO KA, NAKANISHI N, TONG G, LIPTON SA, ZHANG D (2002) Excitatory glycine receptors containing the NR3 family of NMDA receptor subunits. *Nature* 415(6873):793-8.

CIABARRA AM, SULLIVAN JM, GAHN LG, PECHT G, HEINEMANN S, SEVARINO KA (1995) Cloning and characterization of chi-1: a developmentally regulated member of a novel class of the ionotropic glutamate receptor family. *J. Neurosci.* 15(10):6498-508.

DA SILVA LF, WALDER RY, DAVIDSON BL, WILSON SP, SLUKA KA (2010) Changes in expression of NMDA-NR1 receptor subunits in the rostral ventromedial medulla modulate pain behaviors. *Pain* 151(1):155-61.

DAS S, SASAKI YF, ROTHE T, PREMKUMAR LS, TAKASU M, CRANDALL JE, DIKES P, CONNER DA, RAYUDU PV, CHEUNG W, CHEN HS, LIPTON SA, NAKANISHI (1998) Increased NMDA current and spine density in mice lacking the NMDA receptor subunit NR3A. *Nature* 393(6683):377-81.

DINGLEDINE R, BORGES K, BOWIE D, TRAYNELIS SF (1999) The glutamate receptor ion channels. *Pharmacol Rev.* 51(1):7-61.

FUNK GD, SMITH JC, FELDMAN JL (1993) Generation and transmission of respiratory oscillations in medullary slices: role of excitatory amino acids. *J. Neurophysiol.* 70(4):1497-515.

FUNK GD, SMITH JC, FELDMAN JL (1995) Modulation of neural network activity *in vitro* by cyclothiazide, a drug that blocks desensitization of AMPA receptors. *J. Neurosci.* 15(5 Pt 2):4046-56.

GRAY PA, HAYES JA, LING GY, LLONA I, TUPAL S, PICARDO MC, ROSS SE, HIRATA T, CORBIN JG, EUGENÍN J, DEL NEGRO CA (2010) Developmental origin of preBötzing complex respiratory neurons. *J Neurosci.* 30(44):14883-95.

HAMPSON RE, ESPAÑA RA, ROGERS GA, PORRINO LJ, DEADWYLER SA (2009) Mechanisms underlying cognitive enhancement and reversal of cognitive deficits in nonhuman primates by the ampakine CX717. *Psychopharmacology (Berl)*. 202(1-3):355-69.

HONORÉ T, DAVIES SN, DREJER J, FLETCHER EJ, JACOBSEN P, LODGE D, NIELSEN FE (1988) QUINOXALINEDIONES: potent competitive non-NMDA glutamate receptor antagonists. *Science* 241(4866):701-3.

IRELAND MF, LENAL FC, LORIER AR, LOOMES DE, ADACHI T, ALVARES TS, GREER JJ, FUNK GD (2008) Distinct receptors underlie glutamatergic signalling in inspiratory rhythm-generating networks and motor output pathways in neonatal rat. *J. Physiol.* 586(9):2357-70.

KARIHARAN T, SHONESY BC, PARAMESHWARAN, SUPPIRAMANIAM VD (2008) A memory enhancing drug ampakine (CX-717) potentially modulates synaptic AMPA receptor channel properties. *Alzheimer's & Dementia: The Journal of the Alzheimer's Association.* 4(4) Supplement: T502. P2-440

KASHIWAGI M, ONIMARU H, HOMMA I (1993) Effects of NMDA on respiratory neurons in newborn rat medulla *in vitro*. *Brain Res Bull.* 32(1):65-9.

KAWAI M, NAKAMURA H, SAKURADA I, SHIMOKAWA H, TANAKA H, MATSUMIZU M, ANDO K, HATTORI K, OHTA A, NUKUI S, OMURA A, KAWAMURA M (2007) Discovery of novel and orally active NR2B-selective N-methyl-D-aspartate (NMDA) antagonists, pyridinol derivatives with reduced HERG binding affinity. *Bioorg. Med. Chem. Lett.* 17(20):5533-6.

LIU Q, WONG-RILEY MT (2010) Postnatal development of N-methyl-D-aspartate receptor subunits 2A, 2B, 2C, 2D, and 3B immunoreactivity in brain stem respiratory nuclei of the rat. *Neuroscience* 171(3):637-54.

LORIER AR, FUNK GD, GREER JJ (2010) Opiate-induced suppression of rat hypoglossal motoneuron activity and its reversal by ampakine therapy. *PLoS One* 5(1):e8766.

MORGADO-VALLE C, FELDMAN JL (2007) NMDA receptors in preBötzinger complex neurons can drive respiratory rhythm independent of AMPA receptors. *J. Physiol.* 582(Pt 1):359-68.

MOSLEY CA, MYERS SJ, MURRAY EE, SANTANGELO R, TAHIROVIC YA, KURTKAYA N, MULLASSERIL P, YUAN H, LYUBOSLAVSKY P, LE P, WILSON LJ, YEPES M, DINGLEDINE R, TRAYNELIS SF, LIOTTA DC (2009) Synthesis, structural activity-relationships, and biological evaluation of novel amide-based allosteric binding site antagonists in NR1A/NR2B N-methyl-D-aspartate receptors. *Bioorg. Med. Chem.* 17(17):6463-80.

OERTEL BG, FELDEN L, TRAN PV, BRADSHAW MH, ANGST MS, SCHMIDT H, JOHNSON S, GREER JJ, GEISSLINGER G, VARNEY MA, LÖTSCH J (2010) Selective

antagonism of opioid-induced ventilatory depression by an ampakine molecule in humans without loss of opioid analgesia. *Clin. Pharmacol. Ther.* 87(2):204-11.

PAARMANN I, FRERMANN D, KELLER BU, VILLMANN C, BREITINGER HG, HOLLMANN M (2005) Kinetics and subunit composition of NMDA receptors in respiratory-related neurons. *J. Neurochem.* 93(4):812-24.

PACE RW, DEL NEGRO CA (2008) AMPA and metabotropic glutamate receptors cooperatively generate inspiratory-like depolarization in mouse respiratory neurons *in vitro*. *Eur. J. Neurosci.* 28(12):2434-42.

PACE RW, MACKAY DD, FELDMAN JL, DEL NEGRO CA (2007) Inspiratory bursts in the preBötzinger complex depend on a calcium-activated non-specific cation current linked to glutamate receptors in neonatal mice. *J Physiol.* 582(Pt 1):113-25.

PARAMESHWARAN K, UTHAYATHAS S, SIMS C, ROGERS GA, SUPPIRAMANIAM V (2006) An ampakine CX-717 potently modulates the single-channel properties of synaptosomal AMPA receptor. *Society for Neuroscience Abstracts*. Poster# 424.11/C28.

PÉREZ-OTAÑO I, LUJÁN R, TAVALIN SJ, PLOMANN M, MODREGGER J, LIU XB, JONES EG, HEINEMANN SF, LO DC, EHLERS MD (2006) Endocytosis and synaptic removal of NR3A-containing NMDA receptors by PACSIN1/syndapin1. *Nat Neurosci.* 9(5):611-21.

PIÑA-CRESPO JC, TALANTOVA M, MICU I, STATES B, CHEN HS, TU S, NAKANISHI N, TONG G, ZHANG D, HEINEMANN SF, ZAMONI GW, STYS PK, LIPTON SA (2010) Excitatory glycine responses of CNS myelin mediated by NR1/NR3 "NMDA" receptor subunits. *J. Neurosci.* (34):11501-5.

PORRINO LJ, DAUNAIS JB, ROGERS GA, HAMPSON RE, DEADWYLER SA (2005) Facilitation of task performance and removal of the effects of sleep deprivation by an ampakine (CX717) in nonhuman primates. *PLoS Biol.* 3(9):e299.

REN J, POON BY, TANG Y, FUNK GD, GREER JJ (2006) Ampakines alleviate respiratory depression in rats. *Am. J. Respir. Crit. Care Med.* 174(12):1384-91.

REN J, DING X, FUNK GD, GREER JJ (2009) Ampakine CX717 protects against fentanyl-induced respiratory depression and lethal apnea in rats. *Anesthesiology* 110(6):1364-70.

SASAKI YF, ROTHE T, PREMKUMAR LS, DAS S, CUI J, TALANTOVA MV, WONG HK, GONG X, CHAN SF, ZHANG D, NAKANISHI N, SUCHER NJ, LIPTON SA (2002) Characterization and comparison of the NR3A subunit of the NMDA receptor in

recombinant systems and primary cortical neurons. *J. Neurophysiol.* 87(4):2052-63.

SHAO XM, GE Q, FELDMAN JL (2003) Modulation of AMPA receptors by cAMP-dependent protein kinase in preBötzing complex inspiratory neurons regulates respiratory rhythm in the rat. *J. Physiol.* 547(Pt 2):543-53.

SMOTHERS CT, WOODWARD JJ (2007) Pharmacological characterization of glycine-activated currents in HEK 293 cells expressing N-methyl-D-aspartate NR1 and NR3 subunits. *J. Pharmacol. Exp. Ther.* 322(2):739-48.

SMOTHERS CT, WOODWARD JJ (2009) Expression of glycine-activated diheteromeric NR1/NR3 receptors in human embryonic kidney 293 cells Is NR1 splice variant-dependent. *J. Pharmacol Exp Ther.* 331(3):975-84.

SUCHER NJ, AKBARIAN S, CHI CL, LECLERC CL, AWOBULUYI M, DEITCHER DL, WU MK, YUAN JP, JONES EG, LIPTON SA (1995) Developmental and regional expression pattern of a novel NMDA receptor-like subunit (NMDAR-L) in the rodent brain. *J. Neurosci.* 15(10):6509-20.

WESENSTEN NJ, REICHARDT RM, BALKIN TJ (2007) AMPAKINE (CX717) effects on performance and alertness during simulated night shift work. *Aviat Space Environ Med.* 78(10):937-43.

YAO Y, MAYER ML (2006) Characterization of a soluble ligand binding domain of the NMDA receptor regulatory subunit NR3A. *J Neurosci.* 26(17):4559-66.

ZHANG D, HEINEMANN SF, ZAMONI GW, STYS PK, LIPTON SA (2010) Excitatory glycine responses of CNS myelin mediated by NR1/NR3 "NMDA" receptor subunits. *J. Neurosci.* 30(34):11501-5.

ZHENG Y, BALABHADRAPATRUNI S, MASUMURA C, DARLINGTON CL, SMITH PF (2011) Effects of the putative cognitive-enhancing ampakine, CX717, on attention and object recognition memory. *Curr. Alzheimer Res.* 8(8):876-82.

CHAPTER 6

REVIEW AND DISCUSSION

The experimental work reported in this thesis was designed to further our understanding of opioids and ampakines modulation of respiratory neuronal activity. The first data chapter (Chapter 3) of my thesis had two main goals. First, I verified the existence of μ -opioid receptors within the preBötC and determined the synaptic action of opioids on respiratory neurons of the preBötC. Second, I determined how and where positive allosteric modulators of AMPA receptors modulate synaptic activity within the inspiratory network. The second project (Chapter 4) aimed to define the expression and function of μ -opioid receptors on the raphé nucleus obscurus that may contribute to breathing depression associated with opioid administration. The third project (Chapter 5) initially aimed to determine the synaptic actions of low-impact ampakines on respiratory neurons of the preBötC, with a focus on CX717. The study subsequently expanded into an examination of the “not-so-well-known” glycinergic NMDA receptor subtypes that may account for the potentiation of respiratory rhythm by CX717, and provides the foundation for examining a previously unexamined receptor in the context of respiratory rhythmogenesis.

6.1 MU-OPIOID RECEPTORS OF THE RAT PREBÖTC

Previous studies have examined the potential role of the preBötC in opioid-induced respiratory depression (Morin-Surun et al., 1984; Morin-Surun et al., 2001; Greer et al., 1995) but questions remained about opioid mechanisms of action. The study undertaken by Gray et al., 1999 was the first study demonstrating the presence of μ -opioid receptors (MOR) in preBötC neurons by means of immunohistochemical and electrophysiological analyses. This was followed by an important study demonstrating a strong respiratory depression after microinjection of a μ -opioid agonist specifically into neurokinin-1 receptor (NK1R)-expressing preBötC nuclei of anaesthetized adult rats (Montandon et al., 2011). Both studies led to two fundamental conclusions: μ -opioid receptors and NK1 receptors are co-expressed in the same cells and μ -opioid agonists hyperpolarize inspiratory neurons of the preBötC. However, there remains some

controversy as there have been reports stating that preBötC neurons do not express MOR (Ballanyi et al., 2010). In this thesis the data demonstrated that i) μ -opioid receptors 1A (MOR1a) are expressed within the preBötC, ii) there is some colocalization between MOR1a and NK1R in the preBötC and the nucleus ambiguus (NA) compact division, and iii) some preBötC neurons have functional postsynaptic MOR, and others undergo a significant decrease in the frequency of the spontaneous tonic synaptic events when exposed to DAMGO.

Local injections of DAMGO within the preBötC in medullary slice *in vitro* were performed and MOR activation in the preBötC not only induced a decrease in inspiratory frequency but also caused some changes in the bursting pattern (e.g. decrease of inspiratory burst duration). Importantly, naloxone microinjections within the preBötC could block the respiratory depression induced by DAMGO. These results suggest that opioid action on the central inspiratory pattern generator affects both rhythm frequency and strength of the inspiratory drive.

In the immunohistochemical study, motoneurons of the semi-compact division of the NA (characterized by high immunoreactivity for ChAT) were rarely positive for MOR1a, while neurons of the compact division of the NA were highly immunoreactive. The semi-compact division of the NA contains mainly pharyngeal motoneurons whose axons travel through the glossopharyngeal nerve and the pharyngeal ramus of the vagal nerve. The compact division of the NA (NAc) contains mainly densely aggregated vagal motoneurons (Bieger and Hopkins, 1987) comprised of cardiac or pulmonary projecting neurons with inspiratory electrophysiological pattern (McAllen and Spyer, 1978). At the transversal plane of the preBötC, MOR1a⁺ NAc neurons did not stain for ChAT which seems to corroborate with some atypical catecholaminergic vagal neurons that also failed to stain for tyrosine hydroxylase (Blessing et al., 1985). Our data therefore reinforce the heterogeneity in the neuronal organization of the NA and support the subdivision of the NA into functionally distinct compact and semi-compact compartments that both coexist in the medullary transversal plan of the preBötC.

More directly related to opioid action on inspiratory drive, the immunohistochemical study also indicated that MOR1a is strongly expressed in the axon hillock, neurites, and somatic membrane of preBötC neurons, suggesting that MOR are located in key postsynaptic sites. Whole-cell recordings of respiratory preBötC neurons demonstrated a heterogeneous synaptic response and sensitivity to the μ -opioid agonist DAMGO. MOR activation by DAMGO resulted in a decrease in R_N and elicited an outward current in a subpopulation of inspiratory cells, yet no significant effect on inspiratory current amplitude was seen. In other inspiratory cells, no postsynaptic effect of DAMGO was observed but there was a decrease in interburst spontaneous activity, similar to the response of XII motoneurons to DAMGO (Lorier et al., 2010). In contrast, expiratory neurons of the preBötC did not respond to DAMGO, and MOR1a immunohistochemistry through the ventrolateral medulla showed no labeling of MOR1a in the Bötzinger complex (BötC), except in few scattered motoneurons of the external formation of the NA. Those results correlate with previous *in vitro* studies that have demonstrated that expiratory neurons were resistant to μ -opioid agonists (Takeda et al., 2001; Mellen et al., 2003), and immunolabeling study that also showed an absence of MOR labeling in the BötC (Gray et al., 1999).

Finally, hetero-oligodimerization between MOR and non-MOR has been reported (Pfeiffer et al., 2002, 2003). Of particular interest, the μ -opioid receptor 1 (MOR1) has been shown to specifically associate with the substance P receptor subtype neurokinin-1 receptor (NK1R) (Pfeiffer et al., 2003) or with the somatostatin receptor subtype STT2A (Pfeiffer et al., 2002). Those two G-protein coupled receptors are expressed in putative rhythmogenic neuronal population of the preBötC (as reviewed in Chapter 1). Although the coexistence of MOR, NK1R and/or SSTR2A has already been shown in some preBötC neurons (Gray et al., 1999; Gray et al., 2010), the possible native oligodimerization between two or more of these receptors within the preBötC remains undetermined. Pfeiffer and colleagues have demonstrated that the dimerization of MOR1/NK1R and MOR1/SST2A resulted in modulation of the phosphorylation, internalization and desensitization processes of either dimer where, for instance, the internalization of

one dimer would entrain the internalization of the other (Pfeiffer et al., 2002, 2003). The idea that a putative heterodimerization between MOR and NK1R in preBötC cells could result in the alteration of spontaneously generated or evoked respiratory signals within the preBötC is intriguing. The analysis of MOR/NK1R preBötC double-immunolabeling with macroscopic confocal images did not provide the resolution necessary to answer that question, but it does support the idea of oligodimerization between MOR and NK1R in preBötC neurons. As seen in Figures 3.3B, D and H in Chapter 3, MOR1A and NK1R are intimately expressed in the same cellular compartments. The prospect of such interactions (i.e. MOR1/NK1R) within a subpopulation of critical preBötC neurons and their possible physiological outcome on neural control of breathing merits future investigation. For this purpose, the use of non-internalizing versus internalizing μ -opioid-agonists (such as herkinorin and DAMGO respectively; Xu et al., 2007) combined with the use of fluorochrome compounds conjugated with MOR agonist could facilitate that research.

6.2 RAPHE OBSCURUS INFLUENCE ON RESPIRATORY NETWORK ACTIVITY

The use of reduced preparations such as the neonatal rat medullary slice preparation is well-suited for measuring single-cell electrophysiological activity and pharmacological analysis. However, the fact that *in vitro* preparations are only viable in neonates and are isolated from their normal environment and synaptic connectivity raises limitations to data interpretation. The fact that the activation of MOR within the raphé may be limited to *in vitro* conditions and/or early developmental stages cannot be excluded. For instance, tryptophan hydroxylase and serotonin transporter expression in rat raphé nuclei and neuropile of preBötC declines significantly from P12 onward (Liu and Wong-Riley, 2010). Therefore the raphé/preBötC excitatory loop studied in Chapter 4 might be more relevant to younger aged animals.

The contribution of serotonergic raphé obscurus (RNO) neurons to respiratory drive clearly appears to depend on the experimental setting. While methysergide maleate, a 5HT_{1/2} antagonist, can produce severe respiratory drive depression when applied to preBötC in rat medullary slice preparation (Ptak et al., 2009), it does not change baseline breathing of anaesthetized adult mice (Depuy et al., 2010). The effects of exogenously applied substance P on inspiratory drive has been shown both *in vitro* (Pagliardini et al., 2005; Ptak et al., 2009) and *in vivo* (Gray et al., 1999), although no data has been derived from blocking NK1R within the preBötC. The histological data indicates that SP⁺ RNO neuronal somata are specifically positioned at the same transverse plane as the preBötC which is consistent with SP⁺ RNO neurons being important providers of endogenous SP to the preBötC. In addition, data showed that MOR is expressed on somatic membranes of most SP⁺ RNO neurons. Thus, if MOR-induced inhibition was to occur on RNO neurons, a decrease in 5HT and SP excitatory input to the preBötC would likely follow. It is proposed that the observed delayed respiratory drive depression was a consequence of a decrease in endogenous 5HT and SP release within the preBötC.

An increasing number of genetic mouse models are associated with altered 5HT expression. *Gata 2* (Craven et al., 2004), *Gata3* (Van Doorninck et al., 1999), *Mash1* (Pattyn et al., 2004), *Lmx1b* (Ding et al., 2003) and *Pet1* (Hendricks et al., 1999) transcription factors have all been shown to play a role in 5HT neuron identity. These genetic models have provided insights to the transcriptional control mechanisms underlying the development and maturation of neuronal circuits, including respiratory networks (Hodges et al., 2009). The data provided in Chapter 4 showed that SP⁺ neurons of the raphé are also crucial for the raphé / preBötC excitatory loop, and are part of 5HT⁺ neuronal population. It would be interesting to know if SP⁺ neurons can still develop in 5HT-related genetic mouse models and influence respiratory networks activity *in vivo* and *in vitro*.

The role of chemosensitive neurons within the raphé obscurus and their potential modulation by MOR was not part of the study. There is still some controversy surrounding the notion of putative chemoreceptors with medullary

raphé nuclei. Based on the fact that isolated medullary raphé neurons have intrinsic chemoreception properties in culture (Wang et al., 2001; Bouyer et al., 2004), Hodges and Richerson (2010) argue that those neurons are chemoreceptive to surrounding arterial PCO₂ in the whole animal (Bradley et al., 2002; Hodges and Richerson, 2010). This view is in contrast to data from a recent study by Depuy and colleagues who demonstrated that serotonergic medullary raphé neurons were not responding to PCO₂ in mice (Depuy et al., 2010). Accumulating evidence supports the idea that *in vivo*, chemoreceptive properties of yet another population of putative central chemoreceptors (RTN neurons; Mulkey et al., 2004) depend on discrete communication with their surrounding vascular and pH-sensing glia cells in addition to neuronal sensing (Gourine et al., 2010; Guyenet et al., 2010). As discussed by Depuy and colleagues (Depuy et al., 2010), if that is true for all classes of central chemoreceptors such as raphé neurons, then culture models devoid of vascular and glia cells should not be capable of responding to chemoreception challenges the same way that they respond *in vivo*. Further, central serotonergic neurons have recently been shown to mediate arousal responses to hypercapnia (Buchanan and Richerson, 2010) and MOR activation in serotonergic neurons might lead to a decrease in hypercapnia response (Zhang et al., 2009). The “state-dependent central chemoreception” theory states that chemoreceptive sites vary in effectiveness depending on the state of arousal (sleep state versus wakefulness; reviewed in Nattie, 2001). Overall, future work may be directed towards determining whether or not respiratory RNO neurons display chemosensitive properties, as well as analyzing a potential regulation of those chemosensitive features by opioids in relation to arousal state.

Finally, central serotonergic nuclei have recently been proposed to be essential sites for thermoregulation (Ray et al., 2011), although it is not known if respiratory-related 5HT neurons are thermo sensors. If raphé 5HT neurons actually interact with the inspiratory network as they do *in vitro*, thermo sensory 5HT neurons could have a role in integrating sensory inputs onto neuronal networks that control inspiratory activity. The clinical relevance of thermoregulatory role of medullary 5HT neurons could come into play in

particular cases such as stroke or brain injury management that can use a combination of opioids anesthetics and hypothermia during surgery (Statler et al., 2003).

6.3 ALLOSTERIC MODULATORS OF AMPA RECEPTORS MODIFY RESPIRATORY NEURON FUNCTION

Whole-cell data in Chapter 3 have suggested a certain difference in sensitivity of the respiratory preBötC neurons to allosteric regulation of AMPA receptor desensitization and deactivation rates induced by the high-impact ampakines versus cyclothiazide. Biochemistry studies examining the molecular mechanisms underlying the binding affinity between cyclothiazide, CX614 and their respective targets, show that while cyclothiazide is more sensitive to Ser750 (flip) alternative splicing of AMPA receptors over the Asn-750 (flop) variant (Partin et al., 1995), CX614 has a higher binding affinity with the flop variant (Arai et al., 2000). This may account for the higher sensitivity of respiratory preBötC neurons to CX614 and suggests that those neurons may have a high flop/flip AMPA receptors splice variants ratio.

One of the most intriguing aspects of glutamate receptor function is with regards to the regulatory domains of their carboxyl termini that have emerged as critical endogenous modulators of synaptic transmission. Those regulatory domains, like glutamate allosteric modulators, also influence electrophysiological properties of the glutamatergic receptors. Regulatory domains are targets of many intracellular cytoskeletal (example actin), signaling (such as kinases) and regulatory proteins (PDZ domains). Recently, transmembrane AMPA receptor regulatory proteins (TARPs) (Chen et al, 2000; Tomita et al., 2003; Priel et al., 2005; reviewed in Nicoll et al., 2006), cornichons proteins (CNIH; Schenk et al. 2009) and cystine-knot AMPA receptor modulating protein 44 (CKAMP44; von Engelhardt et al., 2010) have been identified as auxiliary proteins that fine tune the electrophysiological properties of glutamate-gated ion channels by slowing (TARPs and CNIH) or accelerating (CKAMP44) deactivation and desensitization

kinetics. Those proteins change the pharmacological properties of AMPA receptors (Tomita et al., 2006; Zhang et al., 2006; Kato et al., 2010; Gill et al., 2011). In particular, the ampakine CX546 was found to exert different degrees of modulation of AMPA receptor kinetics within different brain regions, depending in part on native TARP expression (Montgomery et al., 2009). Similarly, CX614 modulation of AMPA-mediated kinetics in respiratory raphé neurons differs from that in respiratory preBötC neurons. CX614 increased primarily the duration and eventually the amplitude of AMPA-mediated currents in raphé neurons, while all parameters of AMPA-mediated currents in preBötC neurons were rapidly increased by CX614. The existence of auxiliary AMPA proteins in respiratory neurons of the preBötC and the raphé has not been yet studied, but their presence might also account for the differences in sensitivity among diverse allosteric modulators of glutamatergic receptors.

While CX614 had a high efficacy for potentiating glutamatergic synaptic transmission and counteracting respiratory rhythmic drive depression induced by opioid (either through its direct action on preBötC rhythmogenic neurons or via an indirect action within the RNO) its action on AMPA receptor conductance does not seem to significantly affect baseline inspiratory rhythm. Those results were not expected for two reasons. First, local injection of AMPA in the RNO readily stimulates inspiratory activity. Second, 5HT and substance P (which are the main neurotransmitters released from the RNO), are both capable of depolarizing respiratory preBötC neurons (Ptak et al., 2009) and increasing inspiratory rhythm (Pagliardini et al., 2005) under baseline conditions. Therefore the data emphasize that the key aspect of ampakine modulation of excitatory neurotransmission remains the availability of endogenous release of glutamate itself. This would not necessarily mean that glutamate release becomes more available in the presence of opioids relative to baseline conditions, but the enhancement of AMPA receptor binding affinity induced by CX614 (CX614 preferentially modulates deactivation rate of AMPA receptor conductance; Jin et al., 2004) might be sufficient to promote the necessary increase of spiking discharge probability needed to trigger cellular excitation, depolarization of the

membrane potential and downstream excitatory signalling cascades. This could suggest that the deactivation rate of AMPA receptors may play a lesser role in normal physiological conditions, possibly because of saturating concentrations of glutamate in the synaptic cleft. In contrast, in the presence of persistent glutamate release (baseline conditions), one may speculate that the desensitization rate of AMPA receptors play a more important role. This is supported by the fact that cyclothiazide, a positive allosteric modulator of AMPA receptors that preferentially decreases their desensitization rate (Partin et al., 1993; Partin et al., 1994; Aria et al., 2004), increases respiratory activity in normal physiological conditions (Funk et al., 1995).

6.4 THE PARTICULAR CASE OF CX717, A WINDOW TO A NMDA RECEPTOR-DRIVEN RESPIRATORY RHYTHM GENERATION HYPOTHESIS

a) THE CX717 HYPOTHESIS

In contrast to expectations, the electrophysiological study of ampakine CX717 action suggests that it does not significantly increase AMPA-mediated current kinetics in preBötC neurons. Rather, CX717 may affect NMDA receptor conductance through a mechanism that has yet to be determined. NMDA receptors are known to be “coincidence detectors” that depend on depolarization and the binding of glycine and glutamate. Interestingly, the data suggest that CX717 potentiates NMDA-evoked responses in preBötC neurons only at hyperpolarized membrane potentials (below -50 mV) and in the presence of glycine. This result directed the investigation towards the glycine-binding NR3 subunit of NMDA receptors (more specifically NR3A) which is the only NMDA receptor subtype known to function independently to magnesium extracellular concentration and membrane potential. Thus the hypothesis that CX717 acts through NR3A subunits, by allosterically modulating NR1/NR3A dimer kinetics and consequently increasing NMDA receptor conductance, was put forward.

Because CX717 is an allosteric modulator, it cannot act alone, which means that NR3A must already be activated endogenously by its ligand glycine. There are two reasons to believe that endogenous glycine release is not affected by μ -opioid agonist. First, as demonstrated in Chapter 3, MOR in the preBötC is expressed on NK1R positive cells (also demonstrated by Gray et al., 1999 and Montandon et al., 2011). Second, most glycinergic preBötC neurons (including pacemaker neurons) do not express NK1R (Wang et al., 2001; Morgado-Valle et al., 2010). Therefore glycinergic preBötC neurons are more likely not to contain MOR. On the other hand, Liu et al (2002) demonstrated the presence of glycinergic presynaptic boutons on the membrane of NK1R positive neurons of the preBötC, which implies that MOR⁺/NK1R⁺ preBötC neurons do receive glycinergic inputs. There are two possible targets for the release of glycine from those synaptic boutons to MOR⁺/NK1R⁺ preBötC neuronal postsynaptic membranes: the classic glycinergic receptors GlyRs and the glycinergic NMDA receptors subtype NR1/NR3A. Because the reversal potential for chloride ions (main conducting ions of GlyRs) is very depolarized in the medullary slice maintained in elevated extracellular potassium (Ren et al., 2006) and postsynaptic MOR activation can lead to a hyperpolarization of the membrane potential, the electrical gradient of both types of glycinergic receptors (GlyRs and NR1/NR3 receptors) should allow both receptors to yield a net ion current that flows inward upon channel activation. Note that under more physiological conditions such as in brainstem spinal cord preparations or *in vivo*, the reversal potential chloride is normal and thus GlyRs net ionic flux should not be inward. Nevertheless, it appears that in medullary slice preparations, chloride reversed conductances through GlyRs may lead to sufficient membrane depolarization to activate voltage-gated Na⁺/Ca²⁺ channels and induce excitatory actions (Turecek and Trussel, 2001). In fact, glutamate has recently been found to allosterically potentiate GlyRs (Liu et al., 2010). This hypothesis was tested by looking at the effect of CX717 after DAMGO-induced respiratory depression in presence of the GlyRs antagonist strychnine, and CX717 continued to induce a significant potentiation of inspiratory rhythm under those conditions (data not shown). This

does not rule out the possibility that CX717 may act on classical GlyRs, but it does suggest that GlyRs are not directly involved in the increase of inspiratory activity by CX717.

One important aspect regarding native NMDA receptors is the interesting interplay that exists between NR1/NR3 and NR1/NR2 dimers: glycine and glutamate binding show negative cooperativity which gives rise to a glycine-dependent form of receptor desensitization (Das et al., 1998; Chatterton et al., 2002). In other words, the more active is the NR1/NR3 dimer, the less active the NR1/NR2 dimer will be. Coming back to the situation where MOR⁺/NK1R⁺ preBötC neurons, presumably containing NR1/NR2/NR3 receptors, have their membrane potential hyperpolarized by μ -opioids, glycine binding to the NR1/NR3 dimer would therefore decrease NMDA receptor conductance. This concept raises the possibility that part of respiratory depression induced by opioids might also be related to an indirect facilitation of NR1/NR3 action on preBötC neurons, and that opioids may have an indirect or direct action on NR1/NR3 glycinergic receptors. It was noted that, in some preBötC neurons, NMDA-evoked depolarizing responses were substantially decreased by bath application of glycine. In fact, those preBötC neurons are the ones that responded the most prominently to subsequent bath application of CX717. In those neurons CX717 significantly increased NMDA-evoked responses suggesting that CX717 would affect NR3 subunit in a rather unique way: hypothetically by accelerating deactivation and/or desensitization rate of the NR1/NR3 channel, allowing the NR1/NR2 dimer counterpart to yield more current and produce a larger NMDA-evoked depolarization. This is unexpected because ampakines are known to slow deactivation and desensitization rates. Whether the same potentiation of NMDA-evoked responses by CX717 can also occur in presence of DAMGO remains to be determined, but the data suggest that endogenous release of glycine would be a key factor for the hypothesized CX717 allosteric negative modulation to be effective.

b) NMDA RECEPTORS AND RESPIRATORY RHYTHMOGENESIS

The fact that CX717 may increase respiratory drive in the presence of AMPA antagonist NBQX (although transiently) and increase NMDA-mediated responses, suggest that respiratory activity under CX717 could be driven by NMDA independently of AMPA receptors. Further, because the potentiation of respiratory activity by CX717 did not occur in baseline conditions, but was limited to specific conditions (either low extracellular concentration of potassium, presence of glycine or depression of respiratory rhythm by opioids), CX717 action may dependent on the network activity. Therefore a tempting interpretation of the data proposes a form of plasticity within the preBötC where electrical activity necessary for synaptic transmission within the preBötC can respecify glutamate neurotransmitter expression, switching from a type of AMPA receptor regulation at rest, to a NMDA-regulated type of regulation in weak respiratory drive conditions. This concept relates to the idea of “activity-dependent respecification” where neuronal membrane protein expression changes as a function of electrical activity (reviewed in Spritzer et al., 2012). Morgado-Valle and colleagues (2010) had suggested the possibility of NMDA receptors driving respiratory activity independently of AMPA receptors and the data support their findings. A hypothetic dynamic neuromodulation and neurotransmission within the preBötC might be a relevant concept to consider in the future.

One of the most important characteristics of NR3 containing NMDA receptors is their lack of Ca^{2+} permeability. Ca^{2+} is a critical second messenger that triggers a number of different intracellular signalling cascades believed to be crucial for rhythmogenesis within the preBötC (Pace et al., 2007; Rubin et al., 2010; Dunmyre et al., 2011). It is therefore evident that NR3 dominant-negative modulation may also play a role in the rhythmogenesis itself, by modulating Ca^{2+} signalling according to levels of excitations. The exact mode of action of NR3 within the preBötC is unclear and will require further research. NK1R appears to be a relatively reliable marker of preBötC neurons (Gray et al., 1999; Guyenet et al., 2002; Pagliardini et al. 2003). In Chapter 5 it was demonstrated that the neurotransmitter receptor NR3A was highly expressed in the preBötC region.

Previous single-cell RT-PCR study has shown that preBötC respiratory neurons may possess the NR3A gene (Paarmann et al., 2005). The whole-cell recording data suggest that NR3A are functional in preBötC neurons (respiratory and non-respiratory cells). Further research is required in order to determine the proportion of NR3A⁺ cells in the preBötC and their electrophysiological behaviour, but the NR3A subunit holds the potential of becoming a complementary marker of important modulatory neurons in the preBötC.

Apart from the hypothesis that CX717 may directly interact with NR3A subunits to modulate NMDA receptors conductance, the possibility that NR3A of preBötC neurons may also work as a conditional detector, and that CX717 may directly interact with conventional NMDA receptors cannot be ruled out. In fact CX717 has already been shown to potentiate intracellular calcium concentration waves in hippocampal synapses, an effect blocked by NMDA and non-NMDA receptors blockers (Hampson et al., 2009). Because NR3A functions independently of the membrane potential, NR3A may confer to its co-expressing dimers the ability to be active at hyperpolarized potentials. In the experiments, NMDA-evoked responses were not increased at membrane potential over -50mV, which would imply that NR3A contributes to a lesser extent to NMDAR conductance at depolarized potentials relative to hyperpolarized potentials.

6.5 FUTURE DIRECTIONS

The use of low-impact ampakines to counter respiratory depression has clinical promise. Further studies at the molecular level should help to determine the NMDA receptors binding site(s) for allosteric modulators (and more particularly CX717), using crystallography techniques and recombinant receptors expression of NMDA receptors in appropriate mammalian cell models.

The exact mechanism by which modulators bind and regulate the glutamatergic receptor ion channel itself is beginning to unfold (Furukawa et al., 2005; Sobolevsky et al., 2009). Furukawa and colleagues demonstrated that aniracetam, a molecule from which ampakines are structurally derived, binds to a

particular site called site II in AMPA receptor homomeric GluR2, which has equivalence in the NR1/NR2 heterodimer: the site Y535 (Furukawa et al., 2005; see Fig. 6.2.). The authors hypothesized that the residue 535 modulates the deactivation in NMDA receptors. This leads to the proposal that the Y535 site (or its homolog in the NR1/NR3A heterodimer) can be a candidate for the potential binding site of CX717.

Further electrophysiological examination of the effect of CX717 on NR1/NR3 recombinant proteins should confirm whether or not CX717 modulates NR3 subunit directly. Eventually, CX717 may modulate the conventional NMDA receptors, and NR3 subunit may act as a conditional protein, allowing CX717 to potentiate NMDA-conductance at hyperpolarized potentials. In any case, an understanding of the role of NR3 in the preBötC function deserves investigation, from transcription factor profile, neurotransmitter phenotype, as well as aspects of NR3 positive neurons axonal projections and migratory pattern.

From a translational standpoint, because NR3A is expressed only in very specific areas of the brain (Ciabarra et al., 1995), therapeutic tools that target NR3 would provide functional and anatomical specificity. To this end, other low-impact ampakines should be tested in order to assess their potential regulation of NR3 subunits. Alternatively, new modulators specifically targeting NR3 subunits would be worth developing.

Selective inactivation of the NR3 subunit genes with knockout or conditional knockout mice may help us identify respiratory abnormalities linked to NR3 subunits deficiency. A NR3A mutant mouse model has been generated that helped elucidate some important aspects of NR3A function (Das et al., 1998; Piña-Crespo et al., 2010). The Greer laboratory received breeding pairs in June, 2012 and the colony is being established. A combination of *in vivo* and *in vitro* experimental strategies will be used to analyze behavioural and physiological phenotypes of mutants and should help us elucidate the potential implication of NR3A in CX717 modulation of respiratory activity, as well as more generally, be used to probe other pharmacological agents and understand the role of the NR3 subunits in the respiratory rhythmogenesis development and function. Moreover,

despite the detection of NR3A in the preBötC shown by the immunohistochemical data, the ontogeny of NR3A subunit within the preBötC remains uncertain. It has been suggested that the expression of NR3A may be limited to neonatal or juvenile stages of development (Wong et al., 2002). The developmental profile of this subunit using immunohistochemistry will be examined. Interestingly the expression of the NR3B subunit has been found to be weak in embryonic/neonatal stages and up regulated in juvenile extending to adult stages in several brain regions including the preBötC (Matsuda et al., 2002; Fukaya et al., 2005; Liu and Wong-Riley, 2010b). The apparent mutual exclusive changes in the developmental expression of both NR3 subunits may underlie a switch between NR3A and NR3B.

6.6 CONCLUDING REMARKS

In summary, this thesis has addressed important clinically-related modulatory aspects of respiratory rhythm generation, with an emphasis on preBötC synaptic transmission. Further data supporting the presence of pre- and postsynaptic functional μ -opioid receptors on preBötC neurons were obtained and provided a better understanding of the diversity of synaptic responses involved in μ -opioid-induced respiratory rhythm depression. Opioids can impact breathing rate through a direct inhibitory action on preBötC neurons or indirectly via raphé neurons. The *in vitro* analysis of cellular mechanisms underlying ampakine stimulation of inspiratory rhythm led to a better understanding on how ampakines alleviate opioid-induced respiratory depression and which neurotransmitters contribute to the generation the preBötC synaptic drive. AMPA receptor mediated conductance is clearly an important drive of rhythmogenesis within the preBötC and ampakines may promote further enhancement of central respiratory function via surrounding medullary structures (such as the raphé) which provide endogenous synaptic inputs to rhythmogenic preBötC neurons. The discovery of a potential novel receptor target for the ampakine CX717 led us to a much more extensive study analyzing CX717 pharmacological profile on specific recombinant proteins and the expression pattern of a NMDA receptor subtype in the medullary slice. The NR3 subtype of NMDA receptor might have an important role in driving preBötC synaptic activity under specific conditions.

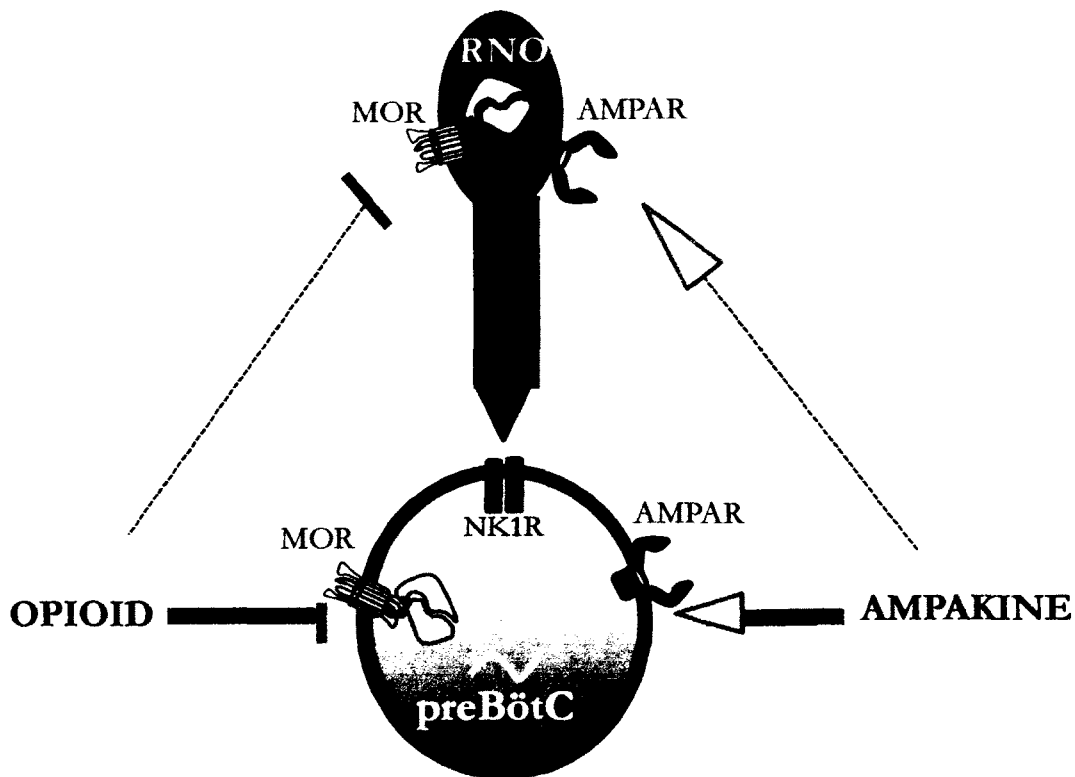


Figure 6.1 Putative “two arms” system of neuromodulation of the inspiratory drive by opioids and ampakines.

The generator of inspiratory drive (preBötzinger Complex; preBötC), may be inhibited directly by opioids via their direct action on mu-opioid receptors (MOR) present in the preBötC, or indirectly via an inhibition of tonic excitatory inputs (serotonergic; 5HT and substance P; SP) coming from the raphe nucleus obscurus (RNO). Ampakine may increase inspiratory drive via AMPA receptors (AMPA) present on the postsynaptic membrane of preBötC neurons, or indirectly promoting excitatory neurotransmitter release via AMPAR present in the RNO.

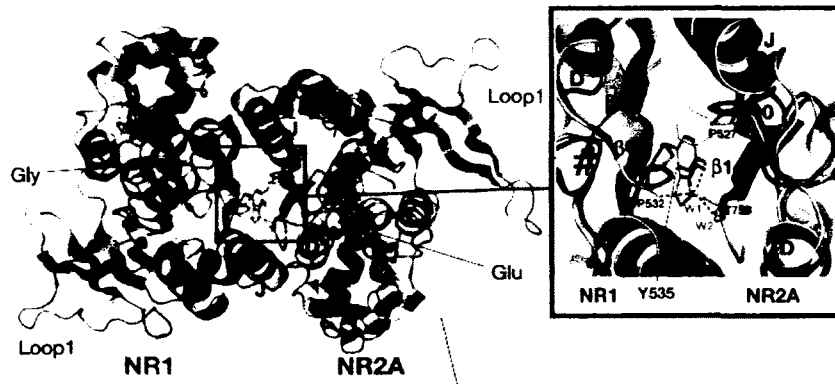


Figure 6.2 A candidate binding site for a low-impact ampakine.

Superposition of NR1–NR2A S1S2 and the GluR2 S1S2–aniracetam complex. Overlay of the GluR2 S1S2 dimer bound to glutamate and aniracetam (Ani, pink) onto the NR1–NR2A S1S2 dimer (green and blue).

[Fig 5 from Hiroyasu Furukawa, Satinder K Singh, Romina Mancusso and Eric Gouaux. Subunit arrangement and function in NMDA receptors. *Nature*. Vol 438|10 November 2005].

6.7 REFERENCES

ARAI AC, KESSLER M, ROGERS G, LYNCH G (2000) Effects of the potent ampakine CX614 on hippocampal and recombinant AMPA receptors: interactions with cyclothiazide and GYKI 52466. *Mol. Pharmacol.* 58(4):802-13.

BALLANYI K, PANAITESCU B, RUANGKITTISAKUL A (2010) Indirect opioid actions on inspiratory pre-Bötzinger complex neurons in newborn rat brainstem slices. *Adv Exp Med Biol.* 669:75-9.

BIEGER D, HOPKINS DA (1987) Viscerotopic representation of the upper alimentary tract in the medulla oblongata in the rat: the nucleus ambiguus. *J. Comp Neurol.* 262(4):546-62.

BLESSING WW, WILLOUGHBY JO, JOH TH (1985) Evidence that catecholamine-synthesizing perikarya in rat medulla oblongata do not contribute axons to the vagus nerve. *Brain Res.* 348(2):397-400.

BOUYER P, BRADLEY SR, ZHAO J, WANG W, RICHERSON GB, BORON WF (2004) Effect of extracellular acid-base disturbances on the intracellular pH of neurones cultured from rat medullary raphe or hippocampus. *J. Physiol.* 559(Pt 1):85-101.

BRADLEY SR, PIERIBONE VA, WANG W, SEVERSON CA, JACOBS RA, RICHERSON GB (2002) Chemosensitive serotonergic neurons are closely associated with large medullary arteries. *Nat Neurosci.* 5(5):401-2.

BUCHANAN GF, RICHERSON GB (2010) Central serotonin neurons are required for arousal to CO₂. *Proc Natl Acad Sci U S A.* 107(37):16354-9.

CHATTERTON JE, AWOBULUYI M, PREMKUMAR LS, TAKAHASHI H, TALANTOVA M, SHIN Y, CUI J, TU S, SEVARINO KA, NAKANISHI N, TONG G, LIPTON SA, ZHANG D (2002) Excitatory glycine receptors containing the NR3 family of NMDA receptor subunits. *Nature.*;415(6873):793-8.

CHEN L, CHETKOVICH DM, PETRALIA RS, SWEENEY NT, KAWASAKI Y, WENTHOLD RJ, BRETT DS, NICOLL RA (2000) Stargazin regulates synaptic targeting of AMPA receptors by two distinct mechanisms. *Nature* 408(6815):936-43.

CRAVEN SE, LIM KC, YE W, ENGEL JD, DE SAUVAGE F, ROSENTHAL A (2004) *Gata2* specifies serotonergic neurons downstream of sonic hedgehog. *Development* 131(5):1165-73.

DAS S, SASAKI YF, ROTHE T, PREMKUMAR LS, TAKASU M, CRANDALL JE, DIKES P, CONNER DA, RAYUDU PV, CHEUNG W, CHEN HS, LIPTON SA, NAKANISHI

- (1998) Increased NMDA current and spine density in mice lacking the NMDA receptor subunit NR3A. *Nature* 393(6683):377-81.
- DEPUY SD, KANBAR R, COATES MB, STORNETTA RL, GUYENET PG (2011) Control of breathing by raphe obscurus serotonergic neurons in mice. *J. Neurosci.* 31(6):1981-90.
- DING YQ, MARKLUND U, YUAN W, YIN J, WEGMAN L, ERICSON J, DENNERIS E, JOHNSON RL, CHEN ZF (2003) Lmx1b is essential for the development of serotonergic neurons. *Nat. Neurosci.* 6(9):933-8.
- DOI A, RAMIREZ JM (2010) State-dependent interactions between excitatory neuromodulators in the neuronal control of breathing. *J. Neurosci.* 30(24):8251-62.
- DUNMYRE JR, DEL NEGRO CA, RUBIN JE (2011) Interactions of persistent sodium and calcium-activated nonspecific cationic currents yield dynamically distinct bursting regimes in a model of respiratory neurons. *J. Comput. Neurosci.* 31(2):305-28.
- FUNK GD, SMITH JC, FELDMAN JL (1995) Modulation of neural network activity *in vitro* by cyclothiazide, a drug that blocks desensitization of AMPA receptors. *J. Neurosci.* 1995 May;15(5 Pt 2):4046-56.
- FUKAYA M, HAYASHI Y, WATANABE M (2005) NR2 to NR3B subunit switchover of NMDA receptors in early postnatal motoneurons. *Eur J Neurosci.* 21(5):1432-6.
- FURUKAWA H, SINGH SK, MANCUSO R, GOUAUX E (2005) Subunit arrangement and function in NMDA receptors. *Nature.* 438(7065):185-92.
- GILL MB, KATO AS, ROBERTS MF, YU H, WANG H, TOMITA S, BRETT DS (2011) Cornichon-2 modulates AMPA receptor-transmembrane AMPA receptor regulatory protein assembly to dictate gating and pharmacology. *J Neurosci.* 31(18):6928-38.
- GRAY PA, REKLING JC, BOCCHIARO CM, FELDMAN JL (1999) Modulation of respiratory frequency by peptidergic input to rhythmogenic neurons in the preBötzing complex. *Science* 286(5444):1566-8.
- GRAY PA, JANCZEWSKI WA, MELLEN N, MCCRIMMON DR, FELDMAN JL (2001) Normal breathing requires preBötzing complex neurokinin-1 receptor-expressing neurons. *Nat. Neurosci.* 4(9):927-30.

GRAY PA, HAYES JA, LING GY, LLONA I, TUPAL S, PICARDO MC, ROSS SE, HIRATA T, CORBIN JG, EUGENÍN J, DEL NEGRO CA (2010) Developmental origin of preBötzing complex respiratory neurons. *J. Neurosci.* 30(44):14883-95.

GREER JJ, CARTER JE, AL-ZUBAIDY Z (1995) Opioid depression of respiration in neonatal rats. *J. Physiol.* 485 (Pt 3):845-55.

GUYENET PG, STORNETTA RL, BAYLISS DA (2010) Central respiratory chemoreception. *J. Comp Neurol.* 518(19):3883-906.

HAMPSON RE, ESPAÑA RA, ROGERS GA, PORRINO LJ, DEADWYLER SA (2009) Mechanisms underlying cognitive enhancement and reversal of cognitive deficits in nonhuman primates by the ampakine CX717. *Psychopharmacology (Berl)*. 202(1-3):355-69.

HENDRICKS T, FRANCIS N, FYODOROV D, DENERIS ES (1999) The ETS domain factor Pet-1 is an early and precise marker of central serotonin neurons and interacts with a conserved element in serotonergic genes. *J. Neurosci.* 19(23):10348-56.

HODGES MR, WEHNER M, AUNGST J, SMITH JC, RICHERSON GB (2009) Transgenic mice lacking serotonin neurons have severe apnea and high mortality during development. *J. Neurosci.* 29(33):10341-9.

KATO AS, GILL MB, HO MT, YU H, TU Y, SIUDA ER, WANG H, QIAN YW, NISENBAUM ES, TOMITA S, BREDT DS (2010) Hippocampal AMPA receptor gating controlled by both TARP and cornichon proteins. *Neuron* 68(6):1082-96.

KOTT S, SAGER C, TAPKEN D, WERNER M, HOLLMANN M (2009) Comparative analysis of the pharmacology of GluR1 in complex with transmembrane AMPA receptor regulatory proteins gamma2, gamma3, gamma4, and gamma8. *Neuroscience* 158(1):78-88.

LIU YY, WONG-RILEY MT, LIU JP, JIA Y, LIU HL, JIAO XY, JU G (2002) GABAergic and glycinergic synapses onto neurokinin-1 receptor-immunoreactive neurons in the pre-Bötzing complex of rats: light and electron microscopic studies. *Eur. J. Neurosci.* 16(6):1058-66.

LIU Q, WONG-RILEY MT (2010A) Postnatal changes in tryptophan hydroxylase and serotonin transporter immunoreactivity in multiple brainstem nuclei of the rat: implications for a sensitive period. *J. Comp. Neurol.* 518(7):1082-97.

LIU Q, WONG-RILEY MT (2010B) Postnatal development of N-methyl-D-aspartate receptor subunits 2A, 2B, 2C, 2D, and 3B immunoreactivity in brain stem respiratory nuclei of the rat. *Neuroscience* 171(3):637-54.

- LIU J, WU DC, WANG YT (2010) Allosteric potentiation of glycine receptor chloride currents by glutamate. *Nat. Neurosci.* 13(10):1225-32.
- LORIER AR, FUNK GD, GREER JJ (2010) Opiate-induced suppression of rat hypoglossal motoneuron activity and its reversal by ampakine therapy. *PLoS One* 5(1):e8766.
- LYNCH G, GALL CM (2006) Ampakines and the threefold path to cognitive enhancement. *Trends Neurosci.* 29(10):554-62.
- MATSUDA K, KAMIYA Y, MATSUDA S, YUZAKI M (2002) Cloning and characterization of a novel NMDA receptor subunit NR3B: a dominant subunit that reduces calcium permeability. *Brain Res Mol Brain Res.* 100(1-2):43-52.
- MCALLEN RM, SPYER KM (1978) Two types of vagal preganglionic motoneurons projecting to the heart and lungs. *J Physiol.* 282:353-64.
- MELLEN NM, JANCZEWSKI WA, BOCCHIARO CM, FELDMAN JL (2003) Opioid-induced quantal slowing reveals dual networks for respiratory rhythm generation. *Neuron* 37(5):821-6.
- MENUZ K, STROUD RM, NICOLL RA, HAYS FA (2007) TARP auxiliary subunits switch AMPA receptor antagonists into partial agonists. *Science* 318(5851):815-7.
- MONTANDON G, QIN W, LIU H, REN J, GREER JJ, HORNER RL (2011) PreBotzinger complex neurokinin-1 receptor-expressing neurons mediate opioid-induced respiratory depression. *J. Neurosci.* 31(4): 1292-301.
- MORGADO-VALLE C, BACA SM, FELDMAN JL (2010) Glycinergic pacemaker neurons in preBötzing complex of neonatal mouse. *J. Neurosci.* 30(10):3634-9.
- MORGADO-VALLE C, FELDMAN JL (2007) NMDA receptors in preBötzing complex neurons can drive respiratory rhythm independent of AMPA receptors. *J. Physiol.* 582(Pt 1):359-68.
- MORIN-SURUN MP, GACEL G, CHAMPAGNAT J, DENAVIT-SAUBIE M, ROQUES BP (1984A) Pharmacological identification of delta and mu opiate receptors on bulbar respiratory neurons. *Eur. J. Pharmacol.* 98(2):241-7.
- MORIN-SURUN MP, BOUDINOT E, DUBOIS C, MATTHES HW, KIEFFER BL, DENAVIT-SAUBIÉ M, CHAMPAGNAT J, FOUTZ AS. (2001) Respiratory function in adult mice lacking the mu-opioid receptor: role of delta-receptors. *Eur. J. Neurosci.* 13(9):1703-10.
- MONTGOMERY KE, KESSLER M, ARAI AC (2009) Modulation of agonist binding to AMPA receptors by 1-(1,4-benzodioxan-6-ylcarbonyl) piperidine (CX546):

differential effects across brain regions and GluA1-4/transmembrane AMPA receptor regulatory protein combinations. *J. Pharmacol. Exp. Ther.* 331(3):965-74.

MULKEY DK, STORNETTA RL, WESTON MC, SIMMONS JR, PARKER A, BAYLISS DA, GUYENET PG (2004) Respiratory control by ventral surface chemoreceptor neurons in rats. *Nat Neurosci.* 7(12):1360-9.

NATTIE EE (2001) Central chemosensitivity, sleep, and wakefulness. *Respir. Physiol.* 129(1-2):257-68. Review.

NICOLL RA, TOMITA S, BREDT DS (2006) Auxiliary subunits assist AMPA-type glutamate receptors. *Science* 311(5765):1253-6.

PAARMANN I, FRERMANN D, KELLER BU, VILLMANN C, BREITINGER HG, HOLLMANN M (2005) Kinetics and subunit composition of NMDA receptors in respiratory-related neurons. *J. Neurochem.* 93(4):812-24.

PACE RW, MACKAY DD, FELDMAN JL, DEL NEGRO CA (2007) Inspiratory bursts in the preBötzinger complex depend on a calcium-activated non-specific cation current linked to glutamate receptors in neonatal mice. *J. Physiol.* 582(Pt 1):113-25.

PAGLIARDINI S, ADACHI T, REN J, FUNK GD, GREER JJ (2005) Fluorescent tagging of rhythmically active respiratory neurons within the pre-Bötzinger complex of rat medullary slice preparations. *J. Neurosci.* 25(10):2591-6.

PATTYN A, SIMPLICIO N, VAN DOORNINCK JH, GORIDIS C, GUILLEMOT F, BRUNET JF (2004) *Ascl1/Mash1* is required for the development of central serotonergic neurons. *Nat. Neurosci.* 7(6):589-95.

PARTIN KM., BOWIE D AND MAYER ML (1995) Structural Determinants of Allosteric Regulation in Alternatively Spliced AMPA Receptors. *Neuron* 14: 833-843.

PARTIN KM, PATNEAU DK, MAYER ML (1994) Cyclothiazide differentially modulates desensitization of alpha-amino-3-hydroxy-5-methyl-4-isoxazolepropionic acid receptor splice variants. *Mol Pharmacol.* 46(1):129-38.

PARTIN KM, PATNEAU DK, WINTERS CA, MAYER ML, BUONANNO A (1993) Selective modulation of desensitization at AMPA versus kainate receptors by cyclothiazide and concanavalin A. *Neuron* 11(6):1069-82.

PFEIFFER M, KIRSCHT S, STUMM R, KOCH T, WU D, LAUGSCH M, SCHRÖDER H, HÖLLT V, SCHULZ S (2003) Heterodimerization of substance P and mu-opioid

receptors regulates receptor trafficking and resensitization. *J Biol Chem.* (51):51630-7.

PFEIFFER M, KOCH T, SCHRÖDER H, LAUGSCH M, HÖLLT V, SCHULZ S (2002) Heterodimerization of somatostatin and opioid receptors cross-modulates phosphorylation, internalization, and desensitization. *J Biol Chem.* 277(22):19762-72.

PIÑA-CRESPO JC, TALANTOVA M, MICU I, STATES B, CHEN HS, TU S, NAKANISHI N, TONG G, ZHANG D, HEINEMANN SF, ZAMPONI GW, STYS PK, LIPTON SA (2010) Excitatory glycine responses of CNS myelin mediated by NR1/NR3 "NMDA" receptor subunits. *J. Neurosci.* 30(34):11501-5.

PRIEL A, KOLLEKER A, AYALON G, GILLOR M, OSTEN P, STERN-BACH Y (2005) Stargazin reduces desensitization and slows deactivation of the AMPA-type glutamate receptors. *J. Neurosci.* 25(10):2682-6.

PTAK K, YAMANISHI T, AUNGST J, MILESCU LS, ZHANG R, RICHERSON GB, SMITH JC (2009) Raphé neurons stimulate respiratory circuit activity by multiple mechanisms via endogenously released serotonin and substance P. *J. Neurosci.* 29(12):3720-37.

RAY RS, CORCORAN AE, BRUST RD, KIM JC, RICHERSON GB, NATTIE E, DYMECKI SM (2011) Impaired respiratory and body temperature control upon acute serotonergic neuron inhibition. *Science* 333(6042):637-42.

REN J, GREER JJ (2006) Modulation of respiratory rhythmogenesis by chloride-mediated conductances during the perinatal period. *J. Neurosci.* 26(14):3721-30.

RUBIN JE, HAYES JA, MENDENHALL JL, DEL NEGRO CA (2009) Calcium-activated nonspecific cation current and synaptic depression promote network-dependent burst oscillations. *Proc Natl Acad Sci U S A.* 106(8):2939-44.

SCHWENK J, HARMEL N, ZOLLES G, BIDL W, KULIK A, HEIMRICH B, CHISAKA O, JONAS P, SCHULTE U, FAKLER B, KLÖCKER N (2009) Functional proteomics identify cornichon proteins as auxiliary subunits of AMPA receptors. *Science* 323(5919):1313-9.

SOBOLOEVSKY AI, ROSCONI MP, GOUAUX E (2009) X-ray structure, symmetry and mechanism of an AMPA-subtype glutamate receptor. *Nature* 462:745–756.

SPITZER NC (2012) Activity-dependent neurotransmitter respecification *Nature Reviews Neuroscience* 13: 94-106.

STATLER KD, ALEXANDER HL, VAGNI VA, NEMOTO EM, TOFOVIC SP, DIXON CE, JENKINS LW, MARION DW, KOCHANNEK PM (2003) Moderate hypothermia may be

detrimental after traumatic brain injury in fentanyl-anesthetized rats. *Crit. Care Med.* 31(4):1134-9.

TAKEDA S, ERIKSSON LI, YAMAMOTO Y, JOENSEN H, ONIMARU H, LINDAHL SG (2001) Opioid action on respiratory neuron activity of the isolated respiratory network in newborn rats. *Anesthesiology* 95(3):740-9.

TOMITA S, CHEN L, KAWASAKI Y, PETRALIA RS, WENTHOLD RJ, NICOLL RA AND BREDT DS (2003) Functional studies and distribution define a family of transmembrane AMPA receptor regulatory proteins. *J. Cell Biol.* 161:805–816.

TOMITA S, SEKIGUCHI M, WADA K, NICOLL RA, BREDT DS (2006) Stargazin controls the pharmacology of AMPA receptor potentiators. *Proc Natl Acad Sci U S A.* 103(26):10064-7.

TURECEK R, TRUSSELL LO (2001) Presynaptic glycine receptors enhance transmitter release at a mammalian central synapse. *Nature* 411:587-590.

VAN DOORNINCK JH, VAN DER WEES J, KARIS A, GOEDKNEGT E, ENGEL JD, COESMANS M, RUTTEMAN M, GROSVELD F, DE ZEEUW CI (1999) GATA-3 is involved in the development of serotonergic neurons in the caudal raphe nuclei. *J. Neurosci.* 19(12):RC12.

VON ENGELHARDT A, MACK V, SPRENGEL R, KAVENSTOCK N, WAN LI K, STERNBACH Y, SMIT AB, SEEBURG PH, MONYER H (2010) CKAMP44: A Brain-Specific Protein Attenuating Short-Term Synaptic Plasticity in the Dentate Gyrus. *Science* 1518-1522.

WANG H, STORNETTA RL, ROSIN DL, GUYENET PG (2001A) Neurokinin-1 receptor-immunoreactive neurons of the ventral respiratory group in the rat. *J. Comp. Neurol.* 434(2):128-46.

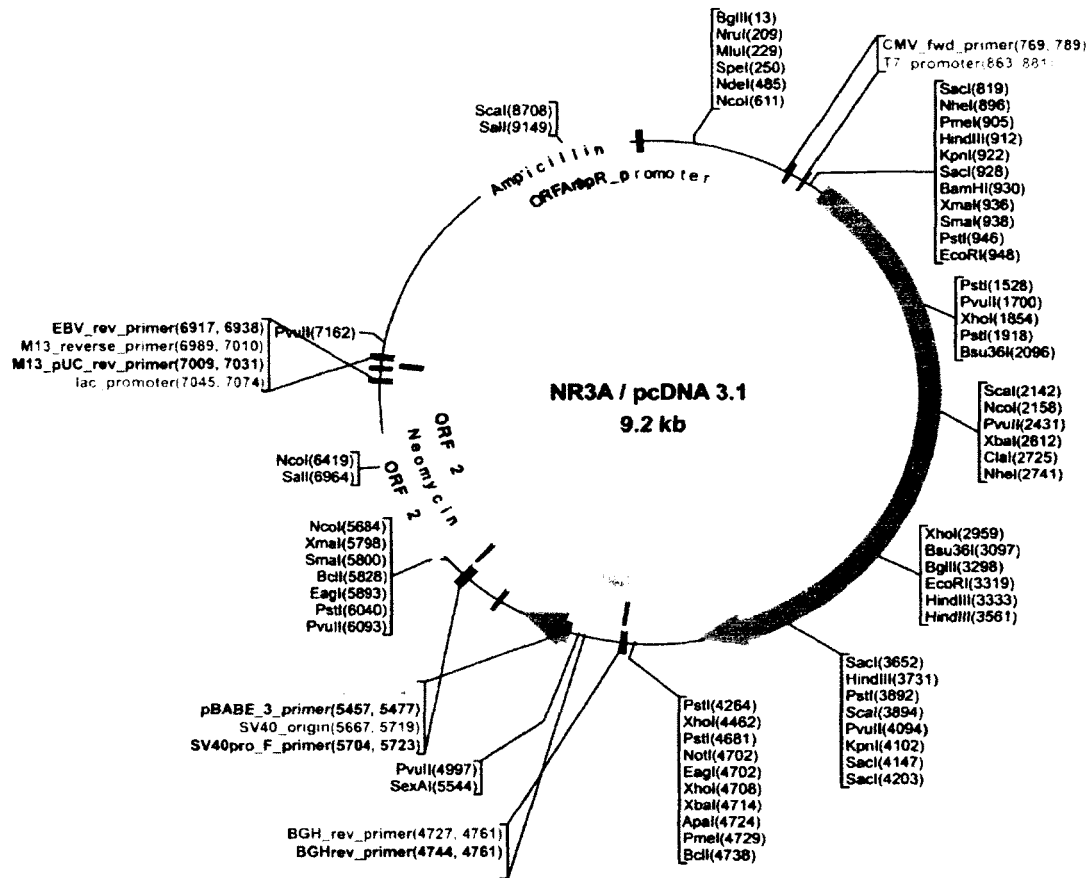
WANG W, TIWARI JK, BRADLEY SR, ZAYKIN RV, RICHERSON GB (2001B) Acidosis-stimulated neurons of the medullary raphe are serotonergic. *J Neurophysiol.* 85(5):2224-35.

WONG HK, LIU XB, MATOS MF, CHAN SF, PÉREZ-OTAÑO I, BOYSEN M, CUI J, NAKANISHI N, TRIMMER JS, JONES EG, LIPTON SA, SUCHER NJ (2002) Temporal and regional expression of NMDA receptor subunit NR3A in the mammalian brain. *J Comp Neurol.* 450(4):303-17.

XU H, PARTILLA JS, WANG X, RUTHERFORD JM, TIDGEWELL K, PRISINZANO TE, BOHN LM, ROTHMAN RB (2007) A comparison of noninternalizing (herkinorin) and internalizing (DAMGO) mu-opioid agonists on cellular markers related to opioid tolerance and dependence. *Synapse* 61(3):166-75.

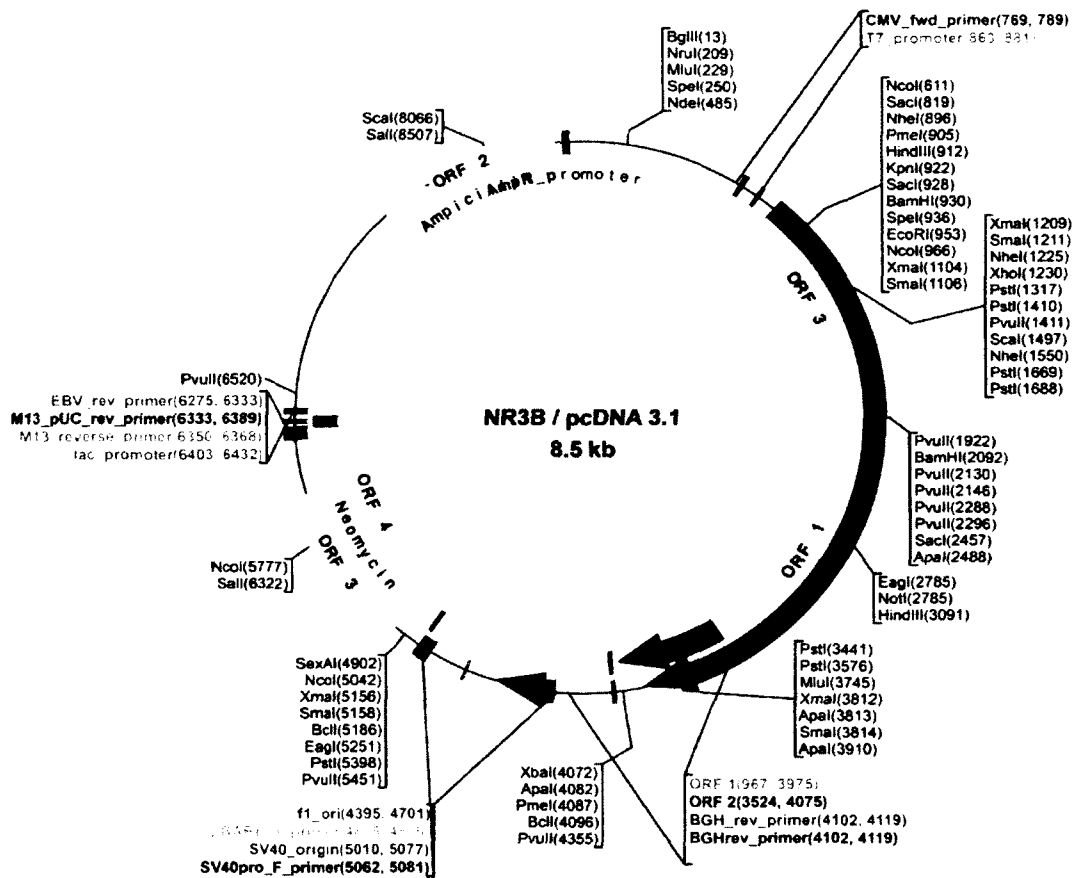
ZHANG W, ROBERT A, VOGENSEN SB, HOWE JR (2006) The relationship between agonist potency and AMPA receptor kinetics. *Biophys. J.* 91(4):1336-46.

ZHANG Z, XU F, ZHANG C, LIANG X (2009) Opioid mu-receptors in medullary raphe region affect the hypoxic ventilation in anesthetized rats. *Respir Physiol Neurobiol.* 168(3):281-8.



Annex 1. Schematic representation of the NR3A/pcDNA3.1 plasmid map.

The *Rattus Norvegicus* NR3A subunit was cloned into a pcDNA3.1 vector for expression of NR3B in HEK293 cells. Note the ampicillin resistance gene and the neomycin resistance gene for selection of the vector in bacteria. The human cytomegalovirus (CMV) early promoter allowed for efficient transient expression of the subclone genes. Note the presence of the bovine growth hormone (BGH) signal to ensure efficient termination of transcription. Open reading frames are indicated as ORF. This plasmid was designed, constructed and provided by Dr. Stuart A. Lipton and Dr. Dongxian Zhang, Burnham Institute San Diego, CA.



Annex 2. Schematic representation of the NR3B/pcDNA3.1 plasmid map.

The *Rattus Norvegicus* NR3B subunit was cloned into a pcDNA3.1 vector for expression of NR3B in HEK293 cells. Note the ampicillin resistance gene and the neomycin resistance gene for selection of the vector in bacteria. The human cytomegalovirus (CMV) early promoter allowed for efficient transient expression of the subclone genes. Note the presence of the bovine growth hormone (BGH) signal to ensure efficient termination of transcription. Open reading frames are indicated as ORF. This plasmid was also designed, constructed and provided by Dr. Stuart A. Lipton and Dr. Dongxian Zhang, Burnham Institute San Diego, CA.